Growth and otolith zone formation of Namibian hake *Merluccius capensis*

Margit R. Wilhelm

Thesis presented for the degree of

Doctor of Philosophy

Department of Zoology

University of Cape Town

February 2012

Supervisors:

Prof. Astrid Jarre

Prof. Coleen L. Moloney

Dr Jean-Paul Roux

Dr M. Deon Durholtz

Declaration

I know the meaning of Plagiarism and declare that all the work presented in this thesis is my own, except where it is properly acknowledged in the text. This thesis has not been submitted in whole or in part for a degree at another university.

.....
Margit Wilhelm

.....
Date

Then the Lord answered Job out of the storm. He said:

. . .

"Where were you when I laid the earth's foundation?
Tell me, if you understand.
Who marked off its dimensions? Surely you know!
Who stretched a measuring line across it?
On what were its footings set,
or who laid its cornerstone —
while the morning stars sang together
and all the angels shouted for joy?
"Who shut up the sea behind doors
when it burst forth from the womb,
when I made the clouds its garment
and wrapped it in thick darkness,
when I fixed limits for it
and set its doors and bars in place,
when I said, 'This far you may come and no farther;
here is where your proud waves halt'?

. . .

Then Job replied to the Lord:
"I know that you can do all things;
no plan of yours can be thwarted. . ."

(Job 38: 1, 4-11; 42: 1-2. New International Version, 1984)

Table of Contents

Acknowledgements

Financial support was provided by the SEAChange Project of the South African Network for Coastal and Oceanic Research, funded by the Branch: Marine and Coastal Management and the National Research Foundation; and by the South African Research Chairs Initiative of the Department of Science and Technology and the National Research Foundation, through the Research Chair in Marine Ecology and Fisheries. The Ministry of Fisheries and Marine Resources (MFMR), Namibia funded the collection of seal scat data, research survey and commercial length-frequency data, biological data, and otoliths, and oceanographic data. The Benguela Current Large Marine Ecosystem (BCLME) funded the first mini-workshop when this project started in 2006, and the Benguela Current Commission (BCC) funded an ageing training workshop contributing to this work in 2010.

I am extremely grateful to Jean-Paul Roux (MFMR) for sharing his brain-child with me. The seal scat hake cohort data!!! It has been a great privilege to be part of this project and to share your enthusiasm and to learn from you about the northern Benguela ecosystem! Thank you for all the conversations and all the ideas to explore, and thank you for teaching me!

Thank you to Deon Durholtz at the Department of Agriculture Forestry and Fisheries (DAFF), Cape Town, for the idea of hake age validation from the seal scat data! Thank you for all the teaching and discussions and hours of otolith reading from the very beginning when the current “ageing working group” started, thank you for always letting me apply my ideas in the region and thank you for believing in me!

I feel immensely privileged to have been able to study at the University of Cape Town (UCT) under the supervision of Coleen Moloney and Astrid Jarre. Thank you for immediately saying “yes” and finding funding for me. Thank you for the support that came in all varieties. Thank you for patiently guiding me from writing my proposal, to statistics and analysis, to being “data smart”, to presentation and writing skills, to putting me in contact with the right people, to getting me where we are today! Thank you for believing in me, for always backing me, and thank you for teaching me!

To a special group of “hake otolith students” Faye Brinkman, Wendy West and Suama Kashava. Thank you for choosing to work with me and for all the invaluable data you collected! And thank you especially to Faye for being part of the “life support” group for much of the time. You don’t know how much it meant to me and how much it contributed to me continuing!

Thank you to lab assistants Emily Richardson, Maya Pfaff and Hanna Neshuku, for putting in that insane amount of hours labelling and separating otoliths! Thank you to Otto Whitehead for taking photographs of otoliths.

Thank you to all the researchers that were part of the seal scat collections, the numerous surveys, the captains and crew of all the research cruises and all the observers for the wealth of data they collected, which contributes to this thesis today.

Thank you to Hanna Neshuku, Sarah Paulus, Anja van der Plas, Paul Kainge, John Kathena, Chris Bartholomae and Carola Kirchner at MFMR for their assistance and their data. A special thanks to Hanna and Sarah for their enthusiasm, and going over and above their call of duty to help me – I am so glad for the new “otolith crew”; Hanna, I remember us sitting with masks on sorting thousands of otoliths in the smelly lab; Anja, thank you for patiently teaching me about oceanography and answering my questions, again and again; Carola thank you for always sharing your ideas and for your support over the years!

Thank you Nadine and Patrick Kohlstädt, Chibo Chikwililwa, and my parents for hosting me in Swakopmund while I was collecting samples. Thank you Heidi Skrypzeck for sharing your office space with me. Thank you Jean-Paul Roux and Jessica Kemper for hosting me in windy Lüderitz for a while.

Thank you to the R gurus for the invaluable geek-help, Dawit Yemane, Tony Booth, Henning Winker, Maya Pfaff, Res Altwegg; wow, you all rock!

Many people have contributed with “bouncing off ideas” and discussions, sparking a new direction, etc; a few I remember are Jean-Paul Roux, Astrid Jarre, Coleen Moloney, Maya Pfaff, Hannes Baumann, John Casselman, Britta Grote, Henning

Winker, Tony Booth, Dawit Yemane, Larvika Singh, Larry Hutchings, Carl van der Lingen, Deon Durholtz, Carola Kirchner, Hilkka Ndjaula.

For reading and commenting on drafts I thank Astrid Jarre, Coleen Moloney, Jean-Paul Roux, Deon Durholtz and Gilly Smith! Gilly, to you also a very special thank you for doing so much more than the administration; always supporting your students, being "der ruhige Pol" around whom everything revolves, and who encourages us and "has our backs" all the time! It's been really great to be in your lab!!

Thank you for drawing the maps, Edward Hill, and for drawing the figure in Chapter 7, Cathy Boucher.

Thank you to John Field for help with administration as the director of MaRe of UCT.

I acknowledge UCT interlibrary loans and the DAFF library staff for helping me find important reference material.

I have amazing friends and family in Cape Town and Swakopmund that have provided the "life support", that is usually needed for a journey like this. There have been many over the years, and I thank you all! But a special mention to Maya Pfaff, Hilkka Ndjaula, Nadine Moroff, Chibo Chikwililwa, Anthony and Daphne Buratovich, Jenny Wicksteed and the rest of the "Goscom group" (my family in Cape Town), Patrice Gopo, Ingrid Vriend, Jean Watermeyer, Chris Warton and the "Monday group", Grant Owens and the "Friday group". For all the support in all varieties, prayers and encouragement, meals and coffees, the literal and the figurative ones. Hilkka, to have had you as my "labmate" for the past 3 years, for helping with the last minute troubleshooting, and just your continuous support, I am so lucky, and I am immensely grateful!

And finally, but actually in the first place, I want to thank my parents, Lothar and Elke Wilhelm. You have stood behind me 200 % of the time. I am extremely grateful and *so* privileged. Thank you for giving me everything I needed for my education, to get me to this point today, and actually being the ones enabling me to explore my passion for fisheries science. Words can not express my gratitude! This is for you!!

Glossary

– after Kalish *et al.* (1995), Panfili *et al.* (2002) and Campana (2001)

Age determination (age estimation) – the process of assigning ages to fish. The term ageing / aging should not be used as it refers to time-related processes altering an organism's composition, structure, and function over time.

Age-group – the cohort of fish that have a given age. The term is not synonymous with year-class (or day-class).

Annulus (pl. annuli) – one of a series of concentric zones on a structure that may be interpreted for age (in this case an otolith), representing one year mark.

Check – a discontinuity (e.g. a stress-induced zone) in a zone or in a pattern of opaque and translucent zones. If the term is used, it requires precise definition.

Cohort – group of fish of a similar age that were spawned during the same time interval. Used with age-group, year-class and day-class.

Core – the area or areas surrounding one or more primordia. In the early stages of otolith growth, if several primordial are present, they generally fuse to form the otolith core

Corroboration – a measure of consistency or repeatability of an age determination method. For example, if readers agree on the age assigned to a fish, corroboration is achieved.

Edge analysis – A method of age validation. The proportion (presence) of the otolith edge type (translucent or opaque) should display a sinusoidal cycle when plotted against season or month of the year with a frequency of one for annuli.

Hatchdate – the date a fish is hatched.

Increment – a reference to the region between similar zones on an otolith. The term refers to a structure but may be qualified to refer to portions of the otolith formed over a specific time interval (e.g. annual, subdaily, daily). Usually an annual increment comprises an opaque zone and a translucent zone.

Marginal increment/margin – the region beyond the last identifiable zone at the edge of an otolith. This term is usually expressed in relative terms, that is, a proportion of the last complete increment.

Marginal increment analysis – A method of age validation. The marginal increment is usually calculated as a proportional state of completion, ranging from near zero (an increment is just beginning to form) to one (a complete increment has formed). When plotted as a function of month or season, the mean marginal increment should describe a sinusoidal cycle with a frequency of one year in annuli.

Opaque zone – a zone that restricts the passage of light when compared with a translucent zone. The term is a relative one because a zone is determined to be opaque on the basis of the appearance of adjacent zones in the otolith (see translucent zone). In untreated otoliths under transmitted light, the opaque zone appears dark and the translucent zone appears bright. Under reflected light the opaque zone appears bright and the translucent zone appears dark. An absolute value for the optical density of such a zone is not implied.

Primordium (pl. primordia) – the initial complex structure of an otolith. It consists of organic matrix and calcium carbonate surrounding one or more optically dense cores 0.5 µm to 1.0 µm in diameter termed primordial granules.

Translucent zone – a zone that allows the passage of greater quantities of light than an opaque zone. The term is a relative one because a zone is determined to be translucent on the basis of the appearance of adjacent zones in the otolith (see opaque zone). An absolute value for the optical density of such a zone is not implied. In untreated otoliths under transmitted light, the translucent zone appears bright and the opaque zone appears dark. Under reflected light the translucent zone appears dark and the opaque zone appears bright. Synonymous with hyaline zone, but the term hyaline zone should be avoided.

Validation – the process of estimating the accuracy of an age determination method. The concept of validation is one of degree and should not be considered in absolute terms. If the method involves counting zones, then part of the validation process involves confirming the temporal meaning of the zones being counted. Validation of an age determination procedure indicates that the age determination method is sound and based on fact.

Verification – the process of establishing that something is true. Individual age estimates can be verified if a validated age estimation method has been employed. Verification implies the testing of something, such as a hypothesis, that can be determined in absolute terms to be either true or false.

Year-class – the cohort of fish that were spawned or hatched in a given year. Whether this term is used to refer to the date of spawning or hatching must be specified as some high-latitude fish species have long developmental times prior to hatching.

Zone – region of similar structure or optical density. Synonymous with ring, band and mark, but the term zone is preferred.

General Abstract

Life history traits and tactics of commercially important Namibian shallow-water hake, *Merluccius capensis*, were investigated in relation to their environment. A time series of length-frequency distributions (LFDs) from otoliths collected from fur seal scat samples was used to identify cohorts and calculate the approximate hatchdates and growth rates of young *M. capensis* from 1994 to 2009. Monthly otolith samples of five of these cohorts (1996, 1998, 2002, 2005 and 2006) were used to evaluate the translucent zone periodicity over the first 21 months of their life. Additionally, LFDs from research surveys and commercial samples were used to calculate growth rates for *M. capensis* up to 65 cm total length (TL), and to further validate the translucent zone formation of three of the five cohorts (1996, 1998 and 2002) on fish up to 3.5 years old. Results showed that spawning peaks occurred once a year in winter (mid-date 23 June). Recruitment strength did not depend on timing of the hatchdates. *M. capensis* juveniles and adults grow twice as fast as previously calculated, making *M. capensis* a more r-selected species than other gadoids. Translucent zones are formed biannually on *M. capensis* up to 3.5 years old. One translucent zone is formed in winter/spring and one or two translucent zones in summer/autumn of each year. Winter/spring translucent zones have the same appearance as summer/autumn translucent zones under the light microscope. The second translucent zone (T2) is usually the first annulus. It is formed between July and September when fish are about one year old and between 15 and 20 cm long. For routine age determination, the first annulus should be assigned at a measurement of between 7.5 and 9.0 mm in diameter. The number of translucent zones after this should be counted and divided by two to get the new (integer) age of the fish. The effects of longitudinal and/or off-the-shelf movements of *M. capensis* on translucent zone formation throughout their life history were studied using densities from research surveys from 1990 to 2007, predicted for fish length and latitude or for fish length and depth using loess smoothers. The first (summer) translucent zone (T1) was strongly linked with young *M. capensis* moving from the mid-shelf to the inner-shelf. The northward movement of 2 to 2.5 year-old fish (30–36 cm) was often associated with translucent zone formation as well. The movement of 1.5 to 2-year-old (24–28 cm) fish from the inner-shelf to the mid-shelf and 3.5 to 4-year-old fish (50–56 cm) from the mid-shelf to the outer-shelf was also sometimes linked with the formation of translucent zones. Fish often moved inshore

and southwards again at ages greater than 3.5 years (> 52 cm), presumably to spawn. Two general areas of spawning aggregation were identified, one in the south (26–29°S) and one in the central area (21–25°S). Hatchdates of young-of-the year from the central spawning aggregation usually peaked in June–July, with a secondary peak in September–October. Those from the southern spawning aggregation peaked in September–October. There is sufficient spatial and temporal mixing between these two aggregations to identify *M. capensis* as one unit stock in the northern Benguela. Strong cohorts usually coincided with bimodal hatchdate peaks from both the central and the southern spawning aggregations. A binomial generalised linear model was used to assess whether the variation in the presence of the first six translucent zones on *M. capensis* otoliths is associated with fish length, cohort, area, depth or maturity stage or a combination of any or all of the variables. The presence of translucent zones was always most strongly associated with fish length, Area had a significant effect on the presence of translucent zones per fish length. Translucent zone formation changed from earliest to latest on fish captured from northern to southern of Namibia. For some translucent zones (notably the first, the third and the fourth), timing also varied among cohorts. Back-calculated translucent zone formation dates were linked with daylight duration, water temperature, water dissolved oxygen content, water temperature change, and water temperature anomalies using a randomization procedure. Events of translucent zone formation were only significantly correlated with warm bottom temperatures. Most translucent zones were formed in summer/autumn at warm bottom temperatures, but annuli were formed in winter/spring at cold temperatures. It is recommended that the link between feeding level and nutritional condition of fish and translucent zone formation on their otoliths is evaluated with additional data. In order to explore possible consequences of these findings for fisheries management advice, the effects of the fast growth rate on the stock dynamics of *M. capensis* were tested using a simple age-structured production model. Results suggested that a fast-growing *M. capensis* stock might be more sensitive to fishing pressure than previously thought, currently being at small spawning stock biomass, and hence at increased risk and sensitive to environmental fluctuations. However, the fast-growing stock might have a quicker recovery rate than previously believed, giving reason to expect an accelerated recovery in case of reduced fishing pressure. The fast-growing stock could also have a higher natural mortality than previously thought, which needs further investigation.

CHAPTER 1

General Introduction

Understanding the life history traits and tactics of a fish species in general is required for understanding the dynamics of a stock, for predicting how it will react to changes in the environment and to fishing pressure, and to assessing its productivity, in order to exploit it in the best possible manner.

Life history strategies and tactics can be described as a series of trade-offs; the relationships between traits; the co-ordinated evolution of all life-history traits together (Stearns, 1976). Details of each strategy are adjusted in each stock in different and variable environments to make each strategy successful. *Tactics* are "rules" (including regulation and compensation processes) that specify how an organism should respond to its own state or environment (plasticity of traits that allows a population to cope with environmental variability). The assembly of these rules is called a strategy. Tactics are permitted by *phenotypic plasticity* – the ability of a particular genotype to vary in response to its environment – and by behavioural adaptations (Stearns, 1989) and differ in species that differ in life-history strategies. The major life history traits are: adult size, survival, age and size at maturity, life span, reproductive lifespan, total reproductive output and fecundity (Stearns, 1976; 2000; Rochet, 2000).

Adams (1980) divided the life history strategies (or combinations of population parameters) of marine fish species into the two broad categories: r-selected strategies and K-selected strategies. The r-strategists are commonly exposed to an unpredictable environment, a high proportion of unpredictable catastrophic mortality, and allocate large portions of energy to reproductive activities. They grow fast, mature early and produce a maximum number of offspring at an early age. Other characteristics that are a result of high productivity are a small body size, short life-span and a high natural mortality rate. Characteristics measurable in fisheries biology are: a low age at first maturity, a high value of k from the von Bertalanffy growth (VBG) equation, a small L_∞ from the VBG equation, high rates of instantaneous natural mortality (M) and low maximum age. Clupeid fish (e.g. sardine, anchovy and herring) are examples of r-strategists. Adams (1980) suggested that fisheries based on a more r-selected strategist would be more productive, could be fished at younger ages and higher levels of fishing

mortality, should have a quicker recovery from over-fishing, but are more heavily influenced by environmental fluctuations. The K-strategist, on the other hand, is exposed to stable environments with predictable mortality sources, and thus rather increases individual fitness through competitive ability. They display slow growth, delayed maturity and low natural mortality rates. They are long-lived fish with a large body size. Measurable characteristics are: high age at first maturity, a low k from the VBG equation, a large L_∞ from the VBG equation, low M, and a high maximum age. Fish such as orange roughy or sturgeons are examples of K-strategist fish. Adams (1980) showed that maximum age, adult size and age at maturity were positively correlated and suggested that fisheries aimed at more K-selected strategists can be based on more predictable catch levels, but once overfished will be slow to recover.

Rochet (2000) examined demographic strategies of four different orders of teleost fish (Clupeiformes, Gadiformes, Perciformes, Pleurinectiformes) by attempting to separate their life history traits into a phylogenetic effect (strategy) and a population component (variability within strategies: tactics). She found that all orders had different life history strategies with different tactics among strategies. She argued that the r- and K-selection theory ignored size effects, fluctuations in mortality and fecundity schedules as well as age structure of most population processes. She hypothesized that if much growth still takes place after maturity, less energy will be allocated to reproduction, resulting in a slower increase of fecundity with size. For example, clupeoid fish, though their age at maturity is young, mature late relative to their maximum size and do not grow much after reproduction. Rochet (2000) also tested how different orders of fish compensate for high adult mortality induced by fishing pressure. Clupeiformes (e.g. sardines and anchovies) compensate for high adult mortality by a steeper increase of fecundity with size, whereas Gadiformes (e.g. hakes and cod) compensate by an increase of fecundity at all ages, and mature at a large size. Perciformes (e.g. horse mackerel and jack mackerel) show very similar trends to Gadiformes, while Pleurinectiformes (flatfishes) have an intermediate strategy (Table 1.1).

Table 1.1 Four orders of teleost species and the summary of their life history strategies and tactics as per Rochet (2000).

Order	Strategies: Adult Size	Life-span	Growth & reproduction	Tactics: Compensation for high adult mortality
Clupeiformes	Small	Long relative to size	First grow, then reproduce. Late maturation relative to size. Steep increase of fecundity with size.	Steeper increase of fecundity with size.
Gadiformes	Large	Short relative to size	Early maturation relative to adult size. Reproduction starts well before end of growth.	Increase of fecundity at all ages. Mature at larger size.
Perciformes	Large	Short relative to size	Same as Gadoids with smaller size at maturity relative to adult size.	Earlier maturity at larger size relative to adult size.
Pleuronectiformes	Intermediate (between two extremes of Clupeoids and Gadoids).			Mature at a larger size or earlier maturity.

The hake species studied in this thesis, shallow-water hake *Merluccius capensis*, belongs to the order Gadiformes and therefore should have overall life history strategies of that order; being large adult size and early maturation with a short life span relative to their size (Table 1.1). However, *M. capensis* needs specific tactics to cope with the highly variable northern Benguela eastern boundary upwelling environment. In this thesis, life history strategies and tactics of *M. capensis* are newly described, and comparisons are made between the "old" and the "new" life history strategy. Since comparisons in this thesis are only made within one species, size effects (Rochet, 2000) do not apply.

1.1 The hakes – species and stock identity

The hakes are typical components of fish communities in upwelling ecosystems. They are members of the subclass Neopterygii, infraclass Teleostei, superorder Paracanthopterygii, order Gadiformes, family Merlucciidae (merluccid hakes) and genus *Merluccius* (1 of 5 genera, 15 of 23 species). These are haddock or offshore silver hake *M. albidus* (Mitchill, 1818), Panama hake *M. angustimanus* (Garman, 1899), southern hake *M. australis* (Hutton, 1872), silver hake *M. bilinearis* (Mitchill, 1814), shallow-water Cape hake *M. capensis* (Castelnau, 1861), south Pacific hake *M. gayi* (Guichenot, 1848), Cortez hake *M. hernandezi* (Mathews, 1985), Argentine hake *M. hubbsi* (Marini, 1933), European hake *M. merluccius* (Linnaeus, 1758), deep-water hake *M. paradoxus* (Franca, 1960), Patagonian hake *M. patagonicus* (Lloris and

Matallanas, 2003), Benguela hake *M. polli* (Cadenat, 1950), Pacific hake (north Pacific hake, or Pacific whiting) *M. productus* (Ayres, 1855) and Senegalese hake *M. senegalensis* (Cadenat, 1950) (Lloris *et al.*, 2005).

The two sympatric hake species that commonly occur in the Benguela region, *M. capensis* and *M. paradoxus*, have distinct genetic profiles (Grant *et al.*, 1988). However, morphologically they are very similar, differing in the number of vertebrae (Franca, 1960), pigmentation of the gill rakers (van Eck, 1969), gill arch morphology (Bentz, 1976), otolith structure and morphology (Mombeck, 1969; Botha, 1971), length of the pectoral fins (Inada, 1981), retinal structure (Mas-Riera, 1991) and sometimes colour of the anal fin (Gordoa *et al.*, 1995). Because these morphological features are not easily detectable and because the species overlap at certain depths, commercial landings have not been separated by species. In addition, *M paradoxus* was not recognised as a separate species until long after exploitation began, with *M. capensis* initially dominating commercial catches. For this reason, the two species have been assessed and managed as a single stock in both South Africa and Namibia since total allowable catches (TACs) were set in the early 1980s (Botha, 1985). They are currently still managed as one unit in Namibia (Kirchner, 2010).

1.2 Ecological and economic importance of hake in the northern Benguela

M. capensis provide the main food source for fur seals in southern Namibia (Mecenero *et al.*, 2006a). They provide a large part of the diet of monk *Lophius spp.* (Gordoa and Macpherson, 1990), another commercially important fish stock in Namibia, and of other demersal fish, sharks, seabirds, whales and dolphins (Jarre *et al.*, 1998; Shannon and Jarre, 1999; Heymans *et al.*, 2004), and other large pelagic predatory fish such as snoek (McQueen and Griffiths, 2004). They are also fed on by larger conspecifics, often as the main food source (Chlapowski, 1977; Roel and Macpherson, 1988; Macpherson and Gordoa, 1994; Punt and Leslie, 1995; Pillar and Barange, 1995). Both hake species also feed on *M. paradoxus*, krill, crustaceans, cephalopods, lightfish, lanternfish, horse mackerel, round herring, anchovy, sardine, bearded goby *Sufflogobius bibarbatus* and other demersal and pelagic fish species. Their diet changes gradually from a high proportion of krill/crustaceans to a high proportion of

fish as they grow older (Botha, 1980; Macpherson and Roel, 1987; Roel and Macpherson, 1988; Punt and Leslie, 1992; 1995; Traut, 1996; Pillar and Barange, 1997; Shannon *et al.*, 2001).

The trophic level of *M. capensis* is estimated to be from 3.97 to 4.45 for small and large *M. capensis* respectively, and 4.11 for large *M. paradoxus* (Roux and Shannon, 2004; Watermeyer *et al.*, 2008). This puts them at a high trophic level compared to other species in the northern Benguela, a similar level to large pelagic fish, seals and seabirds (Shannon and Jarre, 1999).

Hakes have constituted the most valuable demersal resource in the region since 1965 (Crawford *et al.*, 1987). The southern African hake fishery was the largest hake-based fishery in the world in the 1980s (Botha, 1985). The hake fishery is the major source of employment in the fisheries sector in Namibia (van der Westhuizen, 2001), employing 6 334 Namibians onshore and 3 159 offshore in 2003 (Anon., 2004). The sector's contribution to the GDP was worth N$2.9 billion in 2003 (Anon, 2004) and N$2.5 billion in export earnings in 2005 (Weidlich, 2006). The fisheries sector overall contributes around 5.0 % to the total GDP, fluctuating between 4.6 and 7.1 % since 2001, and is Namibia's second largest contributor to the GDP after the mining industry (MFMR, 2003; Investment House Namibia, 2011). The hake fishery contributes around 30 % of the catches (MFMR, 2003), and half of all fishery products in Namibia. This makes the hake fishery Namibia's most valuable commercial fishery (MFMR, 2003; FAO, 2007).

M. capensis are also caught as bycatch in the main fisheries in Namibia: the midwater trawl fishery (targeting horse mackerel *Trachurus capensis* in Namibia), the monk-directed fishery and the orange roughy *Hoplostethus atlanticus* fishery. Bycatch of the hake-directed longline fishery, as well as the trawl fishery in some cases, includes seabirds such as albatrosses, petrels and the Cape gannet *Morus capensis*, threatened or endemic shark species such as blue and mako sharks, the puffadder shyshark *Haploblepharus edwardsii*, the St. Joseph's shark *Callorhinchus capensis* and the whitespotted smooth-hound *Mustelus palumbes*, skates such as the slime skate *Raja pullopunctata*, the munchkin skate *R. caudaspinosa* and the yellowspot skate *R. wallacai*, and dolphin species. Bycatch of the hake-directed trawl fishery also

includes sole *Austroglossus capensis,* Cape fur seals, rat tails, crustaceans, other sharks and skates (Cochrane *et al.*, 2007).

A good knowledge of the life history traits and population dynamics of hake is thus of significance as it directly and indirectly affects the major fisheries and the whole northern Benguela ecosystem.

1.3 History of exploitation and management of hakes in Namibia

Exploitation of hakes in Namibia started in 1964 with catches peaking at 800 000 tonnes in 1972, with open access fishing on hake by fleets mainly from Cuba, Israel, Italy, Japan, Poland, Portugal, South Africa, Spain and the USSR resulting in an initial drastic decline in the stock biomass (Gordoa *et al.*, 1995). From 1976 the fishery was controlled by the International Commission for Southeast Atlantic Fisheries (ICSEAF), implementing a legal mesh size of 110 mm and member country quotas or TAC limits. Despite this, the stock biomass continued to decline. In 1980 the catch had declined to only 170 000 tonnes with the catch never reaching the TAC. Between 1981 and 1989 catches ranged between 300 000 and 400 000 tonnes, improving mainly due to strong year-classes of 1982 and 1983 (van der Westhuizen, 2001).

In 1990 Namibia became independent and the new Ministry of Fisheries and Marine Resources (MFMR) took over management of the fishery on an overfished and heavily depleted resource (Payne and Punt, 1995). Measures that were taken immediately were closure of fishing to all foreign vessels and enforcement of a 200-mile exclusive economic zone (EEZ). In December 1991 the White Paper of MFMR was set out (MFMR, 1991), and this was enacted in the new Sea Fisheries Act by 1992 (MFMR, 1992), updated later with the Marine Resources Act in 2000 (MFMR, 2000), and Namibia's Marine Resources Policy in 2004 (MFMR, 2004).

The hake fleet consists of bottom trawling by sea-frozen / factory operation, and by wetfish operation, as well as a component of longline vessels (~ 8 % of the TAC). Since 1992, the structure of the fleet has changed with a higher proportion of the TAC allocated to wetfish trawlers (~ 80 %, Elago, 2002) to add value to the product and increase jobs in Namibia (Oelofsen, 1999).

When MFMR took over management of the Namibian fisheries, the main aim was to rebuild the hake stocks. Regulations put into place to achieve this were TACs (immediately reducing the TAC to 60 000 tonnes in 1990 and 1991), limiting entry licences, enforcing a minimum mesh size of 110 mm, enforcing catch and discard monitoring, and establishing an observer programme which has allowed at-sea sampling of the catch since 1997 (van der Westhuizen, 2001). A further regulation put into place was a 200-m-depth-restriction (no fishing allowed shallower than the 200 m isobath). In the 2006/2007 season this was extended to a 300-m-depth-restriction for wetfish vessels, a 350-m-depth-restriction for freezer vessels, and closure of the hake-directed fishery in the month of October (Weidlich, 2006).

Since 1991, between 130 000 and 200 000 tonnes of hake have been caught annually (van der Westhuizen, 2001; MFMR, 2003; Weidlich, 2006). The resource is currently assessed as "severely depleted" with the spawning stock biomass at about 80 % of values in 1990 (Kirchner, 2010).

1.4 Assessment and management

In theory, the setting of the TAC in Namibia is based on an operational management procedure (OMP) including the restriction that the TAC cannot be reduced or increased by more than 10 % each year. However, in practice, this is not always enforced (Garcia Rey and Grobler, 2011). The OMP is coupled to a stock assessment based on an age-structured production model (ASPM) (e.g. Butterworth and Geromont, 2001), used since 1998. Input data into the model consist of catch data, commercial catch-per-unit effort (CPUE) indices, a survey biomass index, and proportions of catch-at-age from survey and commercial catches, and mean weight-at-age calculated from survey measurements. The survey index is taken from bottom trawl swept-area abundance surveys that have been conducted along the Namibian coast since 1991, first two to three times per year, and since 1997 once per year in summer (January–February) (Burmeister, 2001; Kainge *et al.*, 2006). The ASPM combines all input data as well as input parameters (growth and mortality parameters) from both species, treating them as a single species (Butterworth and Rademeyer, 2005).

The ASPM relies strongly on annual catch-at-age data to estimate the current biomass and the overall state of the stock. Estimable parameters in the model are the steepness parameter (*h*) on which the stock-recruitment relationship is based, annual recruitment fluctuations, the natural mortality parameter (*M*), and the age-specific gear selectivity functions (Butterworth and Rademeyer, 2005; Kirchner, 2010). All of these rely strongly on the numbers-at age information input into the ASPM. For the latest stock assessment in Namibia (March 2011), only ten (out of 20 possible, 1991-2010) annual age-length keys (ALKs), used to calculate catch-at-age data, were available (Kirchner *et al.*, 2011). Both the species-aggregated model and the lack of age data have been repeatedly identified as serious shortcomings, especially since there is pressure to conduct species-specific assessments in the entire Benguela region, and to manage hake fisheries in South Africa and Namibia together on the assumption of fishing on shared stocks (Anon., 2006; Smith *et al.*, 2011).

M. capensis has always been the more abundant species off Namibia (Gordoa and Macpherson, 1989; Burmeister, 2001; Kainge *et al.*, 2006), but *M. paradoxus* usually makes up between 52 and 71 % of the Namibian commercial catches (Johnsen and Kathena, 2011). Considering the depth-related size distribution of the two species, the 200-m-depth restriction essentially protects juvenile *M. capensis*. Yet the Namibian *M. capensis* stock is not recovering (Butterworth and Rademeyer, 2005; Kirchner, 2010). Causes for this could be related to predation of *M. capensis* by seals or other large predators (Punt and Leslie, 1995; Mecenero *et al.*, 2006a) because of the ecosystem degradation due to the very low abundance of small pelagic fish present in the northern Benguela ecosystem since the mid-1990s (Heymans *et al.*, 2004; Roux, 2004; van der Lingen *et al.*, 2006; Ludynia *et al.*, 2010). Lack of recovery could also be related to cannibalism of juvenile *M. capensis* by larger conspecifics (Chlapowski, 1977; Roel and Macpherson, 1988; Pillar and Barange, 1995), environmental influences on distribution (Mas-Riera *et al.*, 1990; Macpherson *et al.*, 1991) or environmental influences on recruitment (Voges *et al.*, 2002). Further explanation could be the negative impacts of fishing mortality which is strongly dependent on the size of fish harvested. Since the fishery has been restricted to beyond 200 m bottom depth since 1990, the target has been large *M. capensis*, and *M. paradoxus* of all sizes, causing proportionately greater reduction in recruitment of *M. capensis* (Gordoa and Duarte, 1991). For political reasons, TACs have been often set higher than advised by

stock-assessment (Kirchner, 2010; Garcia Rey and Grobler, 2011) and many catches during pre-independence could have gone unreported (MRAG, 2005).

Finding support for the different hypotheses of why *M. capensis* is not recovering despite the bulk of the catches coming from the *M. paradoxus* resource, is confounded by the fact that stocks are not separated in the assessment model, and so species-specific abundance and productivity are poorly understood. Also, because of the limited amount of age data available, the life history characteristics and how these may have changed over time are still very poorly understood.

1.5 Distribution

Distribution of *M. capensis* and *M. paradoxus* in the south-east Atlantic covers the area from Baía de Farto on the west coast of Angola at about 12ºS, 14°E (Cabo, 1965) to Port Elizabeth on the east coast of South Africa at about 35ºS, 25°E with a virtually continuous distribution (Van Eck, 1969; Botha, 1985; Payne, 1989; Gordoa *et al.*, 1995; Payne and Punt, 1995). The biomass of *M. capensis* is larger north of 27ºS (off Namibia) and *M. paradoxus* is more abundant south of 27ºS (southern Namibia and South African West coast) (Botha, 1985; Payne, 1989; Gordoa *et al.*, 1995; Burmeister, 2001). The distribution of the two species is depth-dependent. *M. capensis* occurs from 100 m to generally not deeper than 400 m bottom depth. *M. paradoxus* extends from 300 to 500 m bottom depth (Kawahara and Nagai, 1980; Botha, 1985; Mas-Riera *et al.*, 1990; Gordoa and Duarte, 1991; Burmeister, 2001), but also may occur as deep as 1000 m bottom depth (Mas-Riera, 1991; Kathena, 2004). The depth distribution of the two species is reflected in their retinal structure with *M. paradoxus* showing a more developed scotopic system with higher sensitivity and visual acuity adapted to dim light of their deep-water environment (Mas-Riera, 1991). South of 25°S the distribution of *M. paradoxus* can also extend to areas shallower than 200 m bottom depth (Macpherson *et al.*, 1985).

For both hake species in the northern Benguela fish lengths show a general tendency to increase with depth (Botha, 1985; Gordoa and Macpherson, 1989; Gordoa and Duarte, 1991; Millar, 2000; Burmeister, 2001). This phenomenon has also been observed in other hake species (e.g. Relini *et al.*, 2002; Tserpes *et al.*, 2008). Adult and juvenile

fish of the same species often seem to have different temperature tolerances and so, generally, fish migrate offshore as they grow older. This could be because of expected fast growth rates and thus the need for abundant food supply of young fish in warm water (Macpherson and Duarte, 1991). From the size-dependent depth distribution of *M. capensis* and *M. paradoxus* it follows that large *M. capensis* overlap in distribution with small / juvenile *M. paradoxus* and that there is little overlap of large adult fish of the two species (Botha, 1985; Gordoa and Macpherson, 1989; Burmeister, 2001; 2005).

The north-south and depth-distribution differences between the two species could depend on the width of the continental shelf and the steepness of the continental slope (Payne, 1989), or their preferred temperature ranges, listed as 4–12°C for *M. capensis* and 4–8°C for *M. paradoxus* (Inada, 1981). The north-south and depth-distribution differences between the two species as well as differences between juveniles and adults could result from low-oxygen tolerance levels with *M. paradoxus* preferring more oxygenated water. Oxygen levels increase from north to south in Namibia. Adults prefer more oxygenated water than juveniles and dissolved oxygen levels generally increase with bottom depth (Roel and Bailey, 1987; Mas-Riera *et al.*, 1990; Maree, 1999).

The large overlap in latitudinal distribution and the separation in depth distribution are unique to the hakes in southern Africa. Hake species elsewhere are separated in longitudinal ranges rather than depth ranges (Fig. 1.1; Table 1.2; Lloris *et al.*, 2005).

Table 1.2 The 13 *Merluccius* species of the world, with their sub-species, and their longitudinal and depth distributions. The number is the number used on the map (Figure 1.1) – after Lloris *et al.* (2005).

	Species	**Area**	**Longitudinal range**	**Depth range**
1	Silver hake *M. bilinearis*	North-west Atlantic, North American (Canada and USA) continental shelf and slope	52ºN – 35°N (N & S population)	55–914 m
2	Offshore silver hake *M. albidus*	Western Atlantic, East coast of the USA Georges Bank, Long Island, Virginia, Florida, the Gulf of Mexico & Caribbean Sea to Suriname & French Guiana	40°N – 5°N	160–640 m (92–1170 m)
3	North Pacific hake *M. productus*	Eastern Pacific along Canadian & US West coasts & part of Gulf of California, Mexico	50°N – 16°N	migrates north & shallower in winter
4	Panama hake *M. angustimanus*	Eastern Pacific, Gulf of California to Columbia	27°N – 2°N	80–500 m & open sea
5	South Pacific hake Peruvian sub-species *M. gayi peruanus*	South-eastern Pacific, South America – Peru	4°40′S – 13°56′S	100–500 m
6	South Pacific hake Chilean subspecies *M. gayi gayi*	South-eastern Pacific, South America – Chile	26°21′S – 45°10′S	Summer: 10–50 Autumn: 300 m Winter–spring: 170–190 m
7	Argentine hake *M. hubbsi*	South-western Atlantic, South & East Argentine coast	21°30′S (summer & autumn) – 49°S	Continental shelf; deeper in summer– autumn
8	Southern hake New Zealand subspecies *M. australis australis*	New Zealand	40°S – 55°S	500–900 m (400–450 m on Chatham Rise)
9	Southern hake Patagonian subspecies *M. australis polylepis*	South-eastern Pacific slope (Chile) to south-western Atlantic slope (Argentina)	40°S – 57°S (Sub-Antarctic)	Not much known
10	*M. patagonicus*	South-west Atlantic, Argentinean coast (Comodoro Rivadavia)	45°S – 49°S	95 m
11	European hake *M. merluccius merluccius*	European Atlantic, Bay of Biscay, Portugal, north of Morocco & southwestern Mediterranean	72ºN – 20ºN	30–1075 m
12	European hake *M. merluccius smiridus*	North-western Mediterranean continental shelf and slope	45ºN – 34ºN	50–370 m
13	Senegalese hake *M. senegalensis*	Eastern Atlantic, North African west coast, Morocco to Senegal	32°32′N – 12°25′N	18–800 m
14	Benguela hake *M. polli polli*	Eastern Atlantic, Port Gentil, Angola to north of Namibia	11º26′S – 18º30′S	50–550 m
15	Benguela hake *M. polli cadenati*	Eastern Atlantic, Mauritania, Senegal, Gambia, Guinea-Bissau, Sierra Leone & Liberia	22º30′N – 5º07′S – 500 km break then to 0º15′S	132–910 m
16	Shallow-water Cape hake *M. capensis*	South-east Atlantic, Baihia de Farto, Angolan west coast to Port Elizabeth, South African east coast	12º30′S – 35ºS (25ºE)	100–400 m
17	Deep-water hake *M. paradoxus*	South-east Atlantic, Cape Frio, Namibian west coast to East London, South African east coast. Also found on Madagascar Ridge	18ºS – 35ºS, 25ºE (33°S–44°E Madagascar)	300–500 m

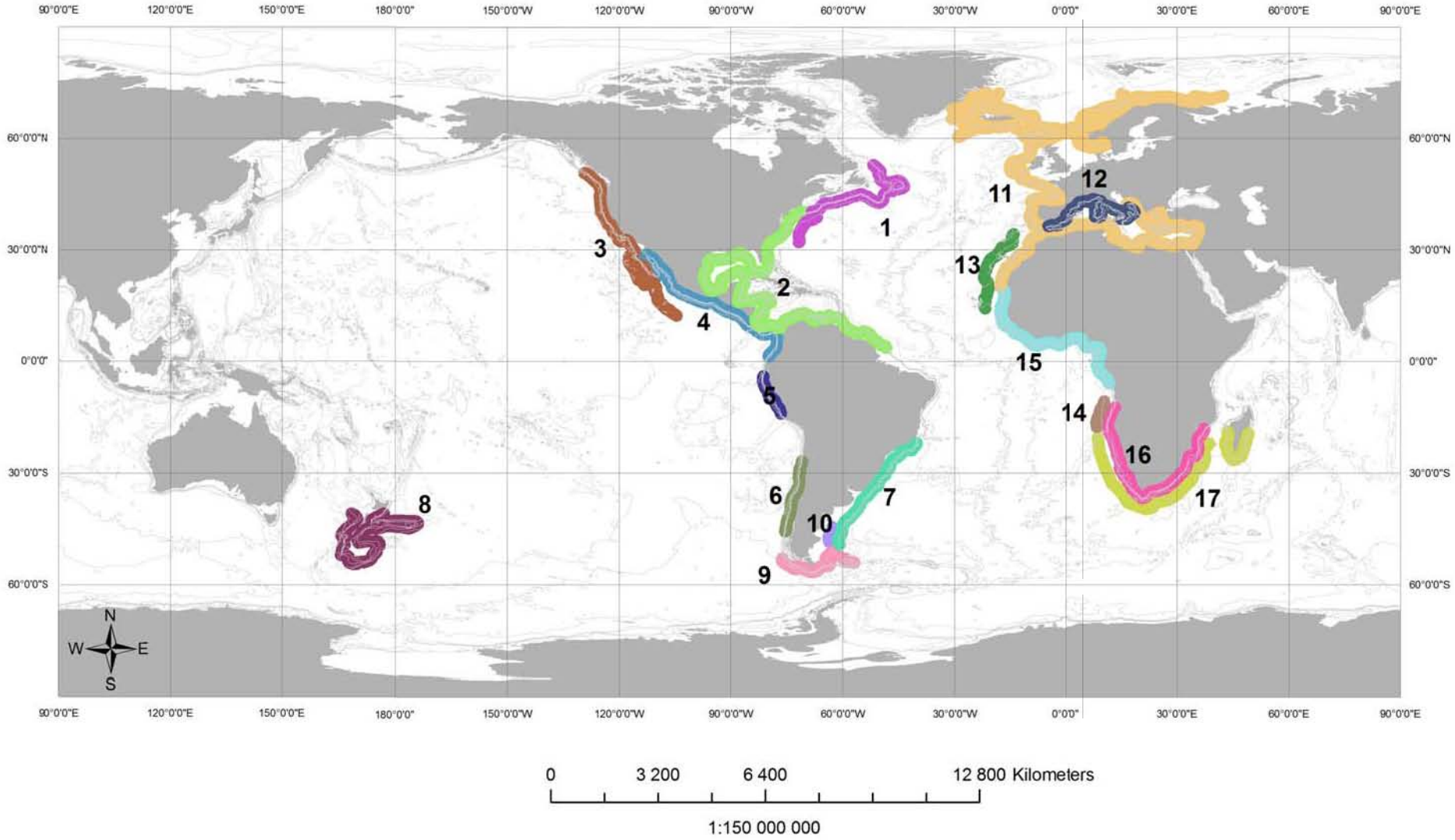

Figure 1.1 Map of the world showing the distributions of the 17 *Merluccius* species listed in Table 1.1 – after Lloris *et al.* (2005).

1.6 Alongshore migration and spawning locations

The Cape hakes exhibit some form of alongshore migration over their life-span, with mean length of both *M. capensis* and *M. paradoxus* generally increasing from northern to southern Namibia (Burmeister, 2001). In ICSEAF studies, *M. capensis* was noted to occur in large densities in northern Namibia close to the Angolan border (17–19ºS) in summer and autumn and in large densities around the Walvis Bay area (22–24ºS) in winter and spring (Anon. 1986, cited by Grant *et al.*, 1987). These migrations were partially attributed to spawning behaviour, hypothesized to coincide with the peak spawning seasons (February–March and September–December) (Botha, 1973; 1980).

Alongshore migrations also seemed to coincide with the southward movement of warm Angolan tropical water or occasional *Benguela Niño* events, the intrusion of warm water and poleward migration of the Angola-Benguela front (Inada, 1981; Shannon *et al.*, 1986; Gammelsrød *et al.*, 1998), or *M. paradoxus* migrating northwards when hypoxic bottom-waters occurred around 27ºS (Mas-Riera *et al.*, 1990). However, no recent north-south temporal shifts in catchability by the fishing fleet have been observed off Namibia, indicating that no seasonal north-south migrations occurred (Gordoa *et al.*, 2000).

Spawning of *M. capensis* in the northern Benguela has been located in the areas listed in Table 1.3. In the southern Benguela, the spawning areas of *M. capensis* seem to extend from 34ºS to 36ºS (Table Bay to the Agulhas Bank) and east of 20ºE on the south coast (Assorov and Berenbeim, 1983; Hutchings *et al.*, 2002).

Table 1.3 Spawning areas and periods of *M. capensis* in the northern Benguela by previous authors.

	Reference	Area	Months	Evidence
1	O'Toole (1976) & O'Toole (1978)	22–24º40'S 19º20'S & Walvis Bay (23–24º30'S)	Nov–Dec Jan–Mar	Presence of most larvae
2	Assorov and Berenbeim (1983)	Walvis Bay (22ºS–25ºS) Cape Frio (20°S–21º30`S)	Spring (Oct–Dec) All seasons, peak in winter–spring (July–Oct)	Presence of mature fish stages IV–V
3	Olivar *et al.* (1988)	20–21°S and 22–23°S 18–23°S	November August	Presence of eggs
4	Olivar and Shelton (1993)	Most of the Namibian coast 18°S–27°S		Presence of larvae
5	Kainge *et al.* (2007)	20ºS, 22ºS–24ºS & around 28ºS	Peak in September (not matched with areas)	High density of adults with gonadosomatic index >1.3 %

Some authors have stated *M. paradoxus* spawns in the same latitudes in Namibia as *M. capensis*, but in deeper water (Porebski, 1976), or around 23ºS (Walvis Bay), and during a warmer season than *M. capensis* (Assorov and Berenbeim, 1983). Other authors believe that there is no indication that *M. paradoxus* spawns in Namibia (Gordoa *et al.*, 1995; Kainge *et al.*, 2007). In South Africa, *M. paradoxus* largely spawns on the Agulhas Bank and between Cape Point and Cape Columbine (Hutchings *et al.*, 2002; von der Heyden *et al.*, 2007b). Burmeister (2005) hypothesized that *M. paradoxus* is shared between Namibia and South Africa, with only one spawning area on the Agulhas Bank and nursery areas off the South African west coast and southern Namibia. However, the evidence for and extent of this extensive long-shore migration of *M. paradoxus* are not clear, since no area-specific length or age distributions have been presented. Also, recently genetic differentiation between Namibian and South African *M. paradoxus* stocks has been identified. However, no stock structure was detected for *M. capensis* (von der Heyden *et al.*, 2007a).

Stock structure, spawning behaviour and alongshore migrations of the two species of southern African hakes are not well understood, and are not as distinct and as well described as, for example, the distribution, spawning and migration cycles described for Pacific hake *M. productus* (Bailey *et al.*, 1982). Pacific hake larvae are found up to 300 nautical-miles offshore between 35 and 26ºN in winter (December–February), being transported northwards between April and August, where they form small inshore aggregations all the way up to 49ºN where they appear as adult fish. By July/August large adults move to the outer continental shelf and then migrate offshore and southwards again to spawn in winter (Bailey *et al.*, 1982). Tagging studies on Chilean hake *M. gayi gayi* showed evidence of migration over 5º of latitude, but no population seasonal pattern has been tested (Saetersdal and Villegas, 1968; Payá Contreras, 2002). Distinct nursery areas have been identified for European hake *M. merluccius* in the Bay of Biscay, Celtic Sea (Kacher and Amara, 2005) and Mediterranean (Maynou *et al.*, 2003). However, migration cycles are also not distinct for this species (Lloris *et al.*, 2005). Peruvian hake *M. gayi peruanus* integrate the anoxic conditions of the continental shelf in their life cycle. Adults are typically found at 5°S and northwards, and juveniles south of this area, which means they undergo alongshore migrations throughout their life (Guevara-Carrasco and Lleonart, 2008).

1.7 Inshore-offshore migration and spawning behaviour

Seasonal inshore-offshore movements of hakes along the South African coast have been noted in the southern Benguela. For example, *M. paradoxus* occurred furthest offshore in winter, and inshore and further south in summer (Millar, 2000). *M. paradoxus* could move offshore to spawn.

Namibian (northern Benguela) *M. capensis*, on the other hand, could move into shallow waters (< 200 m bottom depth) to spawn, with peak spawning occurring in shallowest waters in spring, indicated by the distribution of eggs and larvae (O'Toole, 1978; Olivar *et al.*, 1988; Olivar, 1990; Sundby *et al.*, 2001). Further evidence for inshore and off-the-bottom movement of hake for spawning has been the decrease in catchability of *M. capensis* in the hake-directed fishery between April and September, with a peak in October, while *M. capensis* bycatch in the horse mackerel midwater trawl catches shallower than 200 m bottom depth peaked in October (Gordoa *et al.*, 2006). Deep offshore spawning of *M. capensis* also occurs (Sundby *et al.*, 2001).

Inshore-offshore migration could thus be related to spawning activities. However, it was found that immature fish also show inshore-offshore migrations at certain times, the most likely explanation for this being that fish respond to environmental conditions, following the thermocline or the pelagic production cycle offshore in winter, mainly in South Africa (Shannon, 1986; Millar, 2000; Gordoa *et al.*, 2000). In Namibia, the mid-shelf is defined by a wind-driven upwelling cycle with high inter-annual and seasonal variability (Boyer *et al.*, 2000; Bartholomae and van der Plas, 2007), as well as a poleward undercurrent associated with the advection of anoxic and hypoxic water on the shelf (de Decker, 1970; Salat *et al.*, 1992; Mohrholz *et al.*, 2008). The minimum oxygen tolerance level of 0.5 ml l^{-1} of *M. capensis* (Woodhead *et al.*, 1998; Bartholomae and van der Plas, 2007) and the presence of low oxygen water on the shelf affect the inshore-offshore movement of *M. capensis* over the Namibian shelf (Mas-Riera *et al.*, 1990; Woodhead *et al.*, 1998). Extreme offshore displacement of juvenile fish due to pronounced low oxygen levels on the shelf occurred, for example, in April 1994 (Hamukuaya *et al.*, 1998). Seasonal patterns of inshore-offshore migrations of *M. capensis* in the northern Benguela are not distinct (Botha, 1973; 1980; Gordoa and Macpherson, 1989; Gordoa *et al.*, 2000; Burmeister, 2001).

Apart from moving inshore to spawn, *M. capensis* are also thought to be meso-pelagic spawners, moving upwards above the low-oxygen layer in the water column to spawn (Botha, 1973; Iilende *et al.*, 2001; Sundby *et al.*, 2001). Their eggs have been found over a range of 100–400 m bottom depths, and at 30–150 m depth in the water column in the northern Benguela (Olivar, 1990; Olivar and Shelton, 1993; Sundby *et al.*, 2001). Sundby *et al.* (2001) showed eggs and larvae to be transported southward and shoreward by a subsurface upwelling current, and O'Toole (1978) observed peak abundance of larvae during a time when warm water pushed in that direction.

In the absence of growth data, size distribution data recorded in different seasons have often been misinterpreted as 'migration'. For example, Pillar and Barange (1997) presented length distributions collected from winter and summer surveys for several years (1984–1990), clearly illustrating that *M. capensis* and *M. paradoxus* caught in winter were smaller than those caught in the same area in summer. The authors concluded that this reflects a shoreward shift of the hake stock in summer. However, in the figures, length-frequency distributions from the winter of one year are compared with those of the following summer, i.e. fish were six months older and would have grown by at least 4 cm by the following summer (Morales-Nin, 1991). The 'larger fish' had not shifted shoreward, but the same cohort of fish had undergone growth and now consisted of larger fish. Age and growth information is thus needed to understand the biology of a species and to interpret length frequency distributions correctly.

1.8 Environmental effects and recruitment

The northern Benguela's upwelling system is one of the four major eastern boundary upwelling systems in the world and has been well described by several authors (e.g. Shannon, 1985; 1986; Lutjeharms and Valentine, 1987). Apart from wind-driven upwelling, hypoxic conditions also define the Namibian mid-shelf waters (de Decker, 1970; Salat *et al.*, 1992; Mohrholz *et al.*, 2008).

CPUE of hake has been shown to be dependent on environmental conditions such as sea surface temperature, surface wind and oxygen concentrations. This is explained by hake moving off the bottom, or further offshore, during certain conditions, reducing their availability to bottom trawls, and thus reducing catch rates in those periods (Roel

and Bailey, 1987; Gordoa and Hightower, 1991; Macpherson *et al.*, 1991; Gordoa *et al.*, 2000; Johnsen and Iilende, 2007). Roel and Bailey (1987), Gordoa and Hightower (1991) and Gordoa *et al.* (2000) observed a positive correlation with SST and CPUE of age groups 4 years and older, the main component of the fishery, but a negative correlation with SST and CPUE of age groups 0 and 1 (Roel and Bailey, 1987). The highest CPUE is usually observed in the middle of the day (Johnsen and Iilende, 2007). During warm-water periods or years, (older) hake shoal closer to the bottom (where it is colder) making them more susceptible to bottom trawling and increasing their CPUE, or estimated biomass, as demersal fish in the Benguela benefit from cooler conditions (Shannon *et al.*, 1988). This could result in poor recruitment in warm years (Macpherson *et al.*, 1991).

Voges *et al.* (2002) concluded that one warm-water index and two upwelling indices have significant positive influences on recruitment strength of *M. capensis*. Recruitment strength was calculated from survey length-frequency distribution estimates and age-length keys. None of the relationships were linear, and so "positive" correlations could be coincidental or have indirect effects on recruitment (such as by affecting the catchability as discussed above, or food availability and cannibalism as discussed below). More recently, Roux (2004; 2006) presented a method of calculating *M. capensis* year-class strength (a recruitment index) from the percentage of hake otoliths retrieved in winter samples of fur seal scats in southern Namibia (scaled by the survey estimate of recruitment) between March and September. He showed that recruitment strength is dependent on the strength of the previous year's cohort, suggesting that cannibalism of young hake by one year older conspecifics is the primary driver of *M. capensis* recruitment. Warmer water can lead to increased cannibalism of young hake (Shannon *et al.*, 1988), and so may have an indirect effect on recruitment only.

General recruitment hypotheses done mostly on small pelagic fish state that the timing of availability of small (first-feeding) larvae and their food availability determines the strength of a year class (e.g. Hjort, 1914; Cushing, 1975). This has not been investigated for *M. capensis* in the northern Benguela.

From the early 1990s environmental effects appear to have had a greater (direct or indirect) influence on biomass of species and their migration and recruitment, and the ecosystem in the northern Benguela than before that time (Watermeyer *et al.*, 2008).

To understand the response of a fish species to their environment, it is important to understand their life history strategies and tactics (Table 1.1). In order to study life history strategies and tactics, it is important to obtain age and growth information for a fish stock.

1.9 Age determination and its application

The basic method for annual fish age determination using otoliths consists of reading concentric opaque or translucent (hyaline) zones (bands) around the core of the sagittal otolith. Each zone-pair (opaque and translucent) is assumed to form once per year. The method of interpretation has been well described for hakes, e.g. silver hake (Nichy, 1969; Hunt, 1980), Pacific hake (Beamish, 1979), southern hake (Horn, 1997), Argentine hake (Renzi and Pérez, 1992) and European hake (Hickling, 1933). The method is important because of its application to stock assessments and other life history-related studies on hakes (e.g. Helser and Broziak, 1998; Guevara-Carrasco and Lleonart, 2008; Godinho *et al.*, 2001; Piñeiro and Saínza, 2003). Age information is important in life history studies, stock assessments and fisheries management, and the lack of age data is possibly the main reason why many questions on hakes remain unanswered. Surprisingly few age or growth studies have been conducted on the hakes in southern Africa. Growth has been described for both species combined (Roux 1947; Botha, 1970) and each hake species separately, first described by Botha (1971). It was shown that *M. capensis* grow about 6 cm (4–10 cm) per year from 4 to 11 years and females usually grow faster than males (Botha, 1971; Macpherson, 1976; Pschenichnii, 1976; Pozo Arteaga, 1976; Preñski, 1978; Morales and Payne, 1985; Morales-Nin, 1991; Punt and Leslie, 1991). *M. capensis* usually grow faster and mature younger than *M. paradoxus* (Mombeck, 1969; Chlapowski, 1974; Botha, 1986).

Growth rates and mean lengths-at-age in other hake species are also variable between males and females (Piñeiro and Saínza, 2003) and can be variable between age groups (generally decreasing from larval to juvenile stage and from young to old, Godinho *et*

al., 2001; Piñeiro *et al.*, 2008), between seasons (Morales-Nin and Moranta, 2004; Belcari *et al.*, 2006; Piñeiro *et al.*, 2008), between reared and wild hakes (Arneri and Morales-Nin, 2000; Morales-Nin *et al.*, 2005), between areas (Piñeiro and Saínza, 2003) and between years (Piñeiro *et al.*, 2008; Otxotorena *et al.*, 2010). Annual growth variability has also been observed in *M. capensis* and *M. paradoxus* (Wilhelm *et al.*, 2007).

The "whole otolith" method of age interpretation is used for *M. capensis* and *M. paradoxus*. This method and its criteria for identifying the first and other annuli have been described in photographic guides (ICSEAF, 1983; Wysokiński, 1983; Morales and Payne, 1985). More recently, the criteria have been revisited during several age determination workshops in the region (BENEFIT, 2004; 2005) and have been applied to acquire routine age data for current use in hake stock assessments in Namibia (Wilhelm *et al.*, 2007; Kirchner, 2010).

1.10 Hake age validation

Recently, de Pontual *et al.* (2006) and Piñeiro *et al.* (2007) used otoliths of oxytetracycline-marked and tagged European hake, showing more than one zone pair being formed per year, invalidating the previously-used age determination criteria and growth rate calculations. However, no alternative macrostructure analysis has been proposed since then for interpreting European hake otoliths for age data used for stock assessment purposes. Very similar zone formation patterns have subsequently been observed on Argentine hake otoliths (Goicochea *et al.*, 2010).

In the northern Benguela, validation of the annual occurrence of translucent zones on otoliths has been attempted only for the first annulus of Namibian *M. capensis* (Gordoa *et al.*, 2001), showing that the first translucent zone occurs earlier than one year of age of *M. capensis*. Indirect validation was attempted on South African *M. capensis* and *M. paradoxus* by Botha (1971), showing that translucent zone formation peaks in about September/October (August–November), but the formation of both opaque and translucent zones was recorded in all months of the year.

Interpretation guides on age determination of the two hake species in southern Africa (ICSEAF, 1983; Wysokiñski, 1983; Morales and Payne, 1985) often show conflicting interpretation of similar images. Many interpretation difficulties, especially concerning the first annulus, and thus agreement problems, have been identified during hake otolith reading workshops in the region. Ages assigned to the same fish often differ by 2–3 years, and age validation and description of age determination criteria have been emphasised as a priority for the hakes in the region (BENEFIT, 2004; 2005).

Age validation, guides for otolith interpretation, and investigation of age and growth data of *M. capensis* in the northern Benguela are thus long overdue. This thesis aims to address some of these shortcomings.

1.11 Objectives, hypotheses and thesis structure

M. capensis and *M. paradoxus* have a unique overlap in distributions compared to other hakes. The adults of *M. capensis* and juveniles of *M. paradoxus* thus have a unique interaction through predation (and cannibalism). *M capensis* is of great ecological and economical importance in the Benguela system, but its abundance and causes of non-recovery despite all management measures remains unanswered. Information on life history traits is still lacking. Age data for use in the assessment models is scarce and age validation has not been performed. This study aims to address some of these shortcomings in our knowledge of hake ecology and the responses of *M. capensis* to fishing pressure.

The Cape hakes *M. capensis* and *M. paradoxus* belong to the order Gadiformes. The northern Benguela environment in general is a variable upwelling regime, with *M. capensis*, though meso-pelagic or bottom dwelling, living in a more variable environment than *M. paradoxus*. *M. capensis* should therefore be on the more K-selected side of the scale of life-history strategies, but is still expected to in general resemble the order Gadiformes. This order in general comprises species that have a K-selected life history strategy (compared to other orders), are large but short-lived relative to their size, and mature early relative to their size. However, life history strategies are rarely studied in Namibian *M. capensis* because of the lack of age information and age validation studies available for hakes in the northern Benguela.

The overall objective of this thesis is to understand the life history traits and tactics pertaining to *M. capensis* in the northern Benguela. More specifically, the four overall objectives are (1) to calculate growth rates of *M. capensis* using available data other than those obtained from age information on otoliths (2) to validate translucent zone formation on otoliths using available information and to describe a new age determination method for *M. capensis* (3) to investigate the causes of translucent zone formation on *M. capensis* otoliths and (4) to test the implications of different growth rates for fisheries management.

The growth rates of small *M. capensis* are calculated in Chapter 2 (Objective 1), using the otolith data collected from regular seal scat sampling along the Namibian coast. Based on preliminary work (Roux, 2004; 2006), it is expected that *M. capensis* juveniles grow faster than previously thought. Hatchdate ranges, separated for different cohorts (1993–2008) are also estimated based on these otolith data and compared with recruitment strength to test the hypotheses that (1) hatchdates / spawning peaks occur once a year and (2) recruitment strength is dependent on the timing of hatchdates.

The hypothesis underlying traditional annual otolith age determination and previous studies on *M. capensis* is that translucent zones are formed once per annum. In Chapter 3, this hypothesis is tested for the first three translucent zones on the otoliths of young (< 21-month-old) *M. capensis* (Objective 2). Seasonal changes are assessed in the proportions of the first three translucent zones present in otoliths collected from monthly seal scat samples of selected strong year-classes 1996, 1998, 2002, 2005 and 2006.

In Chapter 4, the data from Chapters 2 and 3 are supplemented with survey and commercial length-frequency distributions (1990–2009) to calculate growth rates for older fish (Objective 1). The results from age readings on otoliths of *M. capensis* are compared with observed modes in the length frequency distributions from research surveys, and diameters at each translucent zone are measured with the aim of deriving a guide for routine age determination methods in Namibia (Objective 2).

The timing and causes of translucent zone formation are investigated in Chapters 5 and 6 (Objective 3) testing the following: Translucent zone formation is not associated with "demersal settlement", but possibly associated with off-the-shelf or north-south movements of hake. The following null hypothesis is also tested: translucent zone formation is not significantly related to a preceding drop in temperature, cold bottom temperatures, low oxygen concentrations or short daylight duration. In Chapter 5, length-frequency distributions of *M. capensis* from hake biomass surveys are described from different areas and depths along the Namibian coast (1990–2007). These length frequency distributions indicate the alongshore and inshore-offshore migration of hake as they grow older and these are related to their otolith translucent zone formation. Results of Chapter 5 are used to further explore findings from Chapter 2, further investigating Hypotheses 1 and 2 of Chapter 2.

In Chapter 6, statistical models are used to test the hypotheses about the effects of environmental and other factors on translucent zone formation (Objective 3). The timing of translucent zones deposited on *M. capensis* otoliths are related to fish length, cohort, area and depth of occurrence, maturity stage, photoperiod, temperature, temperature change or dissolved oxygen concentration along the Namibian coast using a generalised linear model, environmental data, and a randomization test

Finally, Chapter 7 synthesizes results of Chapters 1 to 6 in the context of their contributions to hake ecology and life history strategies of fish ecology. The implications of fast *M. capensis* growth rates to the stock productivity and recovery from fishing are tested using a simple age-structured production model. It is expected that the more r-selected species (faster-growing *M. capensis*) is able to withstand higher fishing mortality, whereas the more K-selected species (slower growing *M. capensis*) takes longer to recover once fished down.

CHAPTER 2

Growth rates and hatchdates of *Merluccius capensis* in the northern Benguela estimated using otoliths from fur seal scat samples

2.1. Abstract

Scat samples were collected at least once a month at several breeding colonies of Cape fur seals along the Namibian coast. *Merluccius capensis* otoliths were obtained from these samples, identified and measured. Cohorts are easily distinguishable from otolith diameter (OD) measurements converted to fish total length (TL). Growth rates of 2- to 21-month-old hake and hatchdates for each of 17 cohorts were calculated from September 1994 to December 2009. TL at age of *M. capensis* did not differ between areas along the Namibian coast (20°S–28°S), indicating that the hakes likely originated from the same spawning population. Growth rates of these young hake were described by the von Bertalanffy growth function $L_t = 33.6 * \left[1 - e^{-0.651 * (t + 0.00917)}\right]$. The estimated mean hatchdate fell on 23 June with the 95 % confidence intervals of a freely fitted model spanning a period of 36 days between 3 June and 9 July (early to mid-winter). Cohort-specific random effects, obtained by fitting a non-linear random effects model to the data, caused hatchdates to vary by 60 days among cohorts, from 21 May (1998 cohort) to 20 July (2005 cohort). The estimated monthly growth rates in the first 12 months of the life of *M. capensis* were 1.3 cm month $^{-1}$, almost double the growth rates previously estimated and used in the stock assessment model. This may have serious implications for the current view of the state of the stock. These impacts need to be investigated further.

2.2. Introduction

The hake fishery is the most valuable commercial resource in Namibia, contributing around 30 % of the catches (MFMR, 2003) and half of all fishery products in Namibia, valued at N$2.5 billion in export values in 2005 (Weidlich, 2006). In 2005, the Namibian Fisheries sector was worth US$ 372.2 million, 5.2 % of the total Namibian GDP that year (FAO, 2007), and decreasing to 5.0 % in 2009 (Investment House Namibia, 2011). The fisheries sector contributed between 4.6 and 7.1 % to the GDP 2001–2009, as the second largest contributor to the total GDP for most years (Investment House Namibia, 2011). Since 1990, the fishery has been managed in the form of a total allowable catch (TAC) which fluctuated between 130 000 and 200 000 tonnes until 2010 (van der Westhuizen, 2001; MFMR, 2003; Kirchner, 2010). The fishery is made up of two species of Cape hake, the shallow-water Cape hake *Merluccius capensis* and the deepwater hake *M. paradoxus* which differ in their biology and distribution (Gordoa and Duarte, 1991; Gordoa *et al.*, 1995; Burmeister, 2001). Since 1998 the two hake species have been assessed as one stock (combined) using an age-structured production model (ASPM) (e.g. Butterworth and Geromont, 2001). Age data in the form of annual age-length keys, based on age determination of individual fish from otoliths, are fundamental input data into the stock assessment in general and the ASPM in particular. Weight-at-age data derived from growth data also form important inputs. In general, estimates of growth and mortality, usually derived from age-based information, are fundamental for understanding the life history of exploited fish populations and for developing their management plans (Beverton and Holt, 1957a; b; Ricker, 1975; Begg *et al.*, 2005).

Roux (1947) first described the growth of southern African hake (only one species assumed – off Table Bay) by using "otolith-ring counts" (counts of concentric translucent zones on otoliths) and length-frequency distribution (LFD) curves, assuming one translucent zone per year. Botha (1970) described growth of only *M. capensis* ("no distinction made between the sub-species") and only from Cape fishing grounds (between 31 and 35°S), and Botha (1971) described growth of both *paradoxus* and *capensis* (considered sub-species of *Merluccius merluccius* at the time) off Lüderitz in Namibia (26–27°S) and Cape Town in South Africa (29–30°S). He also used otolith ring counts, and attempted to validate formation of translucent zones by

edge analysis (Botha 1971). His growth rates were in agreement with those previously reported; Cape hake was similar to other hakes, being a slow-growing fish with uniform growth at older ages. Pozo Arteaga (1976) used the otolith- and LFD-methods to investigate the growth of *M. capensis* off Cunene (17°S) and Cape Cross (22°S) in Namibia, assuming one otolith ring per annum. Pschenichnii (1976) used otolith ring counts to compare growth rates from different years, noting a decrease in length-at-age from 1965 to 1972 (including data from the above authors and Mombeck, 1971). Preñski (1978) examined LFD data and a sub-sample of otoliths of *M. capensis* from most of Namibia and half of the west coast of South Africa (20–30°S, ICSEAF Divisions 1.4 and 1.5), again assuming one ring per year and finding similar slopes in growth rates to previous authors. Wysokiñski (1982) used analysis of modal lengths of young *M. capensis* (10–30 cm total length) to show that they grow very fast in their first year of life. Morales and Payne (1985) read otoliths and described growth rates of both hake species from some of the Namibian coast and the entire South African west coast (25–37°S, ICSEAF Divisions 1.5–1.6). Morales-Nin (1991) used only LFD analysis (ELEFAN) to describe growth rates of *M. capensis* off Namibia similar to those previously described using otoliths. She also described seasonal differences in growth rates, the slowest being found in autumn (February–April). Punt and Leslie (1991) used otoliths and two different growth models (von Bertalanffy and Schnute) to describe growth of both *M. capensis* and *M. paradoxus* off the west coast of South Africa, with estimated growth rates again very similar to those previously described using otoliths. More recently, an agreed method of age determination from otoliths (BENEFIT, 2004b; 2005) has been used to determine growth rates and age data used in the ASPM for Namibian *M. capensis*, though these have not been published (Voges, 1995; Wilhelm *et al.*, 2007).

An important prerequisite for age-based information obtained from fish otoliths is the validation of the periodicity of their zone / increment formation (Beamish and MacFarlane, 1983). Little attention has been given to age validation of the hakes in southern Africa. In addition, growth rates described from otoliths are very sensitive to reader interpretation (Morales and Payne, 1985). The resulting management advice based on data from different readers may differ substantially (Wilhelm *et al.*, 2008). In the absence of age validation of otoliths, annual growth rates calculated independently (e.g. by length-frequency analysis, regarded as a weak age validation method) should

be used as a comparison for the otolith methods (Kimura *et al.*, 2006). Another age validation method, classified as a relatively strong one by Kimura *et al.* (2006), is the "progression of a known year-class in the length-frequency" (Petersen, 1891). Regular LFD data of juvenile fish needed for this analysis, however, are difficult and expensive to obtain from ship-based measurements, and especially from routine surveys.

Standard bottom trawl surveys off Namibia have a partial net size selection of fish smaller than 18 cm total length (TL) and thus miss a large proportion of the juvenile component of the stock. In addition, the surveys do not adequately cover the inner continental shelf off Namibia, the main habitat of juvenile *M. capensis* (Iilende *et al.*, 2001). These bottom trawl surveys are currently only conducted once a year in summer in Namibia, further limiting the length-frequency information on young fish. Although LFD samples from commercial trawlers are obtained regularly from observers, these do not adequately cover the lengths of *M. capensis* < 30 cm TL as the commercial fleet is restricted to a minimum fishing depth of 200 m and the minimum mesh size of 110 mm (van der Westhuizen, 2001). An alternative sampling method for young *M. capensis* is from fur seal predation. Fur seals are meso-pelagic and bottom feeders, distributed along the entire north-south extension of the Namibian coast, and forage primarily on the continental shelf (de Bruyn *et al.*, 2003; 2005; Skern-Mauritzen *et al.*, 2009). *M. capensis* has been strongly represented in their diet in the last 16 years, based on data from fur seal scats collected regularly along the Namibian coast (Mecenero *et al.*, 2006b). The annual mean TLs of *M. capensis* represented in fur seal scats are < 8 cm and between 12 and 14 cm at the more northern colony (Cape Cross), and between 12 and 23 cm at the two more southern colonies (Mecenero *et al.*, 2006b). Fur seals therefore select the juvenile component of the hake stock. Reconstructing fish LFDs from otoliths in scat samples is an affordable, non-destructive and relatively accessible method of sampling (de Bruyn *et al.*, 2005; Mecenero *et al.*, 2006a).

The aims of this chapter are to use measurements of otoliths of young *M. capensis* collected from fur seal scat samples to identify cohorts and determine their growth rates and hatchdates. Otolith diameters were converted to fish total length, with the aim of using fish total length changes over time to calculate an average growth rate and hatchdate for the stock. The variation in hatchdates and growth rates among cohorts was estimated using a non-linear mixed effects model. Based on preliminary

work by Roux (2004; 2006), the following hypotheses are tested: (1) *M. capensis* juveniles grow faster than previously thought. (2) Hatchdate / spawning peaks should occur once a year and (3) recruitment strength should be dependent on the timing of hatchdates.

2.3. Materials and methods

2.3.1 Otolith collection

The data used in this chapter have been collected for an ongoing monitoring programme of the Ministry of Fisheries and Marine Resources (MFMR), Namibia. Cape fur seal *Arctocephalus pusillus pusillus* scat "bag samples" (Mecenero, 2005) have been collected from several mainland breeding colonies along the coast of Namibia on a regular basis (roughly once a month) since September 1994. The following colonies have been sampled most regularly: Van Reenen Bay (VRB; 27°23′S 15°21′E), Atlas Bay and Wolf Bay (combined AWB; 26°49′S 15°08′E and 26°48′S 15°07′E respectively) and Cape Cross (CC; 21°47′S 13°57′E; Figure 2.1; Mecenero *et al.*, 2006a). Since October 2005, two northern colonies, Pelican Point (PP, 22°52′S 14°27′E) and Torra Bay (TB 20°19′S 13°14′E) have been added to the routine collection and, as a result, since then sampling has occurred more frequently along the Namibian coast. One sample at Lion's Head (LH, 27°41′S, 15°31′E) contained hake otoliths and was included in this analysis. At collection scats were selected as either fresh or with a dark core, while completely desiccated scats were excluded. The sampled scats were observed to be less than 5 days old, and the mean is assumed to be 3.5 days between deposition and collection (Kirkman *et al.*, 2007).

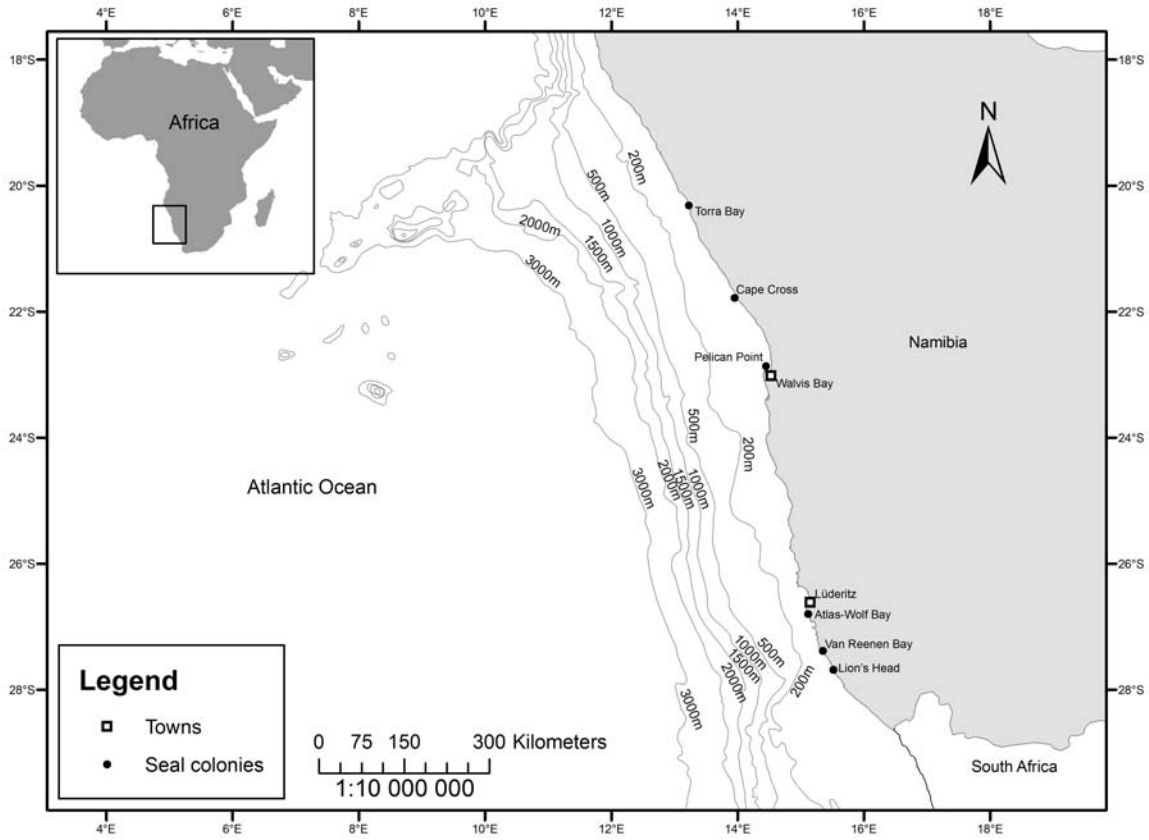

Figure 2.1 Map of Namibia showing the six Cape fur seal mainland study colonies (adapted from Mecenero *et al.*, 2006a).

M. capensis otoliths were recovered from these fur seal scats. They were identified (and separated from *M. paradoxus* otoliths) based on the morphology of the otoliths. *M. capensis* otoliths have a blunter anterior point and deeper radial ridges than *M. paradoxus* otoliths (Mombeck, 1969; Botha, 1971; Smale *et al.*, 1995). This difference is discernible in most digested otoliths (of OD > 4 mm) recovered from the fur seal scats. *M. paradoxus* juveniles (OD < 4 mm) are also typically assumed to be outside the feeding range of fur seals (Gordoa and Duarte, 1991; Burmeister, 2001; Skern-Mauritzen *et al.*, 2009). A full description of the scat sampling and processing procedures is found in Mecenero *et al.* (2006a) and Kirkman *et al.* (2007).

2.3.2 Cohort identification

Each sample of otoliths refers to a collection of otoliths from the same day and the same fur seal colony. The otoliths in each sample were counted and, where possible, otolith diameters (OD, the longest diameter from the anterior to the posterior margin) of whole otoliths were measured with vernier calipers to the nearest 0.05 mm. All otoliths were measured when samples contained < 200 otoliths. Large sub-samples of

otoliths (measurable otoliths) were measured from samples containing > 200 otoliths. These sub-samples were as large as possible and ranged from 203 to 4502 otoliths (usually at least 80 % of the sample). ODs of *M. capensis* otoliths were corrected for erosion occurring during the digestion process by the following equation based on five feeding experiments conducted on four captive adult female fur seals (Millar, 1996):

$$OD_{corrected} = 1.05865\ (OD_{measured}) \quad (2.1).$$

$OD_{corrected}$ was used to back-calculate corresponding fish TL using an empirical TL-OD relationship based on 2901 measurements of *M. capensis* of < 50 cm TL (otoliths from hake > 50 cm TL were not found in the scat samples) from Namibian waters between 1991 and 2006 (Fig. 2.2). The regression equation used to describe this relationship was:

$$TL = a\ (OD_{corrected} - b)^{c} \quad (2.2),$$

where *TL* is the fish total length in cm, *OD* is the otolith diameter in mm, and a, b and c are constants (Fig. 2.2). The fit for Fig. 2.2a was performed using a non-linear fitting technique and the software CurveExpert Basic version 1.4 (Hyams, 2010). The fit for Fig. 2.2b was performed using the Newton algorithm of the Microsoft® Office Excel Solver routine. The log-log fit (Fig. 2.2b) is statistically preferred, but the first (Fig. 2.2a) is used throughout. Table 2.A shows that the maximum relative difference between results from the non-linear and log-log fit is only 4 % for 3 cm fish, and usually < 1 % for all other sizes for both conversions from OD to TL and TL to OD.

Table 2.A Conversion of OD (mm) to fish TL (cm) (first four columns) and TL to OD showing % differences between Fig. 2.2a and Fig. 2.2b conversion equations.

OD (mm)	TL (cm) – Fig. 2.2a	TL (cm) – Fig. 2.2b	% Difference	TL (cm)	OD (mm) – Fig. 2.2a	OD (mm) – Fig. 2.2b	% Difference
1	3.37	3.33	1.2	3	0.74	0.77	-4.0
2	4.89	4.86	0.6	5	2.07	2.09	-0.9
4	8.34	8.32	0.1	8	3.82	3.82	-0.2
6	12.22	12.22	0.0	12	5.89	5.89	0.0
8	16.46	16.47	0.0	16	7.79	7.79	0.0
10	21.02	21.02	0.0	21	9.99	9.99	0.0
12	25.86	25.85	0.1	25	11.65	11.66	0.0
14	30.95	30.92	0.1	30	13.63	13.64	-0.1
16	36.28	36.22	0.2	36	15.90	15.92	-0.1
18	41.82	41.73	0.2	41	17.71	17.74	-0.2
20	47.57	47.43	0.3	47	19.81	19.85	-0.2
22	53.50	53.32	0.4	53	21.83	21.89	-0.3
24	59.62	59.38	0.4	59	23.80	23.88	-0.3

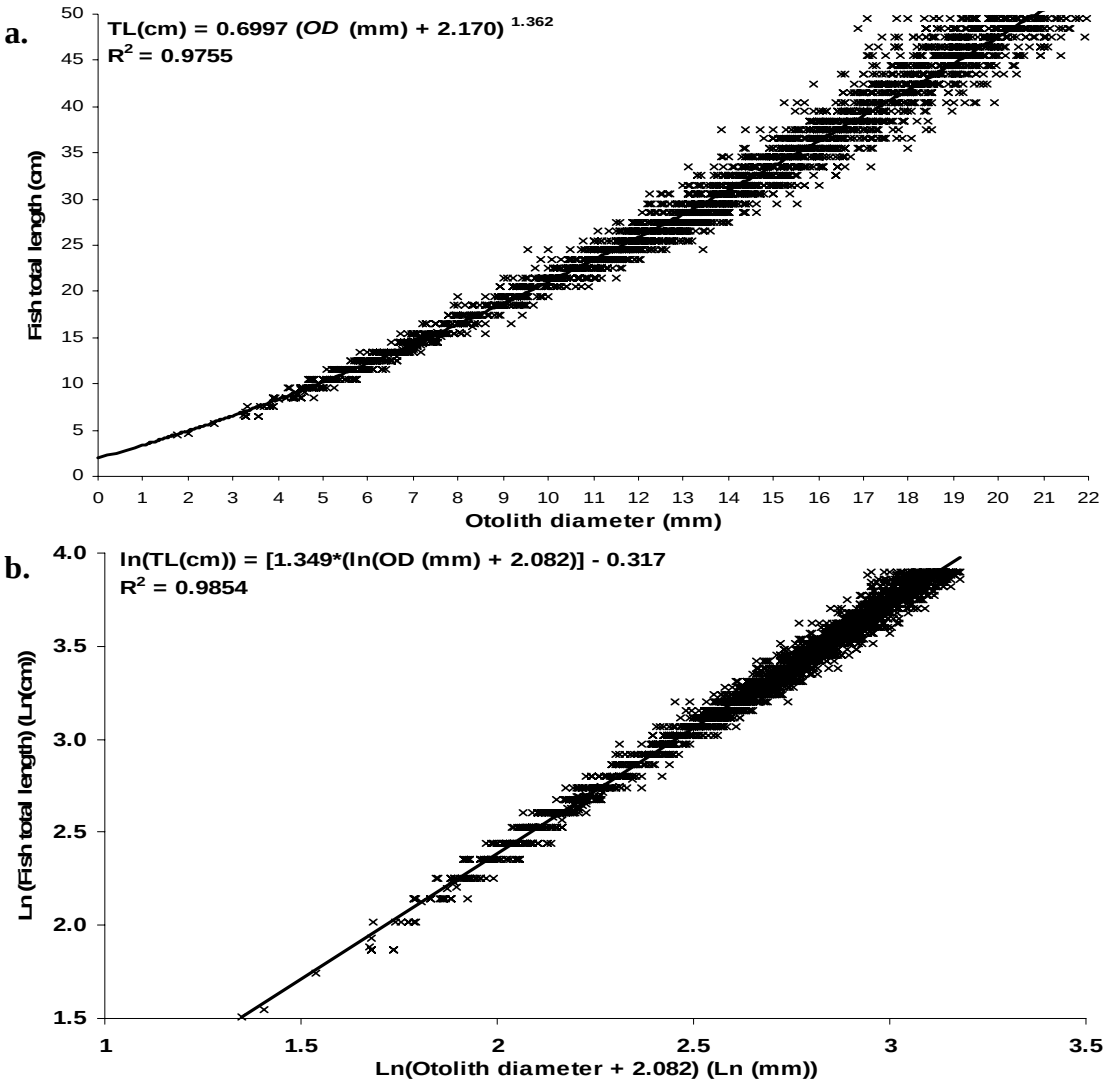

Figure 2.2 *M. capensis* total length (TL) against otolith diameter (OD) obtained from 2901 fish between 6 and 50 cm TL sampled on Namibian biomass surveys 1991–2006 using **a.** a non-linear fit and **b.** a ln-ln relationship.

It was assumed that, in the same way that relative frequencies of otoliths from scats reflect fur seal diet composition (Dellinger and Trillmich, 1988), they would reflect relative frequencies of fish lengths of the same species in their diet and thus in the population. *M. capensis* LFDs were plotted for each sample that contained more than 10 otoliths, from September 1994 to December 2009, and preliminary cohorts were identified by visual inspection. In some samples clearly distinguishable bimodal distributions were detected, usually two successive cohorts, about 10 cm apart, but sometimes from the same cohort. In these cases, distributions were separated into the (sub-) cohorts (see Fig. 2.3 for an example of this method). Mean lengths and standard deviations were calculated for each cohort and plotted against the sample ingestion date. Ingestion date was assumed to be five days before the collection date as the time

of evacuation from fur seal guts ranges between 24 and 48 hours (Millar, 1996), so assuming a mean of 1.5 days for gut evacuation plus a mean of 3.5 for defecation to collection time.

2.3.3 *M. capensis* growth rate, hatchdate and age estimation across all cohorts

An iterative process was used to calculate hatchdate, first assuming all fish were hatched on 1 May, the earliest possible date from visual inspection. The ingestion date was converted to number of days after 1 May of the hatching year to get a first estimate of "*G age in days*". This was converted to a "*G age in years*" by dividing by 365. For example, if a sample was collected on 20 November 2002, consisting of two modes, one at 7 cm TL and one at 19 cm TL, their respective calculated *G age in years* was:

20 November 2002 – 5 days – 1 May 2002 = 198 days (/365) = 0.54 years,
and: 20 November 2003 – 5 days – 1 May 2002 = 567 days = 1.54 years (2.3).

After outlier removal (see below), a von Bertalanffy growth function (VBGF, von Bertalanffy, 1960) was fitted to mean TL (L_t) against *G age in years* (t) for each cohort:

$$L_t = L_\infty \left[1 - e^{-K(t - t_0)}\right] \quad (2.4),$$

where L_t is the expected TL (cm) of each fish at age t (yrs), L_∞ is the asymptotic length (cm), K is the growth coefficient (y^{-1}) and t_0 is the theoretical age (yrs) at length zero. The VBGF parameters were estimated by fitting a non-linear regression to the data by minimising the residual sum of squares (σ^2) using the Newton algorithm of the Microsoft® Office Excel Solver routine:

$$\sigma^2 = \sum_{i=1}^{n} \left(L_i - \hat{L_i} \right)^2 \quad (2.5),$$

where L_i is the observed length-at-age (cm) of each individual in a sample of size n and $\hat{L_i}$ is the predicted length-at-age (cm).

The VBGF parameter estimates were used to calculate the hatchdate, assuming that fish length is 0.2 cm at hatching (Grote, 2010), where $t_{0.2}$ (age (yrs) at length L = 0.2 cm) was calculated by rearranging Equation 2.4 and substituting L_t = 0.2 cm:

$$t_{0.2} = \left[\ln\left(1 - \frac{0.2}{L_\infty}\right) \Big/ (-K) \right] + t_0 \qquad (2.6).$$

The revised hatchdate was calculated as:

$$Hatchdate = (t_{0.2} * 365) + 1 \text{ May of cohort year} \qquad (2.7).$$

The revised hatchdate was used to adjust the fish age estimates by replacing 1 May in Equation 2.3 by *Hatchdate* of Equation 2.7 and the VBGF parameters were recalculated (Equation 2.4). This procedure was repeated until $t_{0.2}$ converged to zero.

Confidence intervals and variance estimates of the VBGF parameters were calculated using parametric bootstrap re-sampling with 1000 replicates drawn from a normal distribution (Efron and Tibshirani, 1986). Standard errors and confidence intervals were constructed using the percentile method of Buckland (1984) (Beamish *et al.*, 2005). This was done using the Newton algorithm in the Microsoft® Office Excel Solver routine.

2.3.4 *M. capensis* growth rate and hatchdate estimation for individual cohorts

A non-linear mixed effects (NLME) model was used to estimate cohort-specific growth parameters. These provide statistical support for analysing population growth parameters and their associated inter-cohort variability, even for noisy or incomplete individual cohort datasets. The assumption is that cohort-specific growth parameters originate from a common distribution as random effects. These were fitted using the library 'nlme' (Pinheiro *et al.*, 2009) in the statistical software R version 2.9.1 (R Development Core Team, 2009) and Equation 2.4, fixing the assumed hatchdate from the results from the iterations (Equation 2.6), with either only t_0 or only K or only L_∞, or only two of the three parameters (t_0 and K, t_0 and L_∞ or K and L_∞), or all three parameters, as random effects for all cohorts. The best model was chosen using the lowest Akaike's Information Criterion (AIC) score (Akaike, 1973; Johnson and Omland, 2004). Hatchdates of each cohort were calculated from their estimated random effect(s) of the best model (Equations 2.6 and 2.7). These were compared to cohort strength, updated from Roux (2004; 2006) (see Section 1.6), which are used as an index in the current stock assessment (Kirchner, 2010).

2.4. Results

2.4.1 Growth rates and hatchdates of young "fur seal-selected" *M. capensis*

The LFDs of the 2002 (and start of 2003) *M. capensis* cohorts are shown in Figure 2.3 as an example of cohort selection. The 2002 cohort first appeared in the fur seal diet at a modal fish total length of 6–7 cm in November 2002. In May 2003, they showed a modal length of 14 cm. By 02 September 2003 they had grown to a length of 19 cm, when the 2003 cohort was seen for the first time at a modal length of 7 cm. A second sub-cohort of the 2003 cohort can be seen at a modal length of 5.5 cm on 20 October 2003 at Cape Cross (CC). From October 2003 to June 2004 (when the 2002 cohort disappeared from the fur seal diet), both the 2002 and 2003 cohorts can be seen together each month. The sample from Cape Cross collected on 20 October 2003 shows an example of a young (4–11 cm) cohort showing a bimodal distribution. Three means (6.1, 9.6 and 18.8 cm) and standard deviations were calculated for that sample. All cohorts from 1994 to 2009 were analysed as described above. The raw data set of LFDs comprised 145 951 otolith measurements, but this was reduced to 139 722 measurements after obvious outliers were discarded. For example the 20.5–24.0 cm fish in the LFD of 25 May 2003, Atlas Bay (AB) were not used because fish were too large to be part of the cohort. In addition, those LFDs for which no clear bimodal distribution or mode could be detected were omitted from subsequent analyses, for example for the 28 February 2003, AB LFD (Fig. 2.3).

Mean lengths (± standard deviations) of each cohort at ingestion dates from September 1994 to December 2009 (Fig. 2.4) indicate that young *M. capensis* first appear in the fur seal diet at 5–8 cm TL between September and December each year and disappear from the fur seal diet at 20–23 cm between September and February, 12 to 14 months later. Six samples were removed for their unusually high mean TL early in the season. Samples that either did not display a clear normal distribution (generally small sample sizes) or contained less than 40 usable otoliths for the cohort were also removed (30 samples). Removal of these left 124 155 measured otoliths, corresponding to ~ 85 % of the original 145 951 otoliths, of which 316 cohort mean lengths were calculated (reduced time series, Fig. 2.6; data courtesy J.-P. Roux, MFMR, Namibia).

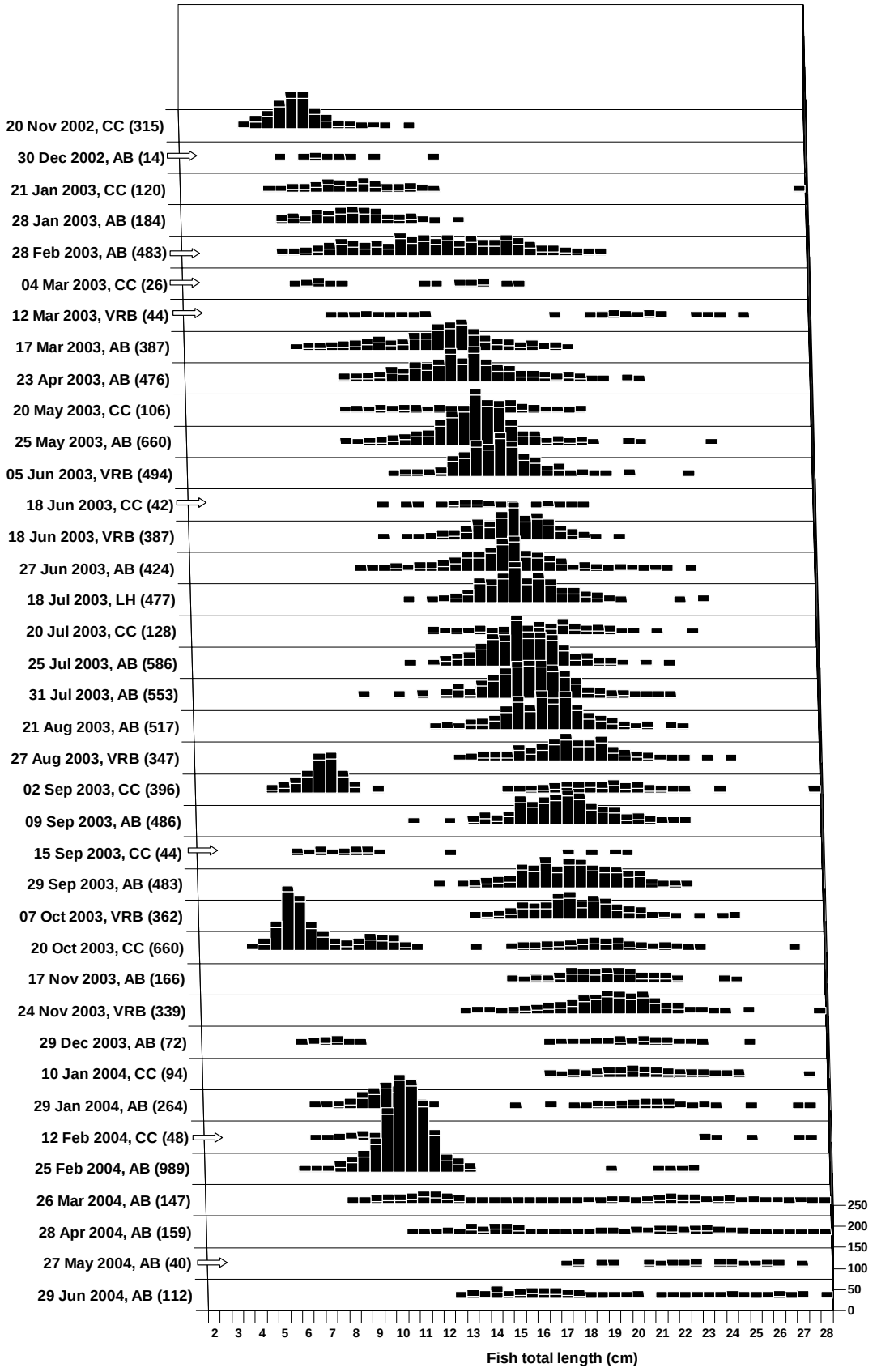

Figure 2.3 Length frequency distributions (LFDs, %) of *M. capensis* from otoliths from fur seal scat samples from November 2002 to June 2004. Date, fur seal colony (CC: Cape Cross, AB: Atlas Bay, VRB: Van Reenen Bay, LH: Lion's Head, Fig. 2.1) and (sample size) are indicated for each LFD. Samples that were excluded from the hatchdate and age estimation sequence are marked with an arrow.

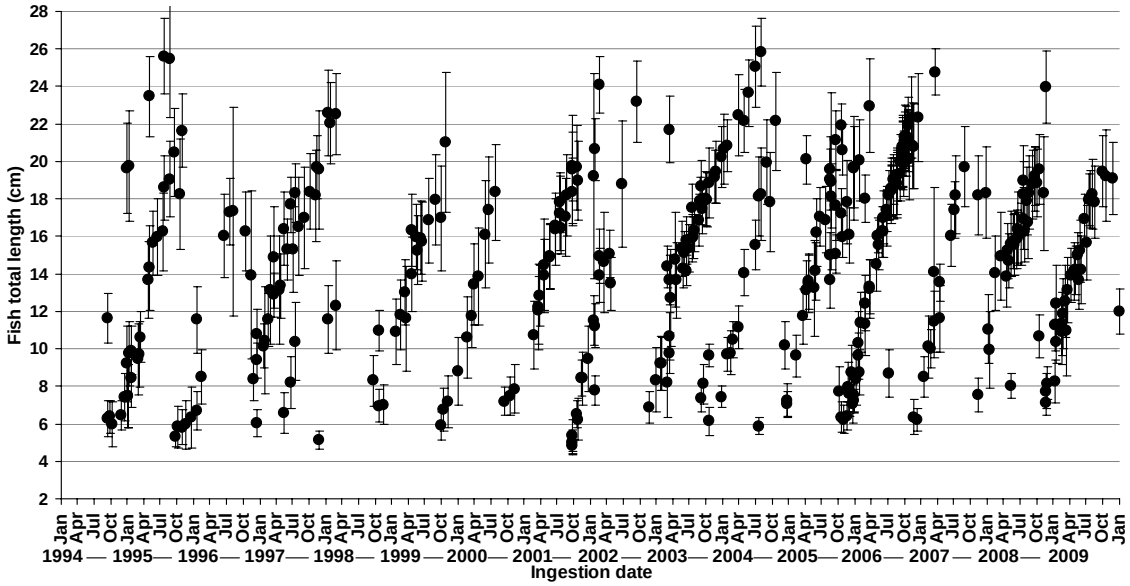

Figure 2.4 Mean (± standard deviation) fish total lengths (cm) of *M. capensis* calculated from otoliths from fur seal scats collected between September 1994 and December 2009.

Table 2.1 shows the parameters of the von Bertalanffy growth function (VBGF) describing mean TL against *fish age* (Figure 2.5). The average hatchdate of all cohorts from 15 September 1994 to 31 December 2009 was 23 June, with the 95 % CI ranging between 3 June and 9 July (36 days, Table 2.1).

Table 2.1 Von Bertalanffy growth function (VBGF) parameter estimates including their bootstrap estimated coefficient of variation (CV) and 95 % confidence intervals (CI) and mean hatchdate (± 95% CI) (n = 316).

	Estimate	**CV (%)**	**95% CI**
L_∞ (cm)	33.6	7.9	[29.7 – 39.9]
K (y^{-1})	0.651	13.0	[0.494 – 0.826]
t_0 (y)	-0.00917	233.5	[-0.0630 – 0.0357]
Hatchdate	23 June		[03 June – 9 July]

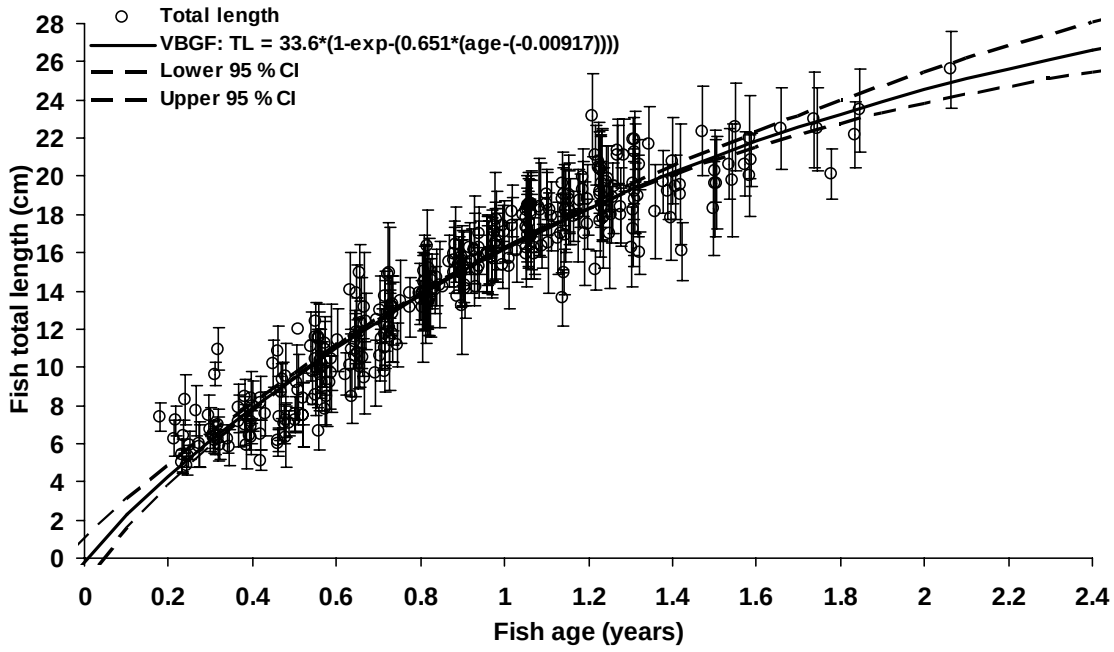

Figure 2.5 Mean (± standard deviation) fish total lengths (cm) of *M. capensis* calculated from otoliths from fur seal scats collected between 15 September 1994 and 31 December 2009 plotted against estimated age (years). A von Bertalanffy growth function (VBGF, solid line) including 95 % confidence intervals (CI, broken lines) is indicated on the plot.

2.4.2 Variation of growth rates and hatchdates between individual cohorts

The overall VBGF (solid line, Figure 2.6) generally fits lengths of all cohorts, but with some possible earlier-spawned sub-cohorts appearing, for example for the 1998 and 2005 cohorts (Figure 2.6).

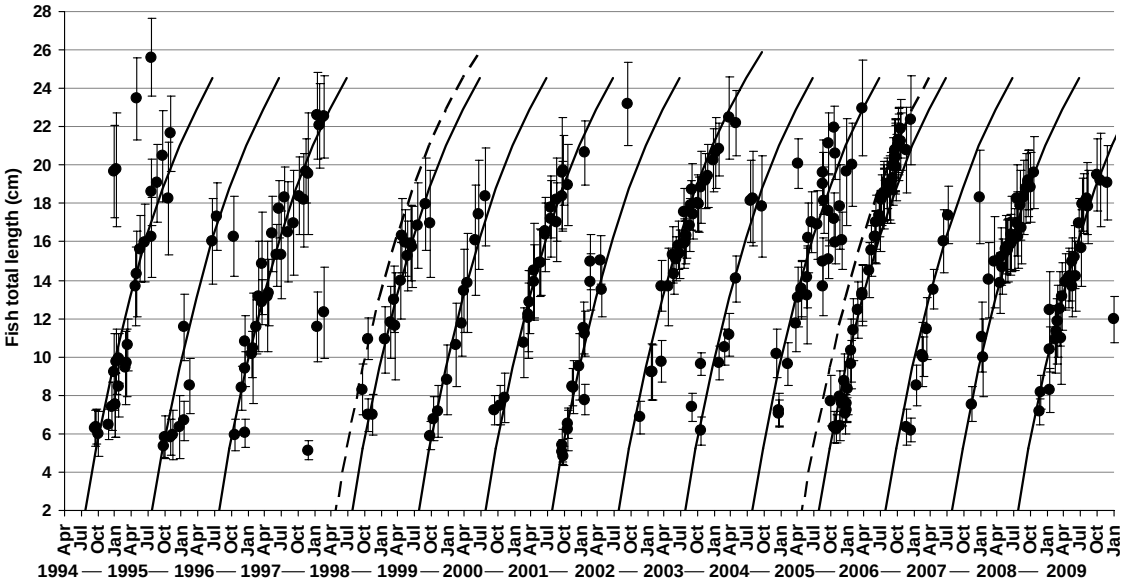

Figure 2.6 Reduced time-series of mean (± standard deviation) fish lengths (cm) of *M. capensis* ingested by fur seals between 15 September 1994 and 31 December 2009. Solid lines show the fitted von Bertalanffy growth curves (Table 2.1) using the estimated 23 June hatchdate for each cohort. Broken lines show additional curves assuming 3 months earlier hatching (23 March) for the 1998 and 2005 cohorts.

The best NLME model fits (AIC = 1087) had K as the only fixed effect, and L_∞ and t_0 as cohort-specific random effects (Table 2.2a). Using this model, each cohort's random effects curve (thin brown line, Fig. 2.7) fits the fixed effects curve (thick blue line, Fig. 2.7) reasonably well, with the exception of 1995 (Fig. 2.7c) and 2006 (Fig. 2.7n) in terms of their hatchdates, and 1998 (Fig. 2.7f), 2001 (Fig. 2.7i), 2003 (Fig. 2.7k) and 2005 (Fig. 2.7m) in terms of their growth rates. The discrepancies are often determined by individual points at the beginning or end of the range of fish TLs. The 2005 cohort (Fig. 2.7m) showed the fastest growth rate and consequently the latest hatchdate, not only determined by individual points at the beginning or end of the range, but by the whole series. Samples in the 2004 cohort (Fig. 2.7l) appeared to represent sub-cohorts (about 5 cm difference between them), with a difference of ± 3 months between hatchdates. Earliest hatchdates calculated from random effects were those of the 1998 and 2003 cohorts (21–23 May), and the latest were those of the 2005 and 2006 cohorts, (16–20 July, Table 2.2b). This is a maximum span of 61 days. Figure 2.7 also shows that, for the most part, samples collected from the different colonies show few differences in lengths-at-age.

Table 2.2a Growth parameters calculated with non-linear mixed effects model (NLME) and the von Bertalanffy growth function (VBGF, Equation 2.4) for *M. capensis* fitted to data from all cohorts 1993–2009 off Namibia.

Fixed effects	Value	Std. error	df	*t*-Value	*p*-Value
L_∞ (cm)	33.2	2.46	297	13.501	$< 2.e^{-16}$
K (year^{-1})	0.667	0.0848	297	7.875	$< 2.e^{-16}$
t_0 (years)	-0.00432	0.0287	297	-0.150	0.881
Hatchdate	24 June				

Random effects	Std. dev	Correlation
t_0 (years)	0.0604	**t_0 (years)**
L_∞ (cm)	2.00	0.732
Residual	1.24	

Level: Cohort	L_∞ (cm)	t_0 (years)
1993	32.7	-0.00407
1994	34.1	0.0434
1995	32.2	0.0296
1996	33.0	-0.00911
1997	34.0	0.0291
1998	31.1	-0.0996
1999	33.8	0.00233
2000	32.3	-0.0522
2001	35.8	0.00832
2002	32.5	0.0162
2003	30.4	-0.0924
2004	31.8	-0.000670
2005	37.2	0.0680
2006	33.2	0.0560
2007	33.1	-0.0374
2008	33.4	0.00850
2009	33.0	-0.0393

Table 2.2b Hatchdates calculated from the estimated t_0 of the NLME model (Table 2.2a) for Namibian *M. capensis*. The corresponding cohort strength was updated from Roux (2004; data courtesy J.-P. Roux, MFMR, Namibia).

Cohort	Hatchdate	Cohort strength (billions of fish)
1993	24 June	2.40
1994	12 July	2.06
1995	07 July	0.41
1996	22 Jun	7.18
1997	06 July	0.94
1998	21 May	4.67
1999	27 June	2.09
2000	07 June	3.03
2001	29 June	0.24
2002	02 July	8.21
2003	23 May	0.86
2004	26 June	2.99
2005	20 July	2.34
2006	16 July	1.78
2007	12 June	4.30
2008	29 June	5.20
2009	11 June	2.14

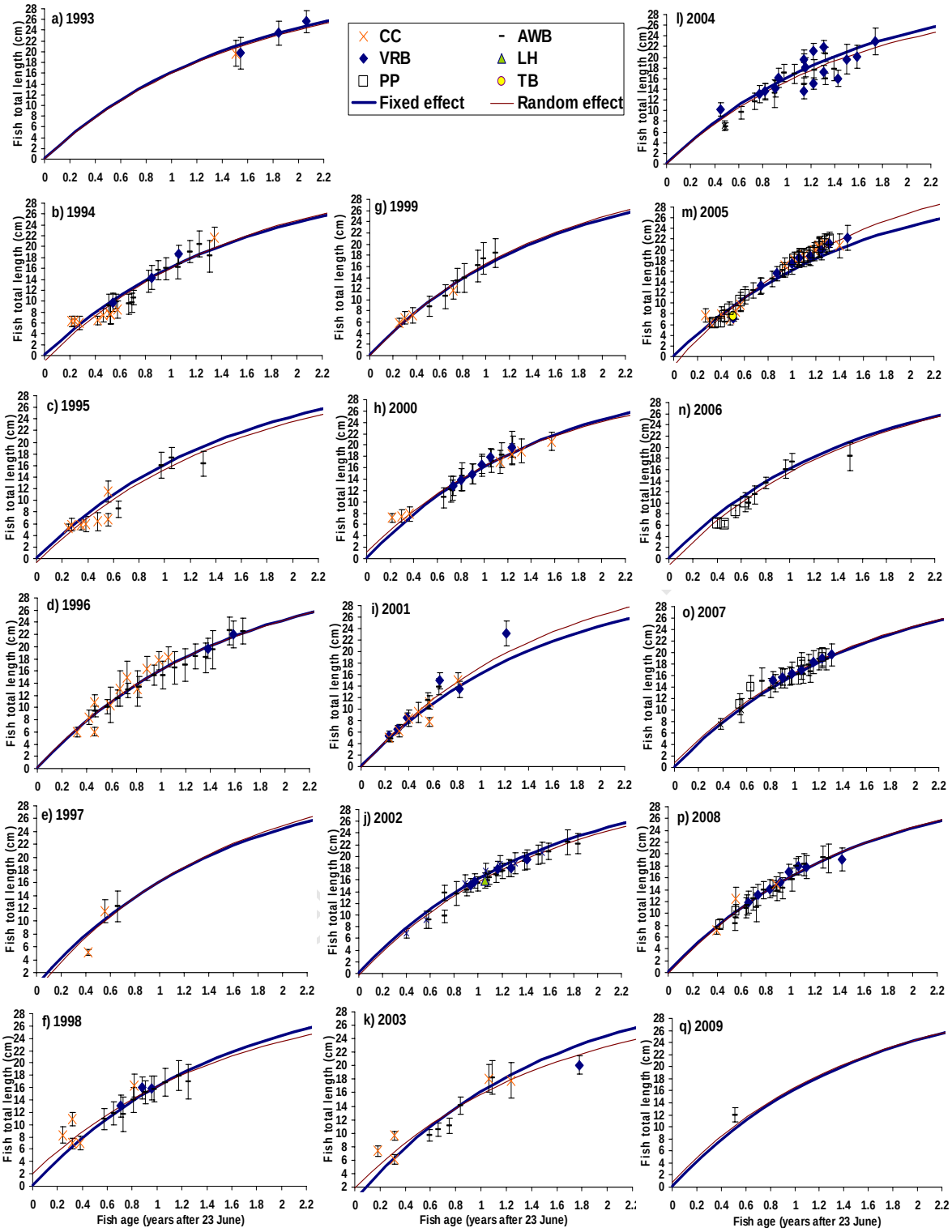

Figure 2.7 Mean (± standard deviation) total lengths (cm) of *M. capensis* (reduced time-series, Fig. 2.6) separated into cohorts. The thick solid lines show fixed effects von Bertalanffy growth function using a non-linear mixed effects model (NLME), and the thin solid lines show the random effects of each cohort's L_∞ and t_0 (Table 2.2) using the estimated 23 June hatchdate for each cohort (Fig. 2.5). The samples collected from different colonies are marked with different symbols: CC; Cape Cross, AWB: Atlas and Wolf Bay, VRB: Van Reenen Bay, LH: Lion's Head, PP: Pelican Point, TB: Torra Bay (see Fig. 2.1).

The cohort strength in billions of fish (updated from Roux (2004; 2006)) and the calculated hatchdate for each cohort are unrelated (Figure 2.8).

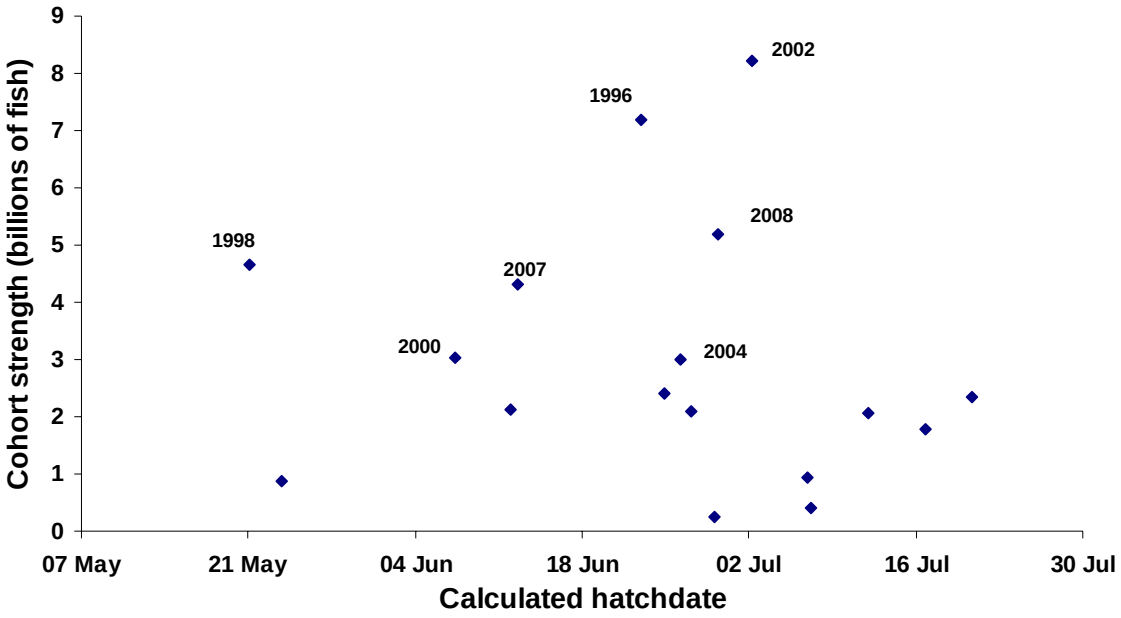

Figure 2.8 Hatchdate of each *M. capensis* cohort (1993 to 2007, calculated from non-linear mixed effects model, NLME, Fig. 2.7) against cohort strength from the seal scat index (updated from Roux, 2004; 2006). The strong cohorts are labelled with their hatching year.

2.5. Discussion

2.5.1 Fast growth rates of young *M. capensis* compared with other hakes

Sampling from fur seals is not random as they may be biased towards a specific area and a specific size range or may change seasonally according to availability of the other prey. However, in most years, fur seals consume hake regularly throughout the year and from the entire available fish length range from 5 to 25 cm total length. They are thus efficient samplers of the available hake in this length range and a useful tool for studying juvenile *M. capensis* growth rates and hatchdates. Cohorts a year apart could be separated clearly. This means they had similar hatchdates in different years and relatively fast growth rates.

According to the growth models calculated in this study, by the end of their first year Namibian *M. capensis* reach a mean total length of 16.2 cm, and after 1.5 years they reach a length of 21.0 cm (Table 2.3, Fig. 2.9). This means they grow at a mean rate of 1.3 cm month $^{-1}$ in their first 18 months. This is almost double that of a previously

described growth rate of Namibian *M. capensis* of around 0.7 cm month^{-1} in their first 18 months (Wilhelm *et al.*, 2007, Table 2.3). Previous studies that showed slower growth rates for *M. capensis*, similar to those obtained by Wilhelm *et al.* (2007), were those obtained by Morales and Payne (1985) and Punt and Leslie (1991) (Table 2.3). Botha (1970 and 1971) showed mean fish lengths of 8 and 7 cm respectively for 1-year-olds and 21 and 18 cm respectively for 2-year-olds, also resulting in fast 1.0–1.1 cm month^{-1} growth rates, similar to those in this study (Table 2.3). Pozo Arteaga (1976), Preñski (1978) and Wysokiñski (1982) showed similar mean growth rates (Table 2.3), but their calculated mean lengths-at-age for 1-year-olds differed by up to 10 cm, whereas the mean lengths-at-age-2 years did not differ as much as those of 1-year-olds (Table 2.3), Wysokiñski (1982) showed the fastest growth rates for young fish (Fig. 2.9). These differences may be accounted for by differences in otolith interpretation (which translucent zone to assign to ages 0, 1 and 2, Morales and Payne, 1985), as well as the length of the youngest fish in the sample, and thus the calculation of t_0 (Fig. 2.9). When length-frequency analyses independent of otoliths were used (Morales-Nin, 1991), t_0 was assumed to be zero and similar monthly growth rates (1 cm month^{-1}) to this study were observed.

This study is the first attempt to calculate growth rates independent of otolith interpretation and with young (< 1-year old) fish, in order to more accurately define t_0. It emphasises the need for age validation for the hakes in the Benguela to re-define current age determination criteria. The results emphasize the importance of using length-frequency analyses for studying age distributions (Morales-Nin *et al.*, 1998; Fournier *et al.*, 1998) in the interim.

The method for back-calculating hatching dates from the smallest fish in this study (5 cm) to hatched fish (0.2 cm) assumes that larvae and juveniles grow at the same rate. The alternative to this would be to calculate the date at metamorphosis (at 1.6–3.0 cm, Grote, 2010), approximately 16 July – 18 August as dates at metamorphosis. This is 30–40 days (Grote, 2010) or 1–2 months (O'Toole, 1976) after hatching and thus would have placed the estimated hatching date between beginning of June and middle of July. The assumption is thus met, bearing in mind that there is a variation of at least one month with these calculations.

In order to simplify results, and after trying many methods, the method of using the mean length for each cohort was decided on so as not to over-sample the youngest fish. Also, L_∞ was freely fitted instead of fixed in order to let the t_0 be estimated as accurately as possible. These two parameters are related and by fixing L_∞ at a high value, this would reduce the early growth rate, and set the hatchdate earlier, whereas it is believed that growth rates calculated here are possibly still under-estimated (see below). However, this meant that the estimated L_∞ (of 33.6 cm) is unrealistic as *M. capensis* grow up to 120 cm long (Table 2.3). The extension of the growth curve to older fish and reasons for this apparent sloping off of the growth curve are addressed in Chapter 4 (see Fig. 4.3).

The influence of individual points, both at small and large lengths is apparent in the 2001 and 2003 cohorts (Fig. 2.7). It is possible that all cohorts grow as fast as the 2005 cohort, and thus overall hatchdates would be later than the end of June.

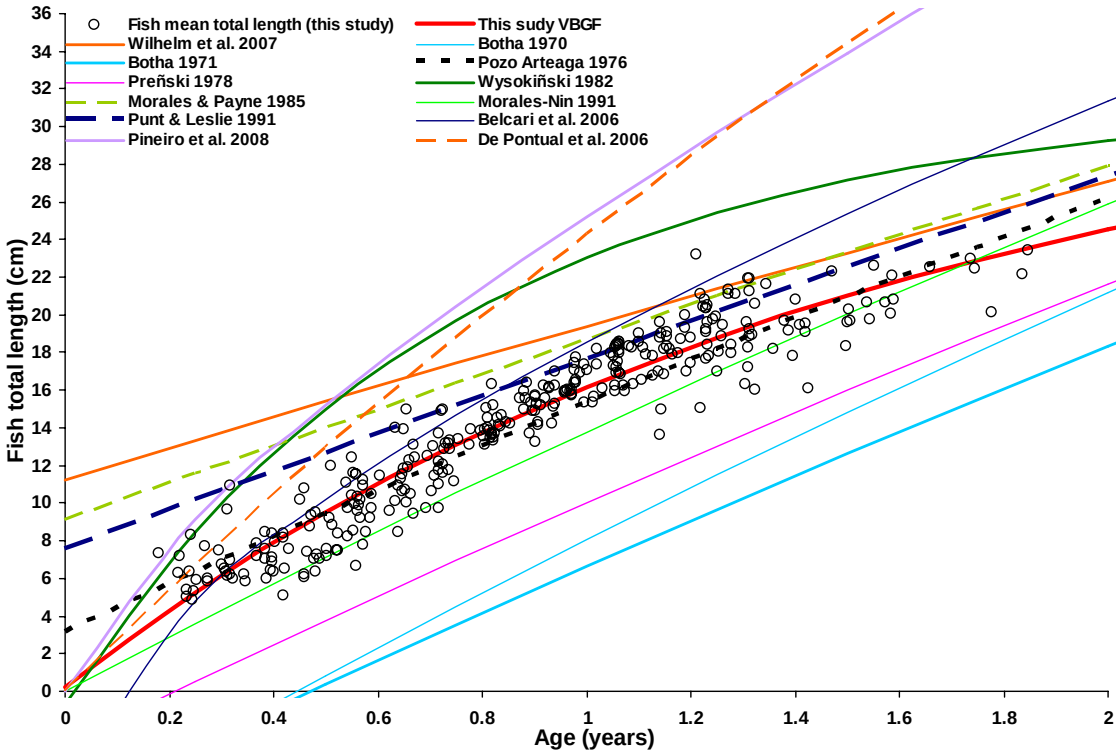

Figure 2.9 Fish total length (cm) against age of *M. capensis* in this study compared with other studies on *M. capensis* in the Benguela (Table 2.3) as well as from tagging studies and daily age determination studies on otoliths of European hake ("Belcari et al. 2006", "Pineiro et al. 2008" and "De Pontual et al. 2006").

Table 2.3 Mean total lengths-at age (cm) and growth rates (cm month^{-1}) of *M. capensis* in this study compared with other annual growth rate studies of *M. capensis* in southern Africa.

Age months	Age years	This study VBGF	Wilhelm *et al.* (2007)	Botha (1970)	Botha (1971)	Pozo Arteaga (1976)	Preñski (1978)	Wysokiński (1982)	Morales & Payne (1985)	Morales-Nin (1991)	Punt & Leslie (1991)
0	0.00	0.20	11.3	-6.9	-6.2	3.2	-2.8	-0.7	9.1	0.0	7.6
3	0.25	5.22	13.3	-3.0	-2.9	6.3	0.5	8.4	11.6	3.6	10.1
6	**0.50**	**9.48**	**15.4**	0.8	0.3	9.4	3.8	15.0	14.0	7.1	12.7
9	**0.75**	**13.11**	**17.4**	4.5	3.5	12.4	7.0	19.7	16.4	10.5	15.2
12	**1.00**	**16.19**	**19.4**	**8.1**	**6.6**	**15.4**	**10.0**	**23.0**	**18.7**	**13.8**	**17.7**
15	1.25	18.80	21.4	11.5	9.7	18.2	13.1	25.4	21.1	17.0	20.1
18	1.50	21.03	23.3	14.8	12.6	20.9	16.0	27.1	23.4	20.0	22.5
21	1.75	22.92	25.2	18.1	15.5	23.6	18.8	28.4	25.6	23.0	24.9
24	**2.00**	**24.52**	**27.1**	**21.2**	**18.4**	**26.2**	**21.6**	**29.3**	**27.9**	**25.9**	**27.3**
27	2.25	25.89	28.9	24.2	21.1	28.7	24.3	29.9	30.1	28.6	29.7
30	2.50	27.04	30.8	27.1	23.8	31.1	27.0	30.4	32.3	31.3	32.0
33	2.75	28.03	32.6	30.0	26.5	33.5	29.5	30.7	34.5	33.9	34.3
36	**3.00**	**28.87**	**34.3**	**32.7**	**29.1**	**35.8**	**32.0**	**30.9**	**36.6**	**36.4**	**36.6**
Growth rate 0–12 months (cm month^{-1})		1.3	0.7	1.2	1.0	1.0	1.1	2.0	0.8	1.1	0.8
Growth rate 6–18 months (cm month^{-1})		**1.0**	**0.7**	**1.2**	**1.0**	**1.0**	**1.0**	**1.0**	**0.8**	**1.1**	**0.8**
L_∞ (cm)		**33.6**	149	116	141	111	125	31.5	210	110	271
K (year^{-1})		**0.651**	0.0609	0.130	0.0911	0.120	0.106	1.33	0.0489	0.134	0.0390
t_0 (years)		**-0.00917**	-1.29	0.444	0.473	-0.240	0.211	0.0160	-0.907	0	-0.730

Growth rates of European hake established from methods other than annual age determination from otoliths also compared well with the fast growth rates of this study. For example, Belcari *et al.* (2006) calculated mean fish lengths of 18.5 cm at age 1 year, with a mean growth rate of 2.0 cm month^{-1} (Fig. 2.9). This is similar to other studies that used otolith microstructure as the age determination method (Piñeiro *et al.*, 2008, Fig. 2.9; Morales-Nin and Aldebert, 1997; Morales-Nin and Moranta, 2004; Otxotorena *et al.*, 2010). Hatchery-reared European hake of up to 13.5 cm TL showed a mean growth rate of 1.8 cm month^{-1} up to 200 days post-hatch (Morales-Nin *et al.*, 2005). Recent re-captures of tagged European hake by de Pontual *et al.* (2006) and Piñeiro *et al.* (2007) showed fast growth rates of hake of 21–40 cm TL (up to 67 cm TL at recapture) growing at 0.032–0.052 cm day^{-1} (0.97–1.58 cm month^{-1} or 12–19 cm year^{-1}), even after 29 cm TL. This is twice as fast as previously recorded from annual age determination studies from otoliths (1933 and 1975–1997, Godinho *et al.*, 2001 and 1954–2000 Piñeiro and Saínza, 2003). De Pontual *et al.* (2006) and Piñeiro *et al.* (2007) showed growth rates very similar to those of Wysokiński (1982) for Namibian *M. capensis* (12–24 cm year^{-1}, Fig. 2.9). Roux (1947) also showed that 40–50 cm *M. capensis* grew at 9–11 cm year^{-1}. Fast (10–20 cm year^{-1}) growth rates of hakes thus have been demonstrated for large hakes elsewhere, similar to the results presented here for *M. capensis* of up to 25 cm TL, but still need to be confirmed for large *M. capensis* (Chapter 4).

2.5.2 *M. capensis* hatchdate periodicity

Hatchdates of the *M. capensis* cohorts detected in the fur seal diet generally fall at the beginning of winter, on average on 23 June with 95 % CIs ranging between 3 June and 9 July (36 days). For the different cohorts hatchdates range (randomly) between 21 May and 20 July (60 days).

Gonadal examinations of *M. capensis* indicated that spawning occurs throughout the year with peaks in winter (mid-July) around Cape Frio (18°S, northern Namibia), and in spring (between October and December) around Walvis Bay (23–24°S), central Namibia (Assorov and Berenbeim, 1983; Gordoa *et al.*, 1995). O'Toole (1978) observed peaks of larval abundance in November–December 1972 off Walvis Bay. Although he did not collect samples between April and July, within the sampling period August to March a summer peak of larval abundance was observed. Olivar *et al.* (1988) found relatively large quantities of eggs and larvae during late winter and noted that "practically no spawning took place in autumn" (from the near-absence of hake eggs in their plankton samples in March–April 1981 in areas of bottom depths between 100 and 200 m, and 17–23°S latitude, compared with August 1980 and November 1979 samples), but that the onset of the spawning season may vary from one year to the next. The peak in gonadosomatic index (GSI) for *M. capensis* samples collected between September 1998 and August 2001 coincided with the winter/spring (July–October) spawning peak (Kainge *et al.*, 2007), but with a weaker secondary peak in summer (February–April). European hake *M. merluccius* also have two peaks in hatchdate distributions (Belcari *et al.*, 2006). The southern (Patagonian) stock of Argentine hake *M. hubbsi* shows peak spawning in spring–summer (November through March, Macchi *et al.*, 2004), whereas those from the northern area (north of 37°S) are mainly spawned during autumn–winter (Christiansen *et al.*, 1986; Norbis *et al.*, 1999).

Fish lengths at age from the far northern (20–22°S) and far southern (as far as 28°S) Namibian fur seal colonies were similar, indicating *M. capensis* in these regions belong to the same population with similar spawning times all along the Namibian coastline. Different spawning times in different areas noted by previous authors have not occurred recent years, but rather peaks of survivors match throughout the distribution of *M. capensis*, i.e. the survivors seem to stem from the same optimal

spawning period. The 1996 cohort is one example of the exception, where Cape Cross samples were a few cm larger than the southern Namibian samples, i.e. had an earlier hatching time (Fig. 2.7d). In Namibia, fur seals forage mainly on the continental shelf within 150 km of the shoreline, and < 500 m bottom depths at the shelf break off northern Namibia (Torra Bay and north of 20°S) and southern Namibia (Atlas Bay and below, Fig. 2.1) and < 200 m bottom depth off central Namibia (Skern-Mauritzen *et al.*, 2009). This may explain the presence of 18–25 cm TL hake in the diet of fur seals from the southern colonies, as these larger fish are probably found on the shelf break between 150 and 250 m bottom depth (Burmeister, 2001; Iilende *et al.*, 2001) and will only be encountered in the south, at the much narrower shelf than in central Namibia (Nelson and Hutchings, 1983). The spatial distributions of juvenile and adult *M. capensis* and hatchdate peaks along the Namibian coast are further addressed in Chapter 5.

The observed mid-winter hatchdate peak of *M. capensis* could simply reflect the centre of the biannual hatchdate distribution, which ranges between earlier summer-spawned fish (e.g. 1998 cohort, Fig. 2.7f), winter-spawned fish (e.g. 2008 cohort, Fig. 2.7p) and later spring-spawned fish (e.g. 2005 and 2006 cohorts, Figs 2.7m and n). If the early growth rates were under-estimated, the hatchdates would have been estimated as being too early and might be closer to spring. The other caution is that individual lengths at age 0 (fish length at hatching) can be quite variable (Pepin and Myers, 1991), and one should consider the range of hatchdates here, rather than individual hatchdates. In some years in which strong *M. capensis* year-classes were observed from the fur seal diet (e.g. 1996, 1998 and 2004, Table 2.2b), survivors seemed to stem from a longer hatching period (Figs 2.6 and 2.7). However, hatchdate in particular does not seem to be related to cohort strength (Fig. 2.8). The strongest year-classes have intermediate hatchdates, which means they could arise from a longer optimal "spawning" or rather, survival, environmental window.

2.6. Conclusions

In this chapter it is shown that fur seal scat analysis can be used as a tool for studying growth rates and hatchdates of juvenile *M. capensis*. The young fish consumed by fur seals over the period 1994–2009 show growth rates twice as fast as those described in a recent publication for 2000–2007 using age determination from otoliths for this species, and comparable with those recently described for *M. merluccius* and *M. gayi*, supporting the hypothesis that *M. capensis* juveniles grow faster than previously thought. *M. capensis* appear to have been hatched mainly in winter (23 June ± 20 days), ranging from 20 May to 20 July among cohorts, supporting the hypothesis that hatchdate / spawning peaks should occur once a year. Recruitment strength did not depend on timing of hatchdates, but it is suggested that the strength of the year class may depend on the length of the spawning season.

CHAPTER 3

Age validation of young *Merluccius capensis* in the northern Benguela using otoliths from monthly fur seal scat samples

3.1. Abstract

The seasonal formation of translucent zones on otoliths was validated using monthly samples of 3 to 21-month-old hake, *Merluccius capensis*, obtained from fur seal scats sampled regularly at the main fur seal colonies along the Namibian coast. A total of 3474 otoliths was analysed from three strong and two weaker cohorts spawned in the winters of 1996, 1998, 2002, 2005 and 2006, respectively. The number of translucent zones was counted, the otolith edges were evaluated, and the otolith diameter (OD) at each translucent zone and total OD of each otolith were measured. Logistic ogives for each translucent zone were firstly fitted to % of otoliths with complete translucent zones against collection date and secondly to % of otoliths with complete translucent zones against total OD. Results showed that young *M. capensis* formed three translucent zones by the time they were 21 months old. During the period of study, the first translucent zone (T1) formed between late summer and autumn (January–April), when hake were only 7–10 months old, being formed when ODs were between 4 and 7 mm and fish total lengths (TL) between 9 and 14 cm. This was previously termed the "demersal ring" but it is formed after hake have already settled to a demersal habitat. A second translucent zone (T2) was formed between late winter and spring (July–September) when fish were between 13 and 15 months old, 7–10 mm OD and 16–20 cm TL, representing the first annulus. The third translucent zone (T3) was formed in summer (December–March) when hake were 18–21 months old at 11.0–12.5 mm OD and fish TLs of 24–27 cm. This translucent zone was previously falsely assumed to be the second annulus and thus previous age estimates have been over-estimated by at least one year. No differences in appearance between summer and winter translucent zones were visible under the light microscope. Biannual translucent zone formation complicates edge analysis, making this method unsuitable for use in age validation of *M. capensis* when not used in combination with number of translucent zones.

3.2. Introduction

The shallow-water Cape hake, *Merluccius capensis* (Castelnau, 1861) and deep-water hake, *Merluccius paradoxus* (Franca, 1960), are members of the order Gadiformes (including cods), Family Merlucciidae (merluccid hakes) and Genus *Merluccius* (Lloris *et al.*, 2005). They occur in high abundances in the Benguela upwelling region, and make up Namibia's most important commercial resource (van der Westhuizen, 2001). Stock abundance trends and catch projections for management recommendations of Namibian hake are modelled by means of an age-structured production model (ASPM, e.g. Butterworth and Geromont, 2001) fitted to abundance indices and catch-at-age data derived from commercial catches and survey catches. The catch-at-age data are important for the ASPMs as the annual recruitment fluctuations / cohort strength, natural mortality and age-specific selectivity functions are estimable parameters, relying on the input catch-at-age data (Butterworth and Rademeyer, 2005). Consequences of age determination biases to these estimated results are often emphasised (BENEFIT, 2004a; Butterworth and Rademeyer, 2005).

Most age determination methods used for annual catch-at-age data of teleost fish rely on counting concentric growth increments on otoliths. One complete growth increment consists of an opaque zone, usually wide and white/pale when viewed under reflected light, thought to form during periods of fast growth, and a narrow translucent zone, which is thought to form at periods of slow growth and appears blue/dark when viewed under reflected light. The basic method for annual age determination using otoliths has been widely described for hakes, for example for silver hake *M. bilinearis* (Nichy, 1969; Hunt, 1980), Pacific hake *M. productus* (Beamish, 1979), southern hake *M. australis* (Horn, 1997), Argentinean / Uruguayan hake *M. hubbsi* (Renzi and Pérez, 1992) and European hake *M. merluccius* (Hickling, 1933), and has been applied to stock assessments and other studies on general hake biology (e.g. Helser and Broziak, 1998; Guevara-Carrasco and Lleonart, 2008; Godinho *et al.*, 2001; Piñeiro and Saínza, 2003). In southern Africa, growth rates of *M. capensis* from annual age determination from otoliths have been described as far back as the 1940s (Roux, 1947). The otolith interpretation methods for both *M. capensis* and *M. paradoxus* were described by Botha (1971), and were used for growth rate calculations by Pschenichnii (1976), Pozo Arteaga (1976), Preñski (1978), Morales and Payne (1985), Morales-Nin (1991) and

Punt and Leslie (1991). Photographic interpretation guides on age determination of the two southern African hake species are also available (ICSEAF, 1983; Wysokiñski, 1983). The method described in these guides, the whole otolith method, involves counting all translucent zones as annuli, and has been used as a guide for the current agreed method of age determination in the region (BENEFIT, 2005). It has been applied routinely to supply age data required for current use in stock assessment (Wilhelm *et al.*, 2007).

Even though the whole otolith method is widely accepted as a method to age fish, and hakes in particular, the method itself is subjective. Similar images in the interpretation guides (ICSEAF, 1983; Wysokiñski, 1983) often have conflicting interpretations, and replicate readings on individual otoliths may differ by up to 6 (age in years assigned) (BENEFIT, 2005). No reliable age determination method of southern African hake has been described based on age validation work. Not only are age validation studies a requirement of any accurate age determination method, they need to be done for each species and all age classes (Beamish and MacFarlane, 1983; Campana, 2001). Gordoa *et al.* (2001) validated the first two annuli on Namibian *M. capensis* otoliths by comparing daily increment counts with the annuli, concluding that counting the first two annuli would mostly over-estimate ages. They also noted that translucent zones were formed throughout the year on *M. capensis* otoliths.

Edge analysis consists of recording the presence of either an opaque or translucent zone on the edge of otoliths and plotting their relative frequency as a function of months, which should follow a sinusoidal cycle with a frequency of 12 months for annuli (Lehodey and Grandperrin, 1996; Vilizzi and Walker, 1999; Campana 2001). Age validation by edge analysis was attempted on South African *M. capensis* and *M. paradoxus* by Botha (1971), showing that translucent zones were formed between August and November on the majority of otoliths, but the formation of both opaque and translucent zones was recorded in all months of the year. Voges (1995) determined Namibian *M. capensis* ages from 1992 and 1993 and found that translucent zones were mostly laid down in July. She found that the length-frequency distributions (LFD) from surveys seemed to match the LFDs at the first seven annuli counted on otoliths. Wilhelm (2005) used the same methods on both *M. capensis* and *M. paradoxus* from 2000 to 2005 and found that the presence of translucent zones on the edge of otoliths

was dominant between June and October and LFD modes generally matched age groups 1 to 7. Length-based methods, however, are problematic, and should best only be applied to young and/or fast-growing fish (Campana, 2001).

The difficulty in interpreting translucent zone patterns on hake otoliths in general is widely recognised in the literature (ICSEAF, 1983; Morales and Payne, 1985; Piñeiro and Hunt, 1989; Morales-Nin *et al.*, 1998; Colloca *et al.*, 2003). Recent age validation studies are re-defining otolith interpretation and growth rates of European hake *M. merluccius* (Morales-Nin *et al.*, 2005; Belcari *et al.*, 2006; de Pontual *et al.*, 2006; Courbin *et al.*, 2007) and on Peruvian hake *M. gayi* (Goicochea *et al.*, 2010). Multiple or secondary translucent zones are often present per year, and split rings or diffuse growth patterns are often present in the southern African hakes as well (ICSEAF, 1983; Morales and Payne, 1985; Piñeiro and Hunt, 1989; Morales-Nin *et al*., 1998). This attribute complicates edge analysis when averaged over all ages, translucent zones and years as edge analysis (the same as length-based methods) should only be applied to young fast-growing fish or restricted to a few (ideally only one) age groups (Campana, 2001). Validating translucent zones on hake otoliths using direct age validation methods is complicated by the difficulty of obtaining known-age hake from either wild populations or reared fish. In Chapter 2, measurements on *M. capensis* otoliths from regular samples of fur seal scats were used to identify annual cohorts, and map the growth rates and hatchdates of these young fish up to the middle of their second year of life.

The aim of this chapter is to use otoliths recovered from fur seal scat samples, assigned to cohorts of approximate known-age (Chapter 2), to investigate the seasonal pattern of translucent zone formation for the first 21 months of the life of Namibian *M. capensis*. The "progression of a known year-class in the length-frequency" (Petersen, 1891) method of age validation is used, described as a reasonably strong method (Kimura *et al.*, 2006). The traditional hypothesis is that *M. capensis* translucent zones are formed once per annum (after the first annulus). In addition, the chapter aims to describe the measurements of the first three translucent zones to derive a more reliable age determination method than is currently used.

3.3. Materials and methods

3.3.1 Cohort selection

Five *M. capensis* cohorts, named after their hatching year, identified in Chapter 2, were chosen for age validation purposes. Three of these cohorts were the strongest cohorts that could be followed through the LFDs in the annual demersal survey samples: 1996, 1998 and 2002 (Fig. 2.8). In addition, two weak cohorts (2005 and 2006) were selected because sampling occurred more frequently after 2005 and they could be compared with the stronger cohorts, and allowed comparisons between two subsequent cohorts.

To ensure that cohorts of approximately the same age were selected, age validation samples were chosen that had mean TLs within a range of ± 1 cm (1996, 1998 and 2002 cohorts) or ± 2 cm (2005 and 2006 cohorts) of the general growth curve. This was done to exclude sub-cohorts spawned more than 1.5 months earlier or later (Fig. 3.1). Each otolith sample consisted of a collection of otoliths from the same day and the same fur seal colony. Individual otoliths were selected from each sample so as to fall within the range of the mean otolith diameter (OD) ± one standard deviation. This reduced the number of samples for the five cohorts from an initial 130 to 94 samples and 3474 otoliths (Table 3.1). Where possible, 40–50 otoliths per sample were chosen for age validation purposes. If scat samples were available from more than one colony from the same day, 40 (or the maximum number of available) otoliths were sampled from each.

Table 3.1 The sampling period, number of samples (collected on the same day at the same fur seal colony), minimum and maximum number of otoliths analysed per sample and the total number of otoliths sampled for age validation for each of five cohorts (named after their hatching year) of juvenile *M. capensis*.

Cohort	Sampling period	No of samples	Min no. of otoliths analysed per sample	Max no. of otoliths analysed per sample	Total number of otoliths analysed
1996	24 Oct 1996 – 27 Nov 1997	13	30	40	500
1998	21 Oct 1998 – 27 Oct 1999	12	12	43	411
2002	20 Nov 2002 – 28 Apr 2004	27	30	50	1015
2005	04 Oct 2005 – 20 Oct 2006	34	30	40	1288
2006	16 Jan 2007 – 27 Dec 2007	8	20	40	260
Total		**94**			**3474**

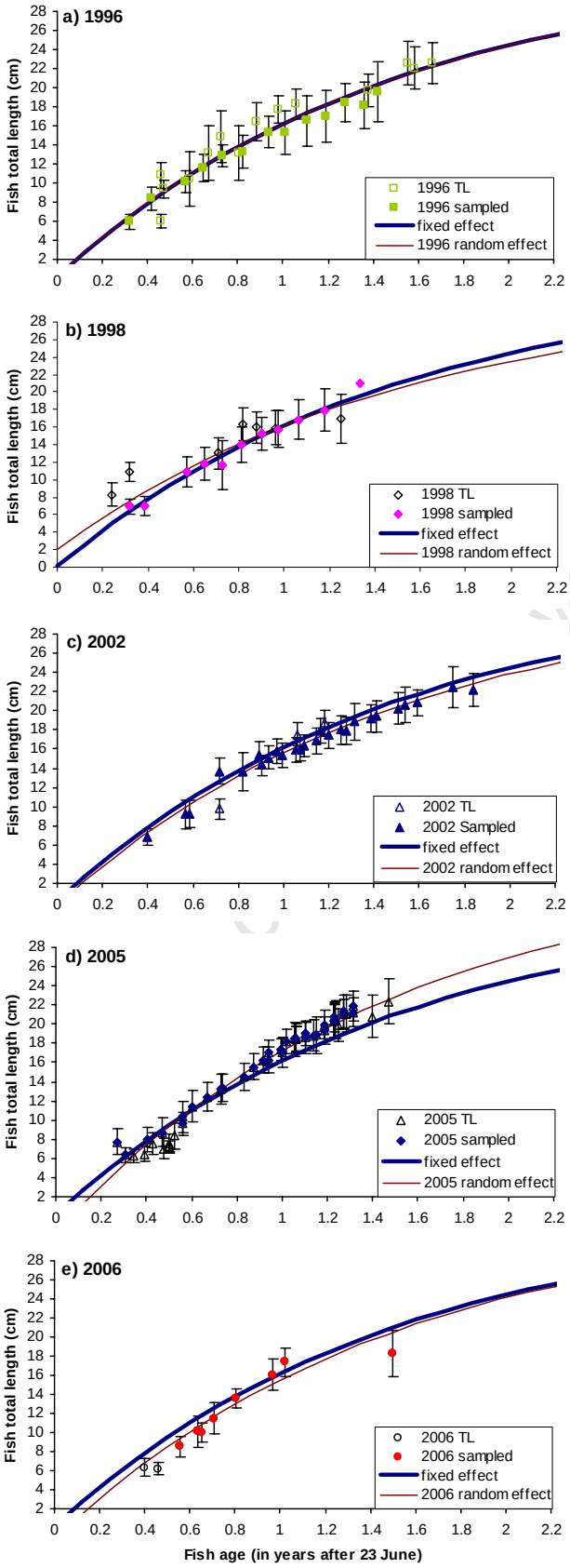

Figure 3.1 Mean (± standard deviation) fish lengths (cm) of *M. capensis*, calculated from otoliths from fur seal scats, plotted against estimated age (years) for the five selected cohorts used for age validation. The open points show all samples originally collected and used for growth rate calculations (Fig. 2.7). The solid points show those selected for age validation in this study). The von Bertalanffy growth function (VBGF, fixed, thick solid lines) and each cohort's random effects VBGF (thin solid lines) are indicated on the plot (see Fig. 2.7).

3.3.2 Otolith interpretation

Only otoliths that did not have a chalky (heavily oxidized) appearance due to digestion or where the visibility of the zonation did not seem to be affected and those with relatively intact margins were chosen for these analyses. Otoliths were submerged in water and viewed whole against a dark background under reflected light using a Leica L2 MZ75 dissecting microscope at 10 x (for otoliths < 10 mm in diameter) or 6.3 x magnification (for otoliths ≥ 10 mm in diameter). The microscope was fitted with an eyepiece micrometer and, for each otolith, the total OD was measured. *Complete* translucent zones (when an opaque zone was visible after the translucent zone) were counted and the OD at each *complete* translucent zone was measured – along the longest axis of the otolith from the anterior to the posterior outer margin of the translucent zone (Fig. 3.2). Only translucent zones that were clearly visible on both anterior and posterior tips were counted and measured. Translucent zones were mostly clearer on the medial (proximal) side (Fig. 3.2). The translucent zones were counted as first, second and third (T1, T2, T3 and so on) as they occurred from the core to the otolith edge. The edge of each otolith was noted to have a translucent zone on the edge as present or absent. The total OD measured was corrected for erosion (Equation 2.1).

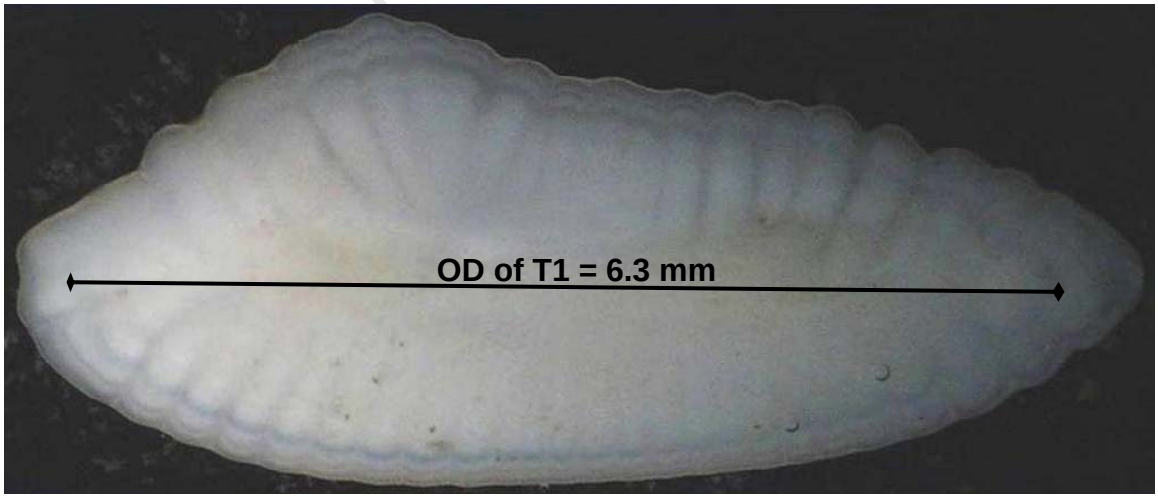

Figure 3.2 Medial side of *M. capensis* otolith recovered from fur seal scat samples at 20 x magnification. Total otolith diameter (OD) = 7.4 mm. OD of the first translucent zone (T1, indicated by the black line) = 6.3 mm. The otolith shows two translucent zones and an opaque edge (i.e. the second translucent zone is complete).

3.3.3 Analysis of time of formation and diameter of translucent zones

For each cohort, the periodicity of translucent zones occurring on the otoliths was tested in the following ways. To separate formation time of the first, second and third translucent zones, proportions of otoliths containing at least one, at least two and at least three (j) translucent zones were plotted against sampling date and modelled using a two-parameter logistic ogive:

$$P_j = \frac{1}{1 + e^{\frac{-(d - d_{50})}{\delta}}} \quad (3.1),$$

where P_j is the expected proportion of fish showing a complete j^{th} translucent zone at date d (in days after 1 January 1996). Estimated parameter d_{50} (in days) was converted to the date at which 50 % of the fish have formed the j^{th} translucent zone (called here "date at 50 % completion" or $Date_{50}$) and δ is the width of the ogive (days).

Parameter estimates were obtained by non-linear minimisation of the binomial negative log-likelihood function:

$$-LL = -\sum_i \left[h_i \ln\left(\hat{P}_{ji}\right) + (n_i - h_i)\ln\left(1 - \hat{P}_{ji}\right) \right] \quad (3.2),$$

where $-LL$ is minimised for the j^{th} translucent zone, n_i is the number of otoliths examined in sample i and h_i is the number of otoliths in the i^{th} sample showing a complete j^{th} translucent zone.

To fully describe otolith growth of young *M. capensis*, ODs (mm) at which 50 % of fish have formed the first, second and third translucent zones (OD_{50}) were also calculated. This was done by fitting a logistic ogive (Equation 3.1) to proportion of fish showing a complete j^{th} translucent zone as a function of total $OD_{corrected}$ (mm). Mean OD (mm) measured at each complete translucent zone for each cohort was also calculated.

Variance estimates of the $Date_{50}$ and OD_{50} parameters were calculated using proportion of fish showing the j^{th} translucent zone at each sampling date, or OD (mm) class, and applying parametric bootstrap re-sampling procedures with 1000 replicates drawn from a binomial distribution (Efron and Tibshirani, 1986). Confidence intervals (CIs) were constructed using the percentile method of Buckland (1984) (Beamish *et al.*, 2005).

All calculations were performed using the Newton algorithm in the Microsoft® Office Excel Solver routine.

3.3.4 Edge analysis

Edge analysis was performed by calculating the proportion of otoliths with a translucent zone present on the edge for each sampling date. Cyclical occurrence of translucent zones was described by a logistic periodic regression model (Flury and Levri, 1999) fitted to the proportion of translucent zones present on the otolith edge against date:

$$\log it\left(\hat{\theta}_i\right) = \beta_0 + \beta_1 \sin\left(\frac{2\pi}{P} T_i\right) + \beta_2 \cos\left(\frac{2\pi}{P} T_i\right) \quad (3.3),$$

where $\hat{\theta}_i$ is the predicted proportion of otoliths with a translucent zone on the edge, T_i is the decimal time in months, and $\log it(\hat{\theta}_i)$ is $ln(\hat{\theta}_i / 1-\hat{\theta}_i)$, thus

$$\hat{\theta}_i = \frac{e^{\log it(\hat{\theta}_i)}}{1 + e^{\log it(\hat{\theta}_i)}} \quad (3.4).$$

1 January was assigned a value of 0 and 1 December a value of 11, thus T (months) was calculated as: 12*[(sampling date – 1 January of the same year)/365]. P is the assumed period (decimal months) of translucent zone formation (12 for an annual cycle and 6 for a biannual cycle), β_0 is the intercept and β_1 and β_2 are the *sin* and *cos* regression parameters respectively (Beamish *et al.*, 2005; Winker *et al.*, 2010). Parameters were estimated using a binomial negative log-likelihood function (Equation 3.2, where h_i is the number of otoliths in the i^{th} sample with a translucent zone present on the edge) and the Newton algorithm of the Microsoft® Office Excel Solver routine.

Seasons were divided into four 3-month periods within the year; summer: 1 December to 28 February, autumn: 1 March to 31 May, winter: 1 June to 31 August and spring: 1 September to 30 November.

3.4. Results

Total OD (corrected for erosion) measured for all 3474 samples ranged between 1.5 mm (1996 cohort) and 13.8 mm (2002 cohort). The maximum number of complete translucent zones on otoliths of each cohort ranged between two (2006 cohort) and five (2002 cohort). The OD measured at each translucent zone ranged between 2.0 mm for the 2005 cohort and 12.3 mm for the 2002 cohort (Table 3.2). Since only *complete* translucent zones were used, the measurements of these would not have been affected by otolith erosion due to digestion. No difference in appearance of zonation was observed between digested otoliths and (previously viewed) non-digested otoliths.

Table 3.2 Minimum (min) and maximum (max) total otolith diameters (OD), numbers of translucent zones (minimum was always 0) and ODs at each translucent zone (T) for each of five *M. capensis* cohorts (named after their hatching year).

Cohort	Min total OD (mm)	Max total OD (mm)	Max number of translucent zones	Min OD of T (mm)	Max OD of T (mm)
1996	1.5	12.5	4	2.7	11.2
1998	2.4	11.2	3	2.6	9.8
2002	2.4	13.8	5	2.5	12.3
2005	1.8	12.1	4	2.0	10.9
2006	3.3	11.5	2	2.8	10.7

3.4.1 Timing of the first three translucent zones

Formation of the first (T1), second (T2) and third (T3) translucent zones was distributed over a period of up to 10 months with considerable overlap and following a logistic ogive (Fig. 3.3).

For the 1996 cohort (Fig. 3.3a), the T1 zone was visible in late October 1996, with 100 % of the otoliths containing at least one complete translucent zone by late June 1997, eight months later. The T2 zone was first visible by February 1997 and T3 by August 1997, both not completed on all otoliths by the end of the series. Six otoliths of the 1996 cohort had a T4 zone from September 1997 onwards.

For the 1998 cohort, T1 was visible only from January 1999 onwards and took until October 1999, about 9 months, to complete on all otoliths (Fig. 3.3b). The earliest T2 was visible in January 1999 and the earliest T3 in June 1999. No T4 was seen.

T1 of the 2002 cohort was first visible in late November 2002 (Fig. 3.3c) and was completed on 100 % of the otoliths by early June 2003 (6.5 months later). As a result, $Date_{50}$ was 27 January 2003, the earliest of the cohorts (Table 3.3). T2 was first visible in March 2003 and visible on all otoliths by February 2004. T3 was first visible in April 2003. Twelve otoliths of the 2002 cohort showed T4, from July 2003 onwards, and on two otoliths a fifth translucent zone (T5) was seen in January 2004 (Fig. 3.3c).

For the 2005 cohort, T1 was already visible by early October 2005, but was only completed on 100 % of the samples by early September 2006, 11 months later. Both T2 and T3 were visible from January 2006 onwards. Two otoliths of this cohort showed T4, in October 2006 (Fig. 3.3d).

Only two translucent zones were apparent in the time series of the 2006 cohort. T1 was first visible by January 2007, but already completed on all otoliths of the sample by June 2007, less than six months later. T2 was visible from March 2007 onwards (Fig. 3.3e). No T3 could be seen on any otolith for this cohort.

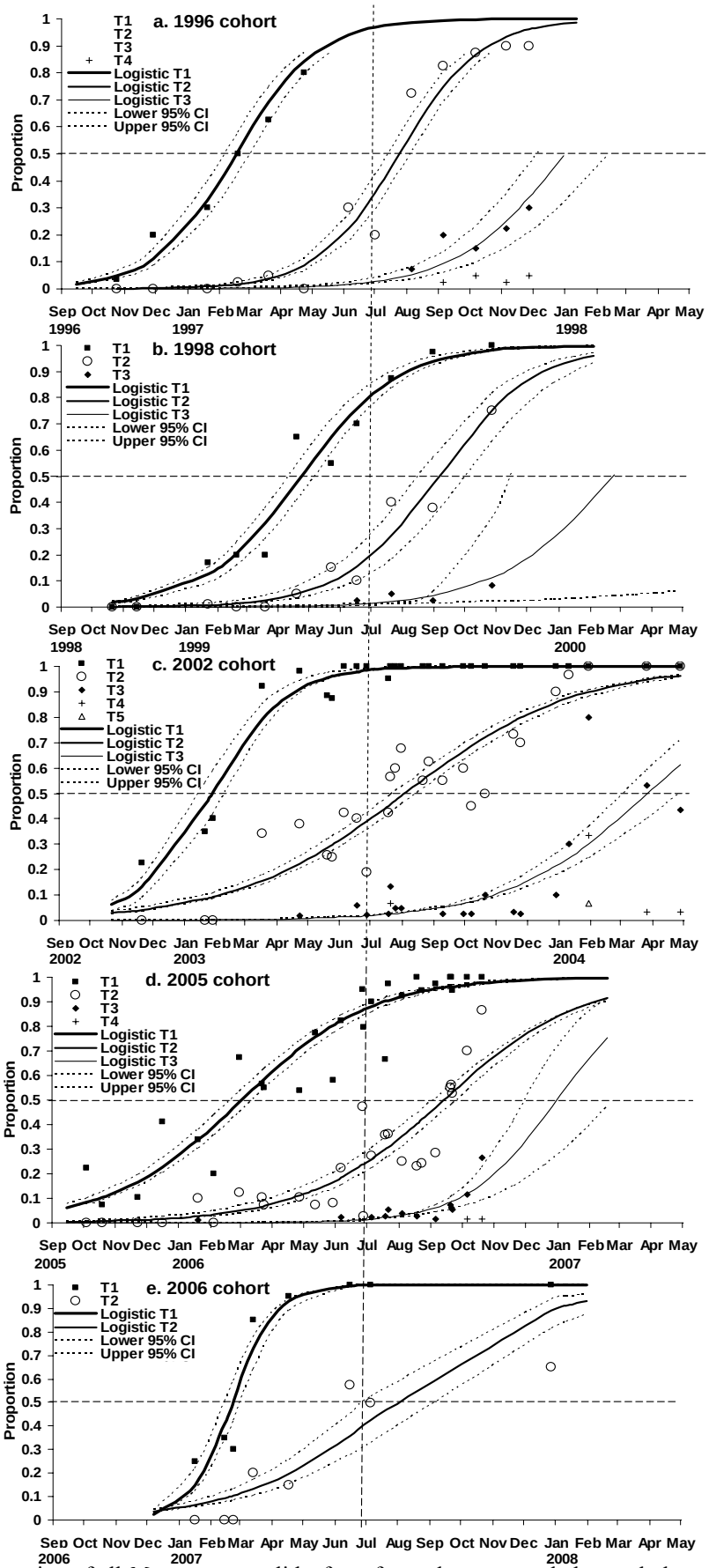

Figure 3.3 Proportion of all *M. capensis* otoliths from fur seal scats sampled at each date showing at least one to five (T1–T5) *complete* translucent zones for five cohorts **a.** 1996, **b.** 1998, **c.** 2002, **d.** 2005 and **e.** 2006. Solid lines represent logistic ogives fitted to each data set and broken lines represent the upper and lower 95 % confidence intervals around these ogives. Horizontal broken lines represent the 50 % line. Vertical broken lines indicate dates at which the fish turn one year old.

Table 3.3 shows that $Dates_{50}$ of T1 usually fell between January and April (summer–autumn), the earliest for the 2002 cohort (27 January) and latest for the 1998 cohort (23 April). T2 was formed between 24 July (1996 cohort) and 12 September (2005 cohort), winter–spring, while T3 was again formed in summer: 30 December (2005 cohort) to 26 March (2002 cohort). The δ values (width of the ogive in days) ranged between 21 days (steepest fit, T1 of the 2006 cohort) and 82 days (T2 of the 2002 cohort, reflected by the long period of formation, Fig. 3.3). The 95 % CIs reflect this range, usually showing CIs of 15–26 days for T1 and T2. T3 usually showed a 2–5-month wide CI, because of the incomplete series of T3 (Fig. 3.3).

Table 3.3 Date at 50 % formation ($Date_{50}$), with their 95 % confidence intervals (CI) derived from 1000 bootstraps, and δ (days) (Equation 3.1) calculated for the first three translucent zones (T1–T3) for five cohorts of Namibian *M. capensis* spawned in 1996, 1998, 2002, 2005 and 2006.

	T1			T2			T3		
Cohort	***Date*$_{50}$**	**95 % CI**	**δ**	***Date*$_{50}$**	**95 % CI**	**δ**	***Date*$_{50}$**	**95 % CI**	**δ**
1996	16 Feb 1997	05 Feb – 01Mar	39	24 Jul 1997	12 Jul – 04 Aug	39	31 Dec 1997	04 Dec – 12 Feb	52
1998	23 Apr 1999	10 Apr – 06 May	47	04 Sep 1999	16 Aug – 01 Oct	47	22 Feb 2000	14 Nov – 22 Jul	57
2002	27 Jan 2003	15 Jan – 08 Feb	37	02 Aug 2003	22 Jul – 14 Aug	82	26 Mar 2004	02 Mar – 25 Apr	69
2005	02 Mar 2006	18 Feb – 12 Mar	62	12 Sep 2006	02 Sep – 24 Sep	66	30 Dec 2006	29 Nov – 22 Feb	43
2006	21 Feb 2007	13 Feb – 28 Feb	21	27 Jul 2007	27 Jun – 30 Aug	72	None		

3.4.2 Diameters of the first three translucent zones

The mean width of a "normal" translucent zone was 0.45 mm ± 0.3 mm. The proportions of otoliths containing T1–T3 translucent zones for different OD classes (mm) showed considerable overlap (Fig. 3.4). The smallest otoliths with a complete T1 were 2.5 mm in diameter (2002 and 2005 cohorts). These two cohorts showed 100 % otoliths with T1 in the smallest (6.5 mm) and largest (9.5 mm) OD classes. OD_{50} of T1 was smallest for the 2002 (4.4 mm) and largest for the 1998 cohort (6.6 mm) (Fig. 3.4; Table 3.4). The 2002 cohort showed the smallest OD_{50} of T2 and T3, while the 2005 cohort showed the largest for both. Mean measured OD at each translucent zone was similar within and between cohorts (5.8–6.9 mm T1, 7.3–8.4 mm T2, and 8.3–9.1 mm T3) (Table 3.4). OD_{50} at T1 was smaller than the mean of T1 of all samples. Projected OD_{50} were estimated higher for T3 than the mean of measured ones because of the incomplete series (Fig. 3.4), again reflected by the 95 % CI values (Table 3.4).

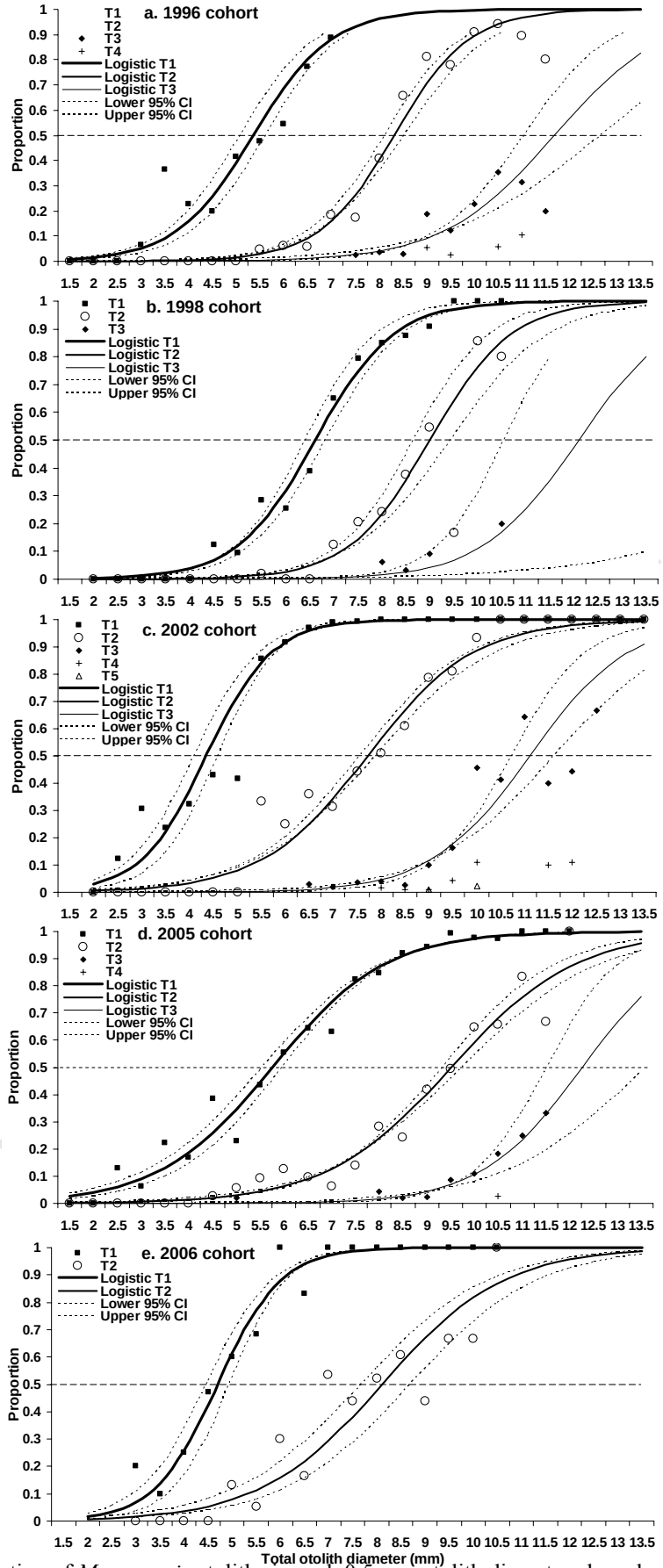

Figure 3.4 Proportion of *M. capensis* otoliths in each 0.5 mm otolith diameter class showing at least one to five (T1–T5) *complete* translucent zones for five cohorts **a.** 1996, **b.** 1998, **c.** 2002, **d.** 2005 and **e.** 2006. The solid lines represent logistic ogives fitted to each data set and broken lines represent the upper and lower 95 % confidence intervals of these ogives. Horizontal broken lines represent the 50 % line.

Table 3.4 OD at 50 % formation (OD_{50}) and δ (cm) (Equation 3.1), mean (± standard deviation, SD) and range of OD (in mm) calculated for the first three *complete* translucent zones (T1– T3) for five cohorts of *M. capensis*, spawned in 1996, 1998, 2002, 2005 and 2006. Data were based on otoliths from fur seal scat samples collected at monthly intervals in Namibia.

			T1			
Cohort	OD_{50}	**95% CI**	δ	**Mean**	**SD**	**Range**
1996	5.4	5.1 – 5.6	0.8	6.6	1.2	2.7 – 10.3
1998	6.6	6.4 – 6.8	0.8	6.3	1.0	2.6 – 9.8
2002	4.4	4.1 – 4.6	0.7	6.4	1.1	2.5 – 10.2
2005	5.8	5.5 – 6.0	1.2	6.9	1.2	2.0 – 10.6
2006	4.7	4.5 – 4.9	0.7	5.8	1.4	2.8 – 8.7
			T2			
Cohort	OD_{50}	**95% CI**	δ	**Mean**	**SD**	**Range**
1996	8.3	8.1 – 8.5	0.8	8.4	1.1	5.1 – 11.2
1998	9.0	8.7 – 9.4	0.8	7.7	0.9	5.3 – 9.5
2002	7.7	7.5 – 7.9	1.1	7.8	1.2	4.9 – 11.4
2005	9.5	9.3 – 9.7	1.3	8.2	1.0	3.9 – 10.4
2006	8.1	7.7 – 8.7	1.3	7.3	1.3	4.3 – 10.7
			T3			
Cohort	OD_{50}	**95% CI**	δ	**Mean**	**SD**	**Range**
1996	11.7	11.0 – 12.7	1.2	9.1	0.9	6.3 – 11.1
1998	12.1	10.5 – 18.1	1.0	8.3	0.8	7.5 – 9.4
2002	11.1	10.7 – 11.6	1.0	9.1	1.3	6.1 – 12.3
2005	12.3	11.5 – 13.6	1.1	8.8	1.0	4.8 – 10.5
2006			None			

3.4.3 Early otolith growth patterns – summary

Figure 3.5 shows the summarised results of Figures 3.3 and 3.4 and Tables 3.3 and 3.4. T1 is usually formed between January and April (summer–autumn) between 4 and 7 mm OD. The estimated ages of young *M. capensis* at that time are between 7 and 10 months. T2 is formed 4.5 to 6.5 months later, between the last week of July at 8.0 mm OD and the first 10 days of September at 9.5 mm OD (winter–spring). Generally, a later translucent zone was formed at a larger OD. T3 (projected) is expected to be formed another 4 to 8 months later, from between the end of December and the end of March (summer–autumn), between 11 and 13 mm OD (Fig. 3.5).

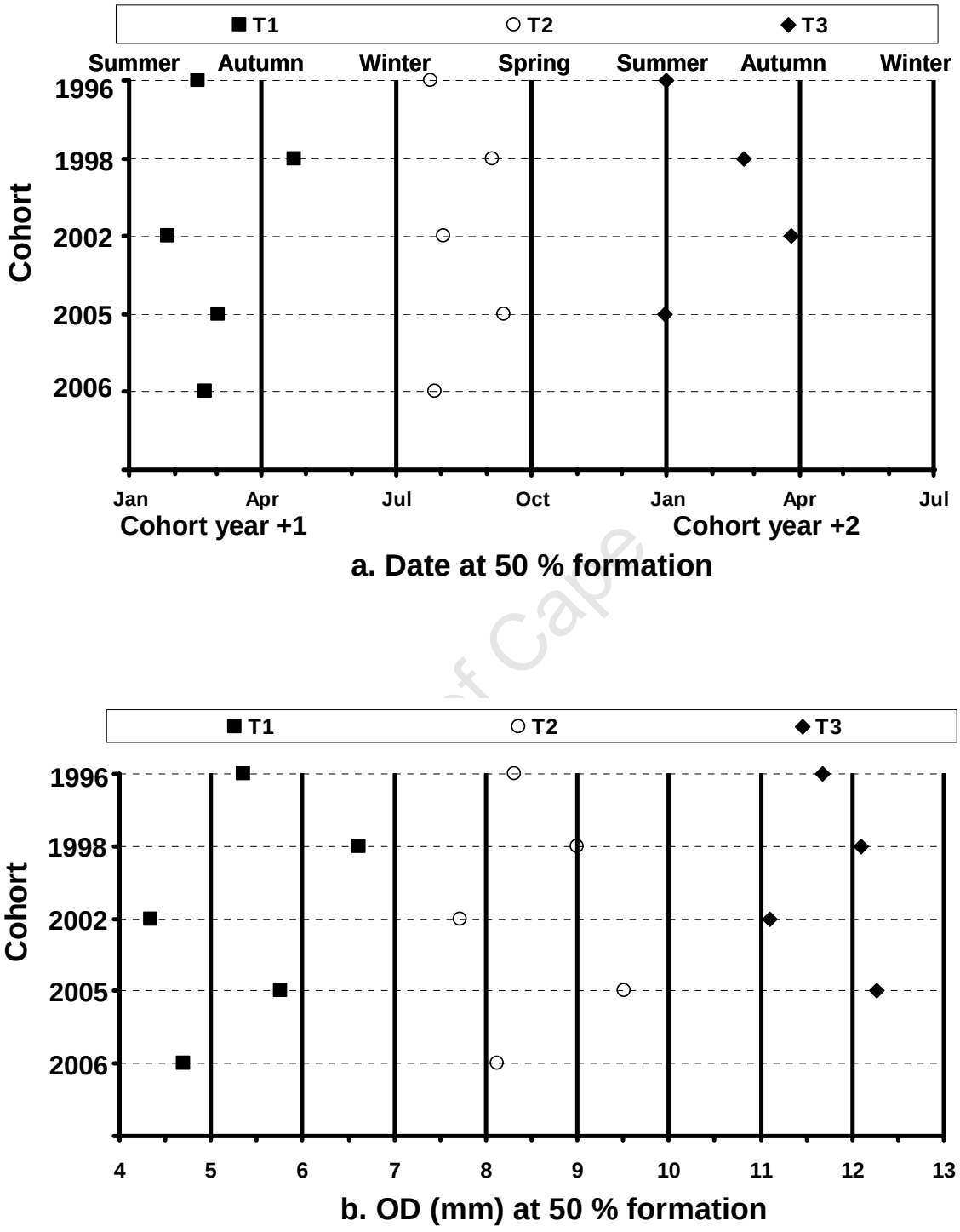

Figure 3.5 a. Date at 50 % formation ($Date_{50}$) and **b.** OD (mm) at 50 % formation (OD_{50}) of the first (T1), second (T2) and third (T3) *complete* translucent zones on otoliths of young *M. capensis* collected from fur seal scat samples for five cohorts hatched in 1996, 1998, 2002, 2005 and 2006.

3.4.4 Edge analysis

The logistic periodic regression fitted to proportions of otoliths with a translucent edge (Fig. 3.6; Table 3.5) showed a better fit for biannual peaks of translucent edges for the 1996 and 2006 cohorts, showing January- and July- peaks and February- and August-peaks respectively. For the other three cohorts an annual peak gave the better fit to the data (April–May for the 1998 and 2002 cohorts, and August–September for the 2005 cohort). The peaks always coincided with at least one of the first three translucent zones' $Dates_{50}$. The timing of the first annual peak of the 1996 cohort (January) (Fig. 3.6a; Table 3.5) coincides with the $Date_{50}$ of T1 and T3 (Table 3.3). The time of the second peak (July) (Fig. 3.6a; Table 3.5) coincided with the $Date_{50}$ of T2 (Table 3.3). The peak proportion of translucent edges shown for the 1998 cohort (April–May) (Fig. 3.6b; Table 3.5) coincided with the $Date_{50}$ of T1 and T3, while the T2 $Date_{50}$ still fell within the end of that peak (compare Table 3.3 and Fig. 3.6b). The 2002 cohort's peak of proportion translucent edges in April–May (Fig. 3.6c; Table 3.5) coincided with the $Date_{50}$ of the T3 (Table 3.3). The 2002 cohort had a high proportion of translucent edges in January 2003, a less clear pattern than for the other years (for which only one monthly sample was available) as well as many points that do not fit either of the two lines for estimated cyclical patterns. The 2005 cohort showed only one annual peak of proportion translucent edges (August–September) (Fig. 3.6d; Table 3.5), coinciding with the $Date_{50}$ of T2 (Table 3.3). The 2005 cohort also showed many fluctuations from the estimated lines. The 2006 cohort showed a clear biannual pattern of proportion translucent edges in February and August (Fig. 3.6e; Table 3.5), coinciding with the $Dates_{50}$ of T1 and T2, respectively (Table 3.3).

Although the pattern of translucent zone periodicity is less clear with edge analysis, the three general repeated patterns observed still seem to be January–February or April–May (summer–autumn) and July–September (winter–spring). This coincides with the formations of the first to third translucent zones (T1–T3), which are often overlapping and continuous over a period of six months (compare Figs 3.3 and 3.6).

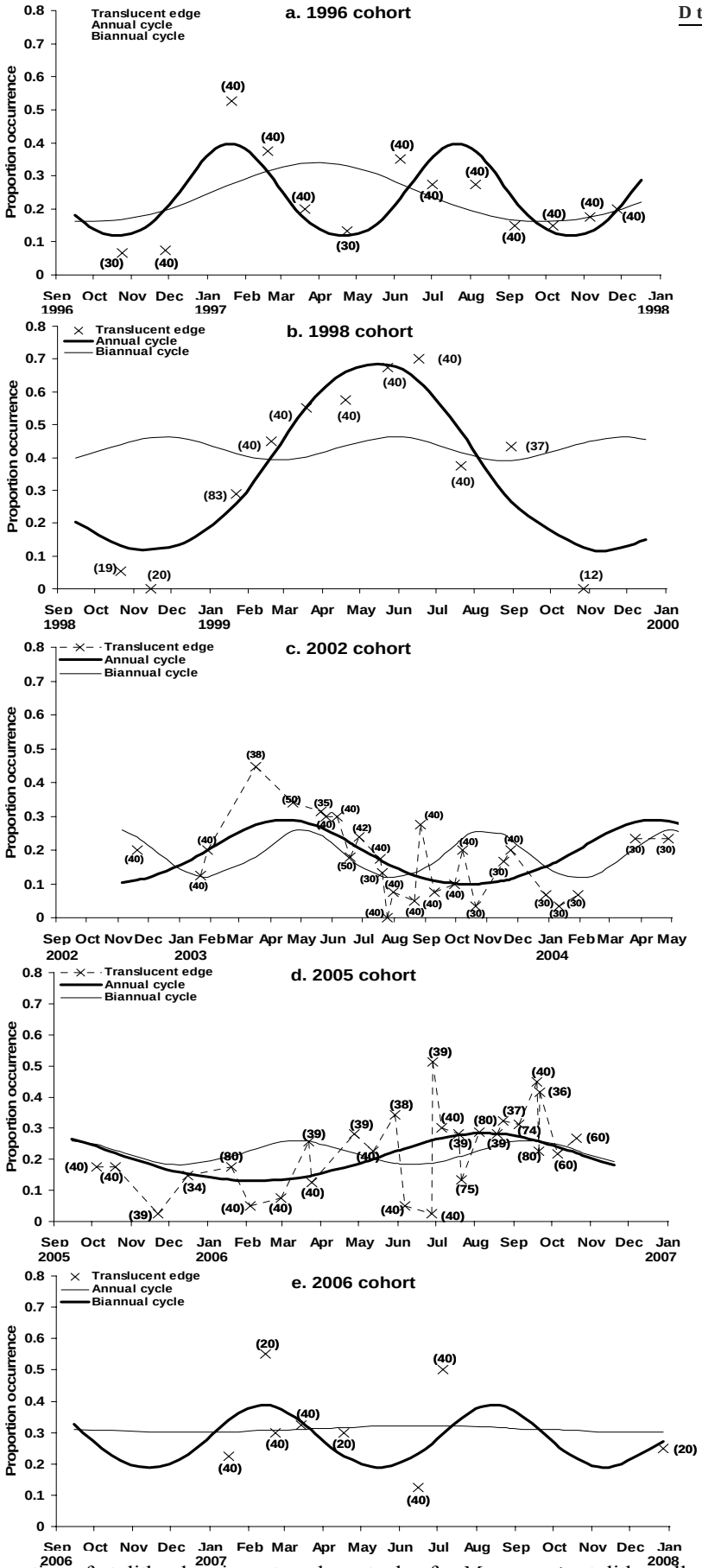

Figure 3.6 Proportion of otoliths showing a translucent edge for *M. capensis* otoliths collected from fur seal scat samples for five cohorts **a.** 1996, **b.** 1998, **c.** 2002, **d.** 2005 and **e.** 2006. Solid lines depict predicted biannual and annual cycles of translucent zone formation fitted by binomial periodic regression. The better-fitting cycle is represented as the thicker line for each cohort. Numbers in brackets denote sample sizes.

Table 3.5 Logistic periodic regression model parameter (Equation 3.3) estimates for annual (period P = 12 months) and biannual (P = 6 months) fits predicting the temporal probability of a translucent zone present on the edge of an otolith for five *M. capensis* cohorts identified from otoliths from fur seal scat samples collected in Namibia. -*LL* refers to the log-likelihood estimates (Equation 3.2). "Peaks" indicates the months in which the presence of a translucent zone on the edge of the otolith was estimated to be at a peak. The best-fit model for each cohort is highlighted (bold).

	Cohort									
Parameter	**1996**		**1998**		**2002**		**2005**		**2006**	
P	12	**6**	**12**	6	**12**	6	**12**	6	12	**6**
β_0	-1.16	**-1.21**	**-0.599**	-0.296	**-1.55**	-1.52	**-1.41**	-1.27	-0.795	**-0.958**
β_1	0.494	**0.487**	**1.062**	-0.138	**0.645**	-0.405	**-0.283**	0.148	0.014	**0.500**
β_2	0.0235	**0.628**	**-0.888**	0.0485	**-0.142**	-0.261	**-0.397**	-0.174	-0.047	**0.053**
-LL	265	**258**	**247**	280	**466**	471	**679**	687	161	**159**
Peaks	Apr	**Jan & Aug**	**May–Jun**	Jun & Nov	**Apr–May**	May & Nov	**Aug**	Mar & Sep	Jun–Jul	**Feb & Aug**

3.5. Discussion

If fish- and otolith growth rates continue at a steady rate, and if otoliths take about 18 months to increase in size by 12 mm (Tables 3.3 and 3.4), a translucent zone of 0.1–0.8 mm would take about 0.2–1.2 months (6 to 36 days) to complete in an individual fish. This is an under-estimate of the range compared to results from microstructure analysis of *M. capensis* otoliths by Gordoa *et al.* (2001), showing a range between 3 and 113 days and an average of 29 days for the translucent zone of an individual fish to complete. The population takes much longer for the completion of each translucent zone.

In the first 18 months of *M. capensis*' life, three translucent zones are generally formed on their otoliths. In the population, each of the three translucent zones is formed over a long period of between 6 and 9 months and over a range of 4–7 mm OD (Figs 3.3 and 3.4). T1 is formed between late summer and autumn, 7–10 months after their estimated 23 June winter hatchdate, and is therefore not an annulus. T1 is formed between 4 and 7 mm OD (Fig. 3.4) and is not always formed or at least not always visible. OD_{50} at T1 was smaller than the mean measured T1 of all samples (Table 3.4), because often the smaller, earlier formed T1 was not visible in larger otoliths. The converted fish total length (TL) range for this OD range is 9.0–13.5 cm (Table 3.6). T2 is formed another 4.5 to 6.5 months after the first, between mid-winter and spring, when fish are between 13 and 15 months old. This means that T2 is the first annulus, which forms on otoliths between 7 and 10 mm in diameter (Fig. 3.5) and at 15.9 to 19.9 cm fish TL (Table 3.6).

T3 is again a summer-formed translucent zone and is also not an annulus, forming at 11.1–12.3 mm OD and a fish TL of between 23.7 and 26.5 cm (Table 3.6). These patterns were surprisingly similar over the time-span of ten years (1996–2006) and comparable between strong and medium-sized cohorts (Table 2.2). The measurements are consistent, but pertain to fast growth rates of a depleted stock and should be revisited when the stock recovers. Even if the hatchdate had been estimated too early (see Chapter 2) this would not change the overall conclusions, as the annulus was taken as later than 23 June (Fig. 3.5).

Comparing results of this study with previous age determination studies on Namibian *M. capensis* shows that what was previously called "age group II" should have been termed age group I (+) (Wysokiñski (1983), on which ICSEAF (1983) is based) as fish of that length are only 1.5 years old (at T3, Table 3.6). Brinkman (2007) also assigned T2 correctly to age 1 (19.3 cm, Table 3.6), but also mostly (incorrectly) counted T3, the summer translucent zone, as the second annulus (25.6 cm, Table 3.6). Both these results were confirmed by Gordoa *et al.* (2001), who showed that reading the first two "annuli" on *M. capensis* otoliths mostly over-estimated age (only agreeing 1/3 of the time), while their estimated fish length was 18–24 cm TL for 1-year-olds (roughly corresponding with T2–T3 in this study, Table 3.6). Annuli (winter translucent zones) are not clearly distinguishable from summer translucent zones, being equally conspicuous and similar in appearance, which is why the summer translucent zones were previously counted as annuli. It is likely that from 1.5 years onwards a translucent zone is formed every summer, but further confirmation of these results of biannual translucent zone formation and possible over-estimation of previous *M. capensis* ages is needed for older fish (Chapter 4).

Table 3.6 Fish total length (TL) in cm at translucent zone formation converted from OD_{50} 95 % CI and range (using Equation 2.2) in Table 3.4 (this study). For other studies, the mean back-calculated fish TL was used when available. All measurements are in cm. Headings (bold) for each study refer to the terms used for translucent zones or age groups. Wysokiñski's (1983) age group O contained a "demersal ring". Brinkman's (2007) translucent zones before her identified first annulus (1) were called pre-annuli (P1–P3) and her f1 is an identified translucent zone after 1. Colloca *et al.*'s (2003) S1 and S2 are summer translucent zones. Goicochea *et al.*'s (2010) measurements were derived from mean TLs at ages from daily increment counts (2009 and 1987 samples combined). "P" stand for pelagic, "D" for demersal and "R" for identified recruitment rings.

	Cohort									
This study Namibian *M. capensis*	**1996**			**T1 (summer)**		**T2 (winter /annulus)**		**T3 (summer)**		
	1998			10.9		17.1		25.1		
	2002			13.5		18.7		26.1		
	2005			9.0		15.9		23.7		
	2006			11.7		19.9		26.5		
	95 % CI (all cohorts)			9.6		16.8				
	Measured TL range (all cohorts)			10.4 – 13.9		15.5 – 20.4		22.3 – 42.1		
				2.0 – 22.4		8.1 – 25.0		9.9 – 26.7		
Other studies on Namibian *M. capensis*	**Wysokiñski (1983)**			**O**		**I**		**II**		**III**
	Mean fish TL			10		16		25		29
	TL range			8 – 12		9 – 22		18 – 31		26 – 31
	Brinkman (2007)		**P3**	**P2**	**P1**	**1**	**f1**	**2**		
	Mean fish TL		7.7	10.9	13.4	19.3	20.9	25.6		
	TL range			5.8 – 16.7		13.4 – 26.1		17.2 – 33.8		
	Gordoa *et al.* (2001)							**1 - from daily increments**		
	Mean fish TL							22.3		
	TL range							18 – 24		
Other hakes *M. hubbsi*	**Norbis *et al.* (1999)**		**P**	**D**		**1**				
	Mean fish TL		8.4	13.5		20.6				
	TL range		3 – 17	6 – 20		13 – 31				
M. merluccius Central Mediterranean	**Colloca *et al.* (2003)**	**P**	**R**	**S1**	**1**	**S2**		**2**		
	Mean fish TL	3.4	8.8	11.1	14.7	20.6		26.3		
	TL St.Dev.	2.1 – 4.7	7.2 – 10.4	9.8 – 12.4	12.7 – 16.7	18.8 – 22.4		23.4 – 29.2		
Northeast Atlantic Iberian Atlantic			**0**	**0**		**1**		**2**		**3**
	Godinho *et al.* (2001)		8.3			16.1		23.4		30.1
	Piñeiro and Saínza (2003)			11.9		20.6		29.0		36.7
M. gayi Peru	**Goicochea *et al.* (2010)**				**0.5**	**1**		**1.5**		**2**
	Mean fish TL				16.1	21.9		27.7		33.5

Previously, translucent zones before the first annulus have been described as "pelagic rings" (the smaller one, said to often "disappear" in fish older than 1 year) and "demersal rings" (ICSEAF, 1983; Wysokiñski, 1983). These were thought to be formed in the juvenile phase, the second one associated with the change in habitat when *M. capensis* move from being mainly pelagic to being mainly demersal dwellers. However, the demersal settlement process for *M. merluccius* (up to 140 m bottom depth) was only 40–60 days long, and typically European hake settled at fish TLs of

1.6–3.0 cm (Arneri and Morales-Nin, 2000; Belcari *et al.*, 2006). For silver hake *M. bilinearis*, settlement took place at a mean age of 35 days at 1.5 cm TL (Steves and Cowen, 2000). Demersal settlement of *M. hubbsi* started at 50 days (15 mm TL) and finished at about 80 days and 30 mm TL (Buratti and Santos, 2010). It is likely that this timing is similar in *M. capensis* as Gordoa *et al.* (2001) showed that the mean duration of the primordia in otoliths of *M. capensis* is 45 days and the second primordium has been described to indicate the demersal phase (Arneri and Morales-Nin, 2000). In addition, young *M. capensis* from 7 cm (2–5 months-old, Chapter 2) have been caught in bottom trawls (up to 188 m bottom depth) and were observed as migrating to full depth on an experimental hake survey (Stenevik *et al.*, 2009). This means that a change from pelagic to demersal habitat is not the reason for the formation of the first translucent zone. The diet studies conducted on Namibian or South African *M. capensis* (Payne *et al.*, 1987; Traut, 1996; Shannon and Roux, 2000) are not sufficiently detailed at the length ranges (11, 18 or 25 cm) to determine changes in diet composition as a cause for translucent zone formation, but no noticeable switch is observed on the large scale.

The presence of *M. capensis* of up to 26 cm in the fur seal diet (Chapter 2) means the fish occur over the inner continental shelf and shelf break, within 200 m bottom depth off central Namibia or within 500 m bottom depth in the north or the south (Wolf- and Atlas Bay). Fur seals' foraging ranges generally do not exceed 150 km from the shoreline (Skern-Mauritzen *et al.*, 2009). They feed most frequently on the continental shelf and on or near the bottom (de Bruyn *et al.*, 2003; 2005). The entire area close to the oceanic bottom on the shelf and shelf break up to 150 km offshore from 20 to 27ºS may be covered by the same water mass, High Salinity Central water, HSCW (also called the Western South Atlantic Central water WSACW, or South Atlantic Central water SACW in the literature) at 8–16ºC and 34.7–35.7 salinity (Duncombe Rae, 2005). However, % coverage of the HSCW may depend on season or mixing (upwelling regime) and may even differ between years in the same season (Mohrholz *et al.*, 2008). This means the fish may undergo some changes in terms of the temperature or salinity they are exposed to through the length ranges sampled in this study. Depth and latitude distributions of *M. capensis* and water temperature as possible reasons for translucent zone formation are addressed in Chapters 5 and 6, respectively.

Studies on other hakes support the back-calculated fish TL from translucent zone measurements found in this study (Table 3.6). Back-calculated fish-TLs at the "pelagic ring", "demersal ring" and age 1 (first annulus) on *M. hubbsi* from the Uruguayan continental shelf (Norbis *et al.*, 1999) roughly correspond to those of T1 ("pelagic" and "demersal" rings) and T2–T3 ("age 1" zone) in this study (Table 3.6). T1 observed in this study covers the length ranges of both the "pelagic" or "demersal" ring of Norbis *et al.* (1999), but the smaller one of the two is sometimes absent on *M. capensis*. Norbis *et al.* (1999) used sliced otoliths on which small translucent zones may always be clearly visible. Alternatively, *M. hubbsi* could be forming an additional translucent zone on otoliths of young fish. Colloca *et al.* (2003) showed more than two pre-first-annulus rings being formed on (Mediterranean) *M. merluccius* otoliths (Table 3.6). They showed a "pelagic ring" (P) back-calculated at 3.4 cm TL, "demersal ring" (or "recruitment ring", R) at 8.8 cm TL, and an additional first summer ring (S1) at 11.1 cm TL corresponding to T1 in this study (Table 3.6). From their first (winter) annulus (1) at 14.7 cm TL their back-calculated measurements were very similar to that of Brinkman (2007) (Table 3.6). Colloca *et al.* (2003) observed that P and R were sometimes absent on large fish as well. These two translucent zones occurred at an earlier stage in the fish's life than did T1 in this study. Both Godinho *et al.* (2001) and Piñeiro and Saínza (2003) observed up to three translucent zones before the first annulus, and sometimes another one ("check") after the first annulus, whereas their mean lengths at age 1 are similar to T2 in this study (Table 3.6). It is possible that *M. merluccius* forms additional early translucent zones compared to *M. capensis*. The original terminology "pelagic" and "demersal" rings (ICSEAF, 1983), and even additional (pre-annulus) rings, may therefore apply to other hake species but not to *M. capensis* and should therefore no longer be used for *M. capensis*. Mean lengths at age 2 of Godinho *et al.* (2001) and Piñeiro and Saínza (2003) compare with the T3 in this study (Table 3.6), suggesting that the "age 2" translucent zone may be a summer translucent zone, incorrectly identified as an annulus. Results from counting daily increments on Peruvian *M. gayi* otoliths of fish between 19 and 39 cm TL (Goicochea *et al.*, 2010) also confirmed this, showing that the length previously termed age 2 years corresponds to length at age 1.5 years (Table 3.6). They found a (winter or summer) "demersal check", an annulus (spring or autumn translucent zone), and a "bi-annual" (spring or autumn) translucent zone on most of these otoliths. The presence of a winter and summer translucent zone (rather than one translucent zone per annum as

previously thought) was also confirmed by OTC- marked recaptured *M. merluccius* (de Pontual *et al.*, 2006).

Biannual translucent zone formation as well as strong overlap in timing of formation of translucent zones (Figs 3.2 and 3.3) complicated the interpretation of edge analysis (Fig. 3.5). It also explains the erroneous conclusions of annual peaks of translucent zone formation of previous edge analysis studies (Botha, 1971; Voges, 1995; Wilhelm, 2005). Edge analysis is only feasible if the majority of fish in the population form a translucent zone at the same time of the year (Beckman and Wilson, 1995; Morales-Nin and Panfili, 2005), which is shown here not to be the case for *M. capensis*. Edge analysis should always be used in combination with the number of translucent zones present on the otolith.

Measurements of OD described here for each translucent zone (Table 3.4) should be used to aid age determination of young fish, i.e. determining the first annulus, and assigning fish to either age group 0 or 1. These should be re-visited when the stock recovers in the future. This has previously been suggested for use of "at least the first annulus" for European hake (GFCM, 1982). This chapter is the first step towards describing new annual age determination methods for *M. capensis*.

3.6. Conclusions and recommendations

In this chapter, otolith samples from *M. capensis* cohorts from the mid-winter spawning periods of 1996, 1998, 2002, 2005 and 2006 were chosen for age validation purposes. The results invalidated the traditional hypothesis that translucent zones are formed once per annum. Translucent zones were formed in the first summer and subsequent winter and summer of the first 21 months of the life of *M. capensis*. Ages were thus previously overestimated as a result of the second summer translucent zone that was incorrectly identified as an annulus. Measurements of the first three translucent zones are presented. Until the stock possibly recovers in the future, these could be used in age determination methods to assign *M. capensis* to age groups 0 or 1. The existence of a hypothesized "demersal ring" is invalidated and it is shown that edge analysis should always be used in combination with number of translucent zones present on the otolith.

CHAPTER 4

Further validation of fast growth rates and biannual translucent zone formation in *Merluccius capensis* otoliths

4.1. Abstract

This chapter addresses the hypotheses that fast growth rates and biannual translucent zone formation demonstrated for *M. capensis* up to 21 months old are also valid for older fish. Growth rates of fish up to 65 cm total length were described using projections from fur seal scat samples to progressive length frequency distributions (LFDs) from demersal research surveys from the period 1990–2009, and monthly commercial LFDs from the period 2007–2009. The growth rates were estimated to be approximately 10 cm year^{-1}, described by the von Bertalanffy growth equation $L_t = 134 * \left[(1 - e^{-0.127 * (t + 0.0490)} \right]$. To validate zone formation in older fish, three of the five cohorts studied in Chapter 3 (1996, 1998 and 2002) were supplemented with otoliths of older fish assumed to belong to the same cohort, based on growth projections. The otoliths were collected during annual demersal research surveys and from commercial samples. Total otolith diameter (OD) and diameters of up to nine translucent zones (T1–T9) were measured on 481 otoliths from fish of up to 50 cm total length. T1 was formed in the first summer (January–April) and T2 in the first winter–spring (July–September) of the hakes' life. T3 was formed in the next summer between December and February (earlier than predicted in Chapter 3), followed by T4 at the end of autumn (April– June, when young hake were not yet two years old). Generally 2–3 translucent zones were subsequently formed per year, up to age ~ 3.5 years, one or two between summer and autumn and one in winter–spring. The winter–spring translucent zones form the annuli. Summer–autumn and winter–spring translucent zones are not distinguishable in appearance under the light microscope. Measurements of translucent zones on survey otolith samples (2002 and 2005) covering the entire fish length range indicated that T2, T4, T6, T8 and T10 zones should be considered annuli. Age 1 should be assigned using diameter measurements of ≥ 7.5 mm. All other translucent zones should be counted and divided by two for the age group assignment after age group 1. A conversion equation from the old age data using the results of 2002 and 2005 survey samples was developed: New age = Integer(0.5*(*Old age* + 0.5)).

4.2. Introduction

Namibian *M. capensis* have been shown to have rapid growth rates and form three translucent zones (two summer translucent zones and one winter translucent zone) on their otoliths during the first 21 months of life (Chapters 2 and 3). Consequently, they have shorter life spans and younger ages at first maturity than previously thought. This could impact current stock assessment results and management advice. Because hake stocks and the overall fisheries sector are such an important economic resource in Namibia (MFMR, 2003; Investment House Namibia, 2011), it is important that further research is undertaken to fully understand the periodicity of the translucent zone formation on older fish, and to re-define their age determination criteria.

In European hake *M. merluccius*, the concept of the non-annual occurrence of translucent zones on otoliths is not new (Morales-Nin *et al.*, 1998). Recently, de Pontual *et al.* (2006) used otoliths of marked and recaptured *M. merluccius* to show that the internationally agreed age determination method over-estimated their ages. Biannual zone pair formation has also recently been observed on Argentinian hake *M. gayi* otoliths (Goicochea *et al.*, 2010). Other fish species for which a biannual cycle of translucent / opaque zone formation (or < 0.8 year^{-1} periodicity) was found are: red snappers *Lutjanus erythropterus*, *L. johnii*, *L. malabaricus* and *L. sebae* (Cappo *et al.*, 2000), sardine *Sardinops sagax neopilchardus* in Albany, Western Australia (ages 2 and 3 years; Fletcher and Blight, 1996), gray triggerfish *Balistes capriscus*, a demersal species off the southeastern coast of Brazil (Bernardes, 2002), and many freshwater fishes such as *Labeo cylindricus* in Lake Chicamba, Mozambique (Weyl and Booth, 1999), common carp *Cyprinus carpio* in Lake Gariep, South Africa (Winker *et al.*, 2010), *Sarotherodon mossambicus* in a subtropical impoundment in Venda, northern South Africa (Hecht, 1980), redband trout *Oncorhynchus mykiss gairdneri* in high desert streams, Idaho (Schill, 2009; Schill *et al.*, 2010) and tilapia *Oreochromis nilotichus* in Lake Awassa, Ethiopia (Yosef and Casselman, 1995). Yosef and Casselman (1995) showed translucent zone formation in January/February and July/August. Casselman (1990) also described "pseudoannuli" formed in mid-summer. Many shark species have also been shown to either form two vertebral zone pairs per year, e.g. basking sharks *Cetorhinus maximus* (Parker and Stott, 1965) and shortfin mako sharks *Isurus oxyringhus* (Pratt and Casey, 1983), or to form zone pairs that are

not related to time (or age or temporal rhythm), e.g. Pacific angel sharks *Squatina californica* (Natanson and Cailliet, 1990), western wobbegong sharks *Orectolobus hutchinsi* (Chidlow *et al.*, 2007) and basking sharks *Cetorhinus maximus* (Natanson *et al.*, 2008). Zone pairs cannot be used to age the last three species, showing the importance of validating the frequency of zone pair formation for all species and for all age classes (Beamish and MacFarlane, 1983; Campana, 2001).

If biannual translucent zone formation observed in young *M. capensis* continue in older fish, this would alter hake age determination and influence stock assessment results (Bertignac and de Pontual, 2007; Wilhelm *et al.*, 2008). The overall aim of this chapter is to test whether the pattern of biannual translucent zone formation seen in up to 21-month-old *M. capensis* (Chapter 3) continues with older fish. Specifically, the chapter aims to estimate growth rates of older *M. capensis* from length-frequency analysis. In addition, the otoliths of young *M. capensis* collected from fur seal scat samples (Chapters 2 and 3) are supplemented with otoliths collected from annual demersal research surveys and commercial catches representing the same cohorts (up to 3.5-year old fish). These new samples are used to investigate the translucent zone formation pattern. The null hypotheses to be tested are that hake growth rates are the same as previously estimated for *M. capensis* using the annual translucent zone hypothesis, and that translucent zone formation occurs once per year after the T3 zone. Otolith diameters (ODs) measured at all translucent zones of three cohorts will be used with the aim to describe new annual age determination methods. Finally, the chapter tests the new age determination methods on samples covering the whole length range of *M. capensis* from two Namibian demersal summer surveys (2002 and 2005). An equation is derived to correct existing ("old") age data for input into the age-structured production model (ASPM) for stock assessment purposes.

4.3. Materials and methods

4.3.1 Length-at-age estimation

Length-frequency analysis (LFA) was performed on 27 progressive length-frequency distributions (LFDs) from research surveys from 1990 to 2009 and 32 monthly LFDs from commercial catches from 2007 to 2009. The 27 survey LFDs were obtained from routine Namibian annual demersal surveys, 18 from January–February summer surveys from 1990 to 2009 (Ministry of Fisheries and Marine Resources, MFMR, Namibia, unpublished data), and 9 additional surveys in 1990–1997 (Burmeister, 2001). From each survey, LFDs were provided for the entire Namibian coast, spanning length ranges from 6 to 95 cm fish total length (TL) divided into 1-cm TL classes. Commercial LFD samples were collected by on-board observers and raised to the vessels' catches and to the fleets' catches for each month, except October (when the hake fishery is closed in Namibia), and December 2008 and 2009 (when no samples were collected) (MFMR, unpublished data). Fish TLs measured during the surveys and commercial sampling were truncated to the nearest cm.

The robust approach of Laslett *et al.* (2004) was used for LFA. This approach involves a first step of estimating mean lengths of modes in an LFD, and then calculating growth rates in a second step. The estimation methods "for finite distribution mixtures" described by MacDonald and Pitcher (1979) and Laslett *et al.* (2004) were used for the first step. It is assumed that:

(1) Lengths of the fish in each age group j are normally distributed around their mean length L_j, and
(2) The standard deviations (σ_j) of lengths around the mean length at age are a function of the mean length at age (CV * L_j), where CV was fixed at 0.12, the mean CV of LFDs from fur seal scat samples in Chapter 2.

The proportion of fish (p_i) expected in length class i in age group j was calculated by drawing from a normal distribution with mean length L_j and standard deviation σ_j = CV * L_j with the probability density component $p_i = g_j(L_i)$, where

$$g_j(L_i) = \frac{1}{2\pi\sigma_j} \exp\left(-\frac{(L_i - L_j)^2}{2\sigma_j{}^2} \right) \quad (4.1).$$

To get a new expected proportion at length (Ep_i), p_i is multiplied by the proportion expected in each age group j (q_j):

$$(Ep_i)_j = q_j p_1 + q_j p_2 \ldots + q_j p_i \quad (4.2),$$

where q_j was obtained by setting an initial proportion (0.2) and initial mean length L_j (10 (when available), 25, 35, 45 and 55 cm) for each age group. Number of age groups a was initially assumed to be five in the survey LFDs. Number of age groups was set to four for commercial LFDs and initial mean lengths at age L_j for these LFDs were set at 25 (when available), 35, 45, and 55 cm.

Residuals were obtained by subtracting total expected proportions at length for all age groups $\sum_{j=1}^{a} (Ep_i)_j$ from the observed proportions at length, and the residual sum of squares (RSS) was minimised by changing values of proportions q_j, and mean lengths L_j estimated iteratively for each age group. The q_j estimate was constrained to be non-negative and to sum to 1 ($\sum_{j=1}^{a} q_j = 1$). The difference between successive means (L_j and L_{j+1}) was constrained to be at least 3 cm, so the separation index (SI, the ratio of the difference between successive means to the difference between their standard deviations) should be at least 2.0 (Gayanilo *et al.*, 2005). If a proportion of an age group (q_j) was estimated as < 0.01, or if visual inspection indicated over-fitting, the number of age groups was reduced to a - 1 until all criteria were met and the best fit was obtained.

In the second step of the LFA, ages were assigned to the mean lengths obtained from the first step, using the following assumptions:

(1) The age of the first mode in the modal progression was assigned using the hatchdate of 23 June (Table 2.1) and the mid-date of each survey. For example for the January–February survey of 1999, the 25-cm mean length group was assigned an age of: 01 February 1999 (mid-date of survey) - 23 June 1997 (assumed hatching) = 587 days = 1.61 years. Subsequent modes would then be assigned ages of that age plus n number of years later.

(2) The L_∞ parameter is greater than that estimated in Chapter 2, likely > 100 cm. This affected how close two modes that were one year apart in age could be set to one another in length.

The von Bertalanffy growth function (VBGF, von Bertalanffy, 1960) was fitted to mean length (L_t) against assigned age in years (t):

$$L_t = L_\infty \left[1 - e^{-K(t - t_0)} \right] \quad (4.3),$$

where L_t is the expected TL (cm) of each fish at age t (years), L_∞ is the asymptotic length (cm), K is the growth coefficient (y^{-1}) and t_0 is the theoretical age (years) at length zero. The VBGF parameters were estimated by fitting a non-linear regression to the data by minimising the residual sum of squares, where a residual was the difference between the observed and the predicted length-at-age L_t.

Variance estimates of the parameters were calculated using parametric bootstrap re-sampling with 1000 replicates drawn from a normal distribution (Efron and Tibshirani, 1986). Standard errors and confidence intervals were constructed using the percentile method of Buckland (1984). All results (LFA, VBGF fitting and bootstraps) were obtained using the Newton algorithm of the Microsoft® Office Excel Solver routine.

4.3.2 Age validation sample selection

Older fish that were assumed to belong to the three strong cohorts (1996, 1998 and 2002) investigated in Chapter 3 were selected for age validation. From the estimated mean lengths-at-age from the fitted VBGF up to 65 otoliths (depending on availability) were chosen from fish of TLs within a range of 4–6 cm spanning the estimated length-at-age from each survey. This range depended on the survey mode and the initial sampled TL range of validation samples. Samples from the 2002 cohort from seal scats included smaller / earlier spawned fish (Fig. 3.1) and so a larger range of fish TLs was selected for this cohort. Additional otoliths were collected from commercial landings in June–August of 2000 and 2001 which allowed 6-monthly sampling for the 1998 cohort. Data for the 2002 survey stemmed from Kashava (2009), 2003 survey data stemmed from Brinkman (2007) and 2005 survey data stemmed from West (2009).

4.3.3 Otolith interpretation and analysis for age validation

Otoliths were analysed in the same way as the otoliths of juvenile fish from fur seal scat samples as described in Chapter 3. Total OD (mm) and OD (mm) at each translucent zone were measured, counting them as T1 to T13 from the centre to the margin of the otolith. Translucent zones were mostly clearer on the medial (proximal) side for otoliths smaller than 16 mm and on the lateral (distal) side for otoliths larger than 16 mm in diameter. No correction for erosion was needed for total OD measurements of survey otoliths.

Proportions of otoliths containing at least *j* translucent zones were plotted against sampling date, OD class (mm) and fish length (cm). Dates at 50 % formation ($Date_{50}$), ODs at 50 % formation (OD_{50}), and fish lengths at 50 % formation (TL_{50}) were calculated using a two-parameter logistic ogive:

$$P_j = \frac{1}{1+e^{\frac{-(d-d_{50})}{\delta}}} \qquad (4.4),$$

where P_j is the expected proportion of fish showing a complete j^{th} translucent zone at time d (in days after 1 January 1996), or at OD class (mm), or at fish total length class (cm), estimated parameter d_{50} is the 50 % formation time (in days after 1 January 1996, $Date_{50}$), or the OD_{50} (mm), or the TL_{50}, and δ is the width of the ogive. Because the survey samples were collected only in January and February, sometimes with only a few (< 5) samples per day, the survey samples were pooled for each week to calculate the proportion of samples containing a j^{th} translucent zone for that week. The date of the middle of the week was used in those cases.

To obtain parameter estimates, the binomial negative log-likelihood function was minimised using the Newton algorithm of the Microsoft® Office Excel Solver routine:

$$-LL = -\sum_i \left[h_i \ln\left(\hat{P}_{ji}\right) + (n_i - h_i)\ln\left(1 - \hat{P}_{ji}\right)\right] \qquad (4.5),$$

where $-LL$ is minimised for the j^{th} translucent zone, n_i is the number of otoliths examined in sample i, and h_i is the number of otoliths in the i^{th} sample showing a complete j^{th} translucent zone.

4.3.4 Evaluation of annual age determination methods

For each of the three cohorts (1996, 1998 and 2002), T1 zones that appeared wide (subjective, generally > 0.8 mm) were measured to test if T1 and T2 "merged" in any case. If a translucent zone would have been previously classified as a "double ring" (ICSEAF, 1983), this was noted. This is a subjective notation by the reader, when one translucent zone appears closer to the previous one, prior to measurements. The percentage of all otoliths on which a particular translucent zone (*Tj*) was visible, where it was classified as "double" was calculated for each cohort. To test if one particular translucent zone was a "double" and if the subjective classification of the reader was supported by measurements, the distance from each translucent zone to the previous one ($OD_{Tj} - OD_{Tj-1}$) was calculated. The mean differences between successive translucent zones were calculated at each translucent zone for each cohort.

Samples covering the survey length range (6–80 cm TL) from the January–February 2002 survey (n = 589) and the January–February 2005 survey (n = 459) were used to test and describe the "new" annual age determination methods. All translucent zones on each otolith were counted. ODs (mm) at individual translucent zones were measured (according to the same criteria as detailed in Section 4.3.3) up to T4 for the 2002 survey (Kashava, 2009), and for every translucent zone (up to T11) for the 2005 survey (West, 2009). A translucent zone was assigned as the first annulus when it was at least 7.5 mm in diameter, according to measurements from Chapter 3 (Table 3.4). Translucent zones that were closer to the core (smaller diameter) than the assigned first annulus were termed "pre-annuli" and counts of more than one pre-annulus were excluded from subsequent analyses. Mean lengths-at-"age" were calculated for both 2002 and 2005 samples under three hypotheses:

(1) one translucent zone is formed per year,

(2) two translucent zones are formed per year,

(3) after T2, three translucent zones are formed per year (T2, T5, T8 and T11 are annuli).

A fourth hypothesis was added for the 2005 survey samples. OD measurements at each translucent zone were used rather than counts to assign individual fish to age groups.

Linear regressions of "new" ages against "old" ages previously assigned to the same individual fish were performed. The "old" age data were obtained using methods and

assumptions described in ICSEAF (1983) and BENEFIT (2004b and 2005), which are currently used for routine age determination for stock assessment purposes in Namibia (MFMR, unpublished data; Wilhelm *et al.*, 2007). The "old" method assumes one translucent zone per year, but also contains subjective assignments of e.g. "demersal rings" and "double rings". "New" ages were obtained from the most likely of the above hypotheses. Linear conversion equation parameters were calculated such that:

"New" age group = Integer (a * "Old" age group + b) (4.6).

4.4. Results

4.4.1 Length-at-age estimation and age validation sample selection

Survey LFDs with their LFA-calculated mean total lengths (cm) show that the modes at fish lengths larger than 35 cm represent smaller proportions than the main modes, usually between 22 and 30 cm TL (Fig. 4.1). Modes identified in the 22–30 cm range are also often closer together than later modes. For this reason, they were assumed to belong to the same cohort, giving bimodal distributions for age group 1.

Commercial LFDs from monthly samples from 2007 to 2009 contained larger proportions of fish > 35 cm than survey LFDs (Fig. 4.2). They also showed about 10 cm differences between subsequent modes, and often 1 cm differences in mean lengths between subsequent months.

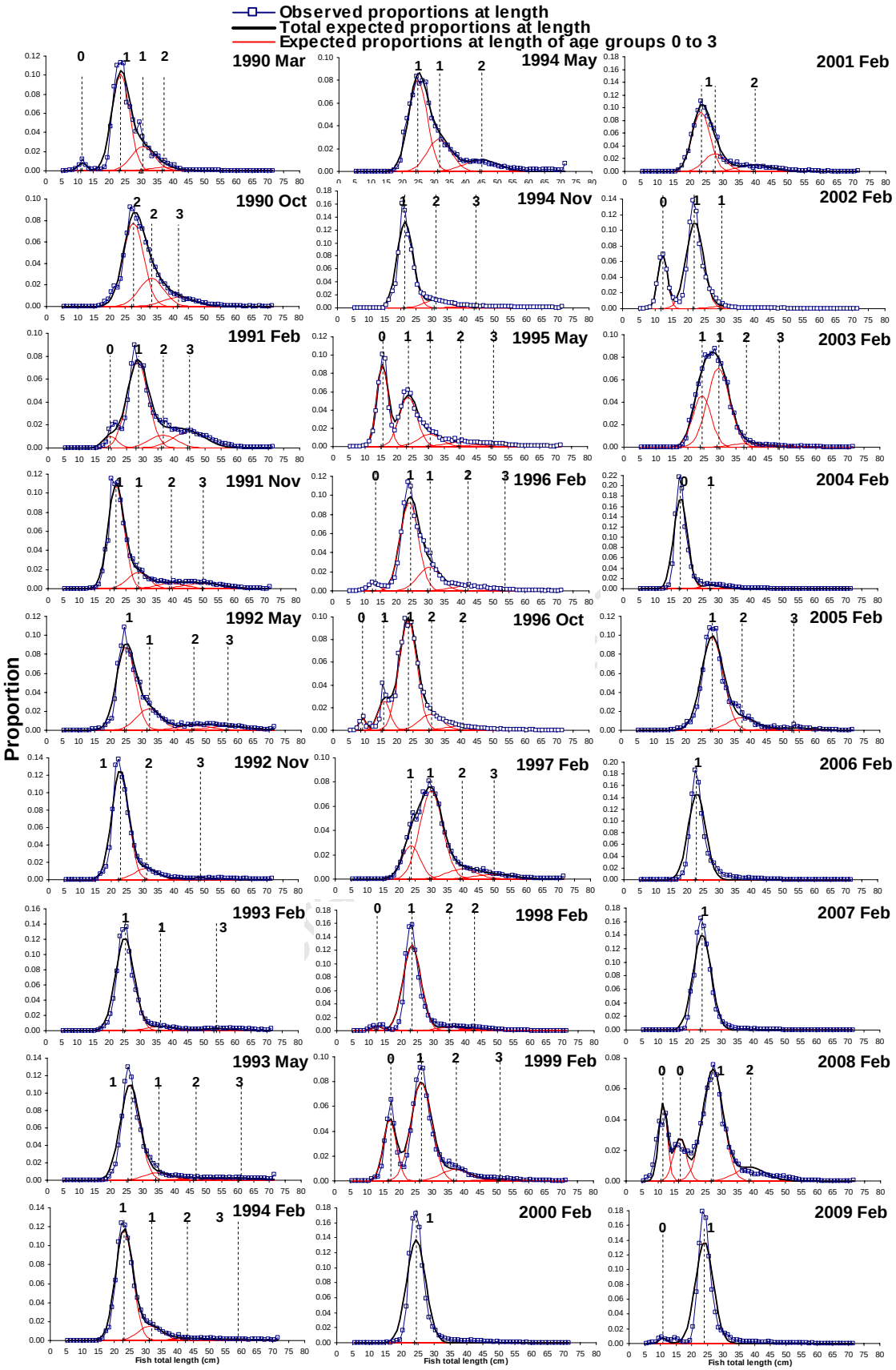

Figure 4.1 *M. capensis* survey length frequency distributions (LFDs) collected off Namibia by the Ministry of Fisheries and Marine Resources (MFMR). Age group modes (indicated by a dashed line and labelled with their assigned age groups) were separated using a minimum residual sum of squares fit length-frequency analysis (LFA) and normal distributions of lengths at each age group with estimated mean lengths and standard deviations of 0.12 * mean length. Age group labels refer to the entire class (e.g. age group 2 refers to ages 2.0 to 2.9).

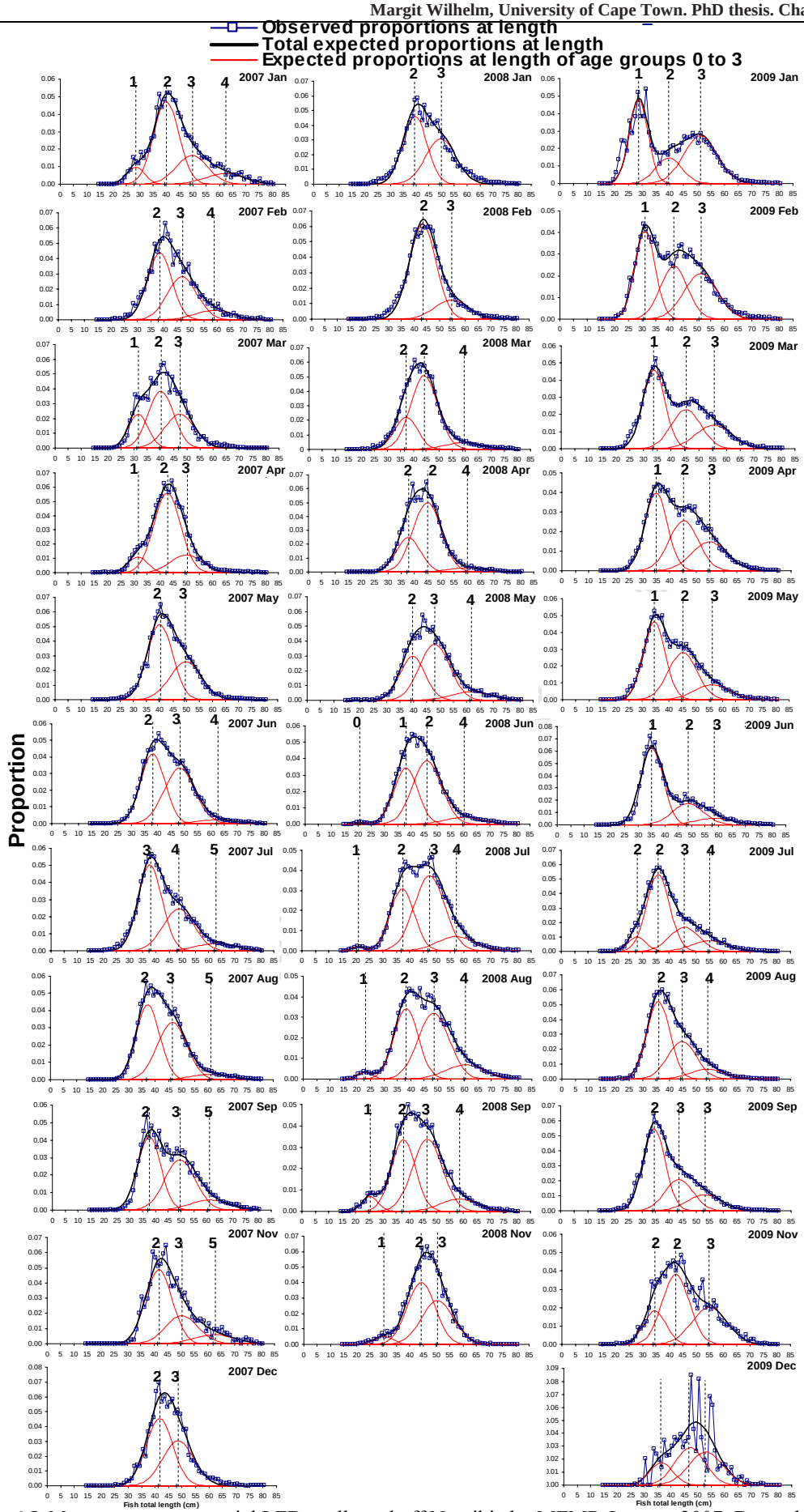

Figure 4.2 *M. capensis* commercial LFDs collected off Namibia by MFMR January 2007–December 2009. Age group means (indicated by a dashed line and labelled with their assigned age group) were separated using an LFA.

The VBGF function fitted to mean TL against age (Fig. 4.3) shows a higher L_∞ parameter estimate (Table 4.1) than previously calculated from only otoliths from seal scat samples (Fig. 4.3). The length ranges of samples chosen from the surveys and commercial samples for the three cohorts are presented in Table 4.2.

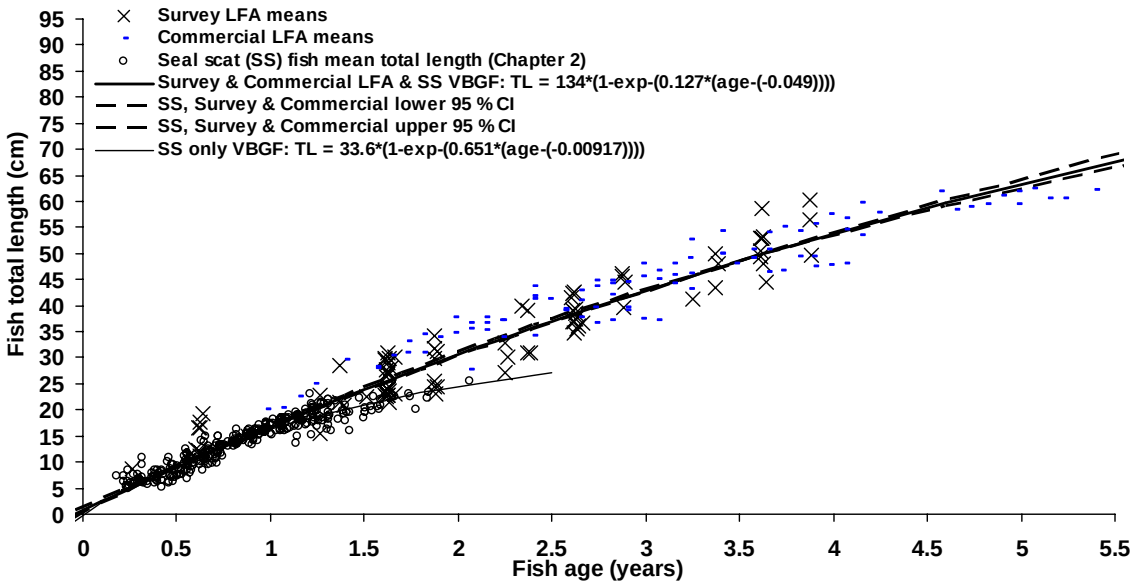

Figure 4.3 Mean fish TL (cm) of *M. capensis* calculated from length-frequency analysis (LFA) from 1990–2009 surveys (crosses), monthly commercial samples 2007–2009 (dashes) and otoliths from fur seal scat samples (SS) September 1994–December 2009 (circles, Chapter 2) against assigned fish age (years). Von Bertalanffy growth functions (VBGF, solid lines) including 95 % confidence intervals (CI, broken lines) are indicated on the plot.

Table 4.1 Von Bertalanffy growth function (VBGF) parameters (Equation 2.4) and calculated lengths at age including their bootstrap estimated coefficient of variation (CV) and 95 % confidence intervals (CI).

Parameter	VBGF	CV (%)	95 % CI	Age (years)	Mean fish length at age (cm)	95 % CI (cm)
L_∞ (cm)	**134**	9.0	[115 – 164]	**0.5**	**9.0**	[9.0 – 9.3]
K (y^{-1})	**0.127**	11.4	[0.156 – 0.0981]	**1.0**	**16.7**	[16.6 – 17.0]
t_0 (y)	**-0.0490**	50.5	[-0.0205 – -0.0937]	**1.5**	**23.9**	[23.7 – 24.4]
n	501			**2.0**	**30.7**	[30.4 – 31.2]
SE	2.72			**2.5**	**37.0**	[36.7 – 37.5]
				3.0	**43.0**	[42.8 – 43.3]
				3.5	**48.5**	[48.6 – 48.7]

Table 4.2 Fish age in years, sampled fish total length (TL) ranges in cm and sample sizes (N) of otoliths from surveys 1998 to 2006 for three cohorts 1996, 1998 and 2002. The sample names indicate the year in which the survey took place and "comm." refers to samples from commercial catches. All other samples were from hake-directed research surveys.

			1996 cohort			**1998 cohort**			**2002 cohort**		
Sample names	Months	Mid-date	Fish age (y)	TL range (4–5 cm)	N	Fish age (y)	TL range (5 cm)	N	Fish age (y)	TL range (6 cm)	N
1998	Jan–Feb	01 Feb	1.5	22–25	28						
1999	Jan–Feb	31 Jan	2.5	34–38	65	0.5	8–12	31			
2000	Jan–Feb	04 Feb	3.5	46–50	25	1.5	22–26	51			
2000 comm.	July	27 Jul				2.0	28–32	18			
2001	Jan–Feb	03 Feb				2.5	34–38	25			
2001 comm.	Jun–Aug	18 Jul				3.0	40–44	12			
2002	Jan–Feb	07 Feb				3.5	46–51	36			
2003	Jan–Feb	08 Feb							0.5	7–12	49
2004	Jan–Feb	04 Feb							1.5	20–25	54
2005	Jan–Feb	30 Jan							2.5	33–38	50
2006	Jan–Feb	31 Jan							3.5	45–50	37
Total					**118**			**173**			**190**
Grand total of survey otoliths sampled											**481**

4.4.2 Translucent zone periodicity

When analysing survey otoliths, it became apparent that the T1 zone (mean of 6–7 mm, Chapter 3) was sometimes not visible on large otoliths, and often the OD of the first visible translucent zone was similar to those noted as T2 and T3 (see Table 3.4).

Between 4 and 13 translucent zones were counted on the otoliths of the oldest fish (estimated age of 3.5 years) from all three cohorts: 1996, 1998 and 2002. The mean number of translucent zones was at least double the fish age from age 1.5 years onwards for all three cohorts (Fig. 4.4).

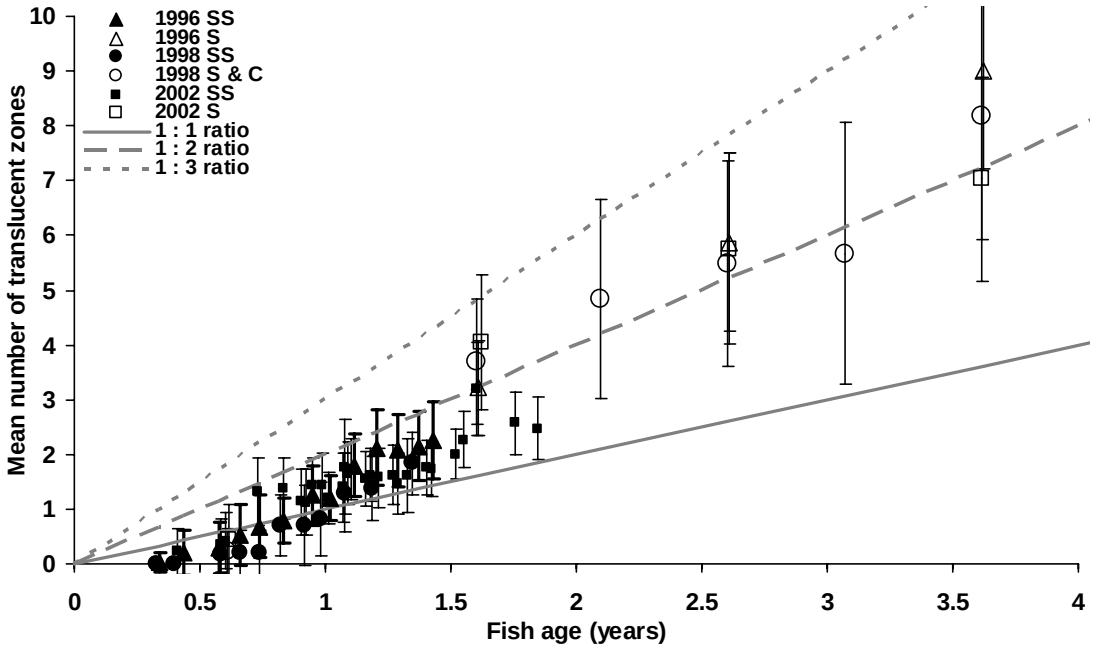

Figure 4.4 Mean (± 1 standard deviation) number of translucent zones per sample (SS = fur seal scat samples (Chapter 3), S = survey samples and C = commercial samples) plotted against the estimated ages for each of three cohorts: (born in) 1996, 1998 and 2002. The solid line represents the 1:1 ratio (one year = one translucent zone).

Translucent zone formation occurs more frequently than once per year (Fig. 4.5). $Date_{50}$ values of each translucent zone are similar between the cohorts. In the first year, spacing between translucent zones was the widest (Figures 4.5 and 4.6, Tables 4.3 and 4.4), two translucent zones being formed in the first year, the first in summer–autumn (end January–April) and the second in winter (July–August), representing the annulus (Table 4.3). After the first year, generally three translucent zones were formed per annum, two in summer–autumn, and one in winter–spring (the annulus). For both the 1998 and the 2002 cohorts only one summer–autumn translucent zone was formed during 2001 (late T6 1998 cohort) and 2005 (very late T6 2002 cohort, Table 4.3). During 2004 (2002 cohort) three translucent zones were formed, but two were formed later than usual, which made T5 of the 2002 cohort a very late spring-formed annulus (Table 4.3). The third translucent zone (T3) seemed to be formed earlier than expected (Table 3.3), i.e. one additional translucent zone is observed here. Only a few otoliths had ten translucent zones or more (9, 12 and 6 otoliths for 1996, 1998 and 2002 cohorts, respectively) so no ogives were fitted to T10.

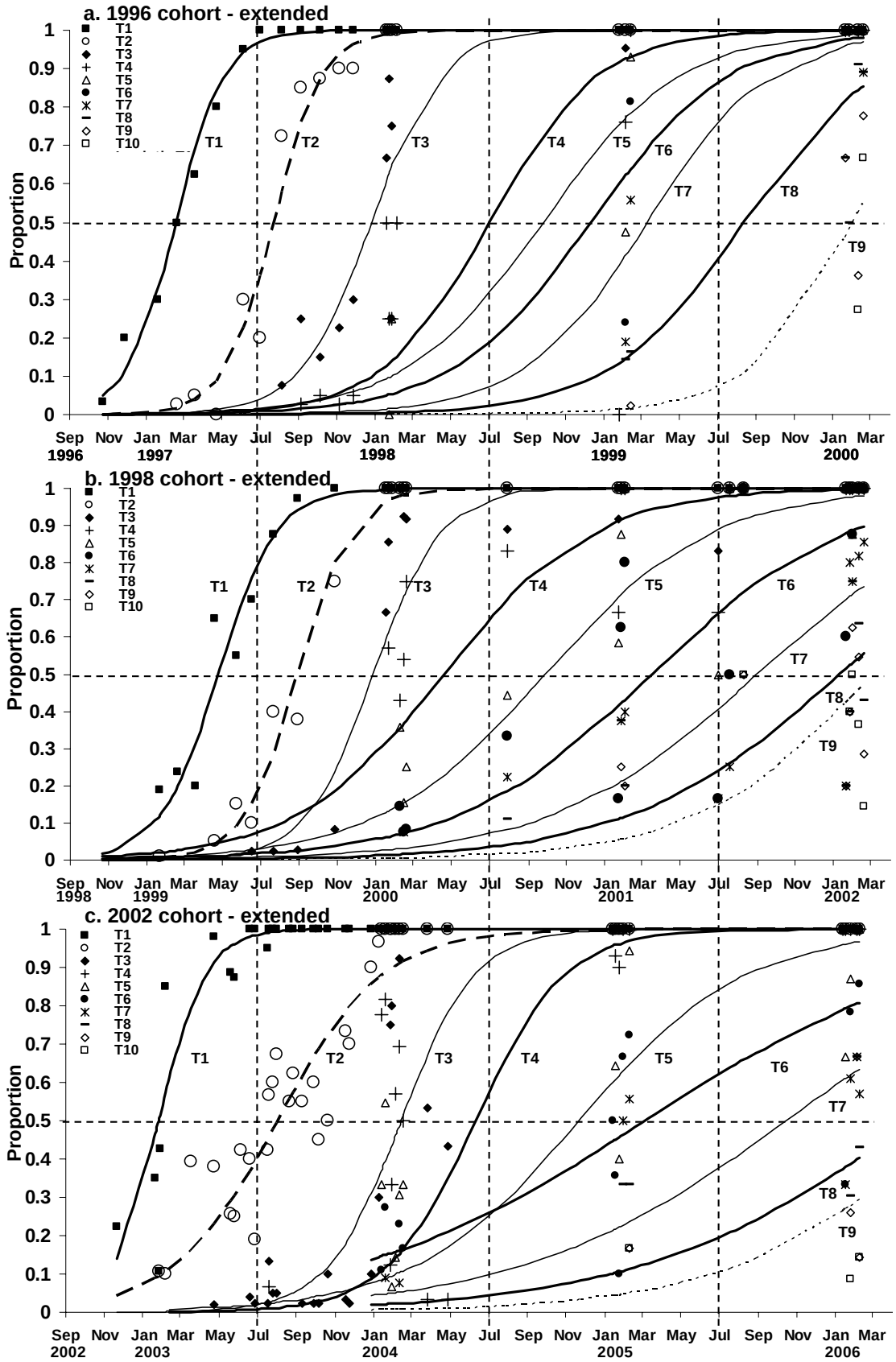

Figure 4.5 Proportions of *M. capensis* otoliths sampled for that date showing at least one to ten (T1–T10) complete translucent zones on the otoliths for three extended cohorts identified from fur seal scat samples and progressive survey length frequency distributions **a.** 1996, **b.** 1998 and **c.** 2002. The lines represent logistic ogives fitted to T1 to T9 in each data set. 50% values and the end of every year of age are marked with dashed lines.

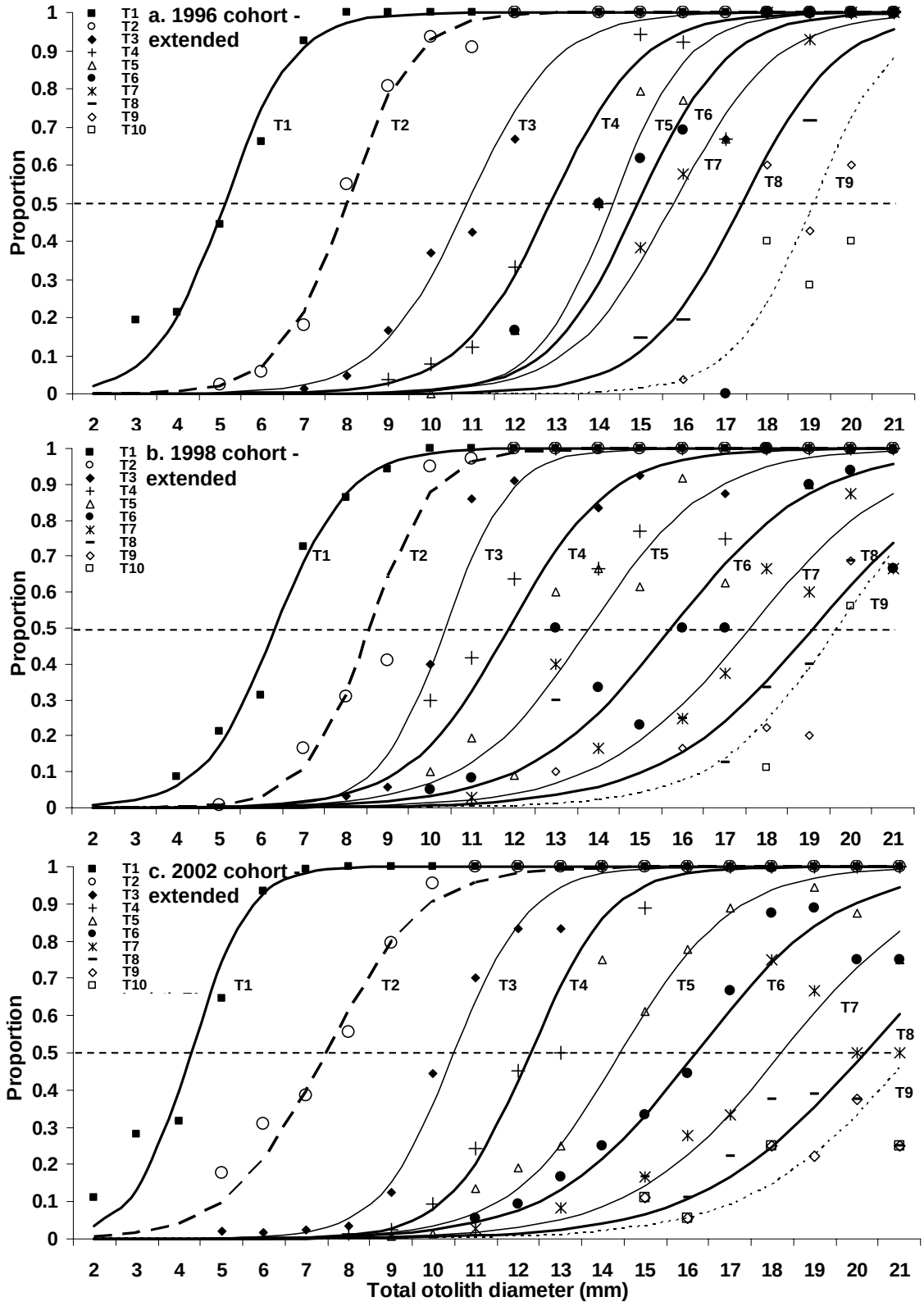

Figure 4.6 Proportions of *M. capensis* otoliths out of all otoliths per 1-mm otolith diameter class showing at least one to ten (T1–T10) complete translucent zones on the otoliths for three extended cohorts identified from fur seal scat samples and progressive survey length frequency distributions **a.** 1996, **b.** 1998 and **c.** 2002. The lines represent logistic ogives fitted for T1 to T9 in each data set.

In Tables 4.3, 4.4 and 4.5 the date of the annulus and the OD and fish TL expected on the date of the annulus (bold) show that the annulus occurs every second, or third translucent zone (or fourth in the case of T8 of the 1996 cohort).

Table 4.3 Date at 50 % formation calculated for nine translucent zones (T1–T9) for three extended cohorts of Namibian *M. capensis*, spawned in 1996, 1998 and 2002 (Fig. 4.5). Winter/spring translucent zones are highlighted (bold) to indicate annuli. Translucent zones that are formed in addition to two translucent zones per year are italicised.

	Date at 50 % formation (*$Date_{50}$*)		
Zone	**1996 cohort**	**1998 cohort**	**2002 cohort**
T1	16 Feb 1997	21 Apr 1999	26 Jan 2003
T2	**23 Jul 1997**	**29 Aug 1999**	**02 Aug 2003**
T3	25 Dec 1997	23 Dec 1999	13 Feb 2004
T4	**03 Jul 1998**	*14 Apr 2000*	**10 Jun 2004**
T5	*24 Sep 1998*	**23 Sep 2000**	*21 Nov 2004*
T6	10 Dec 1998	15 Mar 2001	05 Mar 2005
T7	10 Mar 1999	**30 Aug 2001**	**13 Oct 2005**
T8	**12 Aug 1999**	10 Jan 2002	03 May 2006
T9	02 Feb 2000	05 Mar 2002	**08 Jul 2006**

Table 4.4 OD at 50 % formation (*OD_{50}*, Fig. 4.6) and mean OD measured at nine translucent zones (T1–T9) for three extended cohorts of Namibian *M. capensis*, spawned in 1996, 1998 and 2002. Expected OD at the annuli are highlighted (bold). All measurements are in mm.

Zone	**1996 cohort**		**1998 cohort**		**2002 cohort**	
	OD_{50}	**Mean**	***OD_{50}***	**Mean**	***OD_{50}***	**Mean**
T1	5.1	6.9	6.3	6.7	4.3	6.5
T2	**8.0**	**8.9**	**8.6**	**8.9**	**7.5**	**8.2**
T3	10.9	10.6	10.4	10.8	10.5	10.4
T4	12.9	12.3	11.9	12.3	12.3	12.3
T5	**14.3**	**13.6**	**13.8**	**13.8**	**14.4**	**13.7**
T6	14.9	14.7	15.7	15.1	16.2	15.2
T7	15.8	15.9	**17.6**	16.0	**18.2**	16.4
T8	**17.4**	16.9	19.1	16.7	20.2	**17.0**
T9	19.1	**17.7**	19.7	**18.0**	21.3	18.0

Table 4.5 Fish total length at 50 % translucent zone formation (TL_{50}, cm) for three extended cohorts 1996, 1998 and 2002 and two short cohorts (2005 and 2006, Chapter 3). Predicted mean TL at annulus refers to the mean TL at ages 1, 2, and 3 respectively calculated from the VBGF (Table 4.1). TL_{50} closest to this predicted TL are highlighted (bold) for each cohort.

Predicted mean TL at annulus	Zone	1996 cohort	1998 cohort	2002 cohort	2005 cohort	2006 cohort
	T1	11.0	13.5	9.4	11.9	9.6
16.7	**T2**	**17.2**	**18.4**	**15.9**	**20.0**	**16.9**
	T3	23.6	22.7	22.3	26.3	
	T4	**29.1**	26.7	26.9		
30.7	**T5**	33.2	**32.0**	**32.8**		
	T6	34.8	37.7	38.0		
	T7	37.0	**43.0**	**43.6**		
43.0	**T8**	**44.5**	47.1	48.6		
	T9	48.7	48.8	50.9		

Figure 4.7 shows a summary of the otolith zone formation for all five cohorts: 1996, 1998, 2002 (this chapter), 2005 and 2006 (Chapter 3). $Date_{50}$ of T1 falls between late summer and autumn, T2 in winter–spring, T3 in summer, T4 in autumn for 1996 and 1998 cohorts, and in winter for the 2002 cohort. T5 was formed in spring. T6 was formed over a long period of summer–autumn with an "additional" T7 zone forming in autumn for the 1996 cohort. T8 of the 1996 cohort was formed in winter, coinciding with T7 of the other cohorts (winter–spring). T9 of the 1996 and T8–T9 of the 1998 cohort were formed in summer and T8 and T9 of the 2002 cohort in autumn (Fig. 4.7a). The 2002 cohort appears to have later-formed zones than the other two cohorts from T3 onwards (T3 very late). The 1996 cohort shows T5–T7 very closely spaced between September and April (3 translucent zones within 7 months), which means $Dates_{50}$ generally appear to be more regularly spaced for the 1998 and 2002 cohorts than for this cohort. OD_{50} (Fig. 4.7b) results have the same pattern as the dates (Fig. 4.7a), except for the 2005 cohort where OD_{50} of T1–T3 is wider than for the other cohorts. From Fig. 4.7, annuli in general seem to be: T2, T4/T5 and T7/T8).

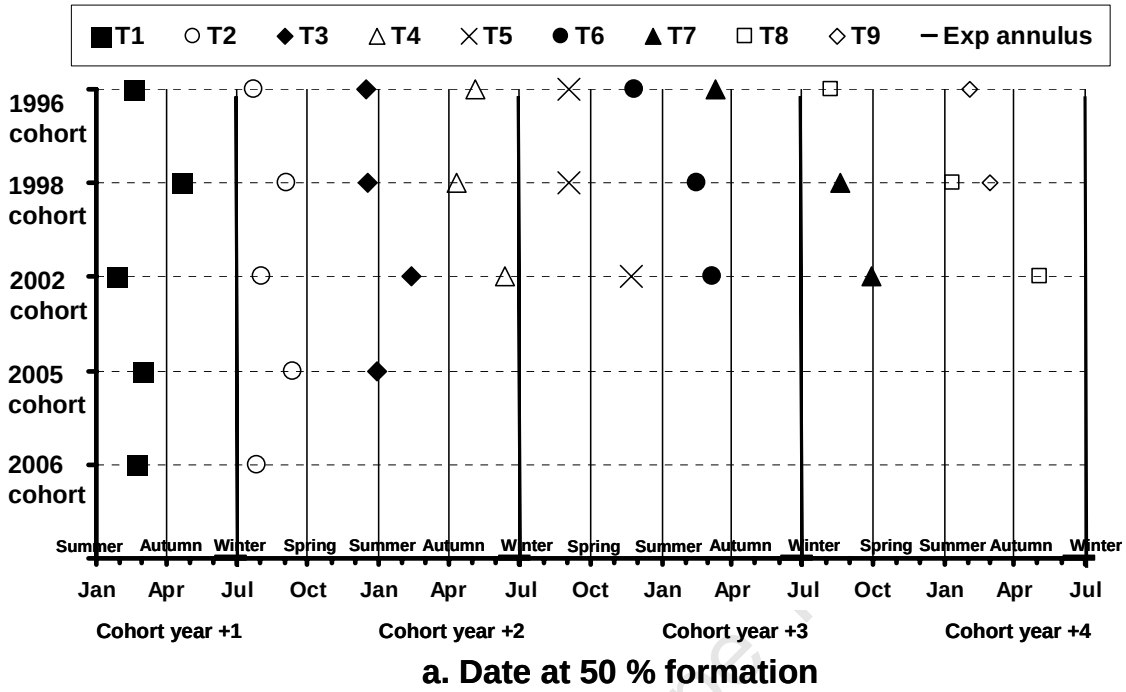

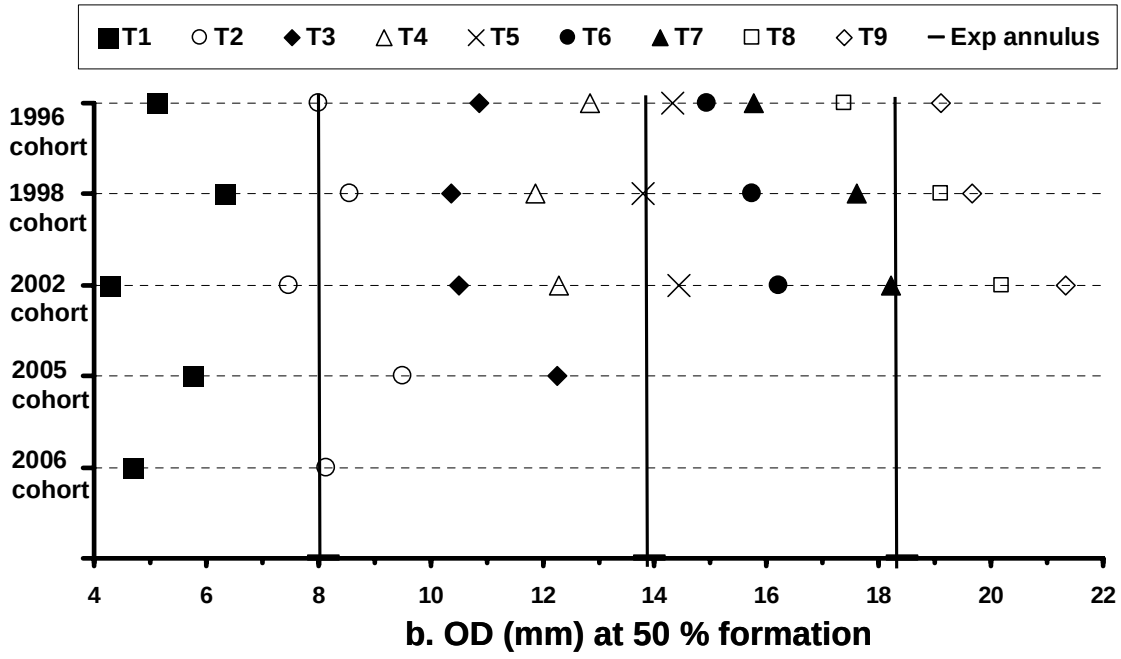

Figure 4.7 a. Date at 50 % formation ($Date_{50}$) and **b.** OD at 50 % formation mm (OD_{50}) of T1–T9 on otoliths of *M. capensis* up to 3.5 years old for five cohorts hatched in 1996, 1998 and 2002 (this chapter) and 2005 and 2006 (Chapter 3). Thick solid lines (Exp annulus) denote the expected position of the annulus (23 June) and expected OD (mm) at ages 1, 2 and 3 years (from Table 4.1 and converted back to OD using Equation 2.2).

4.4.3 Evaluation of annual age determination methods

The width of a "normal" translucent zone was generally 0.4–0.8 mm (from the inside to the outside along the longest axis). No pattern of width or clarity between zones (every other translucent zone being wider or more translucent) could be detected. No pattern of "merging" (the distance between T2 and T1 on small otoliths being as wide as T1 on larger otoliths) was observed. T1 (< 7 mm) however, was often not present, or not visible on large otoliths.

Mean differences in diameter measurements between subsequent translucent zones generally decreased from 1.8 mm to 1.2 mm from T2 to T9 (Figure 4.8). However, this pattern was not defined for the 2002 cohort with the mean difference around 1.5 mm for T2–T7 (Fig. 4.8c). The mean difference between translucent zones subjectively identified as "double" was not significantly different from the mean difference between all the translucent zones measured for each cohort, except for T2 of the 1996 cohort (Figure 4.8a). Numbers (or proportions) of any translucent zones being identified as "double" were not particularly high for any translucent zone in any cohort. Any translucent zone may appear closer to the previous translucent zone at any stage. This means, by measurement, no particular translucent zone appears to be a "double".

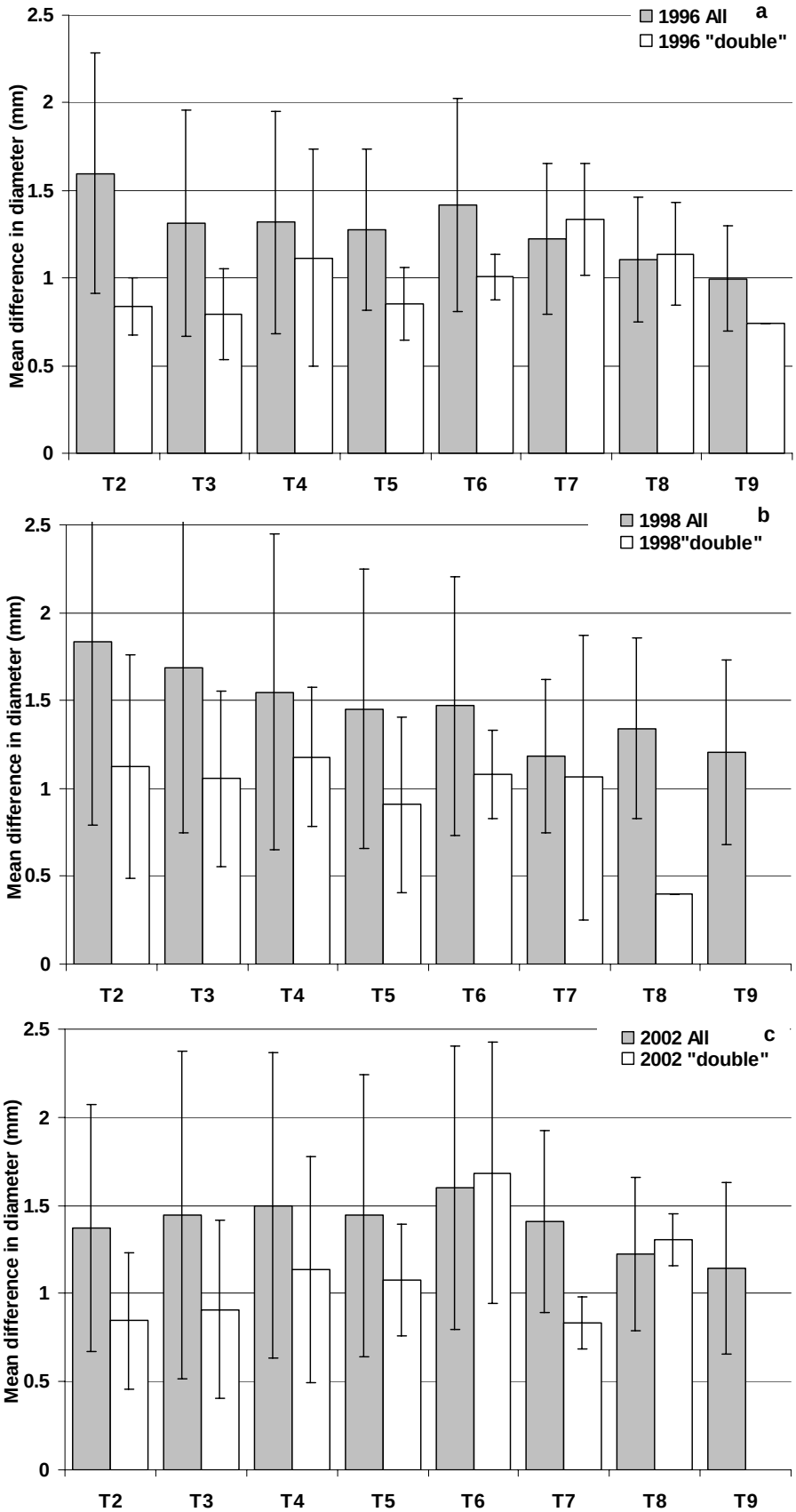

Figure 4.8 Mean difference in diameter (mm) of each translucent zone and its preceding zone (T2 denoting the difference in diameter between T1 and T2, etc) for the three *M. capensis* cohorts (born in) **a.** 1996, **b.** 1998 and **c.** 2002. White bars denote the mean difference in diameter between only those zones subjectively identified as "double". The numbers on the bars indicate sample sizes of each translucent zone.

Graphical inspection of mean lengths-at-age calculated assuming one translucent zone per year (each one being annuli), two translucent zones per year (T2, T4, T6, T8 and T10 being annuli), and three translucent zones per year after T2 (T2, T5 and T8 being annuli) (Fig. 4.9) shows that the biannual translucent zone hypothesis concurs with the expected mean lengths-at-age estimated from LFAs of the 2002 and 2005 surveys, and also with mean lengths-at-age calculated from VBGF for all available LFDs (Fig. 4.9). The method of assigning ages using translucent zone diameter measurements shows lengths-at-age more similar to the VBGF for age groups 5 years and older, whereas the two translucent zones-per year method shows more similar lengths-at-age for the age groups < 5 years. Data from the 2005 survey in general shows a higher variation of lengths at each age (Fig. 4.9b).

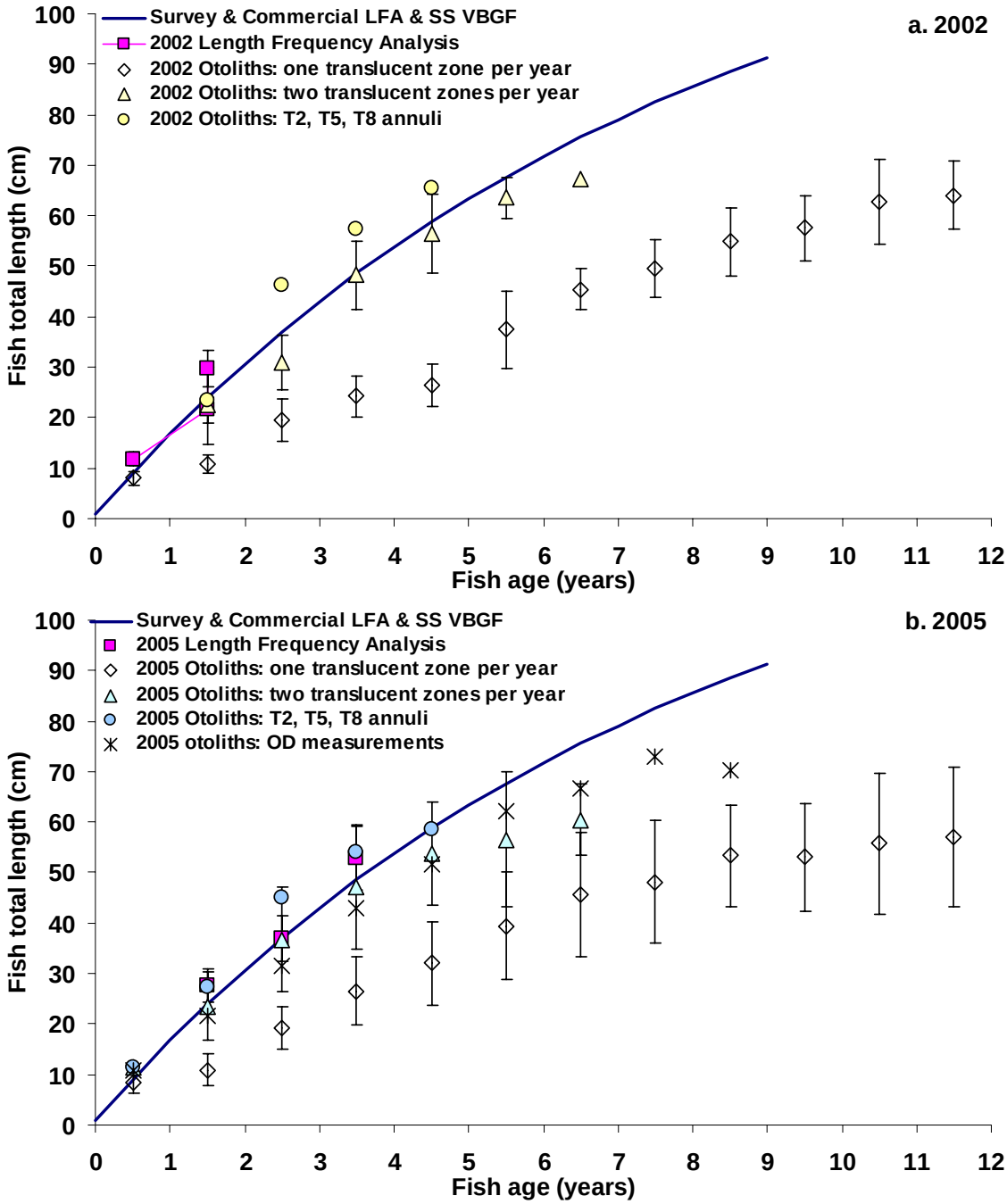

Figure 4.9 Mean lengths-at-age calculated for otoliths collected during surveys in **a.** Jan–Feb 2002 and **b.** Jan–Feb 2005. Mean lengths of the Length Frequency analysis (Fig. 4.1) are shown for each survey. Mean lengths from otoliths were determined assuming (1) one translucent zone per year, (2) two translucent zones per year, (3) zones T2, T5 and T8 were annuli and (4) diameter measurements at each translucent zone (Table 4.4) were used to assign annuli (OD measurements) for 2005 only. Mean lengths from Length Frequency Analysis (LFA), one translucent zone, and two translucent zones per year include one standard deviation. The Von Bertalanffy Growth Function (VBGF) calculated from all available mean lengths from LFA and seal scats (SS) (Fig. 4.3) is also shown. The vertical dashed line indicates the limit of the age validation analysis (Fig. 4.4).

Linear regressions with the fitted parameters of "new" age groups = number of translucent zones counted and divided by 2 ("no of translucent zones / 2") against "old" age groups for 2002 and 2005 survey samples were similar, but with 2002 showing a better fit to the data, and 2005 showing a higher variability at ages 2 to 5 years (Fig. 4.10).

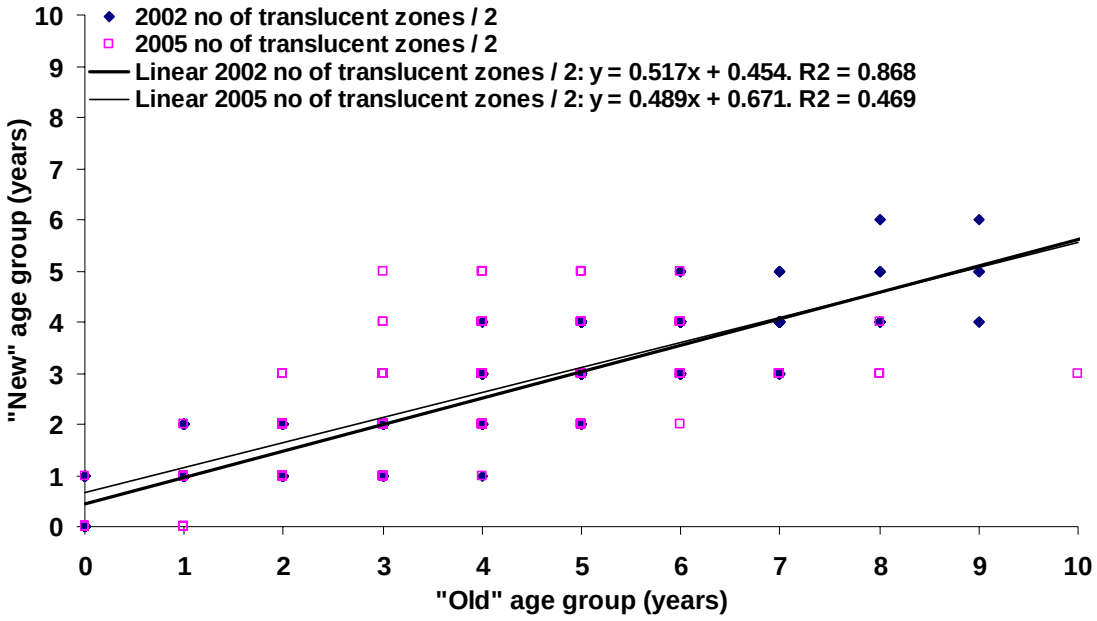

Figure 4.10 "New" age groups (assigned using the biannual translucent zone hypothesis or the measured ODs hypothesis for 2005) against "old" age groups (previously assigned by MFMR, Namibia, using the annual translucent zone hypothesis) with their linear regression parameters fitted.

When using the "no of translucent zones / 2" regression parameters to calculate "new" age groups from "old" both 2002 and 2005 showed identical "new" age groups, with the exception of age group 1 (bold, Table 4.6).

Table 4.6 Conversions from "old" age groups to "New" age groups using regression parameters *a* and *b* such that: New age group = Integer (*a* * Old age group + *b*). Regression parameters *a* and *b* were calculated from New against Old (Fig. 4.10).

Linear conversion	**2002 no of translucent zones/ 2**	**2005 no of translucent zones/ 2**
a	0.52	0.49
b	0.45	0.67
"Old" age group	"New" age group	
0	0	0
1	0	**1**
2	1	1
3	2	2
4	2	2
5	3	3
6	3	3
7	4	4
8	4	4
9	5	5
10	5	5
11	6	6
12	6	6
13	7	7

When all translucent zones were measured and age groups assigned according to the identified OD measurements in Table 4.4, the reader managed to read 30 to 50 otoliths per day (2005 measured OD samples). When only the first four translucent zones were measured and the rest of the translucent zones simply counted, the reader managed to read between 100 and 200 otoliths per day (2002 samples).

4.5. Discussion

4.5.1 Length-at-age estimation and fast growth rates

The identified bimodal distributions of lengths at age group 1 in some years (Fig. 2.7) make length-frequency analysis and growth rate estimation for this species difficult, the same as for European hake (Morales-Nin *et al.*, 1998). However, the separated age groups show that hatching occurs over a long period, probably with bimodal peaks, as has been previously noted (Chapter 2; Assorov and Berenbeim, 1983; Olivar *et al.*, 1988; Kainge *et al.*, 2007; see Table 1.3). Biannual spawning may be one reason for biannual translucent zone formation as spawning has often been associated with slower somatic growth rates and therefore translucent zone formation (Admassu and Casselman, 2000; Bernardes, 2002; Brouwer and Griffiths, 2004; Szedlmayer and Beyer, 2011). However, this has to be an indirect link since translucent zones are also formed in young immature fish.

The reasons for the large difference in the estimated L_∞ parameter between only using young fish from seal scat samples, and those including survey and commercial samples (Fig. 4.3) could be the following:
(1) At the size range of > 23 cm TL hake, fur seals only feed on the fish that remain on the inner-shelf and mid-shelf (Skern-Mauritzen *et al.*, 2009). This may be the slower growing young hake, and hence the sample may be skewed towards small lengths-at-age for fish from 1.5 years onwards. In the survey samples hake are more evenly represented from all areas, resulting in a more realistic L_∞ estimate.
(2) Juvenile and adult *M. capensis* could grow differently – possibly represented by a seasonal or two-stage growth curve. However, the data from commercial and survey samples were not sufficiently detailed to fit such a curve in the current analysis.

Similar to studies on other hake species, e.g. *M. merluccius* (de Pontual *et al.*, 2006; Piñeiro *et al.*, 2007; Fig. 2.9), *M. capensis* continue to grow at fast growth rates up to four years of age, from 17 cm year^{-1} at age 0.5 to 10 cm year^{-1} at age 4. Goicochea *et al.* (2010) also observed winter–spring translucent zones and summer–autumn translucent zones on Perivuan hake *M. gayi peruanus*. About eight translucent zones at 4 cm and 10 translucent zones at 5 cm fish total length (with a high variability of this

number) were visible on Senegalese hake *M. senegalensis* otoliths (Rey et *al.*, 2012), similar to *M. capensis* (Figs 4.3 and 4.4).

4.5.2 Fast growth rates and implications for management

M. capensis seem to grow twice as fast as previously thought, also implying a higher instantaneous natural mortality rate (Beverton and Holt, 1959), a younger age at first maturity, and a younger maximum age, i.e. they have a more r-selected life history strategy than previously thought (Adams, 1980). An r-selected strategy implies a higher stock productivity in general, with the maximum yield-per-recruit occurring at higher levels of fishing mortality and being less sensitive to over-fishing than previously thought (Adams 1980). In line with Adams (1980) and the findings of Bertignac and de Pontual (2007) for European hake, this should be tested for *M. capensis* in Namibia (addressed in Chapter 7).

4.5.3 *M. capensis* translucent zone periodicity and implications for annual age determination methods

Fish spawned at different times of the year, and therefore fish of the same cohort having a different number of biannual translucent zones at any one time, make routine age determination of this species difficult. When an increased length range of fish with greater hatchdate ranges was sampled, as was likely for the survey samples for the 1996, 1998 and 2002 cohorts, a larger number of translucent zones at each date was seen than for seal scat samples (Fig. 4.4). This was also noted for the 2005 survey samples (Fig. 4.9b; West, 2009). Norbis *et al.* (1999) showed differences in translucent zone measurements (and time until translucent zone formation) between autumn–winter- and spring-spawned *M. hubbsi*. Yosef and Casselman (1995) noted one more biannulus present (on average) in fish that were spawned 5–6 months later than those of the same cohort spawned earlier in the season. This makes summer-spawned or early spring-spawned fish difficult to interpret, and makes it difficult to assign a fish to an age-group or annual cohort. Yosef and Casselman (1995) proposed a system to assign ages to tilapia (*Oreochromis niloticus*) using the biannual translucent zones and their biannual spawning and recruitment times. However, this pertained to freshwater fish, where timing of zones as well as spawning seasons were much more clearly

defined than for hake, and so at this stage this system can not be applied to *M. capensis*.

Fitting ogives to proportions of otoliths with translucent zones against date becomes problematic from T4 onwards when only a few points were available (Fig. 4.5). The patterns depicted here (Figures 4.5 and 4.6), nonetheless, show that the rapid, more frequent than annual translucent zone formation observed in young fish (Chapter 3) continues with older fish. The first three translucent zones are formed respectively in the first summer, first winter and second summer of the life of *M. capensis*. A fourth translucent zone is then formed either in autumn or winter at 12 mm OD (25–27 cm TL). The fifth spring-formed translucent zone is the annulus noted on otoliths between 13 and 15 mm in diameter and fish of 30–32 cm TL. This general pattern of 2–4 translucent zones per annum spaced at 3- to 6-month- and 2- to 3-mm OD-intervals thus seems to be consistent from juvenile to 2.5-year-old *M. capensis* for five very different cohorts spanning ten years of observations. After T5, the pattern continues at less regular intervals (2–7 month-intervals) up to 3.5-year-old *M. capensis*.

Translucent zone diameter measurements facilitate proper identification of the first annulus, as has been tested by Brinkman (2007), Kashava (2009), West (2009) and GFCM (1982). However, age determination of fish becomes more difficult with increasing fish age (and increasing otolith diameter) as the number of translucent zones formed per annum increase, and spacing between them is reduced (Fig. 4.8). This makes translucent zone diameter increasingly difficult to measure. There seems to be an overlap of timing of the later translucent zones, with some forming later than expected (e.g. T3 and T4 of the 2002 cohort, Fig. 4.7a), or forming additional translucent zones (e.g. T7 of the 1996 cohort, Fig. 4.7a), further complicating age determination of > 1-year-old *M. capensis*. The time to age a fish took three to four times longer when diameters of all translucent zones were measured than when only the first few translucent zones were measured and the rest of the translucent zones counted. However, the accuracy with which lengths-at-age are determined does not necessarily improve when using translucent zone diameter measurements (Fig. 4.9). The method of counting translucent zones and dividing them by two seems more likely to follow the predicted pattern of growth for fish up to 50 cm (Fig. 4.9). Reasons for the higher discrepancy between observed lengths-at-age from “no of translucent zones

/ 2" and expected lengths-at-age from the VBGF for the 2005 survey samples (Fig. 4.9b) were the higher variation of number of translucent zones seen per length class and the greater number of translucent zones seen. This was also depicted by the weaker fit to "old age data" for 2005 compared with 2002 (Fig. 4.10). In addition, for 2005 all diameters at all translucent zones were measured, and thus only measurable translucent zones were counted (West, 2009). This means the counting (without measurements) method requires less time, and also increases the accuracy of counts of the older fish. The counting over the measurements method should be preferred as it requires a minimal time investment at a small price for accuracy (OD measurements vs. "no of translucent zones / 2" method in Fig. 4.9b). Since the accuracy of assigning ages to older fish is negligible in an assessment where mostly age groups younger than that (in this case < 4 years, previously < 7 years) represented in the catch-at-age input (Wilhelm *et al.*, 2008), the use of the counting method is justified. The sectioning method could overcome the problem of missing the first two translucent zones. This method is successfully applied to hakes (e.g. Norbis *et al.*, 1999; Godinho *et al.*, 2001; Piñeiro and Saínza, 2003). However, the whole otolith method is also successfully applied to hakes including *M. capensis* (e.g. Wysokiñski 1983; Colloca *et al.*, 2003) and has the advantage of a faster processing rate per otolith, and a higher otolith reading precision (BENEFIT, 2004b). For the same reasons that the method of simply dividing the number of translucent zones by two should be preferred over a more time-intensive method, the whole otolith method should be used for routine age determination on *M. capensis*.

Measurements should still be used for the first annulus for future routine age determination. The first visible translucent zone at 7.5 mm OD or more should be assigned to the first annulus (Table 4.4). All translucent zones closer to the core than 7.5 mm should not be considered as annuli and fish with only translucent zones smaller than 7.5 mm in diameter should be assigned to age group 0. The measurements method applied assumes that fast, constant growth rates of about 1 cm month-1 for up to 18-month-old fish (Table 2.3) continue. These have been relatively stable since 1994 (Fig. 2.7). However, these growth rates apply to a "severely depleted" stock (Kirchner, 2010), which may have faster growth rates than a possible recovered stock in the future. Measurements should thus be revised in the case of stock recovery. All translucent zones after the first assigned annulus (assigned by measurement), should be

counted, and the count divided by two to assign an age group after 1. This would solve the "first annulus" discrepancy seen in Table 4.6, which resulted from the T1 zone often being absent, or not seen in older fish, or from "old age groups" having been assigned using the vaguely defined "demersal ring". No "demersal rings", "double rings", or other previously described subjective measures need be noted. For example, according to Fig. 4.7, T6 and T7 of the 1996 cohort and T9 of the 1998 cohort should have been termed "double", but this could not be depicted by mean diameter differences (Fig. 4.8). On average, formation of annuli and additional translucent zones is sufficiently regular (Figs 4.7 and 4.8) that these measurements do not improve age assignments, but increase time and therefore cost of routine age determination.

The reason for old age group 1 remaining as new age group 1 in the conversion (Tables 4.6 and 4.7) is that the first visible translucent zone was previously often regarded as a "demersal ring" and not assigned an age group (ICSEAF, 1983). Admassu and Casselman (2000) also showed that, in general, age could be estimated by counting biannuli and using a multiplier (by months) equation. Old age- to new age group conversions of previously aged *M. capensis* should be used to inform assessments and management. The conversions presented in Table 4.7 should be used for all years. At a minimum, the new age data should be used in sensitivity tests in the stock assessments (see also Chapter 7).

Table 4.7 Conversions to be used for "Old" age groups previously assigned by MFMR, Namibia, to "New" age groups, where New age group = Integer (*a* * Old age group + *b*).

Linear conversion	
a	0.5
b	0.5
Old age group	**New age group**
0	0
1	1
2	1
3	2
4	2
5	3
6	3
7	4
8	4
9	5
10	5
11	6
12	6
13	7

4.5.4 Reasons for translucent zone formation

There are differences in the conclusions reached by different authors about the timing and control of zone formation on otoliths. However, the opaque zone is sometimes believed to form in response to increased growth rates while the translucent zone formation marks periods of slow somatic / otolith growth in temperate zone species, associated with a dip in feeding intensity or cold temperatures (Pannella, 1980; Casselman, 1987; Morales-Nin, 1987; Beckman and Wilson, 1995; Yosef and Casselman, 1995; Pearson, 1996). However, Beckman and Wilson (1995) showed that opaque zone formation in fish from temperate regions in southern latitudes happens throughout the year, with slight increases in winter and summer. This means that translucent zones form in autumn and spring. Periods of translucent zone formation occur in summer/autumn and winter/spring for *M. capensis* in the northern Benguela.

Differences in feeding and nutritional condition in different seasons or as a result of area and depth preferences could cause differences in metabolic rates and growth rates at different times and thus formation of translucent zones. Not enough information on *M. capensis* diet is available by fish length and/or by season to discuss feeding intensity as a cause of formation. This is recommended for future research on *M. capensis*. Habitat and depth-preferences could also be associated with translucent zone formation. Even small (< 20 cm TL) hake follow the diel feeding behaviour of moving from the midwater at night to the bottom during the day (Stenevik *et al.*, 2009). It was shown that therefore the first translucent zone is not formed as a result of their demersal settlement (Chapter 3). However, there may be seasonal migrations that could indirectly cause translucent zone formation. For example, daily migrations related to feeding activity are variable between seasons, related to the upwelling season as well as the inshore-offshore movement of cold water (Gordoa *et al.*, 2006). No seasonal inshore-offshore migrations have been noted for *M. capensis* in Namibia (MacPherson *et al.*, 1991; Gordoa *et al.*, 2000) but fish > 40 cm may undertake spawning migrations from offshore (> 350 m bottom depth), while younger fish mainly inhabit the inner shelf (Gordoa *et al.*, 2006). The spatial aspects of the life history of *M. capensis* are further investigated in Chapters 5 and 6. In general it seems that despite these differences in habitat, seasonal translucent zone formation is consistent from juvenile to adult fish.

The northern Benguela is dominated by a wind-driven upwelling regime. In southern Namibia (Lüderitz upwelling cell, 27ºS) maximum upwelling takes place in summer (December to February) when inshore-offshore temperature differences as well as feeding conditions (theoretically) are at a maximum. Coolest water temperatures occur in winter-spring with mean sea surface temperature (SST) of 11ºC compared with the maximum temperatures, 13–15ºC, in summer–autumn. Further north (Walvis Bay, 23ºS, and north), peak upwelling takes place in winter to spring, between June and November. At that time of the year water temperatures are also at a minimum, with mean SST of 13ºC, and the maximum SSTS between 17 and 19ºC in summer–autumn. Further north at about 19ºS, the SSTs are 2–3°C warmer than at Walvis Bay (Bartholomae and van der Plas, 2007). In this study, fish samples from the northern areas (Pelican Point and Cape Cross) and southern areas (Van Reenen Bay and Atlas and Wolf Bay, see Fig. 2.1) were combined on the assumption that they represented the same cohort of fish, within 1–2 months of the same hatchdate, and thus derived from the same stock (Chapter 2). Since SSTs increase by 3°C from southern to central Namibia and by another 3°C from central to northern Namibia, movement of fish between these areas needs to be further investigated as a possible cause for translucent zone formation (see Chapters 5 and 6).

The translucent zones in general occurred at minimum and maximum temperature periods, but the seasonal SST trends show high daily as well as high inter-annual variability (Bartholomae and van der Plas, 2007). In early 1997, upwelling off the Namibian coast was most active during summer. This means the 1996 cohort formed T1 during an anomalously cold summer–autumn, but formed their T2 during a relatively warm winter (July 1997). February–April of 1999 and 2001 were very warm summers in Namibia, with warm-water events caused by relaxed upwelling (Bartholomae and van der Plas, 2007). Thus, the T1 zone of the 7–9-month-old 1998 cohort, and the T7 zone of the 2.5–2.7 year-old 1996 cohort (Table 4.2) were both formed in the warm summer of 1998/1999. T6 of the 1998 cohort was also formed in the middle of a very warm summer (February 2001). In contrast, T3 of the 2002 cohort was formed in February 2004, a summer with more active upwelling and cold conditions (Bartholomae and van der Plas, 2007).

In general, the fish were thus exposed to large inter-regional as well as large inter-annual variability in temperature and upwelling intensity (amplitude) and length of season (period) during the entire time-span of the studied cohorts (3.5 years), and during the span from one cohort to the next (1996, 1998 and 2002 -spawned fish). In spite of their exposure to high environmental variability, they show relatively consistent translucent zone formation periods. The seasons of *M. capensis* translucent zone formation thus seem to be consistent over the different years and not only related to any specific temperature maxima or minima and seasonal conditions or upwelling events on a broad scale. The roughly 5-monthly cycle of translucent zone formation is consistent between cohorts and years. Additional translucent zones (T7 of the 1996 cohort) or the later formation of translucent zones (e.g. T6 of the 1996 cohort and T3–T5 of the 2002 cohort, Fig. 4.7) could be explained as a result of unmeasured environmental events. Additional translucent zones on sexually mature *M. capensis* could also be indirectly linked with biannual spawning and recruitment peaks.

Translucent zone formation is often assumed to be annual but is still poorly understood and the reasons for zone formation remain unclear (Schill, 2009; Szedlmayer and Beyer, 2011). Much research and resources are invested in determining annual fish ages, which form the basis of growth and mortality comparison as well as stock assessment and life history studies (Campana, 2005; Miller *et al.*, 2010). These results emphasize the importance of age validation studies and highlight the need to extend current research into the causes of translucent zone formation (see Chapter 6).

Formation of the translucent zones in *M. capensis* otoliths appears to be primarily associated with age, generally forming first on 8-month-old fish and then every 5 months after that. Environmental cues, which are variable on a daily basis, within areas, between areas and depths, and inter-annually, could account for the range in the timing of the formation of these zones. Environmental cues could also account for the presence of translucent zones additional to two per year and the variability of internally modulated zone formation. This latter effect is similar to that described by Campana (1984) for daily increment formation in plainfin midshipman *Porichthys notatus*, which he termed “environmental modulation of endocrine rhythms”.

4.6. Conclusions and recommendations

In this chapter, it is shown that fast growth rates of young *M. capensis* shown in Chapter 2 continue on older fish, rejecting the null hypothesis of slow *M. capensis* growth rates similar to those previously estimated.

In terms of the management of *M. capensis* stock in Namibia, it follows that *M. capensis* should have a higher natural mortality rate or a greater stock productivity than previously thought. It is recommended that the sensitivity of the stock assessment models and resulting management advice to this fast growth rate should be tested.

After T2 (the first annulus), translucent zones are formed two to three times per year (roughly every 5 months). T2, T4, T6, T8 and T10 zones are most likely the annuli, though showing no obvious differences in appearance under the light microscope to T1, T3, T5, T7 and T9. This again rejects the null hypothesis generally assumed for annual age validation that translucent zone formation occurs once per year.

The simplest method of age determination should be used. In the first step, the first visible translucent zone at ≥ 7.5 mm diameter should be assigned as the first annulus (regardless of the presence or number of translucent zones before the first annulus). The next step involves counting the number of translucent zones after the assigned first annulus, and dividing the count by two to get the number of age groups after age group 1. The resulting integer should indicate the age group:
Age group = Integer of [1 + (count after assigned age group 1 / 2)].

For the purpose of stock assessment, the new age data to be used should be obtained using the conversion presented in Table 4.7.

Because of the unusual summer- and-winter-overlapping formation of the zones, translucent zone formation does not seem to be primarily related to specific temperatures or seasons. Variables that may influence translucent zone formation (e.g. area, depth, cohort, temperature, feeding and nutrition, fish length or age) should be investigated further.

CHAPTER 5

Spatial distributions of the *Merluccius capensis* stock in the northern Benguela related to translucent zone formation in their otoliths

5.1. Abstract

The spatial distributions of juvenile and adult *M. capensis* were investigated in relation to translucent zone formation on their otoliths. Data were collected from 25 biomass surveys conducted along the Namibian coast from 1990 to 2007. A loess smoother was fitted to the number of fish per 30-min-haul ("density") (1) as a function of fish total length (TL) and latitude; and (2) as a function of fish TL and bottom depth. Nursery aggregations were identified in the central (20.5–25.5°S) and southern (25.5–29°S) areas, with greater densities in the southern area in recent years. Spawning and nursery aggregations appear to have shifted southwards since the 1970s and 1980s. Hatchdates of the young-of-the year (fish < 16 cm TL) were calculated from growth rates presented in Chapter 2. Most hatchdates fell in winter with a secondary peak in spring in the central area, and in spring in the southern area. In general, hatchdates differed between the two areas by 3–4 months with juveniles from the central area hatching earlier. The years of strong recruitment seemed to stem from a long (bimodal) spawning period over the entire Namibian coast. Young *M. capensis* first moved shallower at 9–15 cm, and then deeper, with depth positively related to fish length. Juveniles tended to stay in the same area they were spawned in until they were about 24 cm long (1.5 years old). Fish moved from the inner-shelf to the mid-shelf (24–28 cm) and then northwards when they were between 30 and 36 cm long, probably for feeding and building resources for spawning. They moved to the outer-shelf and then southwards again, and sometimes shallower again to the mid-shelf to spawning area(s) when they were > 52 cm TL. All translucent zones T1–T9 frequently coincided with inner- to mid-shelf and mid-shelf to outer-shelf or north-south migration. Even winter translucent zones were closely associated with off-the-shelf migrations and translucent zones were typically formed at the same rate as migration. The current otolith sampling method on research surveys is sufficient to age the entire Namibian *M. capensis* stock.

5.2. Introduction

Classical marine fish population dynamics assumes that fish populations are structured according to size in different areas (Sparre and Venema, 1998). Demersal fishes of similar sizes have been observed to aggregate according to preference of depth and latitude (e.g. Williams and Ralston, 2002; Tolimieri and Levin, 2006), and have been found to move deeper as they grow "bigger", both for individual species as well as the whole demersal community when limited depth ranges were studied (e.g. Polloni *et al.*, 1979; Gordon and Duncan, 1987; MacPherson and Duarte, 1991). Another reason for the apparent "bigger-deeper" phenomenon for individual species, suggested by Snelgrove and Haedrich (1985), was that immature fish only inhabit shallow depths, while large fish inhabit deep as well as shallow areas. Moranta *et al.* (2004) showed that the "bigger-deeper" phenomenon was not true for all species in the deep-sea.

Many marine fish populations undergo annual spawning migrations by directional and active movement to a preferred habitat (Dorn, 1995), or over their lifetime migrate towards the spawning areas from where eggs and larvae are passively transported towards their nursery areas, and to which adults actively return when they mature (e.g. Hjort, 1914; Saunders and McFarlane, 1997; Hutchings *et al.*, 1998; 2002; van der Lingen *et al.*, 2001; Svendäng *et al.*, 2007). Unit stocks or sub-stocks of the same species are distinguished by their spawning areas and timing, and thus the degree of geographical and temporal mixing (Clayden, 1972; MacLean and Evans, 1981). The "recruitment from nursery areas to the adult stock is potentially the most dispersive phase in a species' life history" (Pawson and Jennings, 1996, p. 205) and the connection between juveniles and adults is an important part of understanding the consistency of a stock, and relevant to fisheries management (Pawson and Jennings, 1996).

Hakes (genus *Merluccius*) show interesting examples of extensive migrations during at least one phase of their life history, including annual spawning migrations (Bailey *et al.*, 1982; Lloris *et al.*, 2005). The populations have been documented to be structured by size according to latitude and bathymetric depths, mostly moving from the continental shelf into deeper waters of the continental slope as their size increases throughout their life history (MacPherson and Duarte, 1991; Relini *et al.* 2002;

Burmeister, 2005; Tserpes *et al.*, 2008), but in some cases the largest individuals being found at intermediate depths (Moranta *et al.*, 2004). More recently, settled juveniles on the shelf break and upper slope have been found in deeper waters than older juveniles (on the mid-shelf) for both silver hake *M. bilinearis* (< 6 cm fish at > 60 m bottom depth; Steves and Cowen, 2000) and European hake *M. merluccius* (< 12 cm fish at > 150 m bottom depth; Bartolino *et al.*, 2008). These shifts were associated with a change in diet from mainly planktonic crustaceans to pelagic fish as well as an increase in the area of the inner ear (Bartolino *et al.*, 2008).

M. capensis are assumed to settle to the oceanic bottom at 45 days (about 3 cm total length, TL), shown by the mean duration of primordia in their otoliths (Gordoa *et al.*, 2001), and move offshore as they grow older and larger (Gordoa and Duarte, 1991; Burmeister, 2001). Both *M. capensis* and *M. paradoxus* in the northern Benguela have shown size- aggregated spatial distributions, with an increasing mean length with depth and a decrease in density of the aggregations with mean length (Gordoa and Duarte, 1991; 1992). This suggests size-based shoaling behaviour (Gordoa *et al.*, 1995). *M. capensis* are thought to be meso-pelagic spawners (Botha, 1973; Sundby *et al.*, 2001). Eggs were found over a range of 100–400 m bottom depths, and at 30–150 m depth in the water column in the northern Benguela. Adults presumably move inshore and upwards above the low-oxygen layer in the water column to spawn, being shallowest towards the end of the spawning season, with the youngest eggs found over shallowest depths (O'Toole, 1978; Assorov and Berenbeim, 1983; Olivar *et al.*, 1988; Olivar, 1990; Sundby *et al.*, 2001). Sundby *et al.* (2001) showed that deep offshore spawning also occurs. They postulated that eggs and larvae are transported onshore and southward by a subsurface upwelling current, concentrating early juvenile hake nearshore.

Spawning *M. capensis* in have been found along most of the Namibian coast between 18°S and 27°S (Olivar and Shelton, 1993). Olivar *et al.* (1988) found *M. capensis* eggs at 20–21°S and 22–23°S in November 1979. They found most eggs in August 1980, between 18°S and 23°S and no eggs in autumn (March–April 1981). Assorov and Berenbeim (1983) showed that spawning adults of *M. capensis* were located around Walvis Bay (23–24ºS) in spring (October–March) and around Cape Frio (20–21ºS) in all seasons with the highest spawning intensity in winter (mid-July). Kainge *et al.*

(2007) found the highest density of adults with a gonadosomatic index above 2.4 % at 20ºS, between 22ºS and 24ºS, and at about 28ºS All of these may or may not have constituted different spawning sub-stocks. No seasonal horizontal migrations (north-south or inshore-offshore) have been observed, as there have been no observed temporal shifts in the catchability of the fishing fleet, fishing only deeper than 200 m bottom depths (MacPherson *et al.*, 1991; Gordoa *et al.*, 2000). However, Gordoa *et al.* (2006) suggest an onshore spawning migration of *M. capensis* in May to September to waters shallower than 200 m bottom depths, with peak spawning occurring in shallowest waters in October. In the southern Benguela, both *M. capensis* and *M. paradoxus* seem to migrate inshore and southwards in summer (Millar, 2000). For both species, Burmeister (2001) observed a decrease in mean length towards the south in Namibia.

In Chapter 2, it was shown that juvenile *M. capensis* collected from Cape fur seal scat samples were mainly spawned in winter (June–July), and mostly fitted the same growth curve, being the same size at the same time for the same cohort, for northern and southern Namibia. This suggests they belong to the same unit stock. It was also noted that the fur seals rarely fed on *M. capensis* larger than 25 cm TL. This suggests the large fish have moved out of the feeding range of the fur seals off the inner shelf and shelf break (Skern-Mauritzen *et al.*, 2009). In Chapters 3 and 4, it was shown that the first three translucent zones were formed at 9–13, 15–20 and 22–26 cm TL of young fish and about every 3–5 cm after that on older fish. The results suggest that settlement of young hake happens long before the first translucent zone is formed. However, it is possible that other depth changes over the life history of *M. capensis* play a role in translucent zone formation because of the associated temperature, diet and area of inner ear changes (Bartolino *et al.*, 2008). For example, the central and northern part of the Namibian coastline is defined by a double shelf-break, dividing the continental shelf into an inner shelf <180 m, mid-shelf 180–350 m, and outer shelf >350 m (Bremner, 1983; Monteiro *et al.*, 2005). Translucent zone formation could be caused by fish moving from one of these shelf areas to the next across these two shelf break boundaries. The sea surface temperature in the north and the south of Namibia differs by about 6°C in summer and winter, and if fish belong to the same stock, they should move between these areas. Temperature differences could also result in the formation of translucent zones on their otoliths if/when they move.

The aims of this chapter are to further address some of the questions regarding *M. capensis* horizontal and vertical distribution and mixing arising from Chapters 2, 3 and 4. The conclusion of Chapter 2 that *M. capensis* stem from a winter spawning period from both southern and central Namibia are further investigated. In addition, the conclusion that translucent zone formation is not caused by demersal settlement but possibly by a shift in energy requirements associated with off-the-shelf or north-south movements of *M. capensis* is tested further. More specifically, the aims of this chapter are to use *M. capensis* length-distributions from surveys along the Namibian coast from 1990–2007 to address the following questions:

(1) a. Which area(s) contain(s) the youngest *M. capensis* and can therefore be termed nursery areas? b. Are there one or several nursery areas along the Namibian coast? c. What are the approximate hatchdate(s) of young fish from the nursery area(s)?

(2) a. At which fish lengths do *M. capensis* change area (move latitude)? b. Is there a relationship between fish length at which *M. capensis* form translucent zones on their otoliths and lengths at which they change latitude?

(3) a. At which fish lengths do *M. capensis* change depth (inner shelf to mid-shelf to outer-shelf)? b. Is there a relationship between fish length at the depth change and fish length at translucent zone formation on *M. capensis* otoliths?

5.3. Materials and methods

The data used in this chapter were collected during hake biomass surveys conducted by the Ministry of Fisheries and Marine Resources (MFMR), Namibia, from 1990 to 2007 (Burmeister, 2001; MFMR, unpublished data). The surveys covered the entire Namibian coastline and the continental shelf and slope, mostly up to bottom depths of 400–600 m (Table 5.1). Most (16) of the 25 surveys were conducted in summer (January–February), four surveys were conducted in May, two in September and three in November.

Survey stations were chosen according to a systematic transect design with a semi-random distribution of stations along transects, based on six depth strata: 1–99, 100–199, 200–299, 300–399, 400–499, 500–599 m bottom depth (Burmeister, 2001). At each station, bottom depth (to the nearest m), latitude (to the nearest minute at the start of the trawl), and hauling duration (minutes) were recorded. For each station, a sample

of *M. capensis* was measured to the nearest cm TL and weighed to the nearest gram. The number of *M. capensis* measured during each survey ranged between 17485 and 42184 from between 98 and 193 bottom trawl stations (Table 5.1; data courtesy P. Kainge, MFMR, Namibia).

Table 5.1 Namibian hake biomass surveys from 1990–2007 with their dates, the total number of hauls including *M. capensis*, depth ranges (of stations including *M. capensis*), areas covered, total numbers of *M. capensis* measured and their length ranges.

Survey	First station	Last station	Mid-date	No. of hauls incl. *M. capensis*	Bottom depth range (m)	Latitude range (°S)	No. of *M. capensis* measured	TL range (cm)
1990	26 Jan	18 Mar	20 Feb	126	76 – 550	17.3 – 29.2	18125	6 – 75
1990-09	14 Sep	04 Oct	24 Sep	110	79 – 402	17.3 – 29.1	23539	6 – 85
1991	27 Jan	27 Feb	11 Feb	175	80 – 416	17.4 – 29.4	26690	6 – 92
1991-11	24 Oct	20 Nov	06 Nov	143	77 – 460	17.4 – 29.2	23617	6 – 84
1992-05	24 Apr	19 May	06 May	149	81 – 504	17.3 – 29.6	23641	7 – 95
1992-11	21 Oct	21 Nov	05 Nov	166	89 – 602	17.3 – 29.6	26024	6 – 90
1993	21 Jan	23 Feb	06 Feb	161	97 – 562	17.4 – 29.6	23998	5 – 97
1993-05	22 Apr	24 May	08 May	176	93 – 554	17.3 – 29.6	27373	7 – 87
1994	21 Jan	21 Feb	05 Feb	122	93 – 557	17.5 – 29.3	19289	3 – 99
1994-05	28 Apr	23 Jun	26 May	193	17 – 588	17.4 – 29.3	42184	4 – 95
1994-11	21 Oct	05 Dec	12 Nov	190	30 – 606	16.8 – 29.6	32433	2 – 98
1995-05	22 Apr	26 May	09 May	128	88 – 580	17.5 – 29.1	23663	6 – 89
1996	10 Jan	17 Feb	29 Jan	168	88 – 453	17.4 – 30.0	34255	7 – 92
1996-09	11 Sep	12 Oct	26 Sep	117	103 – 558	17.4 – 29.3	26086	6 – 84
1997	12 Jan	19 Feb	31 Jan	140	92 – 451	17.4 – 30.8	26014	2 – 89
1998	13 Jan	20 Feb	01 Feb	144	79 – 798	17.4 – 29.5	32558	5 – 88
1999	13 Jan	18 Feb	31 Jan	152	89 – 595	17.3 – 29.6	28460	5 – 98
2000	17 Jan	22 Feb	04 Feb	144	87 – 513	17.3 – 29.3	24281	7 – 94
2001	19 Jan	24 Feb	06 Feb	136	90 – 478	17.3 – 29.3	17485	5 – 86
2002	19 Jan	22 Feb	05 Feb	117	90 – 553	17.3 – 29.0	22821	6 – 85
2003	17 Jan	20 Feb	03 Feb	116	90 – 429	17.3 – 29.0	24559	6 – 85
2004	14 Jan	20 Feb	01 Feb	127	97 – 434	17.3 – 29.3	34253	5 – 84
2005	13 Jan	16 Feb	30 Jan	114	93 – 484	17.3 – 29.3	18760	5 – 80
2006	12 Jan	17 Feb	30 Jan	98	95 – 414	17.3 – 29.3	23012	6 – 81
2007	11 Jan	15 Feb	28 Jan	116	94 – 430	17.3 – 29.3	26449	6 – 86

The number of *M. capensis* measured in each TL-class was raised to the total number of *M. capensis* in the trawl by multiplying the number in the sample by the ratio of total weight (g) in the trawl catch to the sample weight (g). The total number of fish per TL-class for each trawl was then raised to 30 minutes trawl time. The vessel speed and net opening were kept constant at each trawl, assuming that the swept area would be the same for the same towing duration. This resulted in an index of abundance for each TL-class in each trawl as the number of fish per 30 minutes (n 30min^{-1}). For the

purposes of simplicity, the index of abundance is called "density" for the remainder of this chapter.

Similar to Bartolino *et al.* (2008), the density values by trawl were averaged by one-degree-latitude classes and by 20-m-depth classes. These gave a latitude-length matrix and a depth-length matrix for each survey. In each block of the matrix (in each latitude- or depth-class), the density index was normalised to the total number of fish in the *TL*-class, obtaining a relative latitude (*lat*) or depth (*d*) preference index (*R*):

$$R_{TL,lat} = \frac{N_{TL,lat}}{\sum N_{TL}} \text{ and } R_{TL,d} = \frac{N_{TL,d}}{\sum N_{TL}} \quad (5.1),$$

where $N_{TL,\ lat}$ and $N_{TL,\ d}$ are average numbers of fish per 30 minutes trawled in each TL-class in each *lat* or *d* class and $\sum N_{TL}$ is the sum of fish per 30 minutes trawled in the TL-length class over all *lat* or *d* classes in the matrix.

The preference index $R_{TL,\ lat}$ was modelled as a function of length and latitude using a loess smoother, span of 0.1 and divisions of 2 (n 30min^{-1}), in the basic package of R version 2.9.1 (R Development Core Team, 2009) for each survey separately. This surface smoothing assumes an additive model:

$$R_{TL,\ lat} = f\,(TL,\ lat) + \epsilon \quad (5.2),$$

where the two-dimensional surface f (*TL*, *lat*) is defined by the independent variables *TL* and *lat*. The same was repeated for $R_{TL,\ d}$ as a function of *TL* and *d*. Both *TL-lat* and *TL-d* smoothers were fitted twice for each survey, once for fish < 20 cm TL (to include all 16 cm fish, see below) and once for fish spanning the entire length range.

From the growth curve of young *M. capensis* presented in Chapter 2, fish at 16 cm TL are about one year old. The contour plots of $R_{TL,\ lat}$ were used to identify "nursery aggregations" as the centre of the highest density contours, assuming aggregations of fish < 16 cm TL to be young-of-the-year. They were identified as present in the north (< 20.5°S), centre (20.5–25.5°S) and south (> 25.5°S) of the Namibian coast. Their TL at highest density was used to calculate their approximate hatching month using Equations 2.6 and 2.7:

$$t_{TLn} = \left[\ln\left(1 - \frac{TLn}{L_\infty}\right) \Big/ \left(-K\right)\right] + t_0 \quad (5.3),$$

where *TLn* is the TL with maximum density (central) of the aggregation, L_∞ is 33.6

cm, K is 0.651 y^{-1} and t_0 is -0.00917 y from the results presented in Chapter 2 (Table 2.1). The use of this growth curve for juveniles for hatchdate estimation of *M. capensis* is discussed in Chapter 2.

The approximate hatchdate was calculated as:

$$Hatchdate = (t_{TLn} * 365) + \text{survey mid-date} \quad (5.4),$$

using the survey mid-date in Table 5.1.

Density profiling was applied to the $R_{TL,\,lat}$ and $R_{TL,\,d}$ bivariate surfaces. In this method, the maximum value of the surface for each fixed TL is plotted as a function of TL. Similarly, the maximum value of the surface for each fixed one-degree-latitude class was plotted as a function of latitude. The same was repeated for the TL-depth surface, plotting maxima at each fixed TL as a function as TL and maxima at each fixed (20-m) depth category as a function of depth. The minima in these profiles with respect to each latitude and depth represent the values at which length groups are best distinguished and the minima in the density profiles with respect to TL represent depths and latitudes from which clusters change from one to the other preference (Bartolino *et al.*, 2008). This method has been applied to infer movement from static aggregations (Bartolino *et al.*, 2008), and from here on will be termed the TL at which "migration" occurs.

The TL minima from density profiles for each survey were matched with TL_{50} at each translucent zone (T1–T9, Table 4.5). Data for the five cohorts studied in Chapters 3 and 4 1996, 1998, 2002, 2005 and 2006 were used for this purpose. Additional translucent zone counts were used from otoliths collected from five different surveys: "1992-11" (n = 473; West, 2009), 1999 (only T1–T6 zones; n = 280), 2002 (Chapter 4; n = 589; Kashava, 2009), 2003 (only T1–T4 zones; n = 372; Brinkman, 2007) and 2005 (Chapter 4; n = 459; West, 2009). Logistic ogives were fitted to proportion of otoliths showing at least T1–T9 zones against fish TL (cm), by replacing d_{50} in Equation 4.4 with fish TL_{50} (cm).

Separate TL-depth matrices and TL-latitude matrices (Equation 5.1) were constructed using depth-classes in three categories: inner-shelf < 180 m, mid-shelf 180–350 m and outer-shelf > 350 m (Bremner, 1983; Monteiro *et al.*, 2005), and latitude classes in

three areas: north < 20.5°S, centre 20.5–25.5°S and south > 25.5°S. Logistic ogives (see Chapter 4, Equation 4.4, but with TL instead of OD) of the "matching" translucent zones from cohorts and surveys were plotted against the proportion of fish density in each TL-class in each of the three depth areas as well as the three latitude-areas.

5.4. Results

5.4.1 Nursery and spawning areas

Up to three latitude-length clusters were observed for *M. capensis* < 20 cm TL (Fig. 5.1). Most fish < 16 cm TL were found off central and southern Namibia, and for only 6 of 25 surveys (24 %) off northern Namibia (Fig. 5.2). After 1996, no maximum density cluster of fish < 16 cm were found north of 20.5°S. Apart from the February and May 1993 surveys, no fish < 16 cm TL were found north of 20°S. The surveys indicating northern (< 20.5°S) nursery areas were: 1990-09, 1993, 1993-05 and 1996-09. During four more surveys (2000, 2001, 2004, 2006) nursery areas were observed at 21°S (at the northern border of the central area). During most surveys, the fish < 16 cm TL were found in both central and southern areas, with the exception of 1991-11 (only south), 1994-11 (only central area), 1996-09 (north and far south) and 2001 (both in the central area, one close to the northern border) (stars in Fig. 5.2). Surveys with exceptions mentioned above seemed to be mostly spring surveys conducted in the 1990s.

Surveys 1992-05, 1994, 1994-05, 1995-05 and 1997 (Figs 5.1e, i, j, l and o) looked very similar in that there were two nursery aggregations, one at 10 cm TL at 28°S (south), and another at 6 cm at 23°S (centre), with the central and southern aggregations "merging" at 16 cm TL and 26°S.

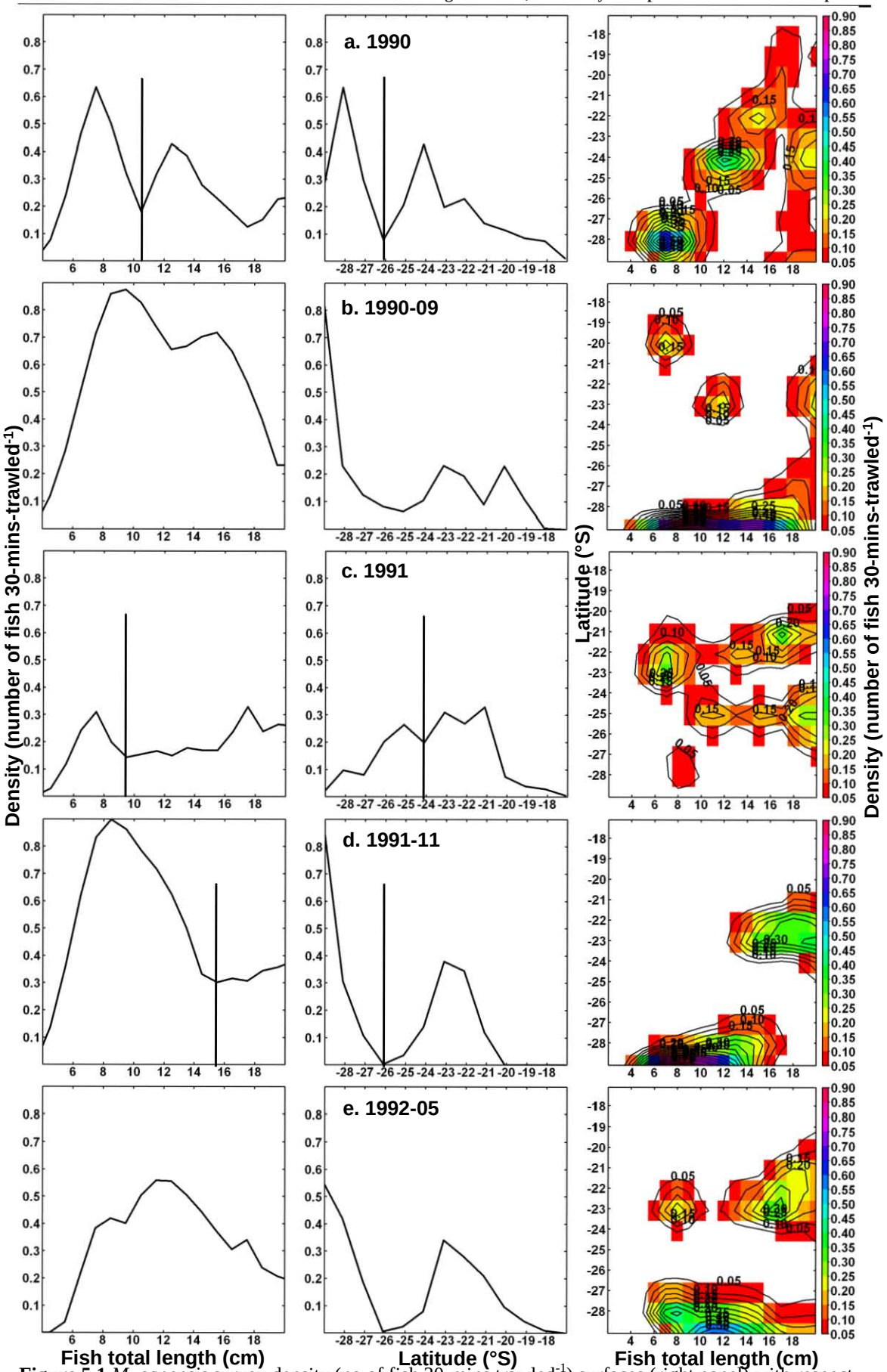

Figure 5.1 *M. capensis* survey density (no of fish 30-mins trawled^{-1}) surfaces (right panel) with respect to fish total length (cm) and latitude (°S) 1990–2007 (a–y) for fish < 20 cm total length. The profiles (left and middle panels) represent maxima on each plane of the surface plots with respect to fish total length and latitude respectively.

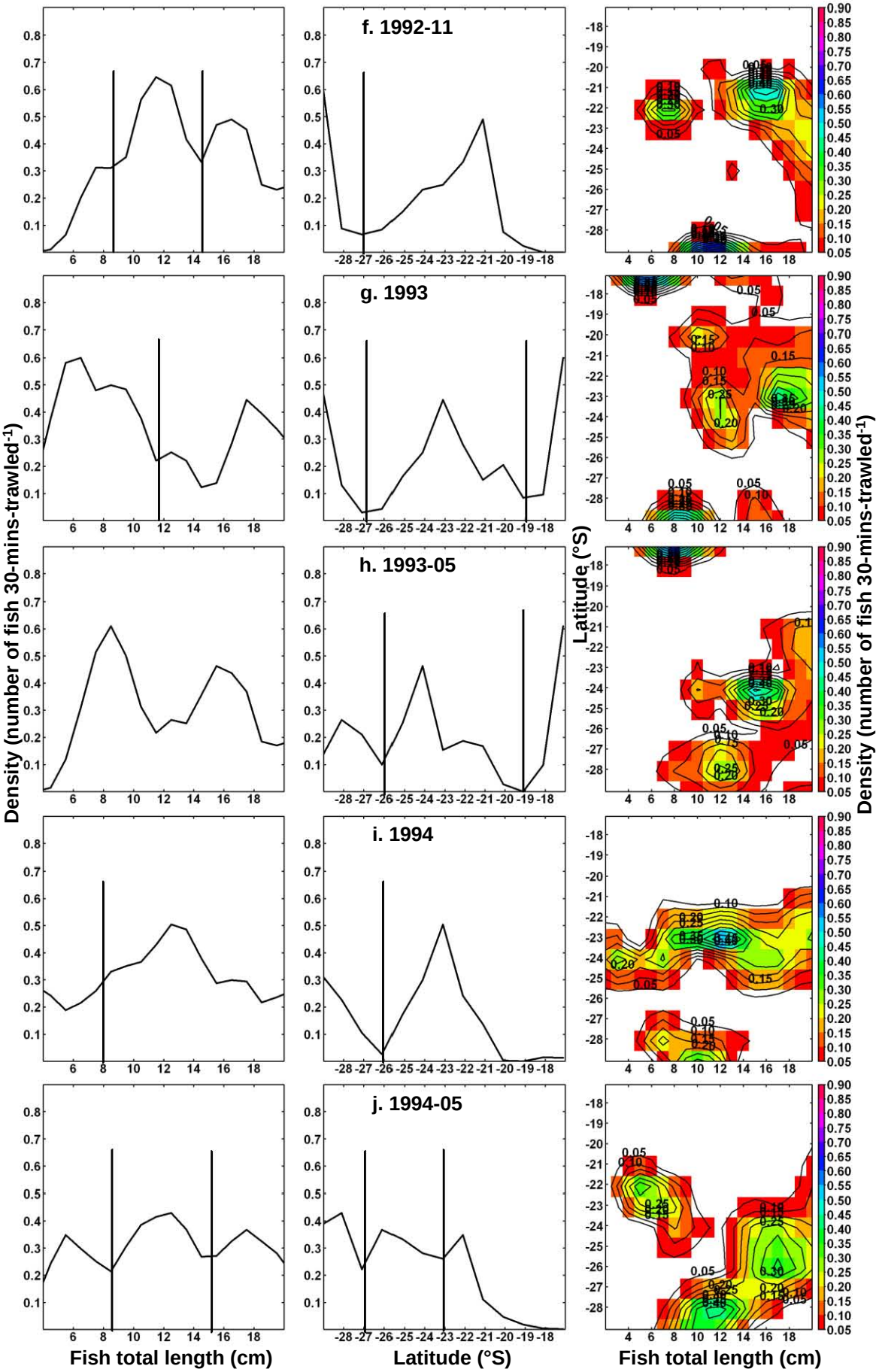

Figure 5.1 (continued)

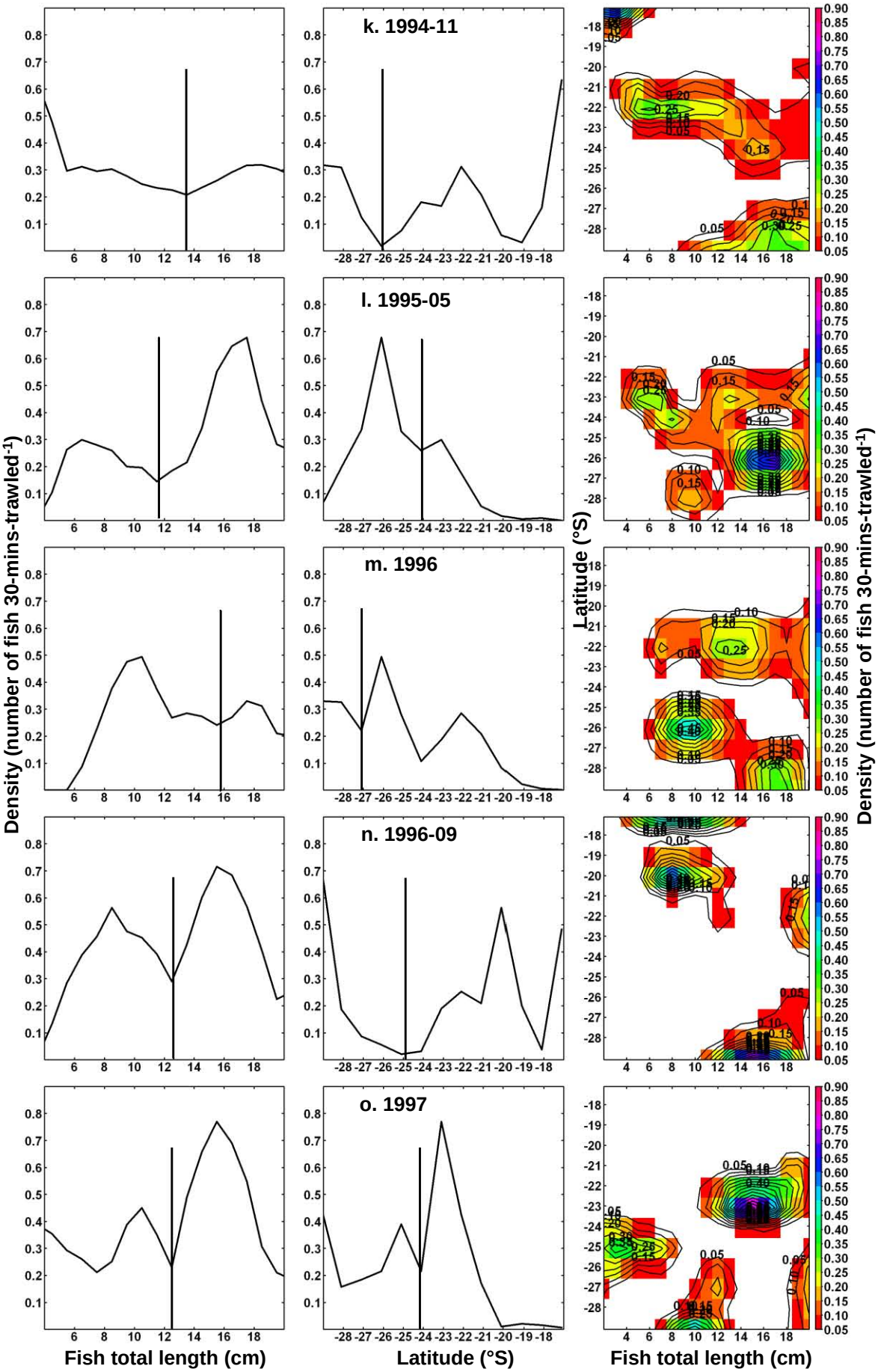

Figure 5.1 (continued)

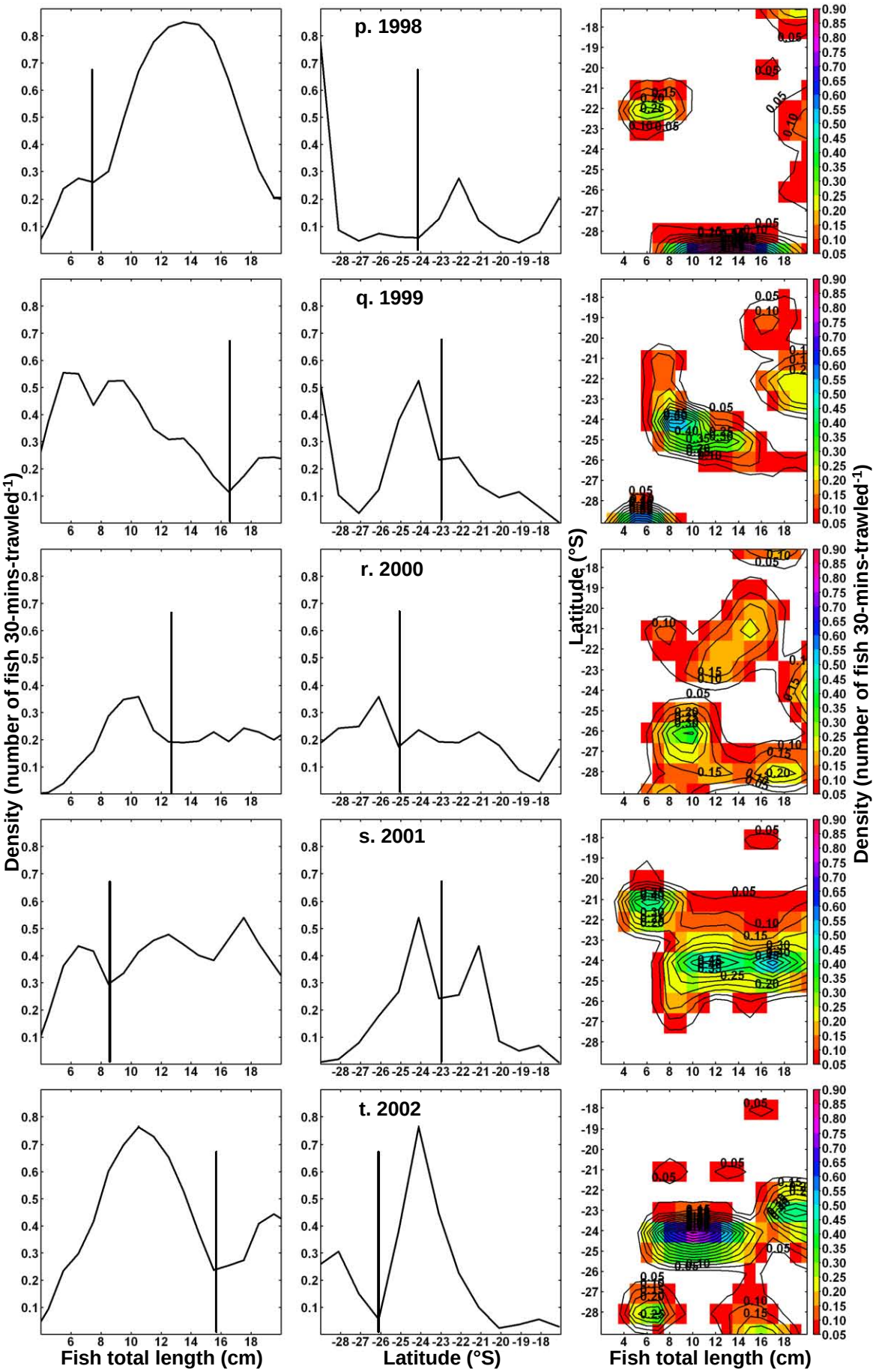

Figure 5.1 (continued)

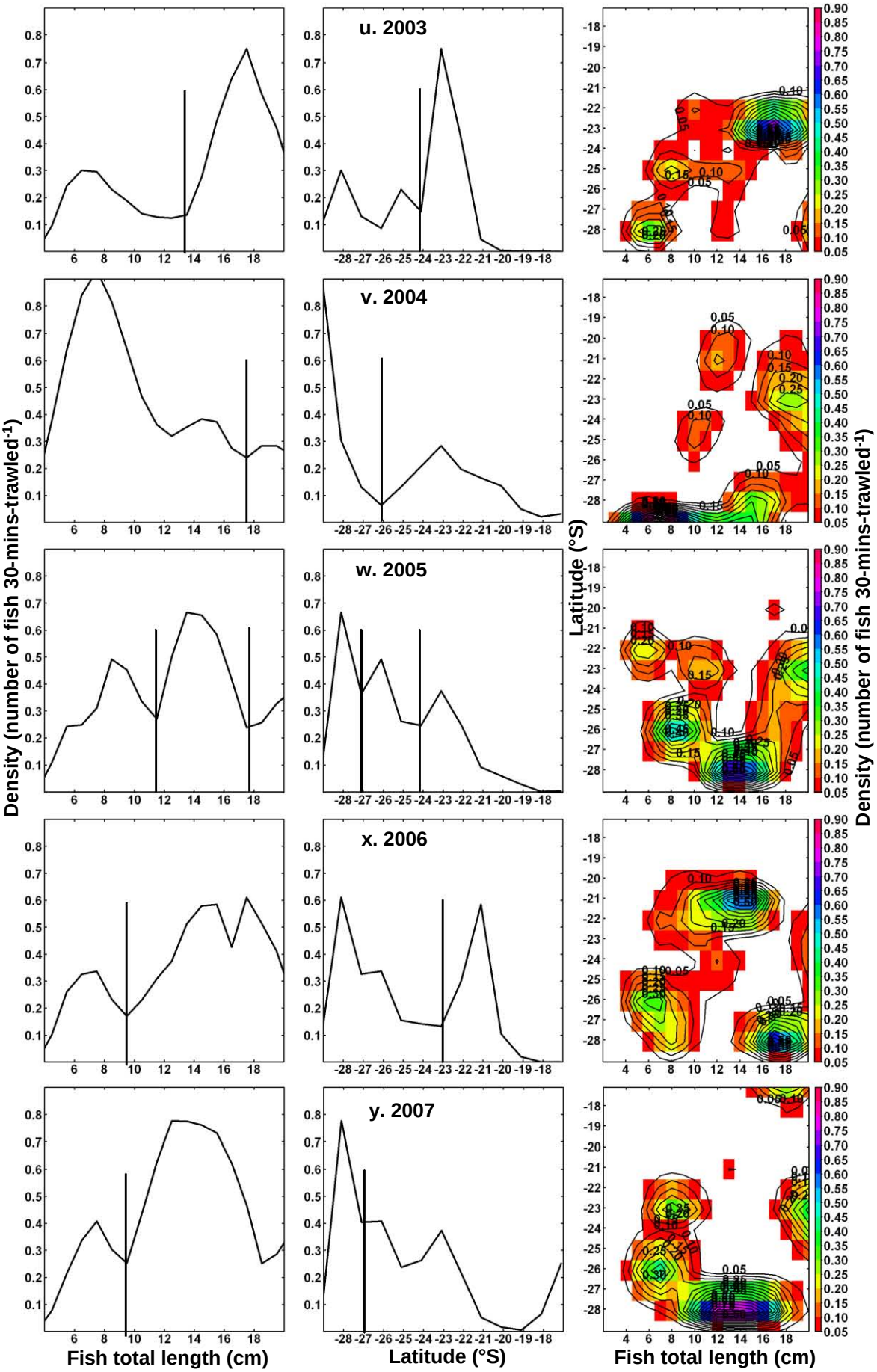

Figure 5.1 (continued)

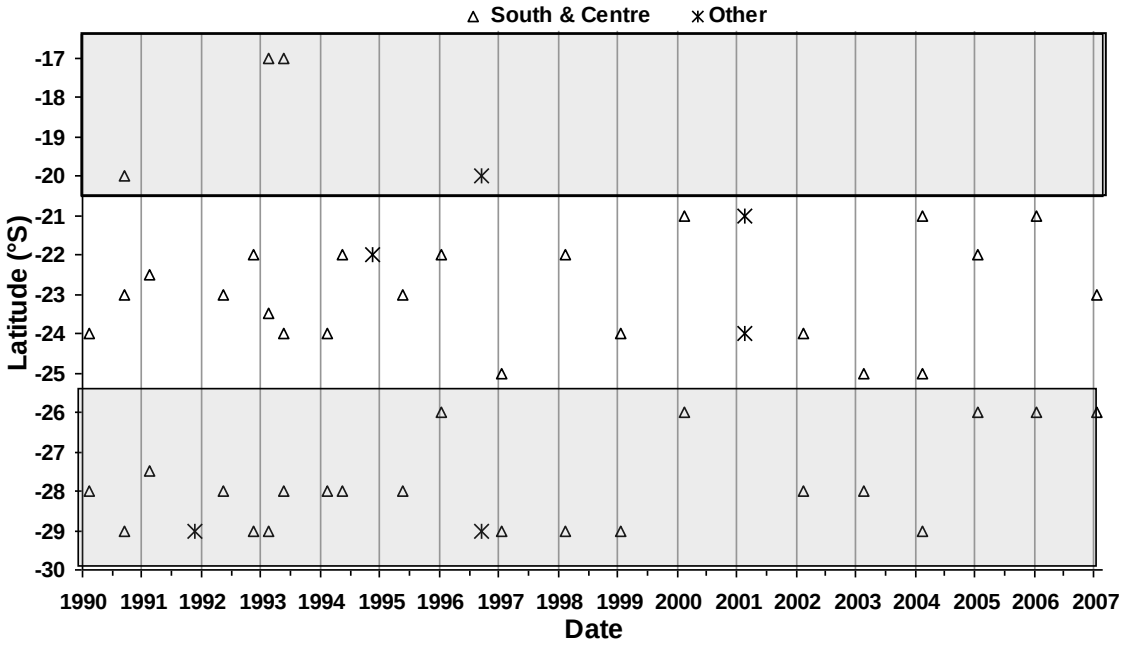

Figure 5.2 Positions of maximum density of *M. capensis* juveniles (< 16 cm TL) from density (*n* 30-mins^{-1} trawled) bivariate surface plots (Fig. 5.1) of 25 bottom trawl surveys conducted off Namibia in February 1990 – February 2007. The three areas north (< 20.5°S), centre (20.5–25.5°S) and south (> 25.5°S) are shaded. Stars indicate surveys in which the juveniles were not found in the centre and south.

In the surveys in which southern nursery areas were identified (which is all surveys except 1994-11 and 2001; Fig. 5.2), aggregations of large fish > 50 cm were also found in the south (Fig. 5.3). Densities of aggregations of fish < 16 cm TL as well as adult fish > 50 cm TL were higher in the south in recent years (since 2002), and higher in the central area in other years (Figs 5.1 and 5.3).

No differences in density between spring surveys (September and November) can be seen (Figs 5.1 and 5.3).

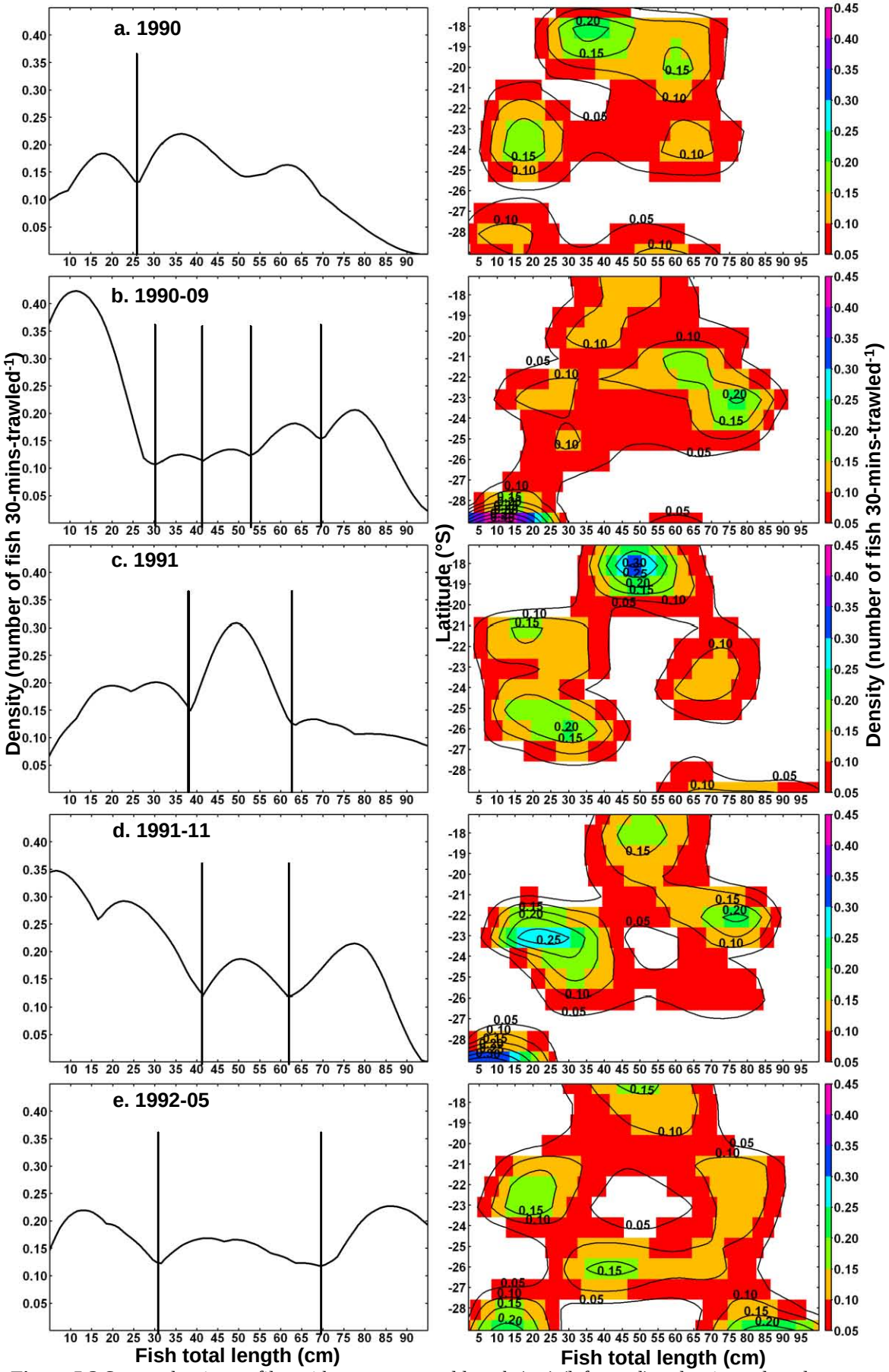

Figure 5.3 Survey density profiles with respect to total length (cm) (left panel) and estimated total length-latitude surface plots (right panel), 1990–2007 for the entire fish length range 4–98 cm of Namibian *M. capensis*.

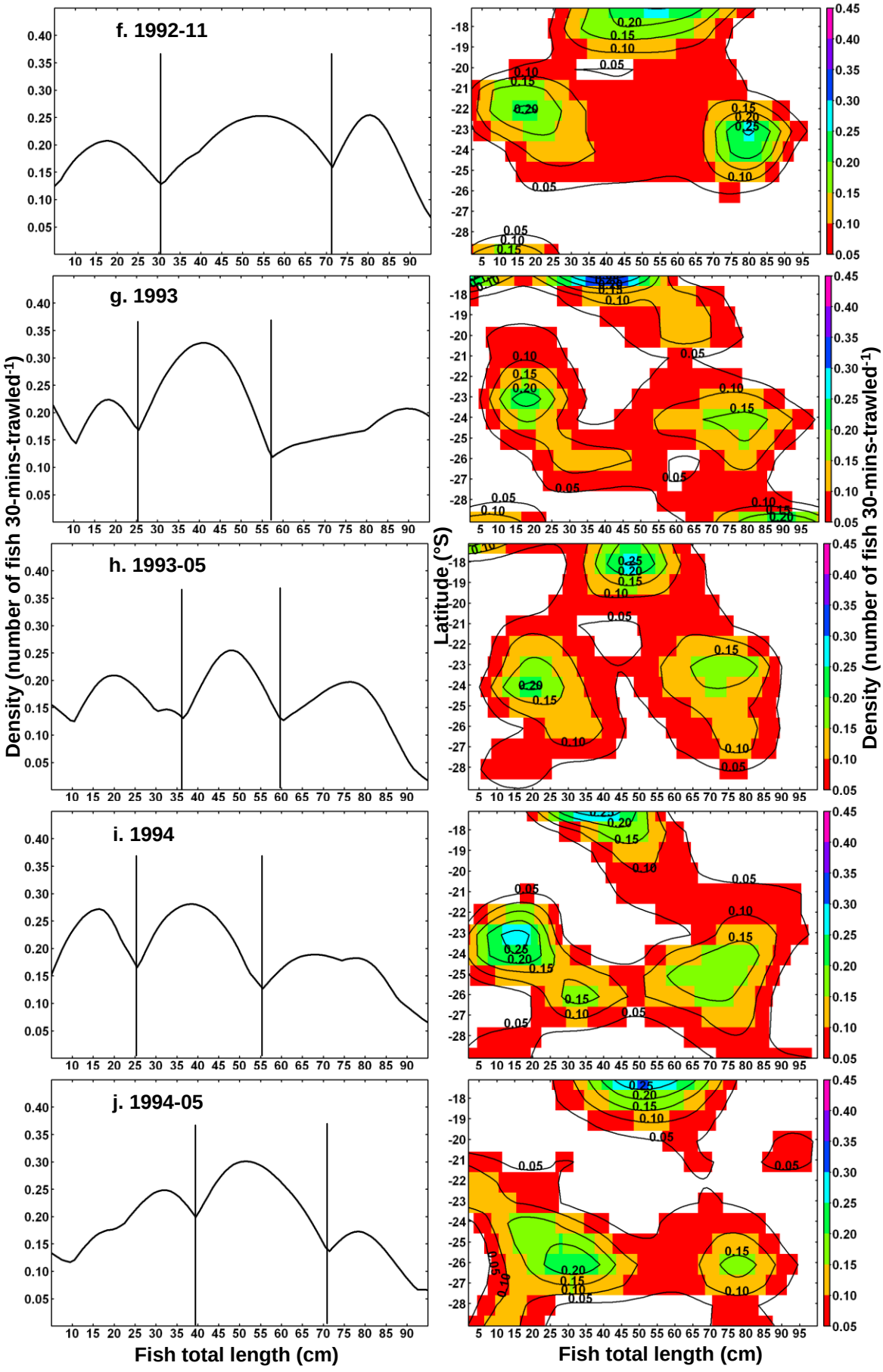

Figure 5.3 (continued)

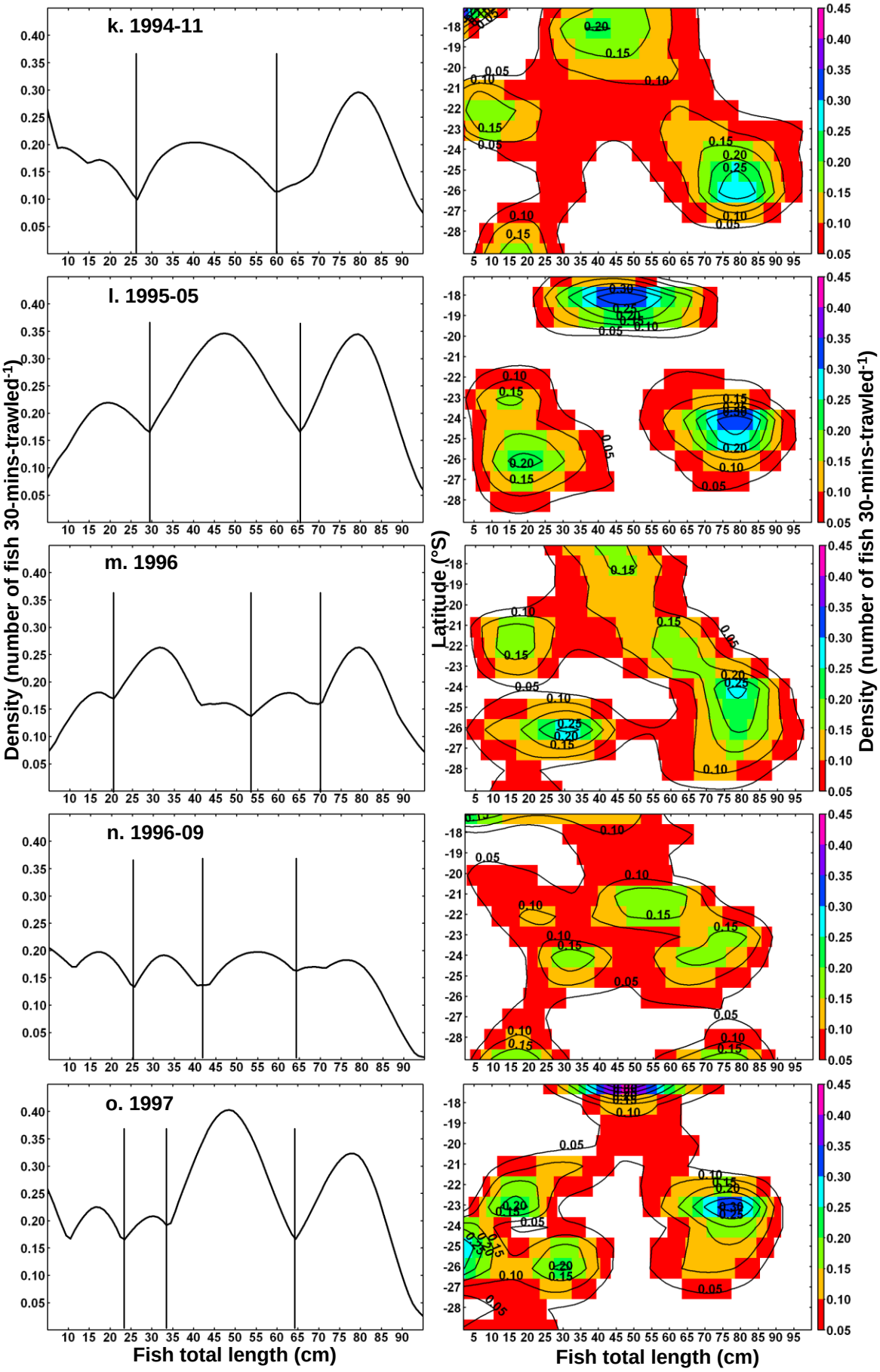

Figure 5.3 (continued)

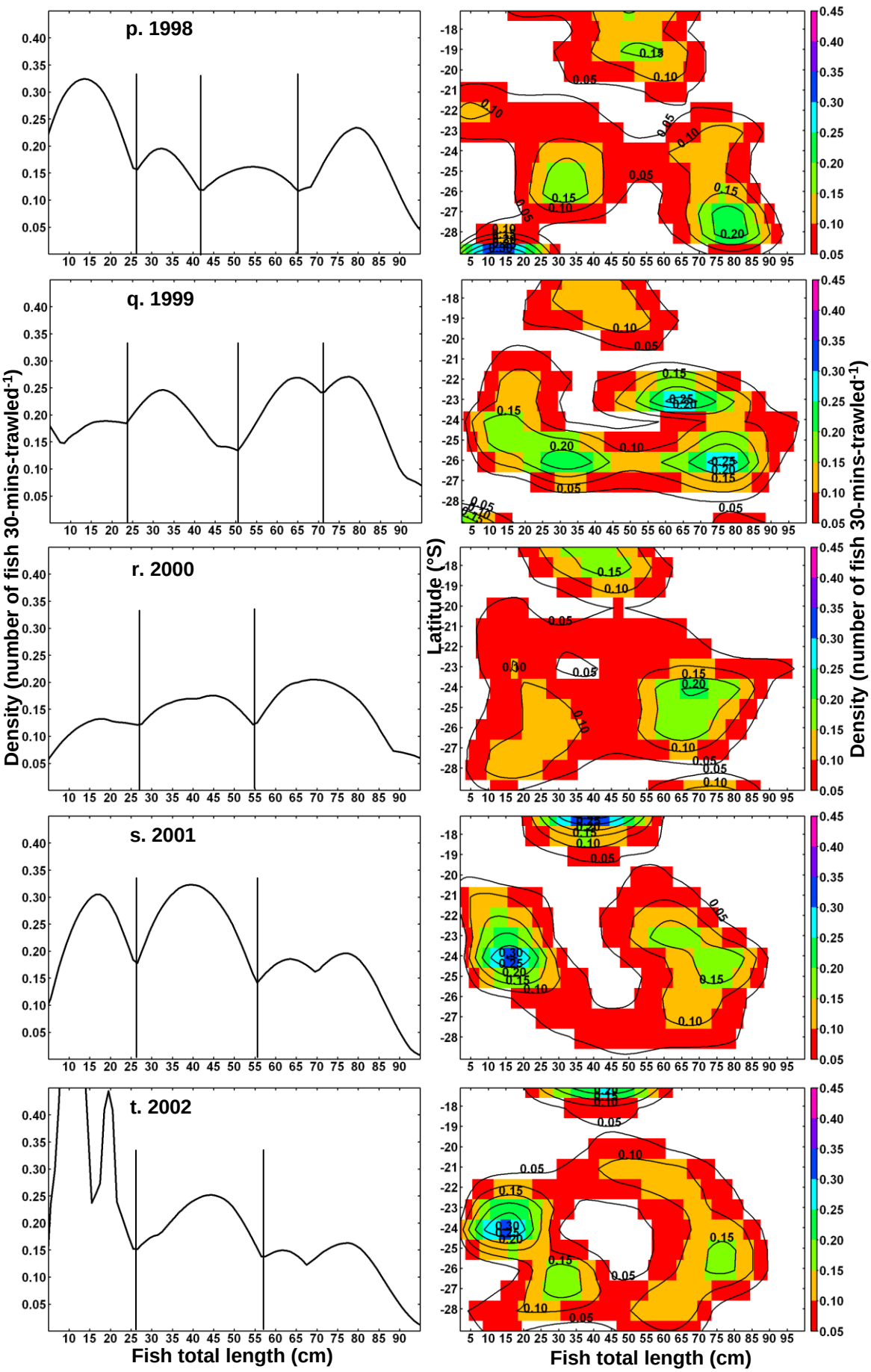

Figure 5.3 (continued)

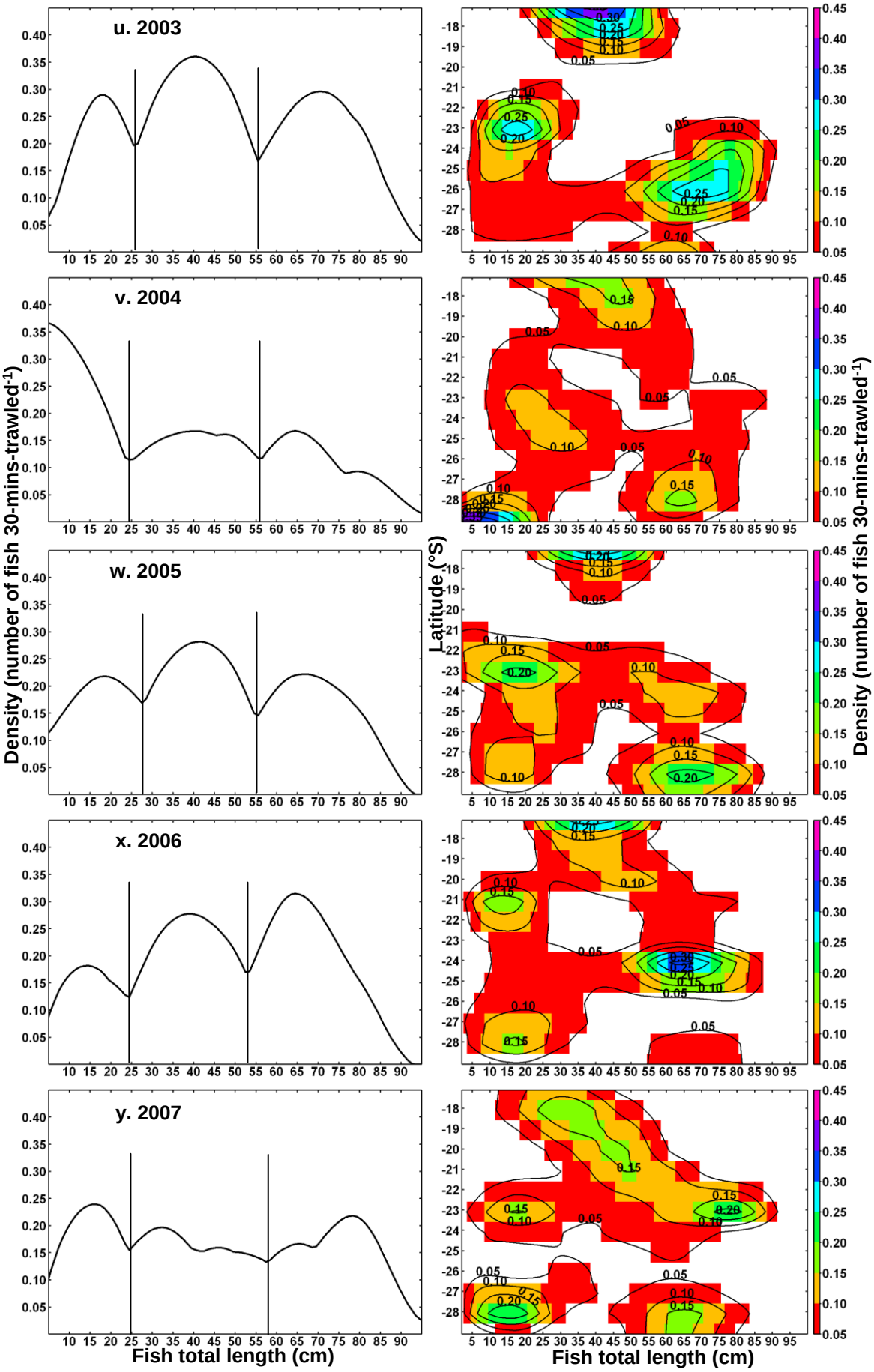

Figure 5.3 (continued)

Most surveys displayed a wide range of hatchdates calculated from the fish in their nursery aggregations (Table 5.2). The fish in nursery aggregations from the central area were older than the southern ones in 16 of 25 surveys (64 %). When aggregations with the same hatchdates were seen again in the next survey, they were in the same general area (arrows in Table 5.2). For this reason, minima in profiles in Fig. 5.1 were not regarded as "movement" but were denoted as two different aggregations.

Table 5.2 Mid-lengths *TLn* (cm) and calculated hatchdates of "nursery aggregations" of Namibian *M. capensis* juveniles < 16 cm TL from density profiles from 25 bottom trawl surveys, February 1990–February 2007 (Fig. 5.1). Surveys for which fish in central aggregations were younger than fish in southern ones are highlighted (bold). Arrows indicate when aggregations with similar hatchdates were seen again in the next survey.

		North (< 20.5°S)		**Centre (20.5–25.5°S)**		**South (>25.5°S)**	
Survey	**Mid-date**	***TLn***	**Hatchdate**	***TLn***	**Hatchdate**	***TLn***	**Hatchdate**
1990	20 Feb 90			12	21 Jun 89	7	15 Oct 89
1990-09	24 Sep 90	7	19 May 90	**11**	**17 Feb 90**	15	30 Oct 89
1990-09	24 Sep 90					9	05 Apr 90
1991	11 Feb 91			**6**	**27 Oct 90**	15	20 Mar 90
1991-11	06 Nov 91					8	10 Jun 91
1992-05	06 May 92			**8**	**09 Dec 91**	8	09 Dec 91
1992-05	06 May 92					11	30 Sep 91
1992-11	05 Nov 92			**7**	**30 Jun 92**	11	31 Mar 92
1993	06 Feb 93	6	22 Oct 92	12	07 Jun 92	8	10 Sep 92
1993	06 Feb 93	10	26 Jul 92				
1993-05	08 May 93	8	09 Dec 92	15	13 Jun 92	12	05 Sep 92
1994	05 Feb 94			3	18 Dec 93		
1994	05 Feb 94			7	30 Sep 93	6	21 Oct 93
1994	05 Feb 94			12	06 Jun 93	10	25 Jul 93
1994-05	26 May 94			**6**	**08 Feb 94**	11	19 Oct 93
1994-11	12 Nov 94			7	07 Jul 94		
1995-05	09 May 95			**6**	**22 Jan 95**	9	18 Nov 94
1996	29 Jan 96			7	23 Sep 95	9	10 Aug 95
1996	29 Jan 96			13	03 May 95		
1996-09	26 Sep 96	8	30 Apr 96			15	03 Nov 95
1997	31 Jan 97			4	24 Nov 96	10	20 Jul 96
1997	31 Jan 97			15	08 Mar 96		
1998	01 Feb 98			6	17 Oct 97	13	06 May 97
1999	31 Jan 99			9	12 Aug 98	5	05 Nov 98
2000	04 Feb 00			14	11 Apr 99	9	16 Aug 99
2001	06 Feb 01	6	22 Oct 00	11	02 Jul 00		
2002	05 Feb 02			10	25 Jul 01	6	21 Oct 01
2003	02 Feb 03			8	06 Sep 02	6	18 Oct 02
2004	04 Feb 04	12	04 Jun 03	10	24 Jul 03	7	29 Sep 03
2005	30 Jan 05			**6**	**15 Oct 04**	8	02 Sep 04
2005	30 Jan 05			**10**	**19 Jul 04**	13	04 May 04
2006	30 Jan 06			13	04 May 05	6	15 Oct 05
2007	28 Jan 07			**7**	**22 Sep 06**	6	13 Oct 06
2007	28 Jan 07					13	02 May 06

Hatchdates fell in all seasons, mainly between June and October in the central area and between September and October in the southern area (Fig. 5.4).

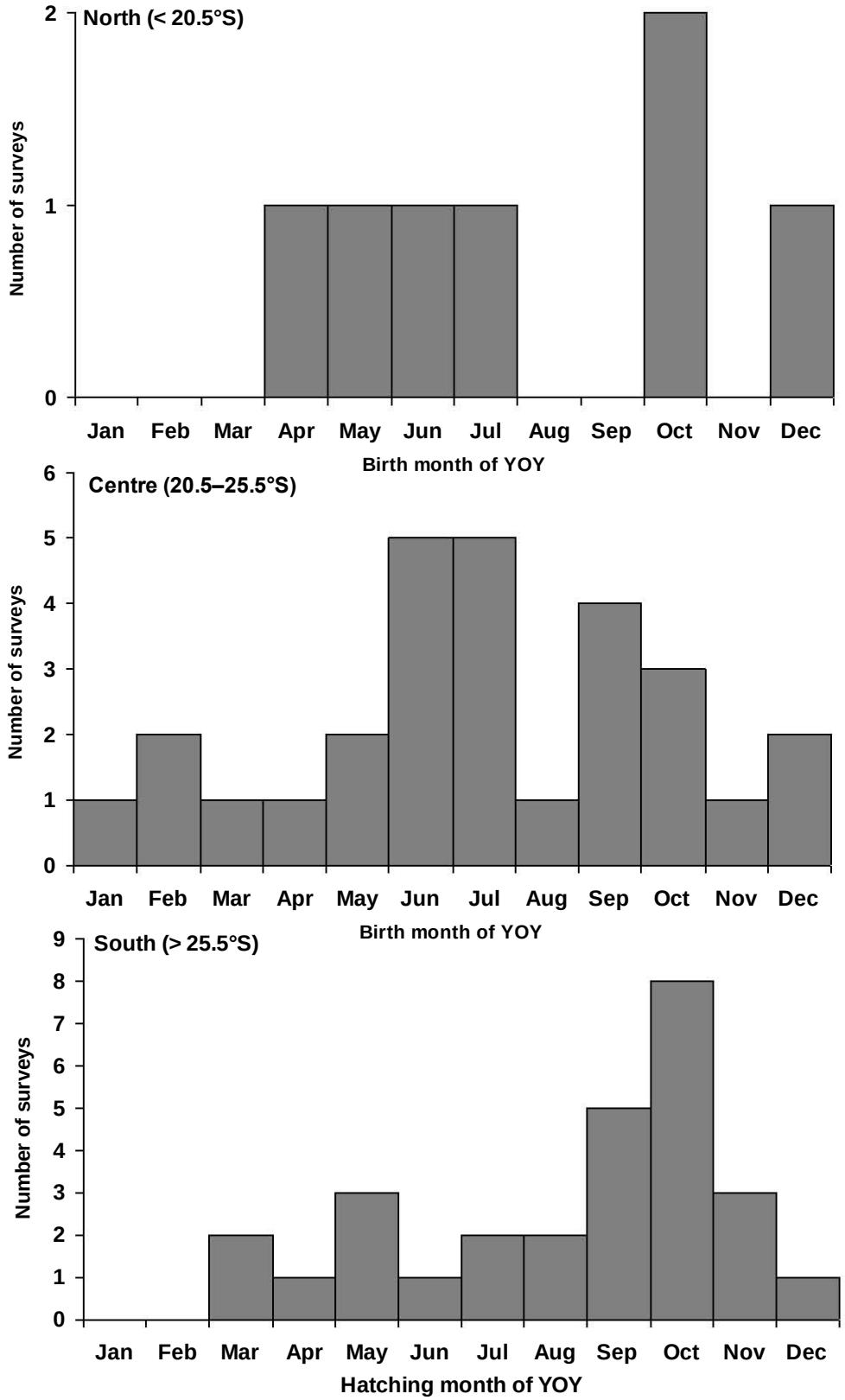

Figure 5.4 Hatchdate periods of Namibian *M. capensis* young of the year (YOY) caught in bottom trawl surveys 1990–2007 in the north < 20.5°S, centre 20.5–25.5°S and south > 25.5°S of Namibia.

5.4.2 Latitude changes with fish length

Latitude-density profiles (Fig. 5.3) showed that, in general, if *M. capensis* migrated after their first year, they moved northwards when they were between 23 and 42 cm TL (Fig. 5.5). Before 1999, they moved northwards twice within that length range, while 2000 onwards, they moved before 30 cm TL. They remained north until they moved south again in the 50–71 cm TL range (Fig. 5.5). The northern aggregation of medium-sized fish (30–50 cm TL) was usually found north of 20°S. TLs of fish "returning south" were < 60 cm from 2000 onwards (Fig. 5.5).

5.4.3 Depth changes with fish length

Density-depth profiles (Appendices 5.1 and 5.2) showed that in 13 of the 25 surveys (52 %) the youngest *M. capensis* were found slightly deeper than the older fish. The young fish moved shallower when they were between 9 and 15 cm TL, then deeper with increasing TL, and sometimes (9 of 25 surveys) shallower again at TLs 57 to 86 cm (Fig. 5.6). The distinct depth-TL clusters in which *M. capensis* moved to deeper bottom depths ranged between 7 and 69 cm TL (Fig. 5.6). These aggregations were not as clearly separated in the density peaks as north-south aggregations (Appendices 5.1 and 5.2). However, there is a significant positive relationship between fish TLs and bottom depths (m) when fish moved deeper (Fig. 5.7). They displayed a "stepped" function for moving shallower: at a mean TL of about 10 cm (from 100–200 m) and again at about 70 cm (from > 200 m) (Fig. 5.7).

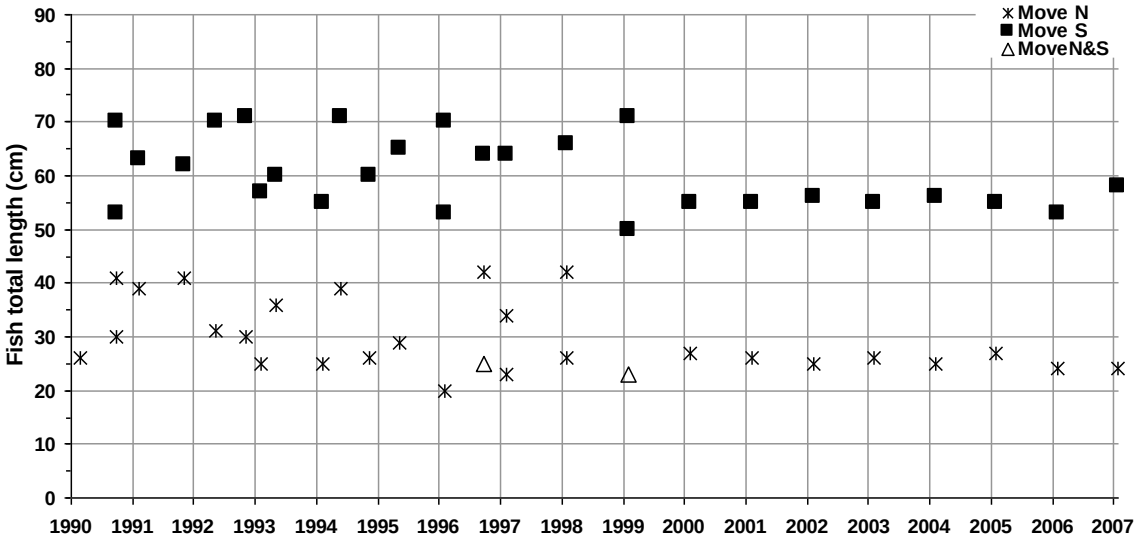

Figure 5.5 *M. capensis* TL (cm) at which they either move northwards (stars), southwards (squares) or both northwards and southwards (triangles), calculated from latitude-length density profiles (Figs 5.1 and 5.3) of 25 Namibian bottom trawl surveys from 1990 to 2007.

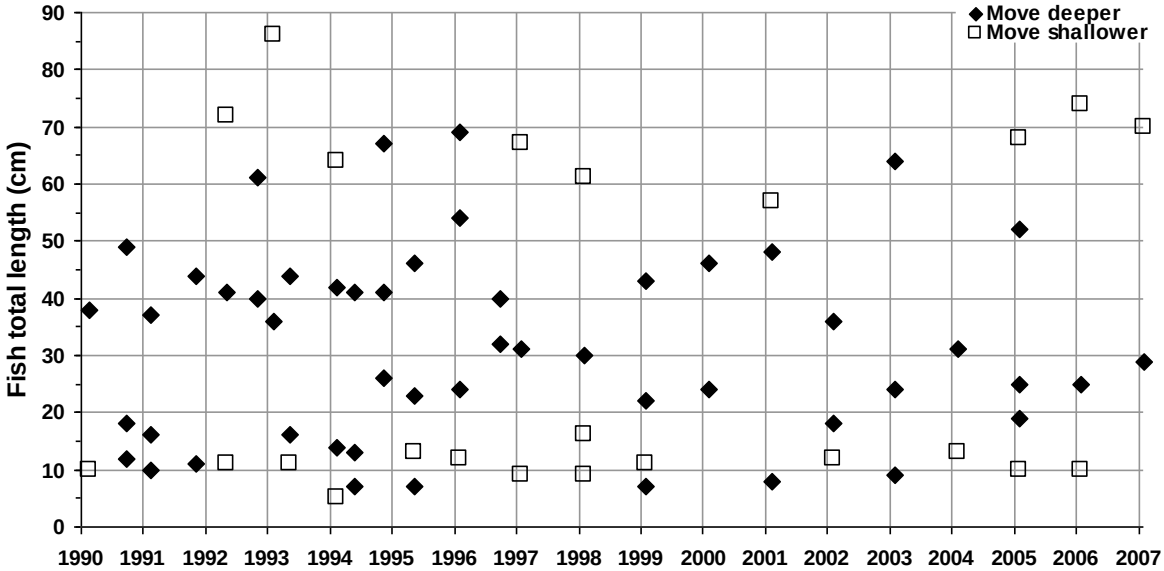

Figure 5.6 *M. capensis* TL (cm) at which they either move deeper (diamonds) or shallower (squares), calculated from depth-length density profiles (Appendices 5.1 and 5.2) of 25 Namibian bottom trawl surveys 1990–2007.

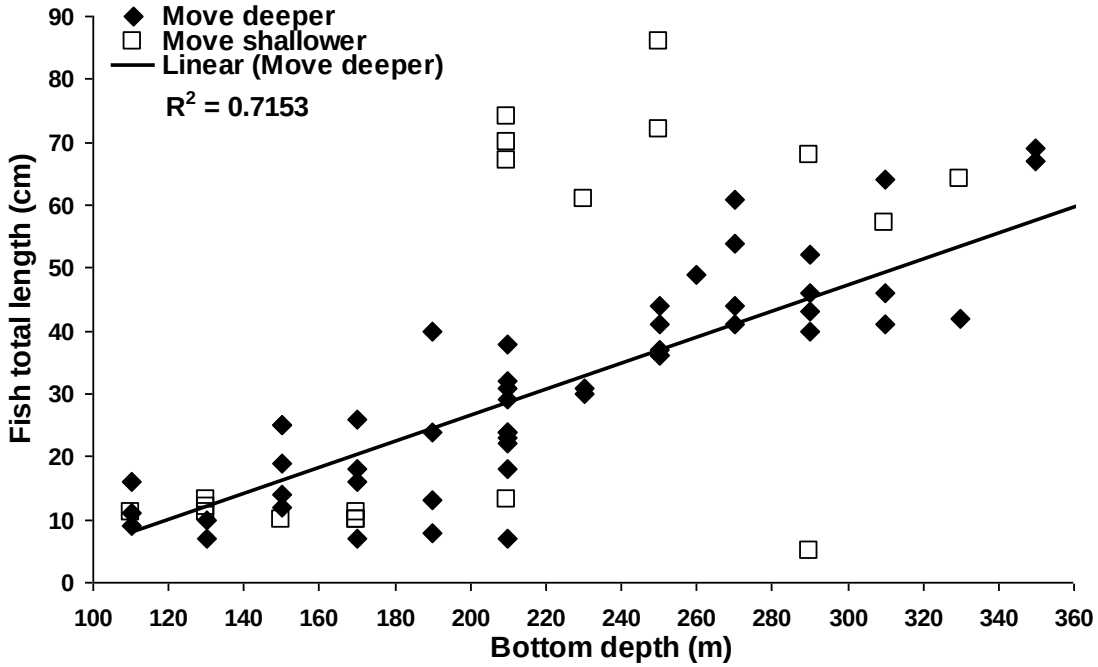

Figure 5.7 Linear relationship between *M. capensis* TL (cm) minima at their depth minima for when they move deeper (diamonds), calculated from depth-length density profiles of 25 Namibian bottom trawl surveys from 1990 to 2007. Open squares indicate movement into shallower depths (not included in the regression).

5.4.4 Latitude and depth changes and translucent zone formation

Figure 5.8 shows TLs at both latitude and depth changes (Figs 5.5 and 5.6) plotted together showing where depth and latitude changes matched. Superimposed on these TLs are the TL_{50} at translucent zone formation of T1–T9 (Table 4.5) of the five cohorts sampled as detailed in Chapters 3 and 4, plotted at their calculated $Date_{50}$ (Table 4.3). Fig. 5.8 also shows TL_{50} at translucent zones T1–T9 calculated from otolith data collected from five surveys, plotted at the date of the survey. Where fish lengths at migration corresponded with TL_{50} at translucent zone formation, these are circled in Fig. 5.8.

The sizes of young fish < 20 cm TL moving shallower corresponded with TL_{50} at formation of the T1 summer translucent zone of the 2002 and 2005 cohorts (2003 and 2006 summer surveys, red, circled in Fig. 5.8a). The TL_{50} at translucent zone formation of fish < 20 cm TL sampled from three individual surveys were also similar to the profile minima of moving shallower: T2 of 2002, T1 of 2003 and T1 of 2005 (blue, circled in Fig. 5.8a).

For medium-sized fish 20–30 cm TL (Fig. 5.8b), moving deeper was frequently associated with (followed or preceded by) moving northwards. These events corresponded with the T3 and T4 zones of the 1996, 1998 and 2006 cohorts (Chapters 3 and 4), formed in the summers of 1997/1998, 1999/2000 and 2006/2007 respectively (red, circled in Fig. 5.8b). Several translucent zones occurring on fish between 20 and 30 cm TL from the five individual surveys also corresponded with moving deeper (T3 of the 1999 survey, T3 of the 2005 survey), or with moving northwards (T3 of the 1992-11 survey, T4 of the 1999 survey, T4 of the 2002 survey, T4 of the 2005 survey), or moving both northwards and deeper (T3 of the 2003 survey) (all blue, circled in Fig. 5.8b).

Two translucent zones in the 30–50 cm TL range corresponded with a deeper movement: T4 of the 1992-11 survey and T6 of the 1999 survey (blue, circled in Fig. 5.8b).

The southward and deeper or shallower migration of fish > 52 cm TL (Fig. 5.8c) occasionally corresponded with TL_{50} of the surveys during which larger fish were sampled (T6 and T7 of the 1992-11 survey, T9 of the 2002 survey and T8 of the 2005 survey).

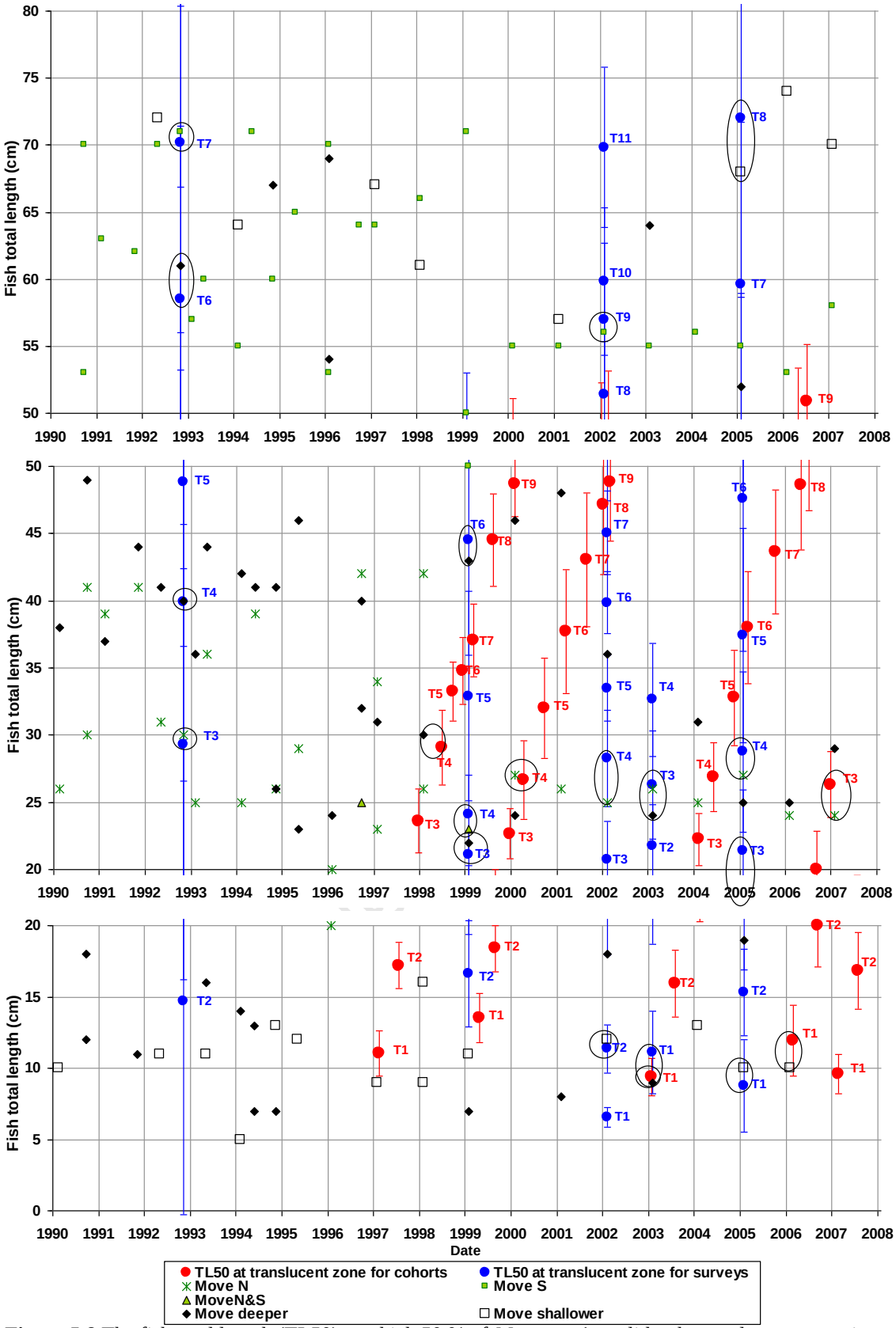

Figure 5.8 The fish total length (TL50) at which 50 % of *M. capensis* otoliths show at least one to nine (T1–T9) complete translucent zones plotted against the calculated $Date_{50}$ of five cohorts 1996, 1998, 2002, 2005 and 2006 (red circles) and TL50 at translucent zones for five surveys (blue circles) plotted at the mid-date of the survey during which the otoliths were collected (though that does not reflect the timing of the translucent zones). Bars represent δ values of the logistic ogives (see Equation 4.4) to illustrate the width of the curve. The movement TLs identified from density profiles of 25 surveys (Figs 5.5 and 5.6) at which *M. capensis* either move northwards (green stars), southwards (green squares) or northwards and southwards (green triangles), deeper (black diamonds) or shallower (open squares) are also presented. Matching "events" (TL at movement corresponding to a translucent zone) are circled.

To test if any "match" of TL_{50} with "migration TLs" was a significant depth-change from inner-shelf to mid-shelf, or from mid-shelf to outer-shelf movement, or coincidental, the logistic ogives (see Equation 4.4) of "matched" translucent zones (circled in Fig. 5.8) were plotted against proportion of the average density on the inner-shelf < 180 m, the mid-shelf 180–350 m, and the outer-shelf > 350 m bottom depth (Fig. 5.9). The gradient of the increase or decrease in proportions of fish present in each depth shelf area category is referred to as the "migration gradient".

Figure 5.9 shows that the shallower movement identified for fish 9–15 cm (Figs 5.1 and 5.5) corresponds to a movement from the mid-shelf to the inner-shelf (blue line) of fish of this size range (1998 survey, 2003 survey, 2006 survey, Fig. 5.9a; 1999 survey, 2002 survey, 2005 survey, Fig. 5.9b). Deeper movement of medium-sized fish happens in two significant stages; movement from the inner-shelf to the mid-shelf between 20 and 34 cm TL, but mostly between 24 and 28 cm TL (50 % values, pink line, Fig. 5.9), and movement from the mid-shelf to the outer shelf between 44 and 58 cm TL, but mostly between 50 and 56 cm TL (50 % values, green line, Fig. 5.9). Shallower movement of large fish is from the outer-shelf back to the mid-shelf or inner-shelf between 54 and 66 cm TL (pink line at the large fish lengths, Fig. 5.9).

Ogives of the proportion of fish with translucent zones at fish TL-class match the proportions of fish on the three shelf areas at the same fish TL exceptionally well (Fig. 5.9). Even for the 1992-11 survey, the ogives of the T6 and T8 zones were less steep than those for other surveys and still compared well with the inner-shelf to mid-shelf, and mid-shelf to outer-shelf migration gradients in that survey (Fig. 5.9b, 1992-11). In addition, T8 of the 2002 survey fits perfectly with off-the-shelf movements of hake of 36 to 50 cm TL (Fig. 5.9b, 2002 survey).

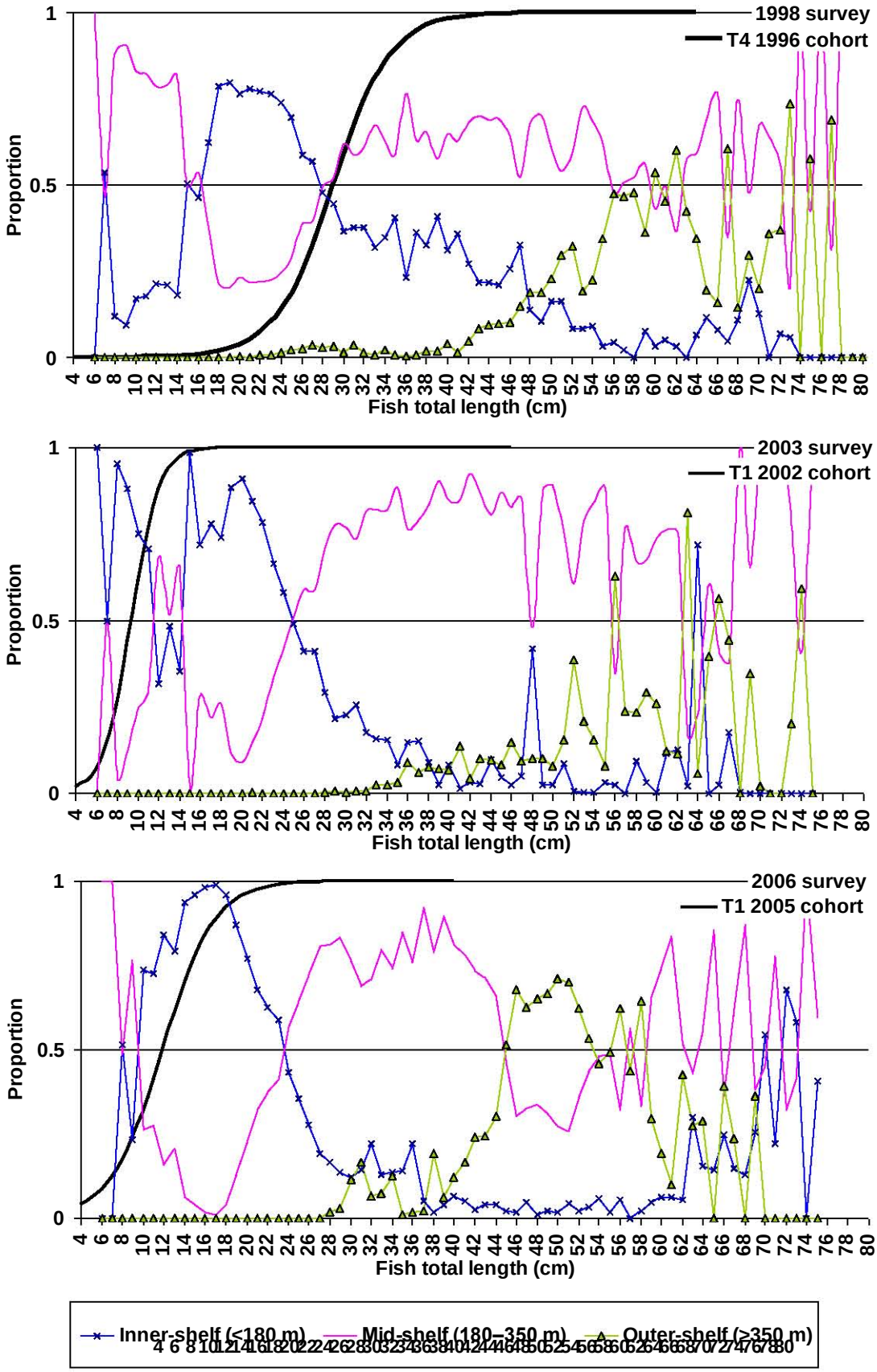

Figure 5.9a Logistic functions (black lines) of proportions of *M. capensis* per 1-cm fish total length class showing translucent zones T1 and T4 (matched with depth-related movement, circled in Fig. 5.8) on otoliths of the cohorts 1996, 1998, 2002, 2005 and 2006 (Chapters 3 and 4). The proportions out of total number of fish per 1-cm-total length class of *M. capensis* found either on the inner- shelf < 180 m (blue), mid-shelf 180–350 m (pink) or outer-shelf > 350 m (green) bottom depth during the relevant biomass surveys are also presented for comparison.

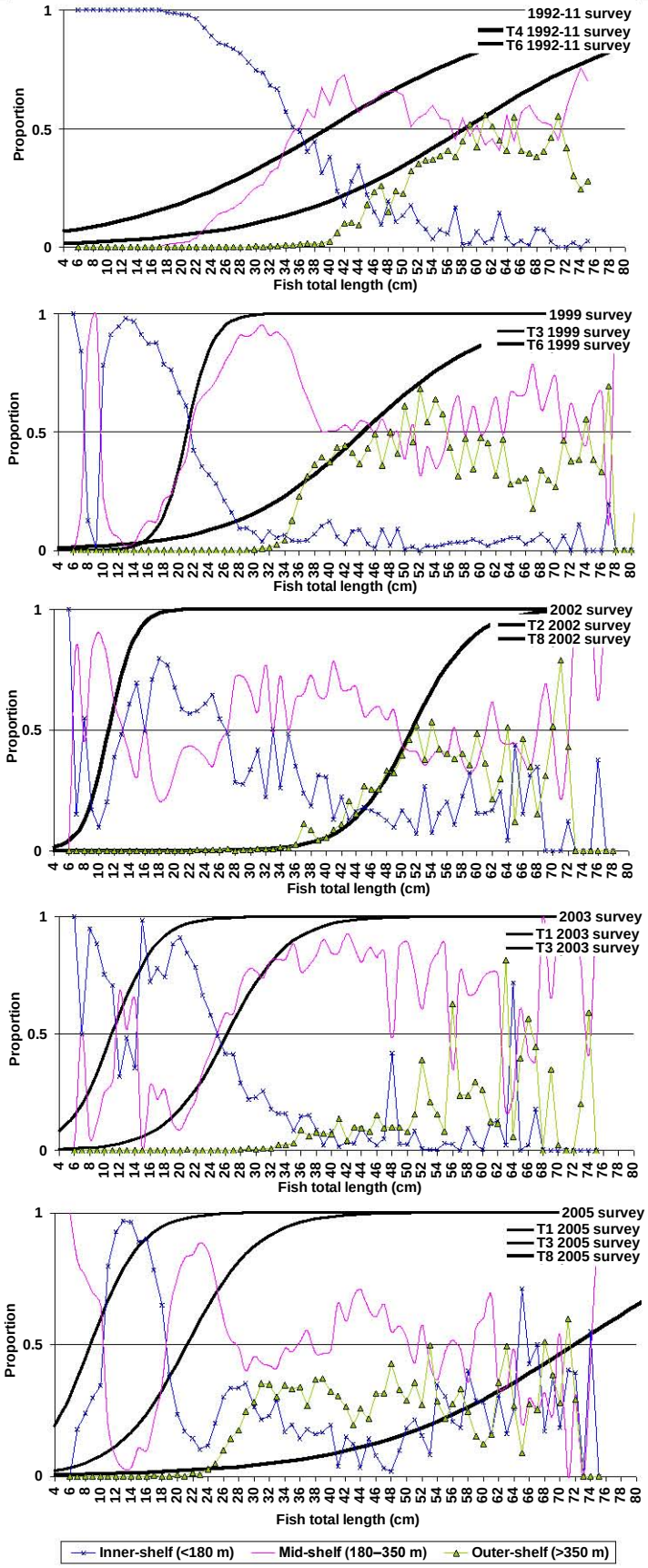

Figure 5.9b Logistic functions (black lines) of proportions of *M. capensis* per 1-cm fish total length class showing translucent zones T1–T4, T6 and T8 (matched with depth-related movement, circled in Fig. 5.8) on otoliths selected from the surveys 1992-11, 1999, 2002, 2003 and 2005. The proportions of the total number of fish per 1-cm-total length class of *M. capensis* found either on the inner-shelf < 180 m (blue), mid-shelf 180–350 m (pink) and outer-shelf > 350 m (green) bottom depth during the relevant biomass surveys are also presented for comparison.

To test if any "match" of TL_{50} with "migration TLs" was a significant latitude-change (from north to central, central to south, etc), proportions of average density in the north < 20.5°S, centre 20.5–25.5°S or south > 25.5°S were plotted for each survey, and the logistic ogives of "matched" translucent zones (circled in Fig. 5.8) were super-imposed (Fig. 5.10).

The main horizontal movement patterns observed were movement from the central to the northern area of fish between 30 and 36 cm TL (green line, Fig. 5.10b), and back again at fish lengths between 52 and 70 cm (pink and blue lines, Fig. 5.10b).

Steepness of ogives of translucent zone formation also matched the migration gradients of proportion of fish in the south (>25.5°S), centre (20.5–25.5°S) and north (< 20.5°S) of the Namibian coast at each TL class (Fig. 5.10).

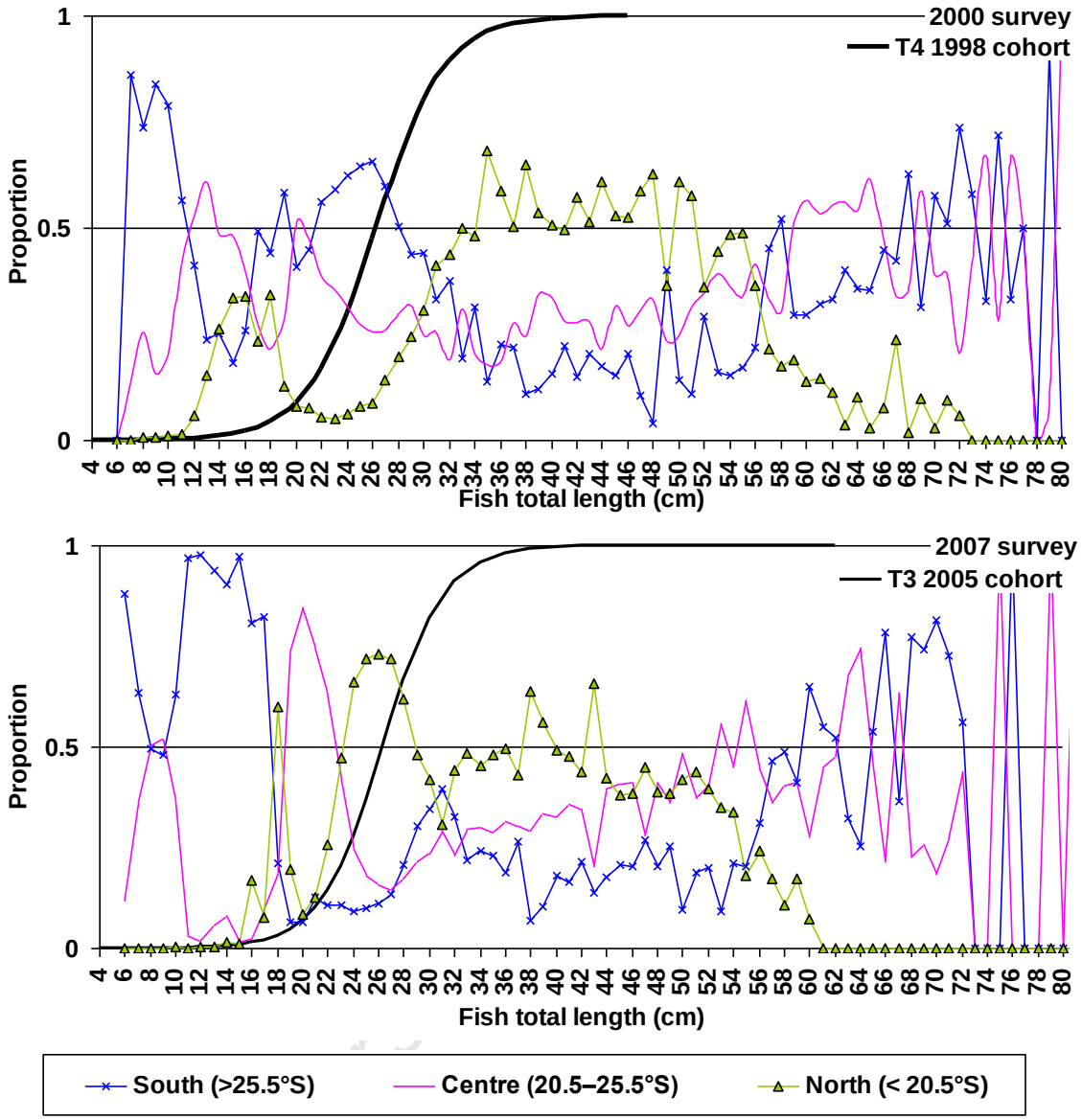

Figure 5.10a Logistic functions (black lines) of proportions of *M. capensis* per 1-cm fish total length class showing translucent zones T1, T3 and T4 (matched with horizontal movement, circled in Fig. 4.8) on otoliths of the cohorts 1996, 1998, 2002, 2005 and 2006 (Chapters 3 and 4). The proportions out of the total number of fish per 1-cm-total length class of *M. capensis* found either in the north < 20.5°S (blue), centre 20.5–25.5°S (pink) or south > 25.5°S (green) of Namibia during the relevant biomass surveys are also presented for comparison.

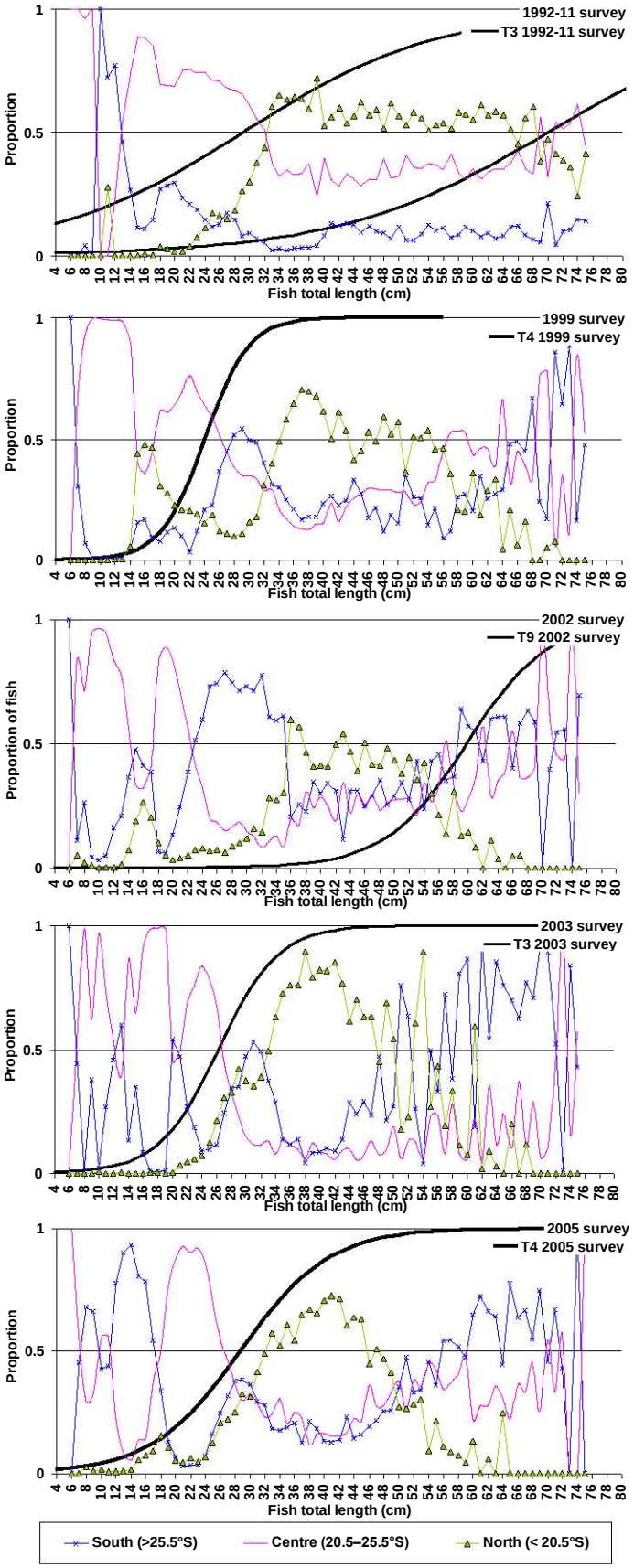

Figure 5.10b Logistic functions (black lines) of proportions of *M. capensis* per 1-cm fish total length class showing translucent zones T1–T4, T7 and T9 (matched with horizontal movement, circled in Fig. 4.8) selected from the surveys 1992-11, 1999, 2002, 2003 and 2005. The proportions out of the total number of fish per 1-cm-total length class of *M. capensis* found either in the north < 20.5°S (blue), centre 20.5–25.5°S (pink) or south > 25.5°S (green) of Namibia during the relevant biomass surveys are also presented for comparison.

5.5. Discussion

5.5.1 Nursery areas and spawning stock units

In recent years, southern (> 25.5°S) and central (20.5–25.5°S) nursery areas were observed for *M. capensis* off Namibia, varying in density among areas and years. Prior to 1997, a northern (< 20.5°S) nursery area was sometimes observed (Fig. 5.2). Assorov and Berenbeim (1983) and Olivar *et al.* (1988) described northern and central spawning areas for different times of the year, centring on winter or early spring, respectively, with data from the late 1960s–early 1970s and late 1970s–early 1980s, respectively. Sundby *et al.* (2001) proposed that spawning products are transported shoreward and southward after being spawned meso-pelagically and offshore, resulting in early juveniles being concentrated nearshore and between 20.5 and 23°S. This is where *M. capensis* presumably settle to the bottom. None of the above studies, however, included areas south of 24.5°S in their surveys, and no subsurface features were mapped south of Walvis Bay (23°S) (Sundby *et al.*, 2001). Thus, the central nursery aggregations identified in this chapter (Fig. 5.2) could originate from spawning products released further northward and further offshore. If it is assumed that the same is true for the southern nursery aggregations, the identified central and southern nursery aggregations could originate from the spawning areas described by Assorov and Berenbeim (1983) and Olivar *et al.* (1988).

However, Kainge *et al.* (2007) showed large *M. capensis* with high gonadosomatic indices around 26°S and 28°S from samples collected between September 1998 and November 2001. In microscopic studies of gonadal development, Singh *et al.* (2011) showed that *M. capensis* reach 50 % maturity at 54 cm TL in the southern Benguela. Assuming this also applies to the northern Benguela, *M. capensis* with TLs ≥ 54 cm then belong to the spawning population. Aggregations of *M. capensis* of > 50 cm TL were mostly present in the central area. When nursery aggregations were found in the south, fish of > 50 cm TL were also found in the south, slightly north of the nursery aggregation (Figs 5.1, 5.2 and 5.3). This suggests there were two separate spawning areas, one off central Namibia (with spawning peaks centred in winter) and one off southern Namibia (with spawning peaks centred in spring). Thus it is very likely that the northern and central spawning areas of the 1970s and 1980s (O'Toole 1978; Assorov and Berenbeim, 1983; Olivar *et al.*, 1988) have now shifted southwards.

Densities of 8–16 cm fish and > 50 cm fish also appear to be higher in the south from 2002 onwards (Figs 5.1 and 5.3). The possible southward shift since 2002 is confirmed by the fur seal diet shown in Chapter 2. In general, seal scat samples containing young *M. capensis* from the southern-most colony (VRB) have increased since 2000 (Fig. 2.7h–p). The exceptions to this are the (weaker) 2003 and 2006 cohorts showing more young *M. capensis* from the seal scats in CC and AWB (Fig. 2.7k and n).

A spawning stock shift has also been observed for Argentine hake *M. hubbsi* (Macchi *et al.*, 2005). Alternatively, there may be a north-south shift of both north/central and central/south spawning and nursery areas in 5-year periods (southward shift since 2002, Figs 5.1 and 5.3) according to temperature, similar to that shown by Horne and Smith (1997) for Pacific hake *M. productus*. This means that the stock may shift northwards again in the future.

If no mixing occurred between adults and juvenile *M. capensis* of central and southern Namibia, they would occupy distinct areas every year with geographical and/or temporal separation. This would indicate different unit stocks (Clayden, 1972; MacLean and Evans, 1981). First looking at geographical separation, aggregations of adult fish > 50 cm TL often do not appear to be geographically distinct (e.g. 1991-11, 1993-05, 1994, 1994-05, 1995-05, 1996, 1997, 2001 and 2003; Figs 5.3d, h, i, j, l, m, o, s and u respectively), and so it appears that, at least for those years, they meet on a common spawning ground (centred around 23–26°S). Surveys 1994-05 and 1995-05 (Figs 5.3j and l) show examples of two nursery aggregations, one with fish averaging 10 cm TL (6 months old) at 28°S (south), and one with fish averaging 6 cm TL at 23°S (centre), with the two "merging" at 16 cm (1 year old) at 26°S, with the spawning aggregation then also "remaining" in that area. The 1992-05 survey (Fig. 5.3e) shows a good example of similar migrations of fish from nursery to spawning adults in the centre and the south. The fish move northwards first at medium sizes (in most recent years between 30 and 36 cm TL, Fig. 5.5, 2 to 2.5 years old) and then southwards again as large adults (> 52 cm TL, Fig. 5.5, > 3.5 years old) to spawn. The Namibian *M. capensis* stock could thus consist of one central spawning aggregation with juveniles originating from the central and southern nursery areas migrating northwards at medium sizes and returning to the central area from the north, or remaining in the central area to spawn at large adult sizes (e.g. 1991-11, 1993-05, 1994, 1994-05, 1995-

05, 1996, 1997, 2001 and 2003). Alternatively, in some years there could be two separate spawning aggregations, not necessarily sub-stocks, with nursery aggregations for each area and fish from both moving northwards at medium sizes and southwards again at large adult sizes to spawn (e.g. 1992-05, 1993, 1999, 2002, 2004, 2005 and 2007; Figs 5.3e, g, q, t, v, w and y).

Looking at temporal separation, at all times of the year surveyed (May, September, November, February) young-of-the-year were present, indicating that *M. capensis* spawn throughout the year with some peaks of higher spawning activity. Spawning peaks were in winter and spring in the central region, and in spring in the southern region (Fig. 5.4), confirming what has been shown from seal scat samples in Chapter 2. Before 2001, hatchdates fell more frequently in summer (Table 5.2). Fish in the central aggregations are typically 3–4 months older than fish in the southern ones in each year (Table 5.2). This confirms the differences in timing of spawning peaks in the different areas proposed by Assorov and Berenbeim (1983) and Olivar *et al.* (1988), but with a southward shift of the two areas, and possibly with a shift of the summer spawning peak towards a few months later (autumn/early winter). Kainge *et al.* (2007) observed *M. capensis* with peak in gonadosomatic index from July to October and another smaller peak December to February (/April). Botha (1986) also identified two spawning periods for *M. capensis* off the west coast of South Africa with the peak of ripe and running (stage 5) fish in August–September and again in December–January, confirming the double spawning cycle with 3–4 months between cycles. In the western Mediterranean reproductive activity of European hake is most active between February and May in the northern Tyrrhenian Sea, but from August to December in the Catalan Sea (Recansens *et al.*, 2008). On the western Mediterranean shelf, European hake YOY between 7 and 11 cm TL were also present all year around (Moralen-Nin and Moranta, 2004) and observed (northern hemisphere) winter and late summer hatchdate distributions (Arneri and Morales-Nin, 2000). Landaeta and Castro (2006) observed peaks in abundance of eggs and larvae of Chilean hake in October–November and February–March. Both examples indicate two spawning cycles per year 3–5 months apart, but with slight differences to the timing of peaks observed in this study. This provides evidence that there are two spawning cycles per year in *M. capensis*. This would suggest there are two major seasonal cycles, not just after maturity, but

affecting somatic as well as reproductive growth. All of this reflects a biannual cycle, and could be indirectly linked to the biannual translucent zone formation.

Hatchdates calculated in Chapter 2 (mid-date end of June) could be an average of biannual hatchdate distributions, e.g. May and September (Fig. 5.4 South). Year-classes would thus be made up of bimodal age-groups, but later merge because of an increase of variability of lengths-at-age (also shown in Chapter 4, Fig. 4.1). Furthermore, the autumn to spring hatchdate period in both the central and southern areas calculated for young-of-the-year from the 2005 summer survey, with biannual and bimodal length- and hatchdate-distributions spanning 4–6 cm and 3–4 months in both areas (Fig. 5.1w; Table 5.2), confirms the bimodal distribution seen throughout the 2004 cohort from seal scat samples (Fig. 2.8l). The 2004 cohort was a relatively strong cohort observed in the seal scat index (Table 2.2b; Fig. 2.8), and a 50 cm (3.5-year) mode could still be seen in the 2008 Feb research survey samples (Fig. 4.1). A similar result was observed for the 1996 cohort (Fig. 2.7d), the second strongest cohort observed in the seal scat index (Table 2.2b; Fig. 2.8), which had a bimodal length distribution in the central area with a wide range of 11 cm, and 8 months between the modes of the length distributions during the 1997 summer survey (Fig. 5.1; Table 5.2). The 1996 cohort was still visible as 2.5-year-olds in the 1999 Feb research survey length-frequency distribution (LFD) (Fig. 4.1). It thus appears that strong cohorts often result from a long spawning / survivorship period over a large area, seen by mid-dates showing the highest year-class strength in Fig. 2.8. The 1998 cohort (fourth strongest, Table 2.2b), showed an early hatchdate (outlier in Fig. 2.8; Table 2.2b) and only a difference of 4 cm and three months between length distributions in the southern and the central area during 1999 summer survey (Table 5.2). However, double modes were present in the seal scat samples at CC (central area) and again later at AWB (southern area) (Fig. 2.7f). More than one survey nursery aggregation was observed in February 1999 (Fig. 5.1q), including one further north, with slightly older than the assumed young-of-the year hake, which would still belong to the early-spawned 1998 cohort. These 0-year olds showed a very large mode in the 1999 Feb survey (Fig. 4.1). The 1998 cohort followed a very weak 1997 cohort (Table 2.2b), which would have minimised cannibalism of young hake of this cohort by older conspecifics (Roux 2004; 2006).

The hatchdates calculated for *M. capensis* for each survey also show that the onset of spawning is variable between years. The earlier onset of spawning (survivors) in the central area could also switch in some years. There was no consistent temporal separation (for example, one area always starting three months earlier) in spawning between the central and southern Namibian *M. capensis* aggregations. There still appears no reason to assume more than one stock of *M. capensis* in the northern Benguela.

5.5.2 Alongshore and inshore-offshore migrations

All the fish represented in the length-distributions were caught in bottom trawls and were thus presumably found on or near the bottom. They were thus assumed to have "settled" to the bottom or to have a partially demersal existence (Steves and Cowen, 2000). This confirms conclusions reached in Chapter 3 that the T1 zone does not relate to a "demersal" or "settlement" zone because the translucent zone is formed at TLs between 9 and 12 cm, about four months after demersal settlement takes place.

Although the young (< 16 cm) fish are only partially selected by the net size of the bottom trawls, seen in the LFDs (Fig. 4.1), it is assumed that they would be equally available during all surveys. So even though their density is under-estimated, their general distribution and changes in distribution from one year to the next should still broadly be captured here.

The youngest *M. capensis* caught in bottom trawls were often found in deeper waters than slightly older conspecifics, moving shallower when they were between 9 and 15 cm TL. This indicates they have changed depths by the time they turn one year old (Fig. 5.6). This shift is similar to that shown for silver hake *M. bilinearis* and European hake *M. merluccius* (Steves and Cowen, 2000; Bartolino *et al.*, 2008). Translucent zone formation ogives of the T1 and T2 zones closely follow the shift of fish between 9 and15 cm length from the mid-shelf to the inner shelf (Fig. 5.9, 2002, 2003, 2005 and 2006 surveys), possibly because of the association of the shift with a change from planktonic to pelagic fish, as well as an increase in the area of the inner ear (Bartolino *et al.*, 2008).

As fish grow older, they move deeper (Figs 5.6 and 5.7), with a shift from the inner-shelf to the mid-shelf at 24–28 cm TL (1.5–2 years old), and a shift from the mid-shelf to the outer-shelf at around 50–56 cm TL (3.5 to 4 years old). The fish also show a definite northwards shift at 30–36 cm TL (Fig. 5.10a), after they have moved from the inner-shelf to the mid-shelf. They then move southwards again at larger sizes (> 52 cm TL, > 3.5 years old) while also moving shallower, presumably to spawn (O'Toole, 1978; Assorov and Berenbeim, 1983; Olivar *et al.*, 1988; Olivar, 1990; Sundby *et al.*, 2001; Singh *et al.*, 2011). This explains the phenomenon of finding young fish only in shallow waters while older fish are found in shallow and deep waters on the shelf break and upper slope (Snelgrove and Haedrich, 1985). The distribution and movement of *M. productus* off British Columbia is also affected by the shelf-break location (Mackas *et al.*, 1997).

Benguela-Niño events have been documented for 1963, 1984 and 1995 (Gammelsrød *et al.*, 1998). The 1995 *Benguela-Niño* event lasted from the end of 1994 to the middle of 1995. In 2001 a warm-water event was recorded, which did not quite qualify as a *Benguela-Niño* event as it only lasted until April and the warm water intrusion did not go as far south as the *Benguela-Niño* events (Bartholomae and van der Plas, 2007). Low oxygen conditions were recorded in 1994 (preceding the *Benguela-Niño*), 2000 and 2001 (beginning of the year, during the warm-water event) and 2005 (Bartholomae and van der Plas, 2007). The warm-water events of 1994 and 2001 could explain the absence of southern nursery aggregations during those surveys (Fig. 5.2 stars). The low oxygen conditions of 1994 and 2005 could explain why fish of < 10 cm TL were found in waters deeper than 200 m bottom depth (Appendix 5.1). Hamukuaya (1998) also noted that low oxygen conditions in 1994 displaced juvenile hake offshore. However, this was not observed during the 2000 and 2001 surveys (Appendix 5.1).

There were not enough surveys available from different times of the year to confirm summer to autumn northward migrations (Gordoa *et al.*, 2000) or autumn to spring shallower migrations (Gordoa *et al.*, 2006) previously observed for Namibian *M. capensis*.

The lack of movement structure of fish larger than 60 cm TL from 2000 onwards could be explained by the decrease in density in aggregations of fish of >70 cm TL by or the

densities increasing in the south in summer months (Fig. 5.3), hence masking the apparent movement of the large fish

Migration or shifts in the (horizontal) distribution can be affected by temperature, feeding, spawning and low oxygen conditions (Mas-Riera *et al.*, 1990; Dorn, 1995). Depth changes with fish size can be caused by food availability (Stefanescu *et al.*, 1992), inter- and intra-species competition and predation (Moranta *et al.*, 2004), or salinity and light (Tolimieri and Levin, 2006). Temperature, food availability, salinity and light could also directly cause slow somatic growth and result in translucent zone formation (Pannella, 1980; Casselman, 1983; 1987; Morales-Nin 1987; Beckman and Wilson, 1995; Yosef and Casselman, 1995; Pearson, 1996). This study confirms the strongly size-aggregated distribution and depth-preferences of *M. capensis* (Gordoa *et al.*, 1995), with the additional result that these seem to correspond with translucent zone formation on their otoliths.

5.5.3 Translucent zone formation related to alongshore and inshore-offshore migrations

For the 1996, 2002, 2005 and 2006 cohorts (Figs 5.9a), depth-changes from the mid-shelf to the inner-shelf (moving shallower) of fish around 9–15 cm TL corresponded with formation of the summer T1 zones. T2 of the 2002 survey, T1 of the 2003 survey and T1 of the 2005 survey were also associated with moving shallower (Fig. 5.9b). These are all presumably pre-annuli, even if already the second pre-annulus in the 2002 survey.

In the range of 25–36 cm fish (1.5–2.5 years old), (summer/autumn) T3 or T4 zones of the cohorts were closely associated with their migration from the inner-shelf to the mid-shelf (T4 of the 1996 cohort, Fig. 5.9a 1998 survey) and at the same time a migration either from the southern to the central area or the central to the northern area (T4 of the 1998 cohort, T3 of the 2005 cohorts, Fig. 5.10a). In the surveys shown in Figs 5.9b and 5.10b, in the same TL-range and associated with the same migration patterns there were not only summer translucent zones but also winter translucent zones / annuli (T4 of 1992-11 survey, Fig. 5.9b; T2 and T4 of the 1999 survey and T2

and T4 of the 2005 survey, Fig. 5.10b). This is assuming that the pattern continues, in which T2, T4, T6 and T8 zones are annuli, as seen in the cohort (Chapters 3 and 4).

The northwards movement from the central to the northern area of Namibia of fish of 30 to 36 cm fish is presumably to feed and gain energy for maturation following the Angola-Benguela front which is a feeding and spawning area for pelagic fish (Crawford *et al.*, 1987). The northward migration is followed by movement from the mid-shelf to the outer-shelf of fish of 50 to 56 cm TL. The off-the-shelf migration is also associated with formation of summer translucent zones as well as (winter) annuli (T6 of the 1992-11, 1999 and 2002 surveys, Fig. 5.9b).

The movement of large (> 52 cm) fish from the outer-shelf back to the mid-shelf or inner-shelf is matched with the southward (return) migration of large fish from the north to the central area, presumably as they make ready to spawn (Figs 5.8–5.10; see also synthesis Fig. 7.1). These (spawning) migrations are associated with the formation of summer translucent zones as well as winter translucent zones (annuli) of these large fish (T8 of the 2005 survey, Fig. 5.9b; T7 of the 1992-11 survey and T9 of the 2002 survey, Fig. 5.10b).

It is possible that winter translucent zones (annuli) are caused by cooling temperatures and resulting decreased somatic growth rates, as has been shown for different fish species (e.g. Pannella, 1980; Casselman, 1983; 1987; Morales-Nin 1987; Beckman and Wilson, 1995; Yosef and Casselman, 1995; Pearson, 1996). However, most translucent zones seem to be formed in summer and autumn (Fig. 4.7) and most translucent zones (with the exception of an T5 and less frequent events of T2 and T6) are associated with either onshore, offshore, northwards or southwards migrations (Figs 5.8, 5.9 and 5.10). Also, translucent zone patterns on *M. capensis* otoliths are quite regular from all surveys (Figs 4.5, 4.6 and 5.8). Translucent zones are also formed when there is no apparent movement (Fig. 5.8).

From Figs 5.9 and 5.10, it appears that translucent zone formation corresponds to a cue the fish are responding to. At the same rate at which they move from the mid-shelf to the inner-shelf as young fish, then from the inner- to the mid-shelf and from the mid-shelf to the outer-shelf, and back again to the mid-shelf as large adult fish, presumably

to spawn, they form a translucent zone (Fig. 5.9). As young fish move from the southern to the central area, then from the central to the northern area at medium sizes, and back again to the central area at larger sizes, to spawn, they also form a translucent zone at the same rate (Fig. 5.10). The migration could be a response to an internal cue ("ontogenetic migration", Bartolino *et al.*, 2008). Migration should be followed by a decrease in somatic growth rate because of allocation of resources to migration, or a feeding or diet change associated with the habitat change, or adaptation to the change in temperature associated with the depth- or latitude change (Bartholomae and van der Plas, 2007). The formation of translucent zones should follow the reduction in somatic growth rates because of a lack of calcium formation in the otolith. Results also indicate that translucent zones often form "ahead of" the migration (e.g. Fig. 5.10b, 2003 survey). In the fish total length range 22–38 cm each total length class has a higher proportion of fish that have the T3 zone present than have moved northwards. The north-south movement could be triggered by the same cue as the translucent zone formation.

Translucent zone formation still occurs at regular intervals but with variation among cohorts and years. Regularity may be caused by innate rhythms triggered and modified by external cues, causing differences between cohorts. By all appearances, translucent zone formation on *M. capensis* otoliths is firstly a response to an internal cue (endogenous) triggered by external cues, and secondly further modulated by additional external cues (exogenous). However, the link between temperature and food availability or fish condition and translucent zone formation needs to be investigated further. Some of these are addressed in Chapter 6.

5.6. Conclusions and recommendations

Length distributions of *M. capensis* from different areas and depths along the Namibian coast collected during 25 hake biomass surveys, 1990–2007 were used to show that the *M. capensis* population has two spawning and nursery aggregations in the central (20.5–25.5°S) and southern (> 25.5°S) area. Aggregations of *M. capensis* appear to have shifted southward in recent years. The timing of hatchdates between the two areas differs by 3–4 months. Most hatchdates calculated for the young-of-the year from the central nursery aggregation were in June–July, with a secondary mode in September–October. Hatchdates of fish from the southern aggregation were in September–October. This reflects a biannual cycle, which may be indirectly related to biannual translucent zone formation.

Strong cohorts observed from the seal scat index and followed through to survey length-distributions seem to stem from both peaks in both areas, i.e. a long spawning period over a large area.

M. capensis first move shallower before they turn one year old (< 16 cm TL). They then move deeper with increasing size, inner-shelf to mid-shelf at 24–28 cm and mid-shelf to outer-shelf at 50–56 cm TL. They sometimes again move shallower at > 52 cm TL to spawn. Whether they have one or two spawning aggregations in different years, fish from both aggregations move northwards at 30–36 cm TL, ages 2–2.5 years and southward again at > 52 cm TL, > 3.5 years to spawn.

Formation of all translucent zones T1–T9 (T5 not recorded) coincides with depth-related as well as with north-south-related migrations.

In terms of otolith sampling, the current method of otolith sampling should be sufficient to cover the entire stock as it appears to be a single stock. Sampling currently takes ten fish per cm-length-class in each of the northern and the southern legs of each survey. This means that even if northern and southern aggregations show differences in biannual age distributions, this sampling method covers both areas sufficiently to be separated at a later stage after age determination.

Appendix 5.1

Namibian *M. capensis* survey density profiles with respect to total length (cm) (left panel) and bottom depth (m) (centre panel) and estimated total length-depth surface plots (right panels), 1990–2007 for fish < 20 cm total length.

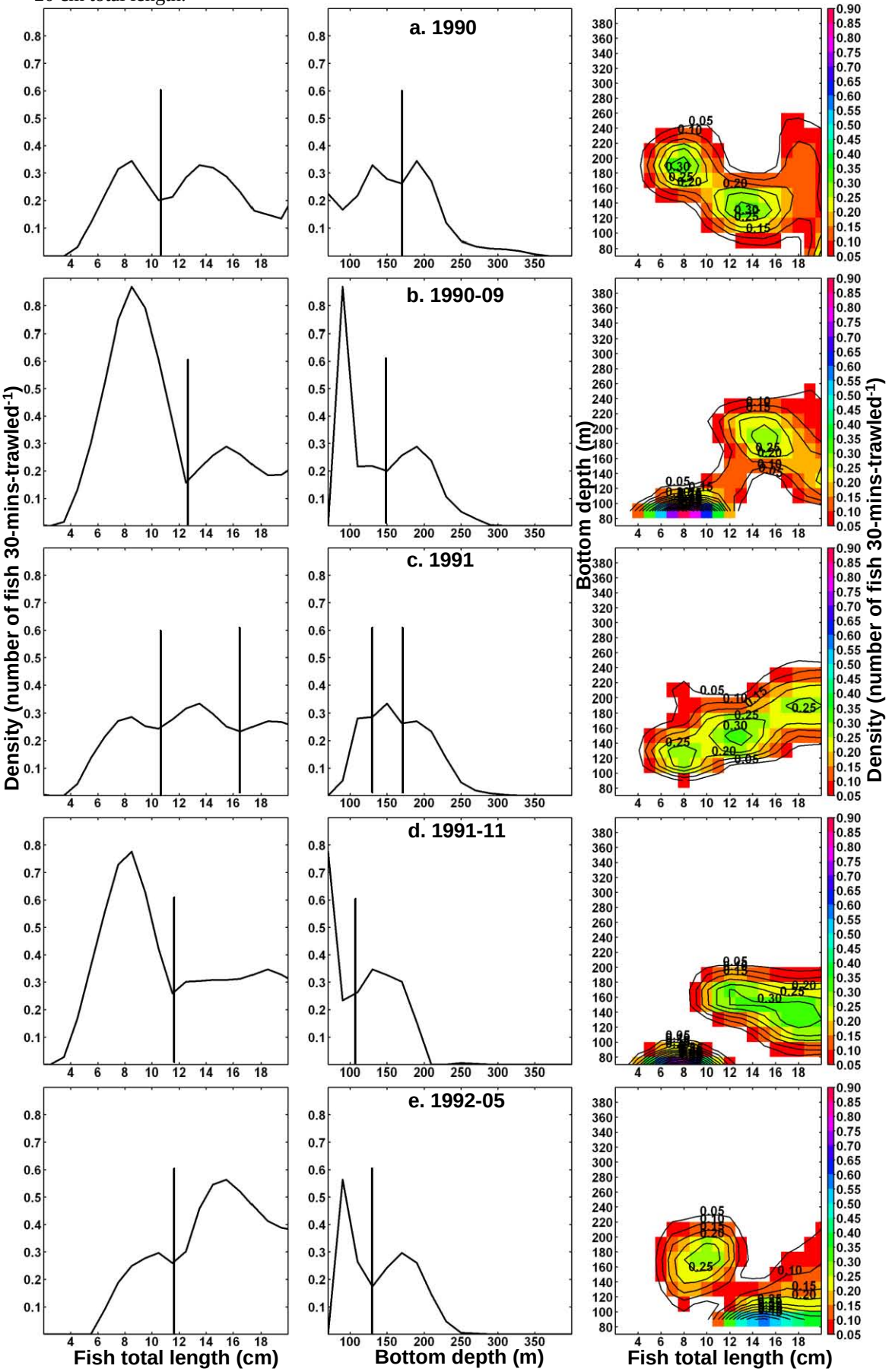

Appendix 5.1 (continued)

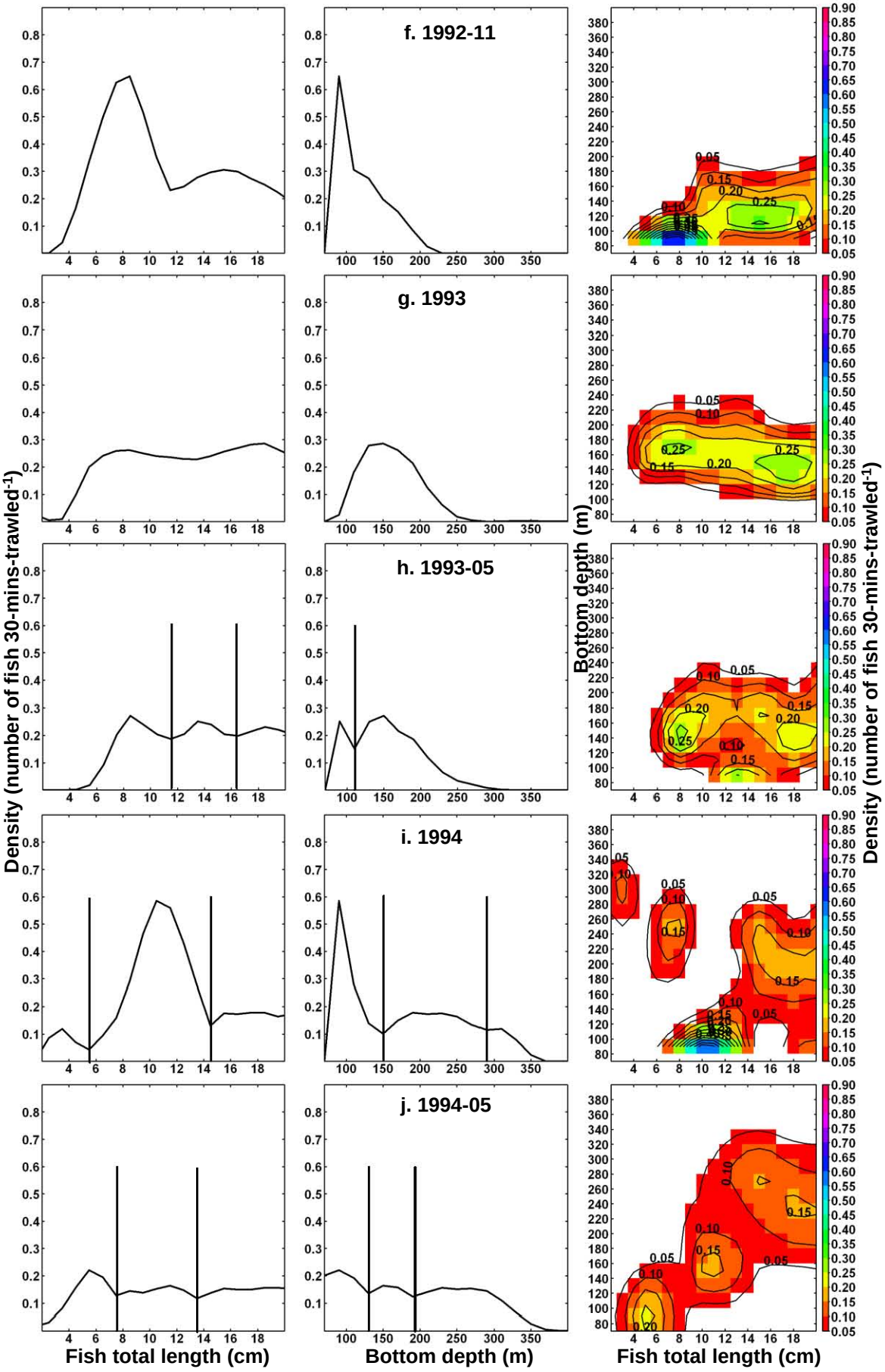

Appendix 5.1 (continued)

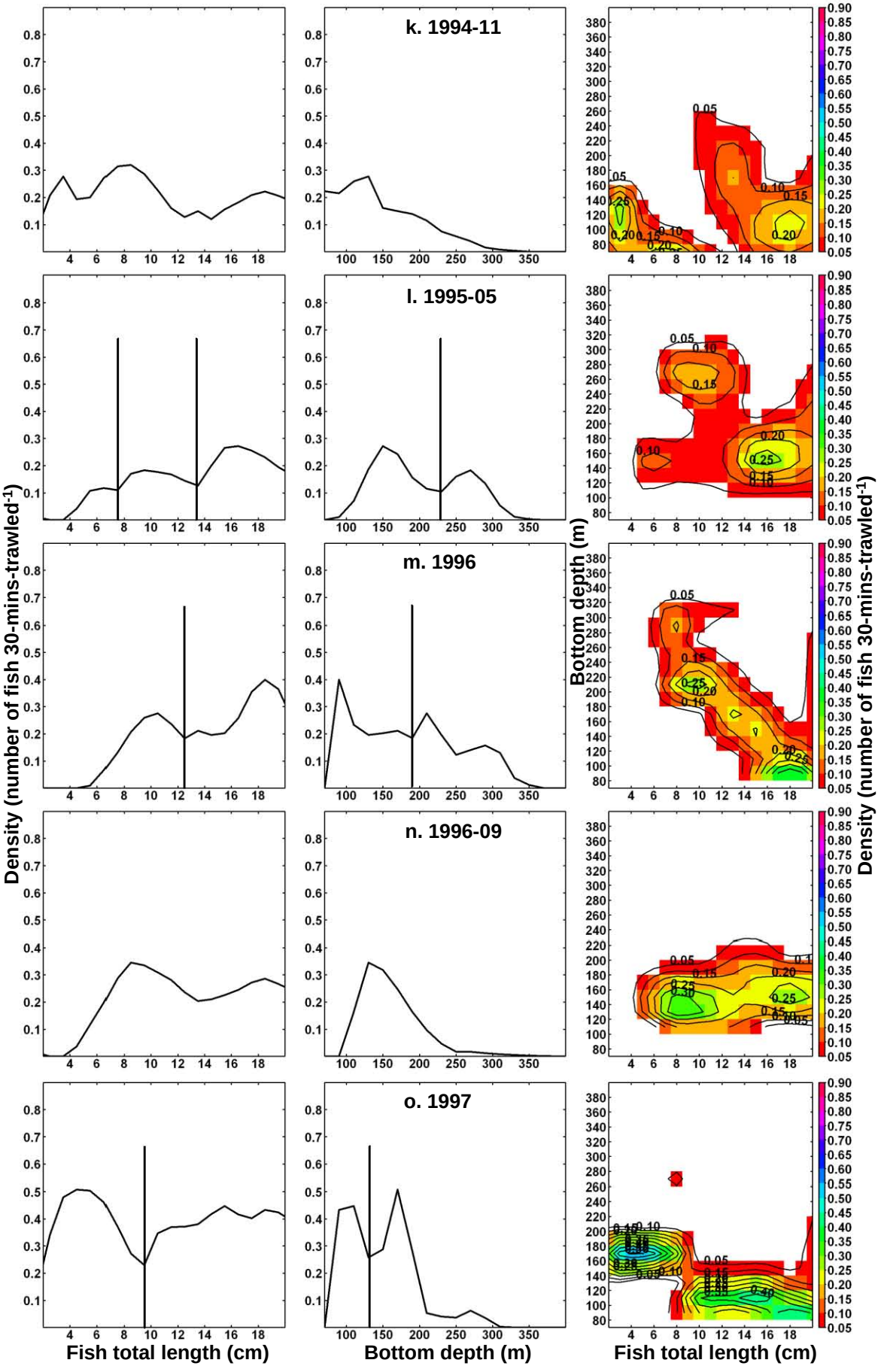

Appendix 5.1 (continued)

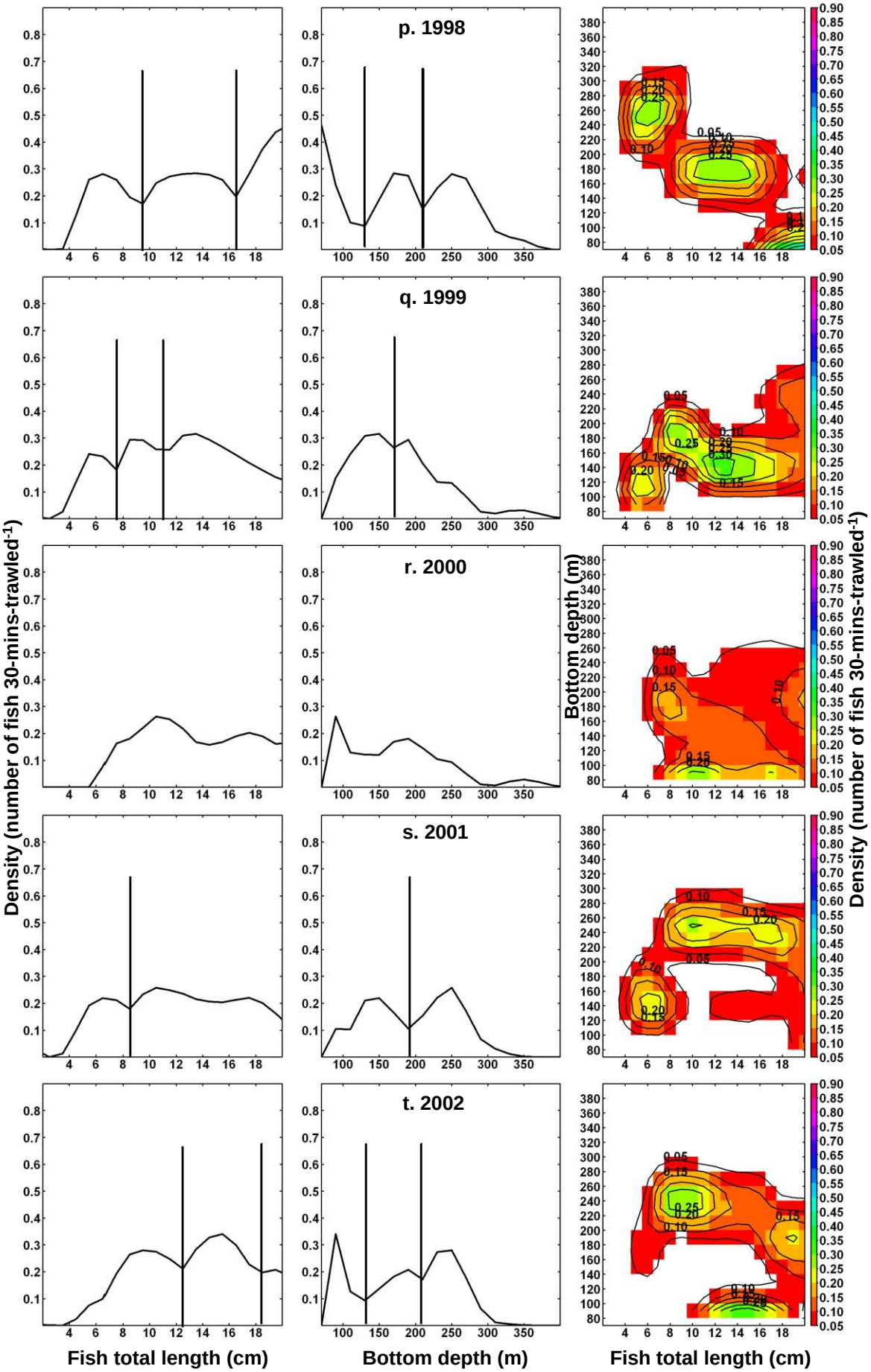

Appendix 5.1 (continued)

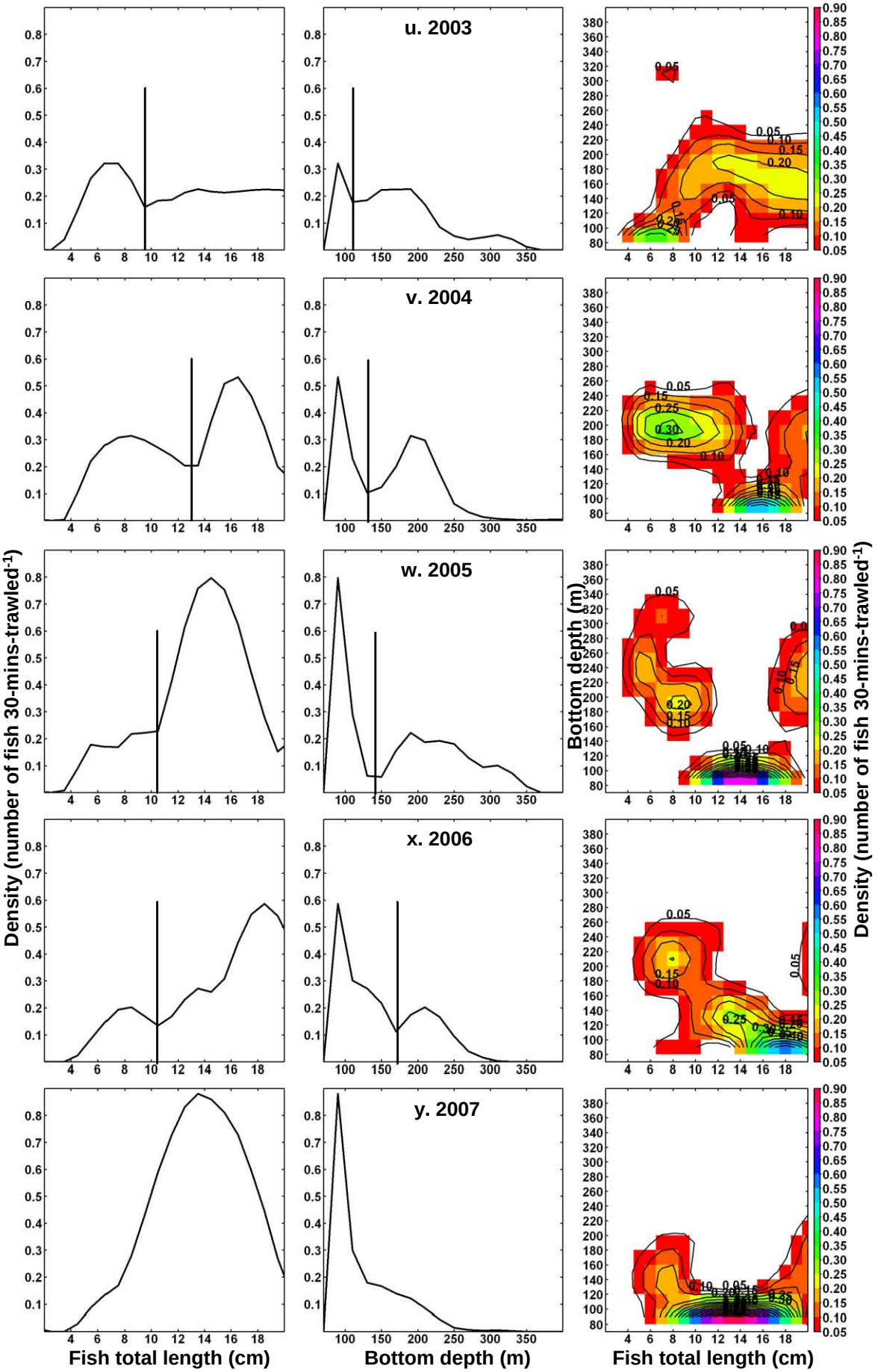

Appendix 5.2

Namibian *M. capensis* survey density estimated total length-bottom depth surface plots (right panel), and density profiles of maxima of surface plots with respect to total length (cm) (left panel), 1990–2007, for the entire total length range 4–98 cm.

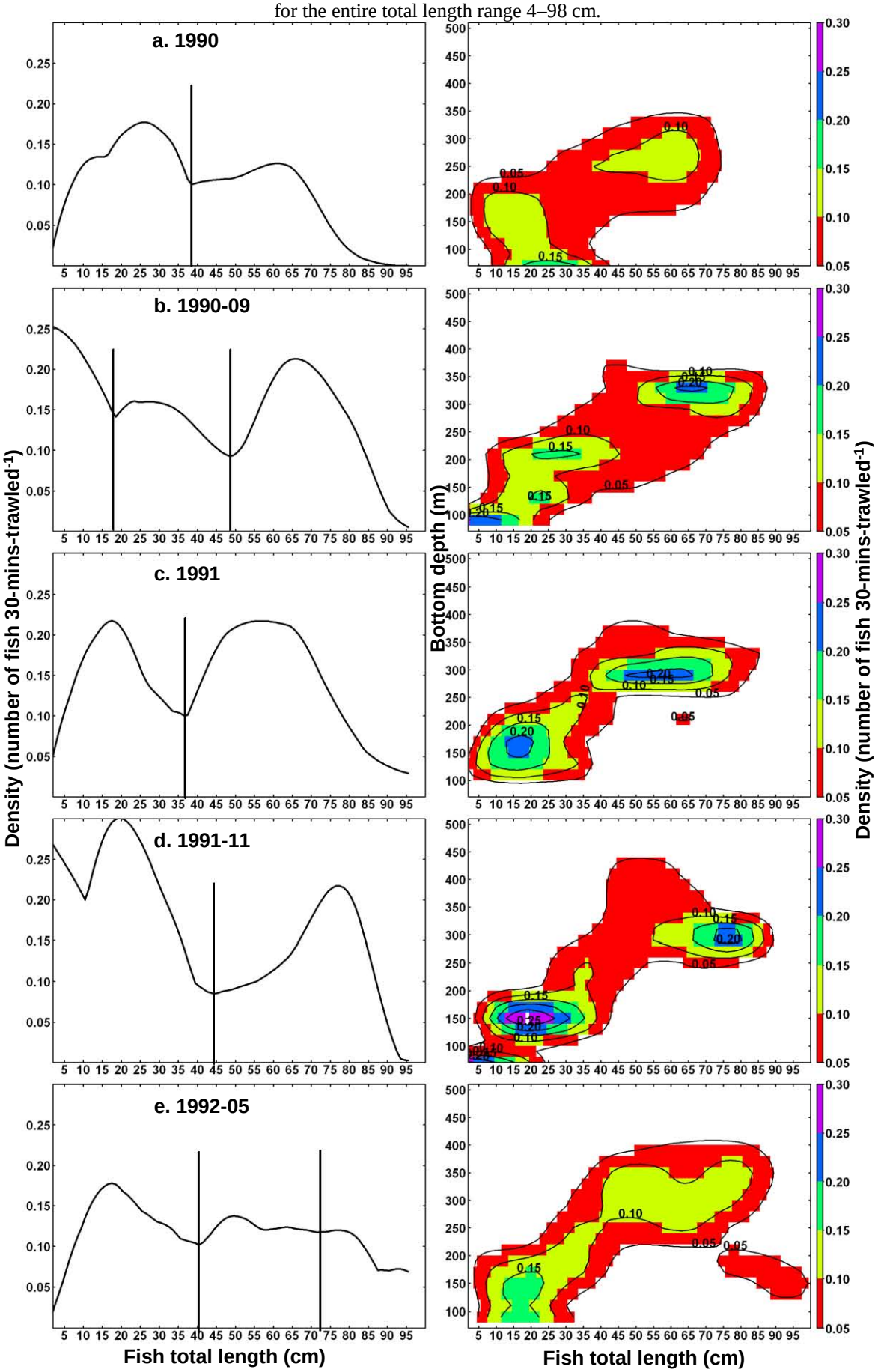

Appendix 5.2 (continued)

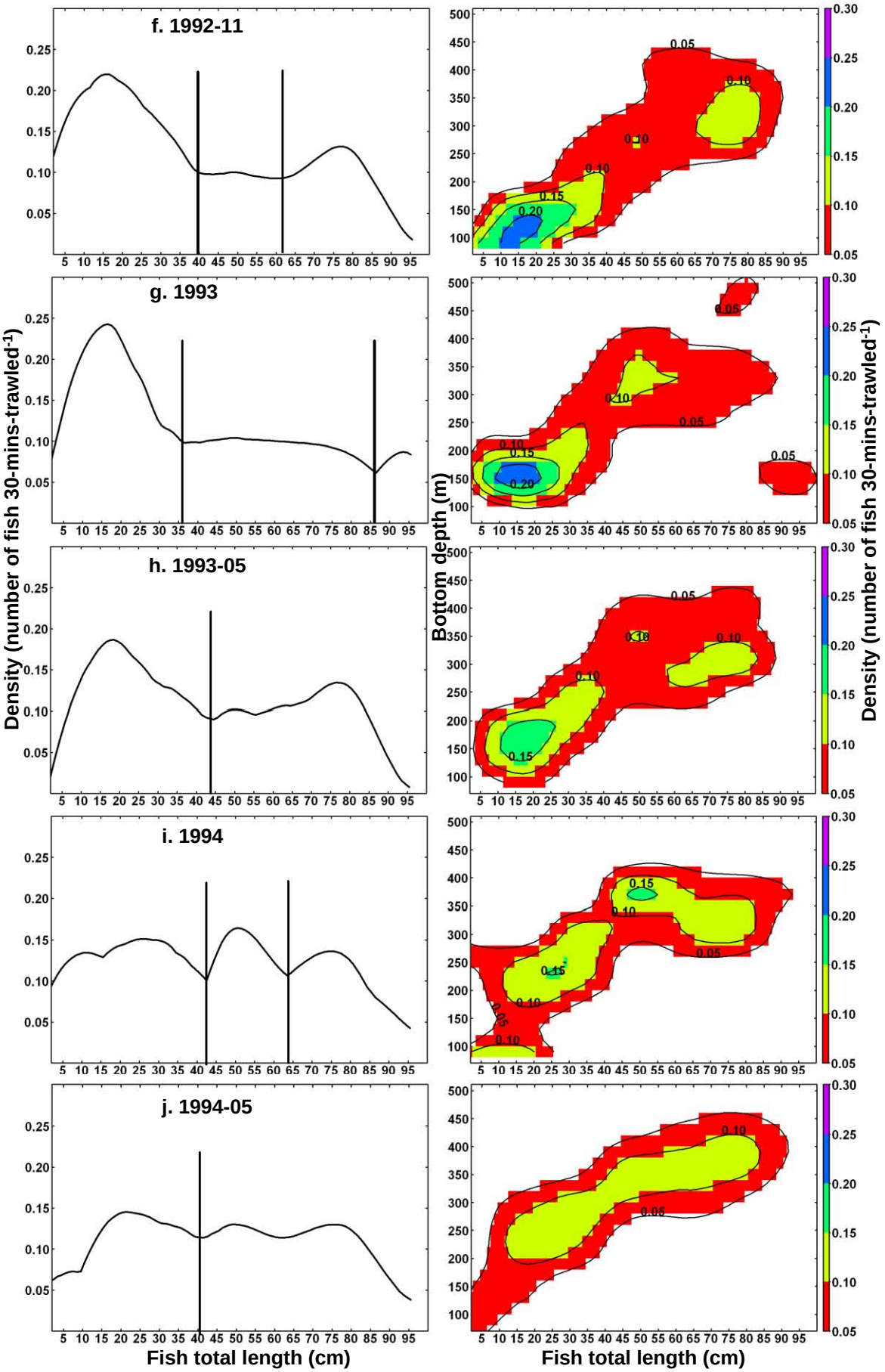

Appendix 5.2 (continued)

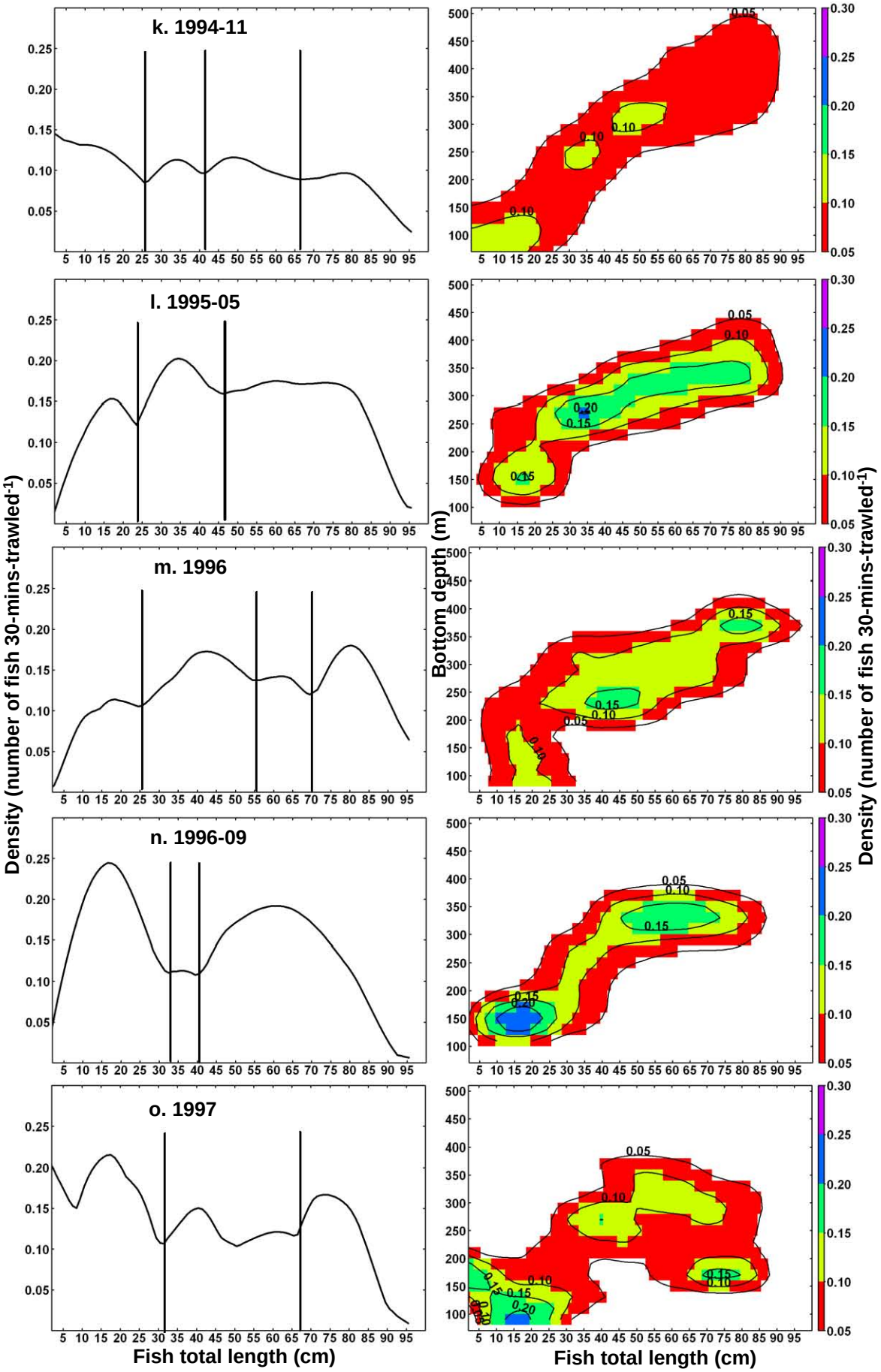

Appendix 5.2 (continued)

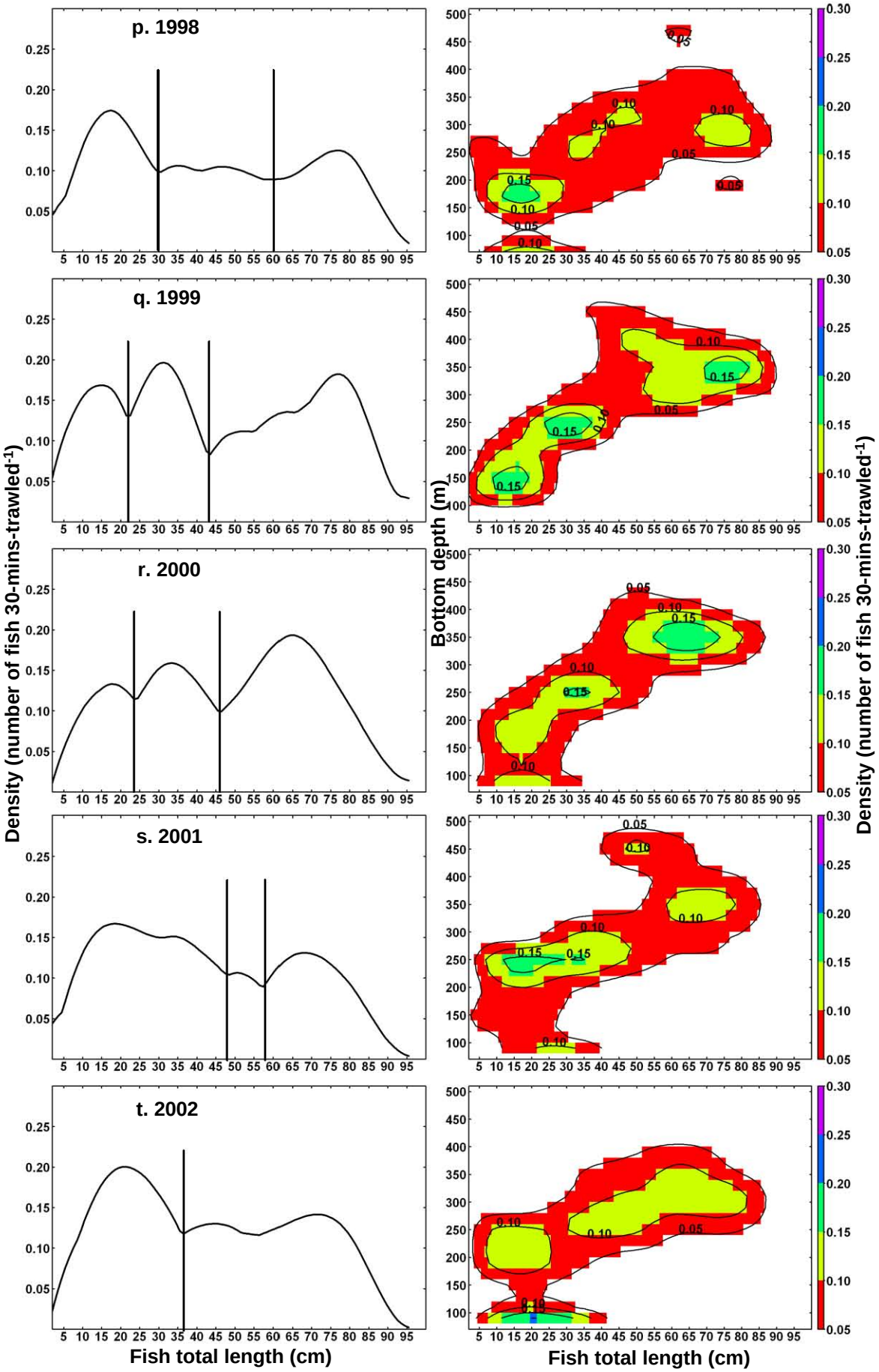

Appendix 5.2 (continued)

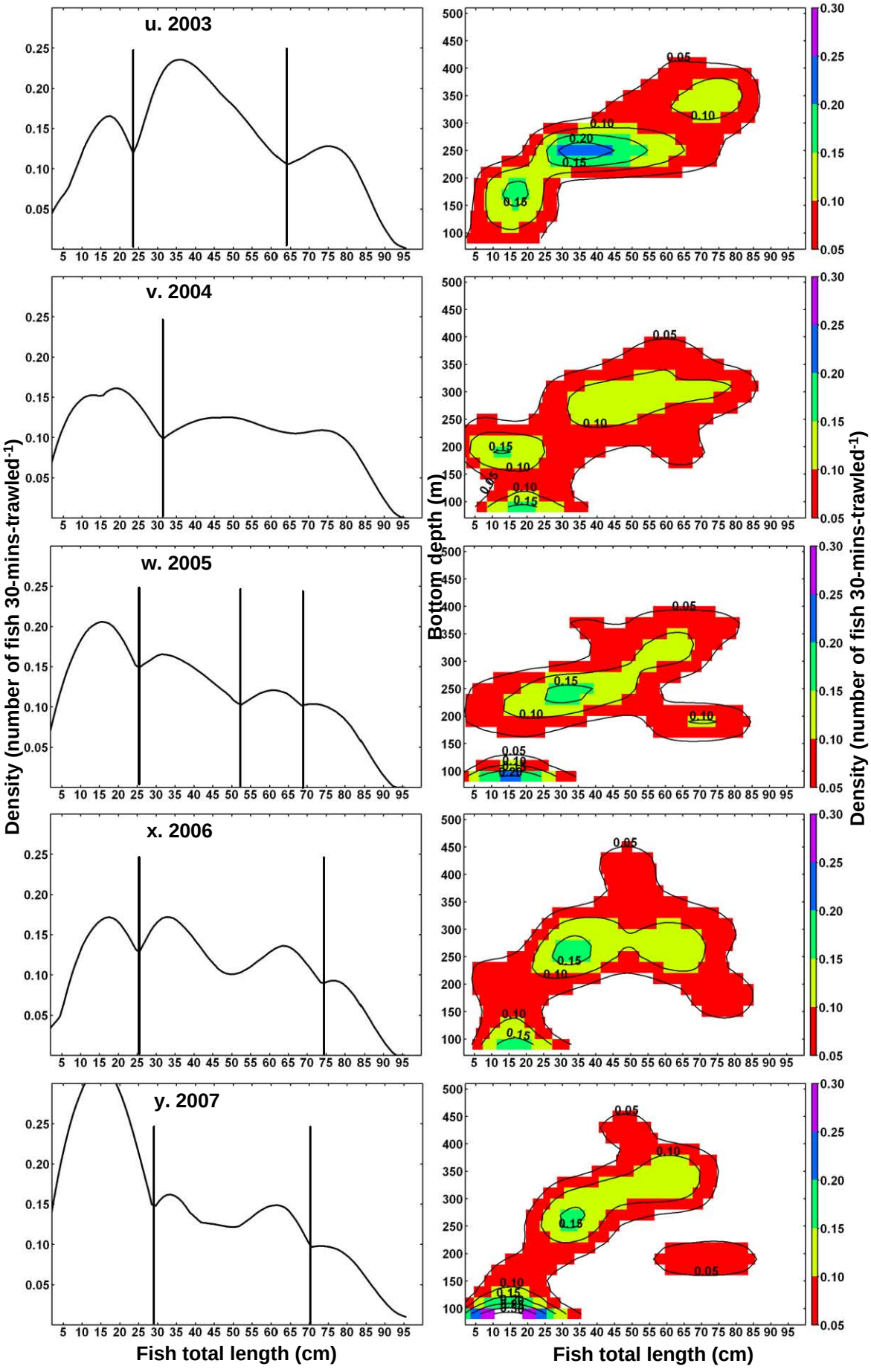

CHAPTER 6

Influence of environmental and other variables on otolith zone formation of *Merluccius capensis*

6.1. Abstract

Factors influencing the timing of translucent zone formation on *M. capensis* otoliths were tested with statistical models. In the first approach a binomial generalised linear model (GLM) was used to predict the presence of zones T1–T6 for fish length and maturity stage, area and bottom depth in which the fish were captured, and the cohort the fish belonged to. The best model was selected using Akaike's information criterion, and was consistently the model in which the presence of a translucent zone was explained by fish length as well as by area and for zones T1, T3 and T4 also by cohort. The additional formation of translucent zones per fish length, or early formation of translucent zones increased from the south to the north of Namibia. Zones T1, T3 and T4 were formed earliest on fish belonging to the 2002 cohort. In the second approach, translucent zone formation dates were back-calculated and linked to environmental variables such as daylight duration, sea surface temperature (SST), a change in SST, SST anomaly, bottom temperature and bottom oxygen concentration preceding the translucent zone formation "event" using a randomization procedure. In this procedure, the mean of the specific variable measured at all *n* translucent zone formation events was compared with the mean of the variables measured at *n* events distributed randomly along the time series under the null hypothesis that translucent zone formation events are independent of the environmental variable tested. Translucent zone formation events were significantly correlated with warm bottom temperatures as most translucent zones were formed in summer/autumn. No significant temporal correlation between translucent zone formation events and daylight duration, a change in temperature, water oxygen concentration or temperature anomaly was detected. There were no apparent links between cold or warm years and additional translucent zone formation on specific cohorts. The area-specific differences in translucent zone formation timing could be explained by warm temperatures or high variability in temperature, or the influence of the width of the continental shelf in northern Namibia. The presence of a certain number of translucent zones on *M. capensis* otoliths was always most strongly associated with fish length.

6.2. Introduction

Determining the (annual) age of fish and understanding the periodicity of translucent and opaque zones on fish otoliths is important in fisheries science. Various studies have addressed questions of periodicity and the cause of annual zone formation on otoliths (e.g. Pannella, 1971; Casselman, 1983; 1987; Beckman and Wilson, 1995; Pearson, 1996). However, there is much inconsistency among the results of these studies and among different species, and relatively little understanding of the causes. Morales-Nin (2000; 2001) concluded that the traditionally assumed constancy of zone formation in deep-water fish complicates our understanding of the mechanism, and posed four questions: "(1) What is the mechanism that relates the growth marks in the otoliths with the age of the fish? (2) Is it possible to validate the proposed mechanism with observed results? (3) How do phylogeny and stock affect the otolith increment patterns? (4) How do the environmental and physiological responses and processes affect check and zone formation?" (Morales-Nin, 2001, p. 381). These questions largely remain unanswered for most species, and remain a challenge for future fisheries research (Schill, 2009; Miller *et al.*, 2010; Szedlmayer and Beyer, 2011).

In *Merluccius capensis*, the translucent zone was defined as the "winter growth zone, deposited in winter/spring and associated with periods of slow growth" (ICSEAF, 1983, p. 2). Translucent zones or "winter rings" were said to form because of a winter slowing in the rate of calcification (Pannella, 1980), but have more recently been observed to form in (northern hemisphere) summer–autumn in North Sea cod *Gadus morhua* also (Pilling *et al.*, 2007). Beckman and Wilson (1995) reviewed 104 studies on annual age validation comparing a wide variety of species and regions. They showed that there was a difference between zone formation in tropical and temperate regions. In temperate and sub-polar latitudes opaque zones were generally formed during high or increasing water temperatures associated with fast somatic growth (Kimura *et al.*, 1979; Brothers, 1979), and so translucent zones should theoretically be associated with cold water temperatures and periods of slow growth. Sometimes physiological responses to low water temperatures were identified as the most important factor causing zone formation, followed by food supply (Pannella, 1980). Schramm (1989) showed that opaque zones (associated with periods of slow growth) were formed in response to increases and decreases in water temperature, and more

effectively after rapid temperature changes, on hatchery-reared bluegills *Lepomis macrochirus*. In Atlantic *G. morhua*, the growth of the translucent zone followed increased metabolic stress resulting from reduced feeding (Hüssy and Mosegaard, 2004). Pilling *et al.* (2007) showed that the onset of translucent zone formation in North Sea *G. morhua* followed peak seasonal temperatures and low feeding rates in the southern North Sea, but that the temperature declined before the zone was completed in the population. They suggested that the combined metabolic stress of reproduction, growth and migration enabled continued translucent zone formation in the population even at low temperatures and high food availability.

In many studies the presence of zones corresponded with the spawning period (e.g. Beckman *et al.*, 1990; Morales-Nin and Ralston, 1990; Brouwer and Griffiths, 2004) or the onset of the reproductive period (e.g. Yosef and Casselman, 1995) or fish sex and maturity stage (e.g. Morales-Nin *et al.*, 1998), with the suggestion that there is relationship between rate of calcification and reproduction (Pannella, 1971). However, the link is not consistent between species. Beckman and Wilson (1995) reviewed 27 studies in which annuli were matched with spawning. Of these, 39 % matched translucent zones with spawning, 19 % matched opaque zones with spawning, and for 37 % the spawning period spanned both translucent and opaque zones. They concluded that correlation between spawning and zone formation could be coincidental. Translucent zone formation also occurs on sexually immature fish, at constant temperature and with unlimited food supply throughout the year, but may be related to daylight duration as this has a seasonal cycle affecting activity and metabolic rate (Wright *et al.*, 1992; Brouwer and Griffiths, 2004; Szedlmayer and Beyer, 2011). Beckman and Wilson (1995) showed that there is substantial variability, even within species at similar geographical levels, and concluded that the causes of zone formation are a composite of endogenous and environmental factors. Morales-Nin *et al.* (1998) showed that there was no seasonal signal in zone formation on European hake *M. merluccius* otoliths and concluded that zone formation is controlled by a combination of environmental and endogenous factors that have different influences at different ages, sex and maturity stages of the fish.

Spawning or other biological (endogenous) events may have a more significant physiological effect than environmental seasonality on zone formation. This was

shown, for example, in tropical regions (Pannella, 1974) and in a recent study on Benguela hake *M. polli* and Senegalese hake *M. senegalensis* in Mauritania, which is also in tropical latitudes (Rey *et al.*, 2012). Geffen and Nash (1995) found that "check" formation on juvenile plaice *Peuronectes platessa* was influenced by the fish' activity patterns, which were influenced by the tidal cycle. However, check formation was not influenced significantly by temperature anomalies or daylight duration. They concluded that check formation matched ontogenetic changes in activity and feeding. *M. capensis* and *M. paradoxus* translucent zone formation, though according to general theory linked to spawning, feeding and environmental conditions, was also suggested to happen according to an underlying process regulated by an innate biological rhythm (ICSEAF, 1983).

The northern Benguela system is variable in terms of daily temperature fluctuations because of the wind-driven upwelling system (Boyer *et al.*, 2000; Bartholomae and van der Plas, 2007). In the Namibian mid-shelf area in mid-latitudes, the area near the seabed, where young hake reside, is perennially oxygen-poor (Woodhead *et al.*, 1997; Mohrholz *et al.*, 2008). Juvenile hake are tolerant to low oxygen concentrations, but with a low tolerance limit of 0.5 ml l^{-1} (Woodhead *et al.*, 1998; Bartholomae and van der Plas, 2007). Low oxygen water has affected the depth distribution and survival of Namibian hake (Mas-Riera *et al.*, 1990; Hamukuaya *et al.*, 1998; Woodhead *et al.*, 1998). Oxygen concentration is thus a factor that needs to be considered when investigating the causes of translucent zone formation on Namibian *M. capensis* otoliths as this would affect the metabolic and growth rates of hake, as well as their migration, and hence would have a direct or indirect effect on translucent zone formation.

In Chapters 3 and 4 it was shown that Namibian *M. capensis* generally form two to three translucent zones on their otoliths at least up to when they are 3.5 years old, starting at the age of about 6–8 months, when they are still sexually immature. The periods of translucent zone formation were mid-winter/spring and summer/autumn, hence did not seem to relate to a particular temperature regime (Chapter 4). However, translucent zones may have been formed after a decrease in temperature or at the onset of an event, e.g. upwelling. In Chapter 5 it was shown that translucent zones were associated with off-the-shelf as well as north-south movements of hake. Not all

translucent zones were linked with migration and differences between cohorts were not clearly associated with differences in migration in those particular years. The association of feeding / nutritional condition (Geffen and Nash, 1995), fish length, cohorts, area and depth (Chapters 3, 4 and 5), fish spawning activity or maturity stage (e.g. Morales-Nin *et al.*, 1998; Brouwer and Griffiths, 2004), as well as environmental variables such as temperature (e.g. Pannella, 1974), increase or decrease in temperature (e.g. Schramm, 1989), daylight duration (e.g. Brouwer and Griffiths, 2004; Szedlmayer and Beyer, 2011) and oxygen concentration (e.g. Hamukuaya *et al.*, 1998) with translucent zone formation on *M. capensis* need to be separated further.

The overall aim of this chapter is to further investigate environmental and biological causes of timing and variability in timing of translucent zone formation on *M. capensis* otoliths using statistical models together with *in situ* and satellite-derived environmental data. Since the temperature at the time of capture of the fish will have little effect on a translucent zone formed a few months before, and since the area or depth in which the fish was at the time of a back-calculated formation date of a translucent zone cannot be known exactly, aims were tackled in two parts asking the following questions (1) Is the presence of a particular translucent zone (T1–T6) dependent on the fish length, cohort of the fish, the area and depth in which the fish was captured or the maturity stage of the fish? (2) Is the back-calculated formation date of the translucent zone dependent on daylight duration, change in water temperature, temperature, temperature anomaly or water oxygen content preceding the formation date? In order to answer this question, a further aim was to describe the oceanographic conditions along the Namibian coast from 1996 to 2007. (3) If timing of translucent zone formation differs between cohorts, are these differences caused by differences in water temperature between the particular years?

6.3. Materials and methods

Data which had been assigned to cohorts in Chapters 3 and 4 were used for analysis in this chapter. These consisted of a total of five cohorts from fur seal scat samples (Chapter 3, n = 3474 otoliths) and three extended cohorts with additional survey otoliths (Chapter 4, n = 451 otoliths). On each otolith, complete translucent zones were counted and otolith diameter (OD) at each translucent zone measured in mm (see Fig. 3.2). Total OD was also measured for each otolith from seal scat samples, corrected for erosion (Equation 2.1) and used to calculate fish total length (TL) for each fish (Equation 2.2). Samples from fish ≤ 50 TL were used and only up to the sixth translucent zone on each otolith (T1–T6) was analysed.

6.3.1 Presence of translucent zones in relation to fish length, cohort, area, bottom depth or fish maturity stage

Only survey otoliths were used for comparisons in this section (Chapter 4, n = 451). The reason for this is that during a research survey the exact area and depth of capture were recorded for each fish, while feeding ranges of fur seals from different colonies overlap (Skern-Mauritzen *et al.*, 2009) so the exact area and depth of capture of hake from fur seal scats is unknown. Also, the exact fish TL and fish sex and gonad maturity stage were recorded for each fish on a research survey, while these were unknown for fish from fur seal scats. In addition, it was observed that small T1 zones were often only visible on small otoliths (Chapter 4). These were mostly collected from scat samples. Including otoliths from scat samples would therefore skew the comparisons of translucent zone presence for the different categories.

A binomial generalised linear model (GLM) applied on binary data with a logit link (Zuur *et al.*, 2009) was used to predict the presence of a particular translucent zone (T1–T6), 1 if the translucent zone was present and 0 if absent, in terms of fish TL (cm), and other variables (described below).

The best candidate model was selected using the model selection approach (Buckland *et al.*, 1997; Johnson and Omland, 2004), based on the lowest Akaike Information Criterion (AIC) (Akaike, 1973). The AIC is based on the log-likelihood while penalising for additional parameters used in each model, and provides a quantitative

measure of relative support for each hypothesis (Johnson and Omland, 2004).

Candidate models assumed the presence of a particular translucent zone *j* (*Hi* on fish *i*) was dependent on:

(1) Fish total length (cm) (*L*, as a proxy of age) only,

as well as *L* and either

(2) Cohort (*C*, 1996, 1998 or 2002) that fish had been assigned to (Chapter 4)

(3) Area (*A*, north <20.5°S, centre 20.5–25.5°S or south >25.5°S, Chapter 5) of the Namibian coast in which the fish were collected,

(4) Depth category (*D*, inner-shelf <180 m, mid-shelf 180–350 m or outer-shelf > 350 m bottom depth, Chapter 5) at which the fish were collected or

(5) The maturity stage of the fish (*S*, inactive, active and spent; see below).

Additional candidate models included TL (1) and two variables each of models (2)–(5), three variables of each, as well as a global model incorporating all five variables. The global model is therefore:

$$logit(\pi_i) = \beta_0 + \beta_L L_i + \beta_C C + \beta_A A + \beta_D D + \beta_S S \quad (6.1),$$

where β_0 is the intercept, only *L* is a continuous variable, all others are categorical (fixed term) variables (explained above in the candidate models), β_L is a constant, β_C, β_A, β_D and β_S are fixed factor coefficients with three levels. π_i is the probability of finding H_i on a particular fish. H_i is binomially distributed with probability π_i and n_i = 1 independent trials. The expected mean of H_i is given by π_i and variance by $\pi_i(1-\pi_i)$. $logit(\pi_i)$ means that:

$$\pi_j = \frac{e^{\beta_0+\beta_L L+\beta_C C+\beta_A A+\beta_D D+\beta_S S}}{1+e^{\beta_0+\beta_L L+\beta_C C+\beta_A A+\beta_D D+\beta_S S}} \quad (6.2).$$

Exploratory analyses showed that there were no significant differences between back-calculated fish total lengths at each translucent zone of male and female fish (see Appendix 6.1). Thus, to simplify the model, male and female fish were used together and the presence of a particular translucent zone was related to their maturity stage (*S*). Maturity stages were assigned to each fish during research surveys by macroscopic analysis according to five stages after Botha (1986). For the purpose of this analysis, testing the effect of spawning activity on translucent zone formation, the five stages were divided into three levels: inactive (stages 0 and 1, juvenile and inactive fish),

active (stages 2 and 3, active and ripe fish) and spent (stages 4 and 5, ripe-and-running and spent fish).

The global model was assessed for goodness-of-fit based on the distribution of residuals (Zuur *et al.*, 2009). All analyses were performed with the basic library in R version 2.9.1 (R Development Core Team, 2009).

6.3.2 Timing of translucent zones in relation to environmental factors

6.3.2.1 Back-calculation of translucent zone formation dates

The method to estimate timing of translucent zone formation made use of back-calculation of fish lengths at each translucent zone and Fabens' (1965) version of the von Bertalanffy growth function (VBGF). Back-calculation generates lengths (and dates) at non-represented sampling dates and so the formation dates of zones T3–T6 could be calculated more confidently using data described in Chapter 4 (n = 3925; see Tables 3.1 and 4.2). With Fabens' (1965) method, date at (the end of each) translucent zone could be calculated without assuming a cohort has a certain hatchdate (or t_0) and thus without assuming a certain age at a particular date of capture.

Back-calculation of fish total lengths (TL) at each translucent zone (i) was performed by applying Equation 2.2 to the measurements of OD at each translucent zone:

$$TL_i = 0.6997\ (OD_i + 2.170)^{1.362} \qquad (6.3),$$

where TL_i (cm) is the fish TL at translucent zone i, OD_i (mm) is the diameter measured at translucent zone i. TL was calculated for up to six translucent zones on each otolith.

The time of formation ($t_{1,i}$) of translucent zone i was calculated by first calculating change in length since translucent zone i (Fabens, 1965; Bal *et al.*, 2011):

$$\Delta L_i = L_{2,j} - L_{1,i} = (L_\infty - L_{1,i}) * (1-e^{-K\,(t2,j\,-\,t1,\mathrm{i})}) \qquad (6.4),$$

where $L_{1,i}$ is the TL at translucent zone i and time 1 ($t_{1,\mathrm{i}}$ is the unknown in this case) and $L_{2,j}$ is the TL at capture of fish j, which is time 2 ($t_{2,j}$), K is the growth rate of 0.127 (year^{-1}), L_∞ is the asymptotic length of 134 (cm), the last two calculated for the overall *M. capensis* population in Chapter 4 (Table 4.1). Rearranging Equation 6.4 to solve for $t_{1,i}$, on fish j:

$t_{2,j} - t_{1,i} = \Delta t$, time in years since translucent zone i (from capture time of fish j, t_2,j)

$$\Delta t = ln[1 - \{(L_{2,j}-L_{1,i}) / (L_\infty - L_{1,i})\}]/-K \qquad (6.5),$$

and so $t_{1,i} = t_{2,j} - (\Delta t * 365)$ (6.6).

For each cohort (1996, 1998, 2002, 2005 and 2006), dates of formation of each translucent zone (T1–T6) were binned into weekly intervals. Translucent zone formation "events" were defined as those weeks in which at least one translucent zone of one cohort had a number of translucent zones greater than a selected threshold. This threshold was selected in advance as the average number (back-calculated days) per week per translucent zone per cohort, plus two standard deviations. This threshold was simplified to a percentage for each cohort. For the 1996 and 1998 cohorts it was 4 %, for the 2002 cohort it was 3.5 %, for the 2005 and 2006 cohorts it was 6 % (see Fig. 6.3).

6.3.2.2 Environmental data

Daylight duration for each day for a whole year was calculated as the number of hours from sunrise to sunset at Walvis Bay (23°S), obtained from http://www.sunrise-and-sunset.com/en/namibia/walvis-bay/. Water temperature and water oxygen data were compiled by the Ministry of Fisheries and Marine Resources (MFMR), Namibia, and comprised two main datasets. (i) Sea surface temperature (SST) data obtained from the high resolution local area coverage NOAA satellites, restricted to the Namibian area (8°–17°E, 17°–29°S), with an initial spatial resolution of 1.1 km (source: http://iridl.ldeo.columbia.edu/SOURCES/.NOAA/ NCEP – IRI Data Library; Bartholomae and van der Plas, 2007). An algorithm was applied to process the raw data, which were finally provided as weekly averages of SST in 1° wide blocks (regular 60x60 km grids) adjacent to the Namibian coast for each latitude starting at 17°S and ending at 29°S, for the years 1996–2006 (data courtesy C. Bartholomae, MFMR, Namibia). (ii) Depth-specific CTD (conductivity- temperature-depth) data and bottle measurements obtained from research surveys, including (near) monthly sampling of the oceanographic monitoring line 23°S (off Walvis Bay). The sea water temperatures and dissolved oxygen content (ml l^{-1}) at the sea bottom (± 10 m) at station 2340 (40 nautical miles offshore on the 23°- monitoring line, 144 m average bottom depth) were used as a proxy for the conditions young hake experience (see later). A 27°S-line and a 20°S-line were also sampled by MFMR, but data from the 23°S line showed the most comprehensive temporal coverage during the period 1996–

2007, so only the 23°S line was used for the purposes of this chapter (data courtesy A. van der Plas, MFMR, Namibia).

Annual cyclical fluctuations of daylight duration, SST and bottom temperatures (Y) were described by a periodic regression model fitted to the observed temperature or time in hours from sunrise to sunset:

$$\hat{Y}_i = \beta_0 + \beta_1 \sin\left(\frac{2\pi}{P} M_i\right) + \beta_2 \cos\left(\frac{2\pi}{P} M_i\right) \quad (6.7),$$

where $\hat{Y}_i$ is the predicted daylight duration (h), bottom temperature, or SST (°C) value at time M_i (in decimal months). 1 January was assigned a value of 0 and 1 December a value of 11, thus M was calculated as: 12[(sampling date – 1 January of the same year)/365]. P is 12, the assumed seasonal annual period (months), β_0 is the mean bottom temperature (or SST or daylight duration) and β_1 and β_2 are the *sine* and *cosine* model coefficients, respectively, which together define the phase shift and amplitude of the oscillations (Bliss, 1958; de Bruyn and Meeuwig, 2001). Parameters were estimated by minimising the sum of squares of the residuals between expected values ($\hat{Y}_i$) and observed values (Y_i) in the Newton algorithm of the Microsoft® Office Excel Solver routine.

The applicability of the SST at 23°S to the SST at the other latitudes was validated with pairwise correlations. The bottom temperature at the 2340 station was also correlated with bottom temperatures at deeper stations on the same line as well as with salinity and bottom oxygen concentrations on the same station (pairing them for the same date). Correlation matrices were drawn up using R version 2.9.1 (R Development Core Team, 2009) and the library 'AED' (Zuur, 2010). The bottom temperature data were also validated by SST-bottom temperature lagged correlations, calculating the lag between daylight duration, SST and bottom temperature from the differences in predicted peaks of the periodic cyclical oscillations.

SST anomalies were calculated by subtracting the predicted cyclical seasonal SST ($\hat{Y}_i$) from the observed SST.

The weekly temperature change (ΔT°) was calculated as:

$$\Delta T°_w = T°_w - T°_{w-1} \quad (6.8),$$

where the change of temperature ($\Delta T°$) of week w is temperature in week w minus the temperature of the previous week.

6.3.2.3 Randomization procedure

A randomization procedure similar to that described by Ladah *et al.* (2005) was used to test for temporal correlation of translucent zone formation events with (1) daylight duration, (2) real time SST, (3) lagged SST, (4) real time SST change ($\Delta T°_w$), (5) lagged SST change, (6) real time SST anomalies, (7) lagged SST anomalies, (8) bottom temperature at the 2340 station and (9) bottom oxygen at the 2340 station. The "lagged" values refer to the lag duration between SST and bottom temperature in order to use SST as an indicator of bottom conditions. From Chapter 3, a translucent zone would take between 6 and 36 days to form in an individual fish, i.e. 21 days on average, and so an additional lag of three weeks was added to "real time" to test conditions that might have caused the start of translucent zone formation events.

Weekly SSTs were assigned to translucent zone formation events. Available bottom temperatures were assigned to the particular week in which they were collected, assigned to translucent zone formation events. Missing data of bottom temperatures were substituted with the cyclical mean for the corresponding week. Only weeks for which bottom oxygen data were available, were included in the test.

The test statistic C for temperature change values was based on Equation 6.8, where w becomes the week along the time series when an event occurs, and $\Delta T°$ for all event weeks is averaged to get a value of C:

$$C = \sum_{w=1}^{n} \Delta T_w^{\circ} \Big/ n \quad (6.9),$$

where n is the total number of events identified. The value of C should be negative if translucent zone formation usually occurred after a temperature drop or positive if translucent zone formation occurred after a temperature increase. The test statistics for other variables were also calculated as the mean values of all event weeks of DD (daylight duration), T (SST or bottom temperature), TA (temperature anomaly), or O (bottom oxygen).

The null hypothesis of the randomization procedure states that the translucent zone formation events (events) are independent of each environmental variable tested, and their occurrence along the time series is thus random. If the null hypothesis is true, the values of *DD*, *T*, *C*, *TA* or *O* calculated for the original dates of events (DD_{obs}, T_{obs}, C_{obs}, TA_{obs} or O_{obs}) will not differ significantly from the values calculated for *n* events allocated at random along the time series *(*DD_{rand}, T_{rand}, C_{rand}, TA_{rand} or O_{rand}). A randomization algorithm with 5000 iterations was used to get an empirical probability distribution for the test statistics *DD*, *T*, C, *TA* and *O* under the null hypothesis. The p-value for each test statistic was calculated as $(x + 1)/(I + 1)$, where *x* is the number of DD_{rand}, T_{rand}, C_{rand}, TA_{rand} or O_{rand} values that were greater than DD_{obs}, T_{obs}, C_{obs}, TA_{obs} or O_{obs} and *I* is the number of iterations = 5000. The null hypothesis was rejected when $p < 0.025$ (2-tailed test) (Ladah *et al.*, 2005).

The earlier or later or "additional" formation of each translucent zone was visually related to anomalous environmental conditions during the life of the particular cohorts.

6.4. Results

6.4.1 Presence of translucent zones in relation to fish length, cohort, area, bottom depth or fish maturity stage

Models with the smallest AIC for T1, T3 and T4 were those in which presence of bans H_i was explained by fish TL, cohort and area (AIC = 80.2, 97.4, and 290.4, respectively, Appendix 6.2, Table A6.2a.i, iii, and iv). The presence of zones T2, T5 and T6 was best explained by TL and area (Appendix 6.2, Table A6.2a.ii, v and vi).

Predicted values for the best model for each translucent zone are presented in Figure 6.1. Estimated coefficients for each model parameter are presented in Appendix 6.2, Table A6.2b. Although some translucent zones were not represented in some categories (e.g. T1 and T3 of the 1996 cohort, Figs 6.1a and c), translucent zones were consistently formed earliest (on smallest fish total lengths) in the north, and latest in the south (Fig. 6.1). Comparing among cohorts, T1, T3 and T4 were formed earliest on fish belonging to the 2002 cohort, but still consistently within each cohort, the translucent zones were formed earliest to latest from north to south with fish from the central and southern areas more similar in timing (Figs 6.1a, c and d).

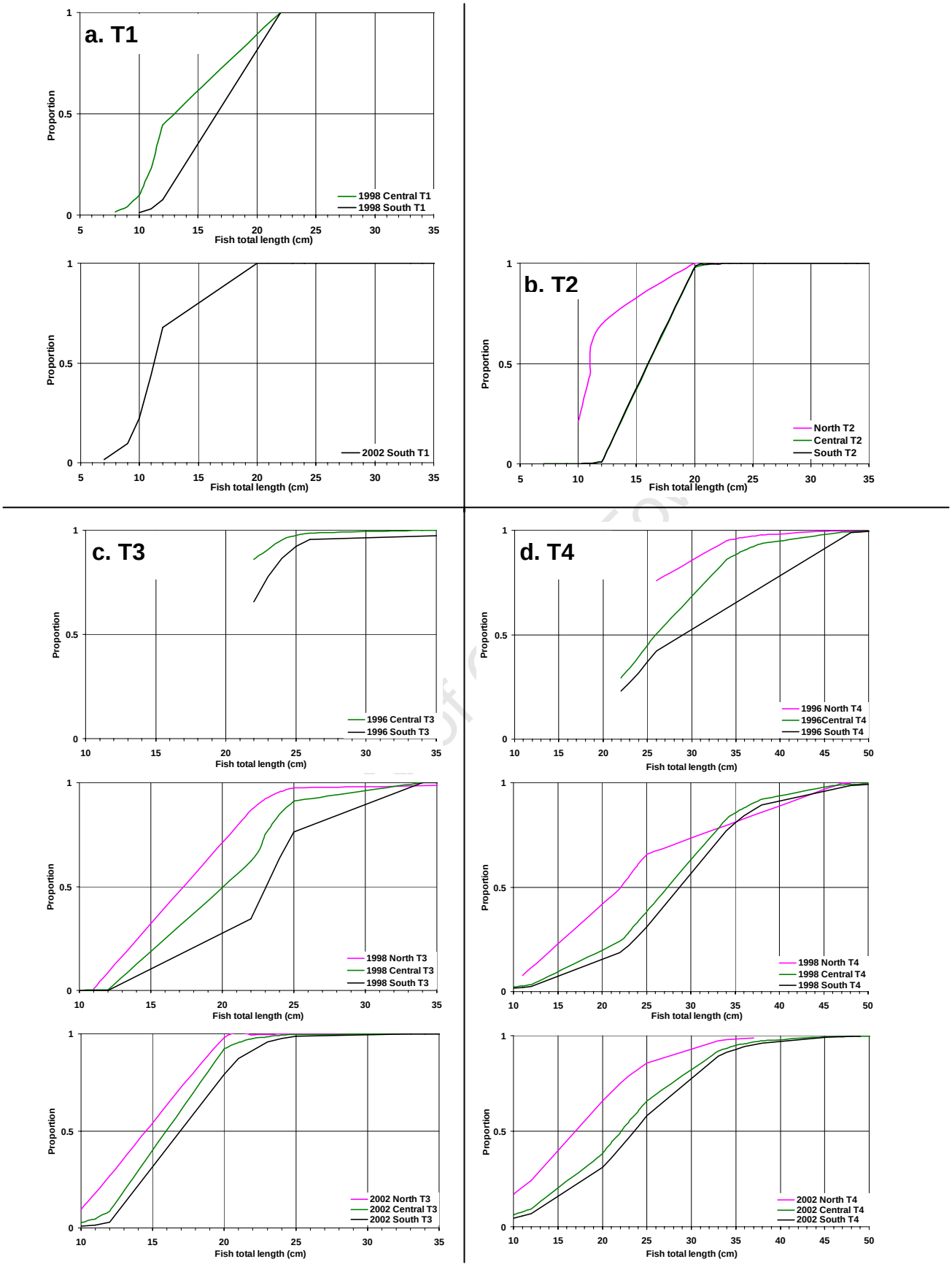

Figure 6.1 Binomial GLM-predicted probability (proportion) of translucent zone **a.** T1, **b.** T2, **c.** T3, and **d.** T4 present on *M. capensis* otoliths against fish total length (cm). GLM predictions are shown by area North (pink), Centre (green) and South (black) and by cohort 1996, 1998 and 2002 (different panels), where applicable (for model selection and model parameter coefficients and fits, see Appendix 6.2, Tables A6.2a.i–iv and b.i–iv).

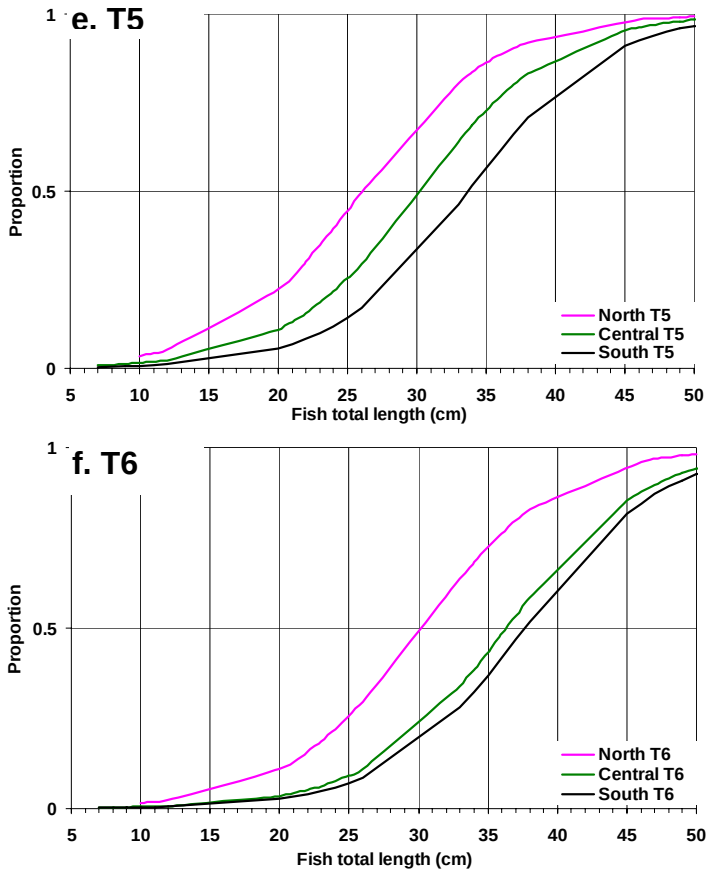

Figure 6.1 Binomial GLM-predicted probability (proportion) of translucent zone **e.** T5 and **f.** T6 present on *M. capensis* otoliths against fish total length (cm). GLM predictions are shown by area North (pink), Centre (green) and South (brown) along the Namibian coast (for model selection and model parameter coefficients and fits, see Appendix 6.2, Tables A6.2a.v and vi and b.v and vi).

Area consistently had the strongest influence on translucent zone formation, with fish caught in the north showing earliest formation of the zones T1 to T6, and so the highest number of translucent zones per fish total length is expected in the north. This could be detected when plotting mean number of translucent zones per fish total length class against total length class (Fig. 6.2). From a fish total length of about 30 cm onwards, the mean number of translucent zones per cm total length was consistently highest in the north and lowest in the south, differing by one to three translucent zones (Fig. 6.2a). Differences in number of translucent zones per fish TL between cohorts are not as marked as differences between areas but the 2002 cohort showed most number of translucent zones in fish up to 30 cm TL. For fish larger than 40 cm TL the 1996 cohort showed most number of translucent zones per cm fish total length (Fig. 6.2b).

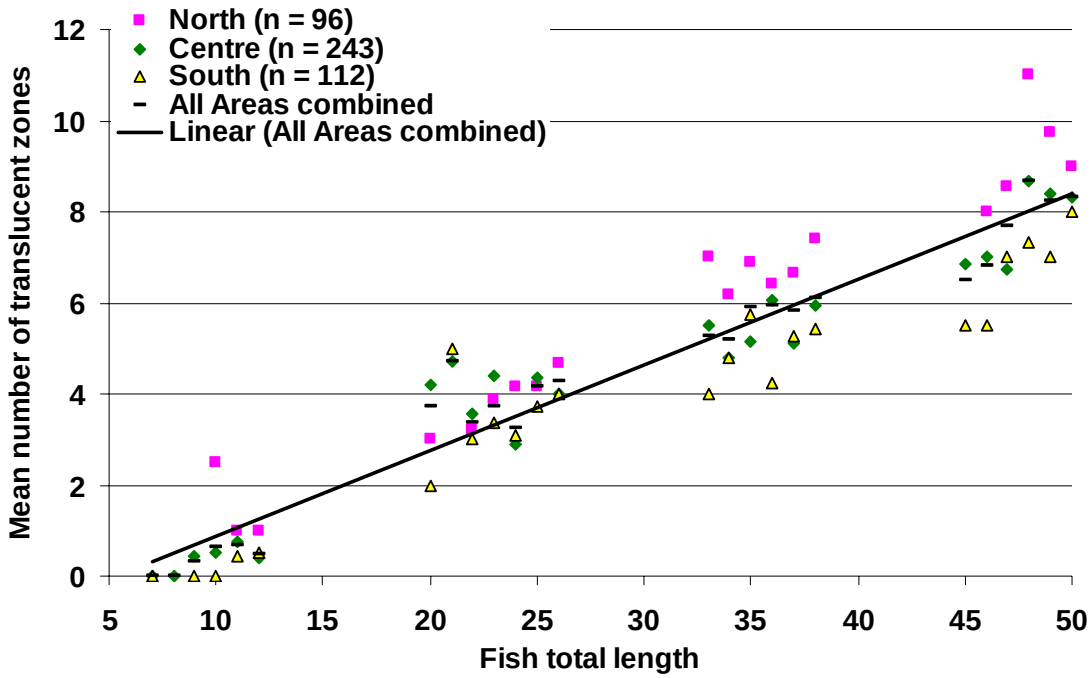

Figure 6.2a Mean number of translucent zones on *M. capensis* otoliths per cm-total-length-class separated by areas North (17–20.5°S), Centre (20.5–25.5°S) and South (25.5–29°S) along the Namibian coast.

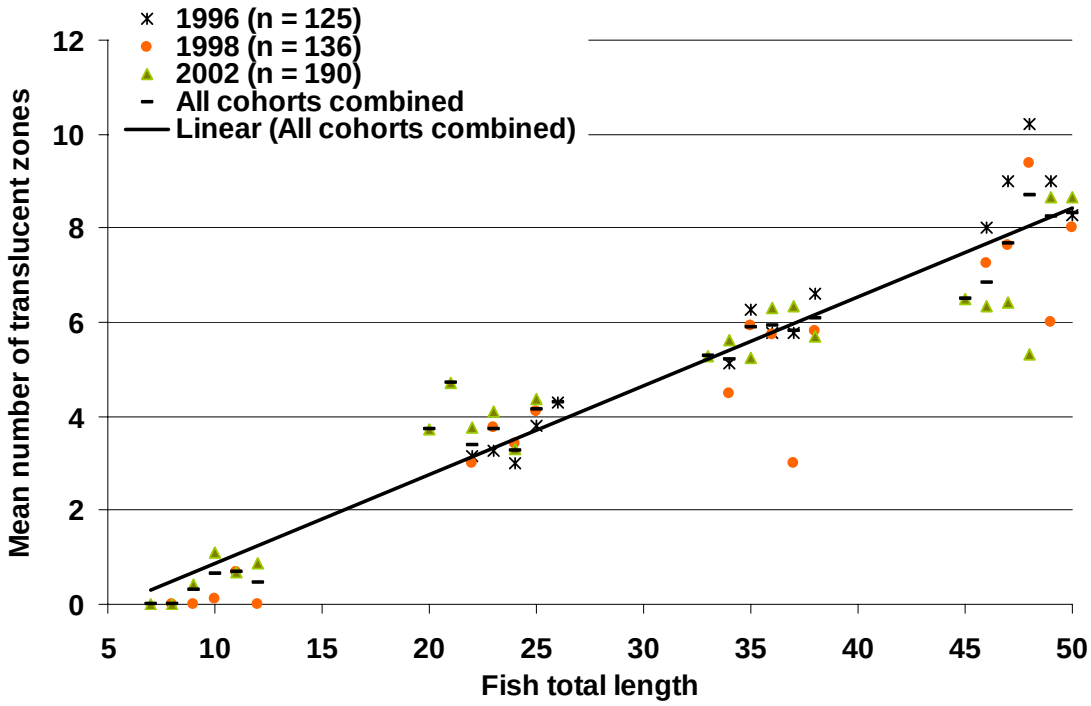

Figure 6.2b Mean number of translucent zones on *M. capensis* otoliths per cm-total-length-class separated by three cohorts of 1996, 1998 and 2002.

6.4.2 Timing of translucent zones in relation to environmental factors

6.4.2.1 Timing of translucent zones

Proportions of back-calculated translucent zone formation dates showed that the first six translucent zones can form at any time over a long period of a year or more (Fig. 6.3). Weeks in which at least one translucent zone showed a proportion higher than the pre-defined threshold (Fig. 6.3; Table 6.1) consisted of 80 "event" weeks in total for all cohorts (Table 6.1).

Table 6.1 The number of back-calculated translucent zone formation "event" weeks identified for five *M. capensis* cohort using different cut-off proportions (Fig. 6.3).

Cohort	Proportion threshold	Number of identified event weeks
1996	0.040	25
1998	0.040	16
2002	0.035	22
2005	0.060	8
2006	0.060	9
Total		**80**

"Events" most frequently occurred in summer/autumn (February–April) and less frequently in winter/spring (August–October) and summer (November–December) (Fig. 6.3). The first "event" of formation of T1 was in March (early autumn) of the first year of each of the 1996, 1998, 2002 and 2006 cohorts (Fig. 6.3). The 2005 cohort showed the first event of T1 in May (late autumn) of 2006, much later than the other four cohorts. For fish of the 1996 and 2002 cohorts, events of T1 continued longest (until late autumn). T2 seemed to be an additional pre-annulus in fish of the 2006 cohort, probably because of the shorter sampling range (not all fish had an T2 zone present in the last sample collected December 2007, see Figs 3.3 and 3.4, so a possible higher proportion of later events was not represented in the sampling range). Fish of the 1996 and 2002 cohorts had later "secondary" events of T2 formation in early winter (June) of 1997 and in spring (October) of 2003, respectively. From T3 onwards, events happened continuously and were strongly overlapping. Timing of formation of zones T3–T6 often had "secondary" events, a few months apart, so that no "early" or "late" formation compared with other cohorts could be disentangled (Fig. 6.3).

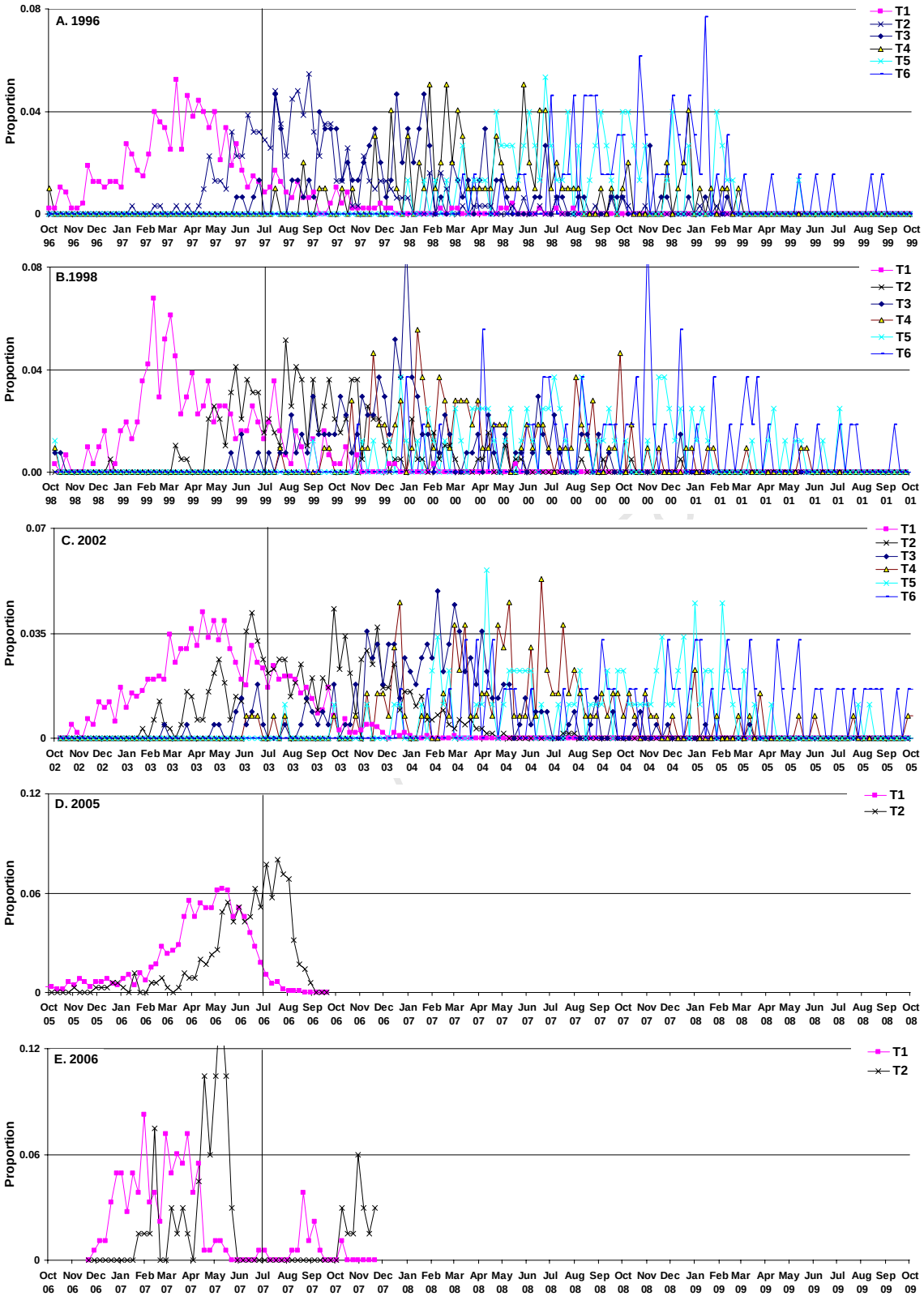

Figure 6.3 Proportion of translucent zones on *M. capensis* otoliths at each back-calculated formation date (binned into weeks) out of the total number of translucent zones for which formation dates were back-calculated (per translucent zone T1–T6) for each cohort **A.** 1996, **B.** 1998, **C.** 2002, **D.** 2005 and **E.** 2006. Horizontal lines indicate the threshold proportion for each cohort. Weeks for which the proportion of translucent zones was above the threshold line, were defined as "event" weeks. Vertical solid lines mark 1 July of every year.

6.4.2.2 Environment

SSTs at all latitudes were strongly correlated with SSTs in the 23° block with temperature in general increasing from south to north and strength of correlation decreasing with distance away from each latitude (Fig. 6.4). The correlation coefficient (r) of SST in the 17° block (most northern) against SST in the 23° block was 0.8 and r of SST in the 29° block (most southern) against SST in the 23° block was 0.9 (Fig. 6.4). This means there was sufficient correlation to use SST in the 23° block as indicator for relative conditions along the whole coast from here onwards.

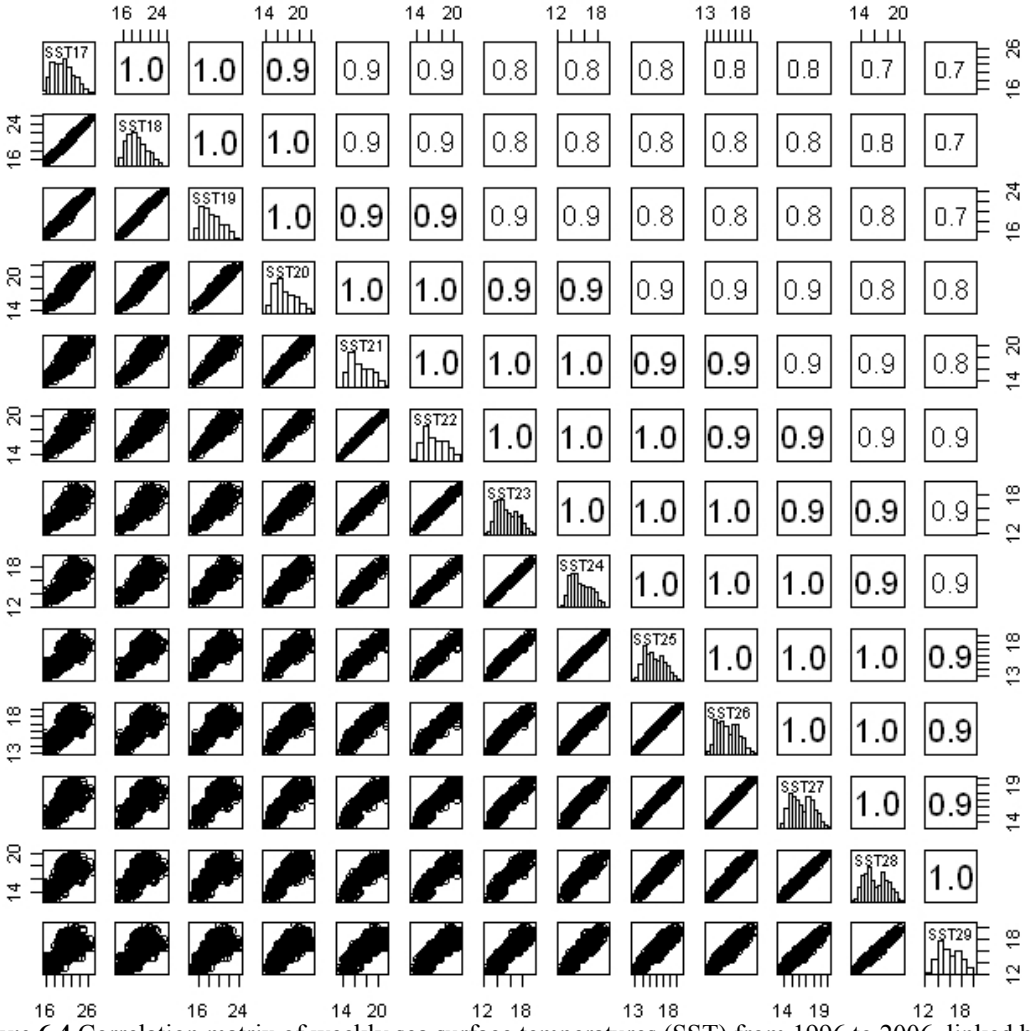

Figure 6.4 Correlation matrix of weekly sea surface temperatures (SST) from 1996 to 2006, linked by the week of collection, in 1° blocks along the Namibian coast (r, rounded and font size scaled according to p-value), frequency distributions and scatterplots. Abbreviated names of the variables are shown in the diagonal histograms: numbers 17–29 indicate each 1°-block from 17°S to 29°S along the Namibian coast. All axes are in °C.

The bottom temperatures at station 2340 were linearly correlated with SSTs at 23°S at with SSTs > 16 °C showing a higher variability of bottom temperatures (Fig. 6.5). Bottom temperatures at the 2340 station (average of 144 m bottom depth, i.e. inner-

shelf) were correlated with bottom temperatures at the deeper stations, with bottom temperatures in general decreasing with depth (Fig.6.5). The 2350 station (50 nautical miles offshore) had an average bottom depth of 226 m (mid-shelf) and the 2360 station (60 nautical miles offshore) had an average bottom depth of 346 m (shelf-break of mid-shelf). Since the location of fish at the time of translucent zone formation could not be known, but most fish < 50 cm would be found on the inner-shelf or mid-shelf (Fig. 5.9), and bottom temperatures at stations 2340 and 2350 were reasonably correlated (r = 0.5, Fig. 6.5), the 2340 station was used as relative indicator for conditions young fish were exposed to. Salinity showed a correlation of 1.0 with bottom temperature. Bottom oxygen concentrations were negatively correlated with bottom temperatures at the 2340 station, but with higher variability at temperatures < 16 ° C (Fig. 6.5). Since temperature is a very good indicator for salinity, but not for oxygen at high temperatures, temperature and oxygen were used as indicators of conditions from here onwards.

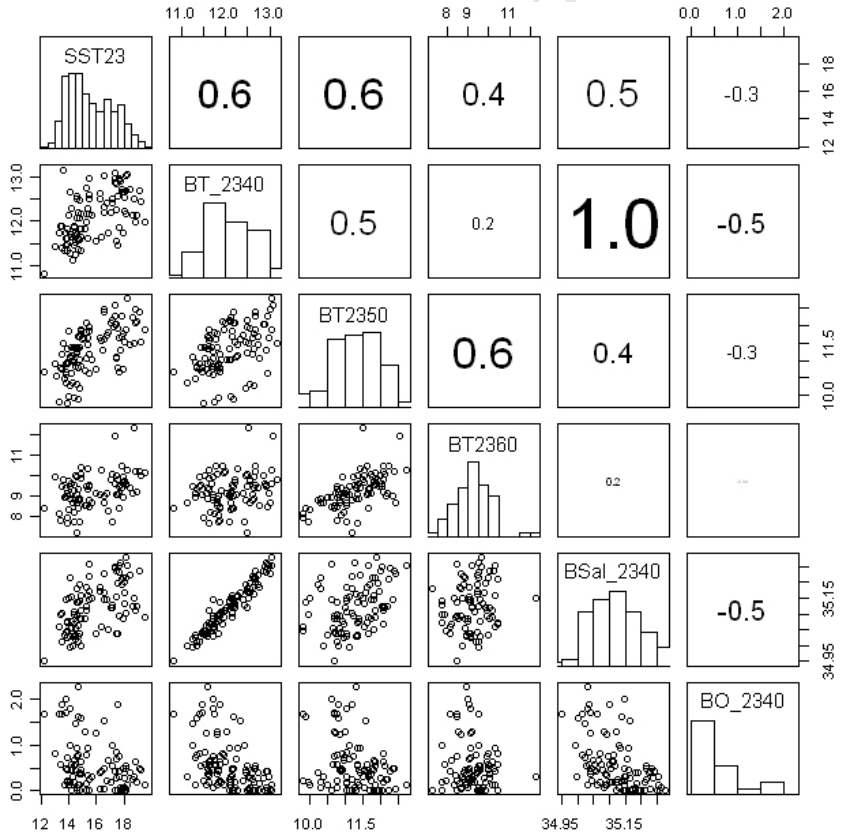

Figure 6.5 Correlation matrix of SST in the 23°S block (SST23) against various sea bottom stations' variables linked by the week of collection (r, rounded and font size scaled according to p-value), frequency distributions and scatterplots. Abbreviated names of the variables are shown in the diagonal histograms: BT_2340: bottom temperature at station 2340 (mean of 144 m depth), BT2350: bottom temperature at station 2350 (mean of 226 m depth), BT2360: bottom temperature at station 2360 (mean of 346 m depth). All temperature measurements were in °C. BSal_2340: the bottom water salinity (ppm) at station 2340, BO_2340: bottom water dissolved oxygen (ml l^{-1}) content at station 2340.

In general, at 23°S, the difference in daylight duration is 2.7 hours between the maximum (21 December) and the minimum (21 June). SST in the 23°S block peaks 9 February at 17.5°C and troughs 10 August at 13.6°C, while bottom temperature at station 2340 peaks 25 March at 12.6°C and troughs 24 September at 11.6°C (Fig. 6.6). SST at 23°S lags daylight duration by six weeks, and bottom temperature at station 2340 lags SST at 23°S by another six weeks (Fig. 6.6; see also Appendix 6.3). This means that the 6-week-lagged SSTs could be used as relative indicator of bottom temperature at the 2340 station (given the missing weeks of bottom temperatures). The 3-week-lagged changes in SST and SST anomalies were used as general indicators of *onset* of an event, e.g. upwelling.

The translucent zone formation "events" on *M. capensis* otoliths (from Fig. 6.3, super-imposed in Fig. 6.6) generally appeared to occur during the times of peak or trough of bottom temperatures, and also in the range in between. The events also spanned the times of peaks or troughs of daylight duration or SSTs.

Comparing SST anomalies with observed bottom temperatures (Fig. 6.7) shows that the bottom temperature time series, though less regular, reflects the overall conditions quite well, for example the relatively cold summer in December 1996 to March 1997 and the secondary peaks in May 2003 are reflected both in the SST and the bottom temperature time series (Fig. 6.7). Translucent zone formation events (super-imposed on Figs 6.6 and 6.7) occurred during anomalously cold conditions (e.g. March 1997, March and May 2003, February–May 2004), anomalously warm conditions (e.g. March–June 1999, November 2003, Apr–Jun 2006), and average conditions (Fig. 6.7).

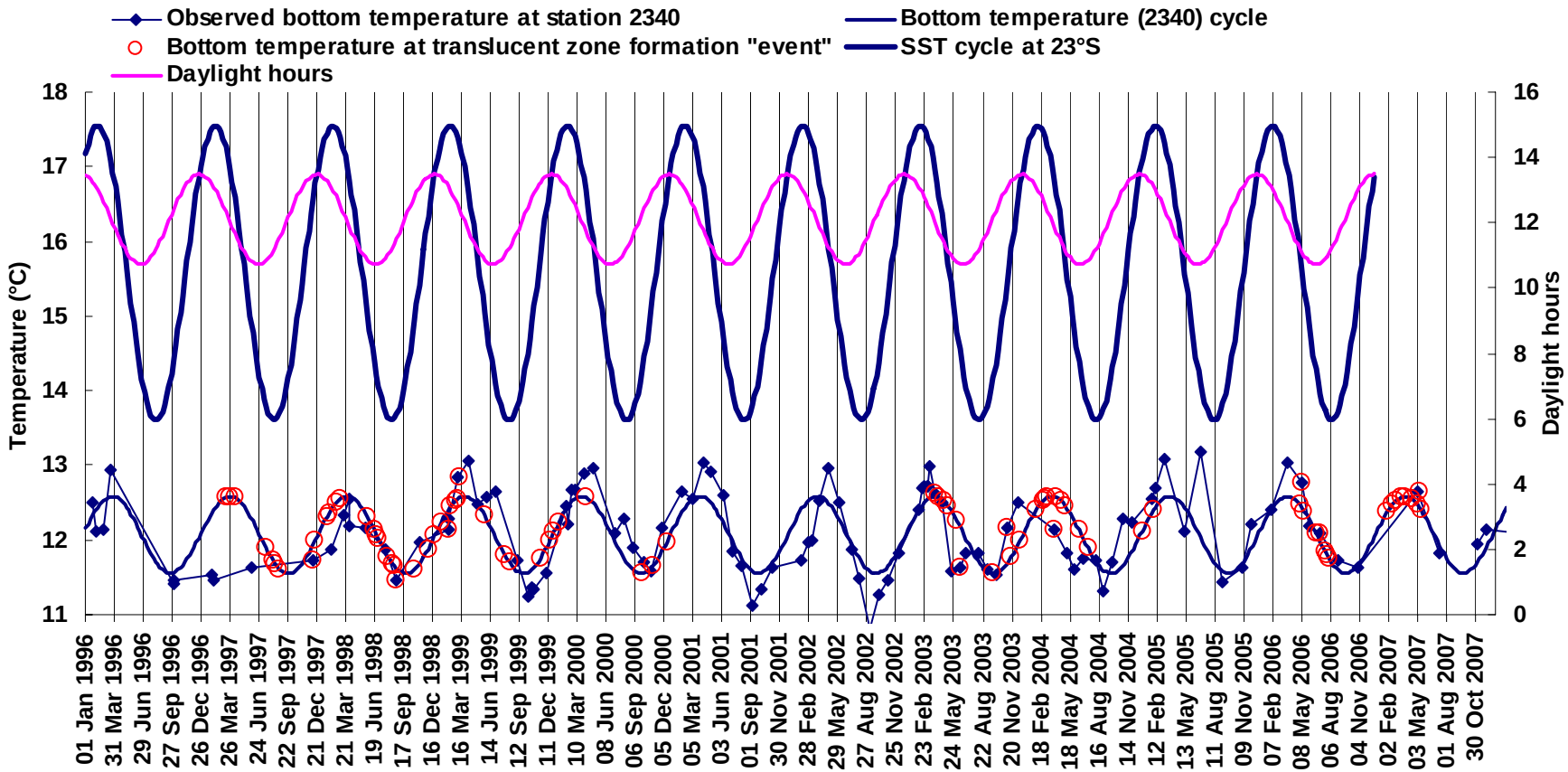

Figure 6.6 Time series of daylight duration (hours), cyclical sea surface temperatures (SST) (°C) at the 23°S block, water bottom temperature (°C) at the 2340 station and the cyclical mean of bottom temperatures off Namibia between 1 January 1996 and 30 October 2007. Identified translucent zone formation "events" (Fig.6.3) are shown on the graph as red circles on the observed (or predicted) bottom temperatures at the week of the event.

The cohorts' individual timing for the first two translucent zones with the prevailing conditions (Figs 6.3 and 6.7) summarise as follows: The latest T1 event occurred for the 2005 cohort in April–June of 2006 during warm conditions. The late "secondary events" of T2 formation occurred in September 1997 (1996 cohort) and October 2003 (2002 cohort); both were warm springs.

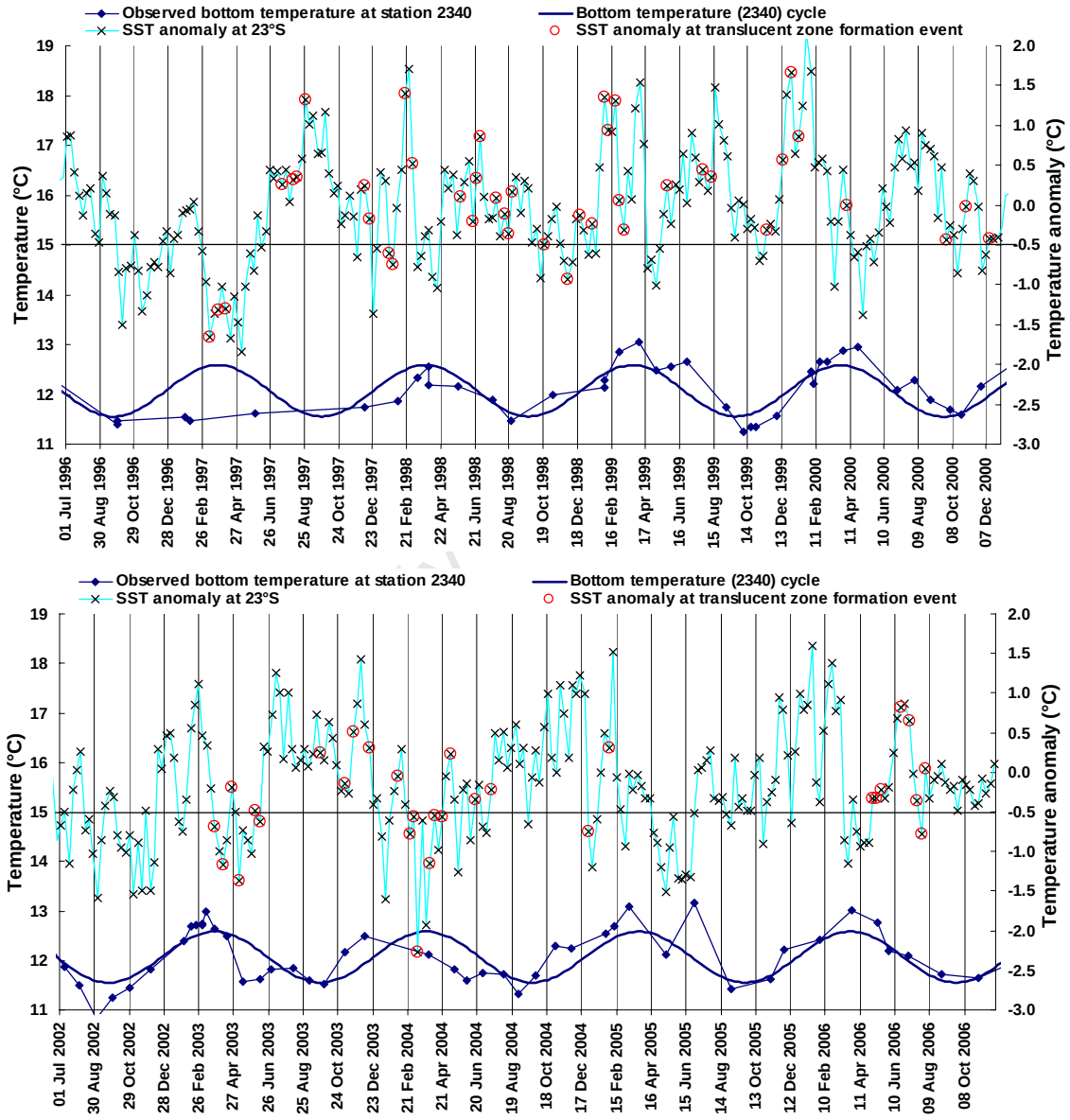

Figure 6.7 Time series of water bottom temperatures (°C) at the 2340 station and the cyclical mean of bottom temperatures and sea surface temperature (SST) anomalies from the cyclical SST mean (Fig. 6.6) off Namibia (i) between 1 January 1996 and 01 January 2001 and (ii) between 01 July 2002 and 1 December 2006. Identified translucent zone formation "events" (Fig.6.3) are shown on the graph as red circles on the SST anomaly during the week of the event.

6.4.2.3 Linking translucent zone formation events to environmental conditions with the randomization procedure

Translucent zone formation events (events) were significantly correlated only with warm bottom temperatures (T_{obs} = 12.16°C; p = 0.013; Fig. 6.8E). The 9-week lagged SST reflecting bottom temperature was also on the warm side, but not significantly correlated (T_{obs} = 15.8°C; p = 0.14; not shown). Events occurred during average daylight duration (12.14 hours; p = 0.28; Fig. 6.8A), average SSTs (15.7°C, p = 0.27, Fig. 6.8B) and a negative change (decrease) in 9-week lagged SST, but not significantly correlated (-0.052°C week^{-1}; p = 0.23; Fig. 6.8C). Events were not significantly correlated with SST anomalies, though these tended to the negative (cold), both for 3-week-lagged (-0.014°C; p = 0.039; Fig. 6.8D) and 9-week-lagged (TA_{obs} = - 0.12°C; p = 0.069; not shown). Events occurred during a period of relatively high bottom dissolved oxygen concentration, but not significantly correlated (O_{obs} = 0.69 ml l^{-1}; p = 0.17; Fig. 6.8F).

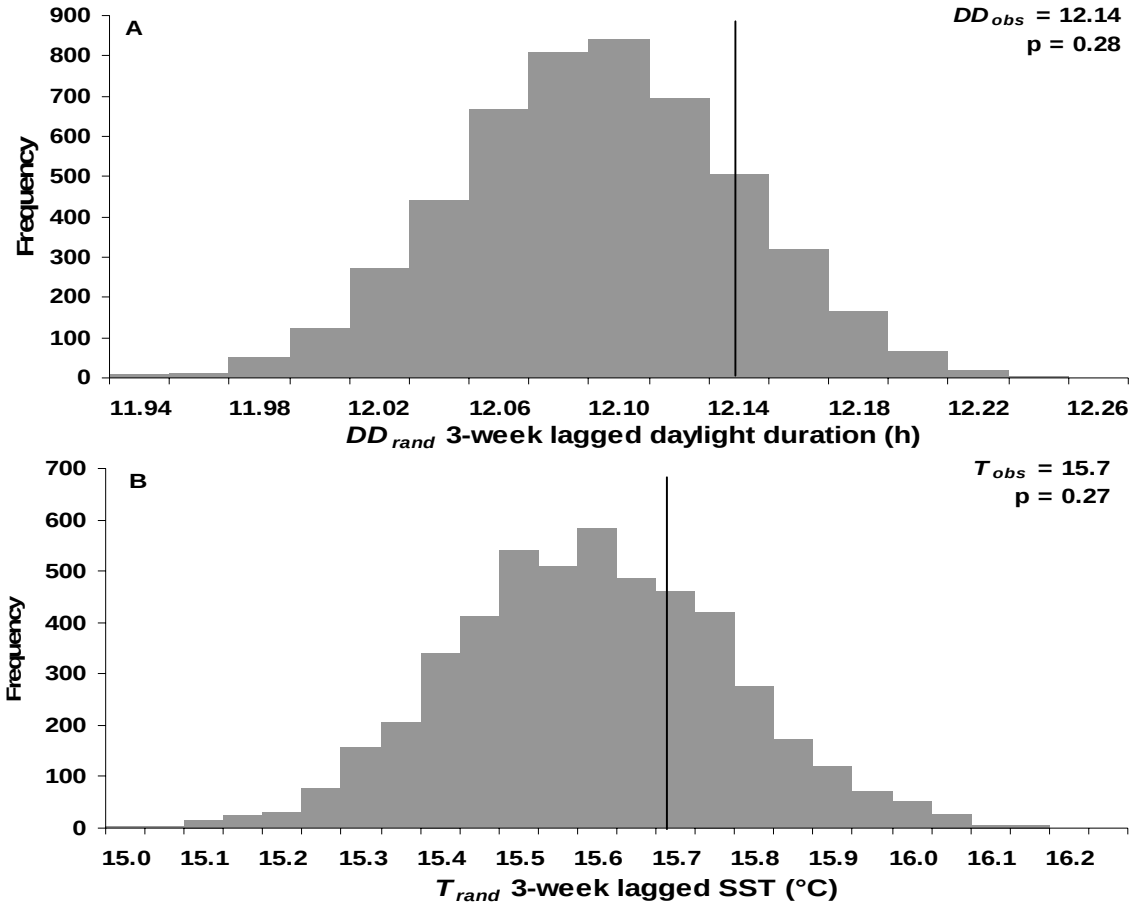

Figure 6.8 Frequency distributions of test statistics resulting from the randomization test to determine temporal correlations between hake otolith translucent zone formation events and environmental covariates **A.** Daylight duration and **B.** Sea surface temperature (SST). Covariates were lagged to translucent zone formation events by 3 weeks. Vertical lines show the positions of DD_{obs} or T_{obs} on each distribution.

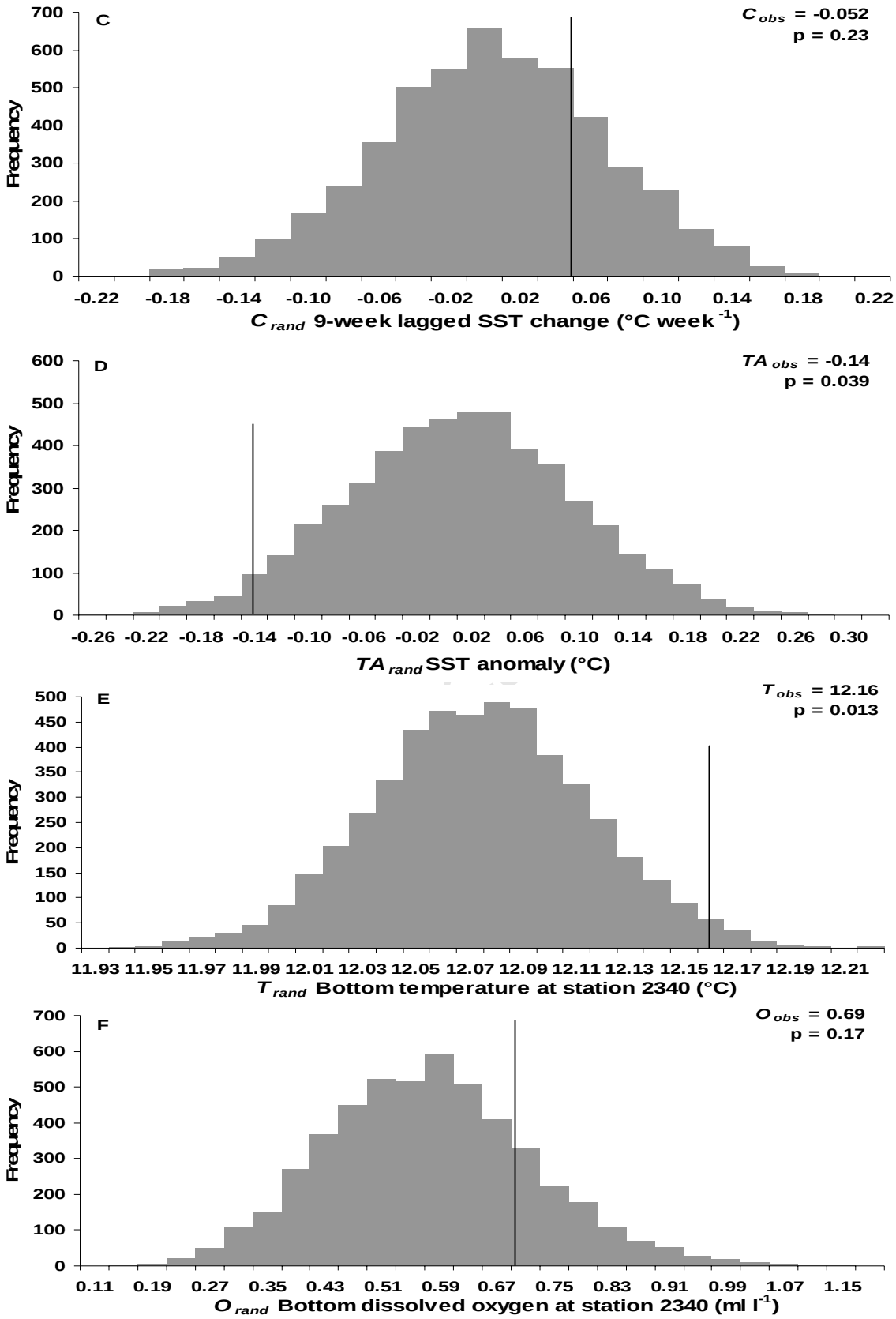

Figure 6.8 Frequency distributions of test statistics resulting from the randomization test to determine temporal correlations between hake otolith translucent zone formation events and environmental covariates **C.** 9-week lagged SST change, **D.** SST anomalies at the 23°S block, **E.** bottom temperature and **F.** bottom dissolved oxygen at station 2340. All covariates were lagged to translucent zone formation events by 3 weeks (unless otherwise stated). Vertical lines show the positions of C_{obs}, TA_{obs}, T_{obs} or O_{obs} on each distribution.

Investigating the significant correlations of translucent zone formation events with warm bottom temperatures in more detail, shows that events occurred at the minimum and maximum bottom temperatures measured, but warm temperatures outweighing the cold temperatures (Fig. 6.9), which brought the test statistic to a high value of 12.16°C (Fig. 6.8E).

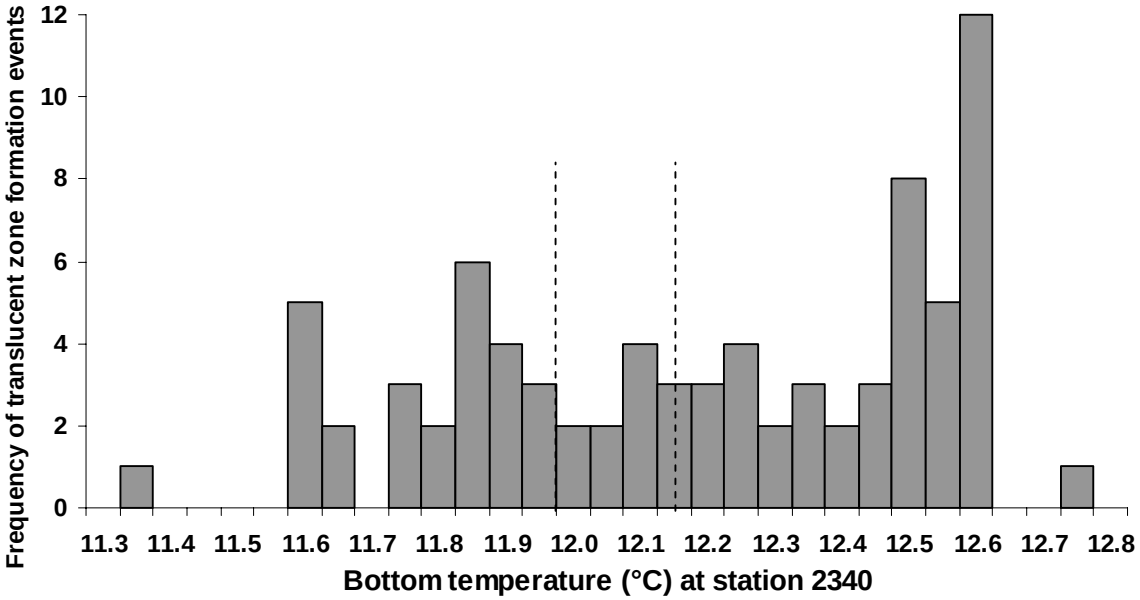

Figure 6.9 Frequency distribution of the bottom temperature at station 2340 (off Walvis Bay at 144 m bottom depth) measured during the 80 weeks of translucent zone formation events. Dashed lines indicate the 95 % confidence intervals of the randomization test (Fig. 6.8E).

6.5. Discussion

This chapter demonstrates a first step towards decoupling the influences of different variables, which are currently available with this dataset, on translucent zone formation of *M. capensis*. Translucent zone formation was always most closely associated with fish length. It also showed differences in timing (per fish length) between areas as well as between cohorts. Area had the strongest influence on timing of translucent zones or additional translucent zones, the general trend being that number of translucent zones per fish length increased from south to north along the Namibian coast. In Chapter 5 it was shown that *M. capensis* "moving" from south to north coincided with (the fish lengths of) translucent zone formation on their otoliths. This would explain why fish caught in the north should have one additional translucent zone to fish (of the same length) caught in the south.

However, in this chapter it was shown that fish caught in the north consistently had at least two additional translucent zones per cm fish length compared to fish caught in the south (Fig. 6.2a). This means that once fish are in the north more translucent zones form in addition to the ones formed at northward migration, which presumably only occurs once in the lifetime of the fish (Chapter 5).

A method for routine annual age determination is described in Chapter 4. Figure 4.9 shows a higher variation of length-at-age for fish from the 2005 survey compared to fish from the 2002 survey, especially for fish older than 4 years. It is possible that this variability is caused by area-specific sampling differences between the two years. Assigning ages by translucent zone diameter measurements would improve the accuracy of age determination of older fish (see Fig. 4.9b). However, the presence of each translucent zone is usually most strongly related to fish length (see Appendix 6.2, Table A6.2b). Given this, and given the importance of finding the optimum time-required- to-accuracy-needed trade-off for age determination, and given that age groups above 4 years carry a negligible weight in the stock assessment model fitting (see Chapters 4 and 7), the simpler age determination method should still be preferred. This means that fish need not be separated by area for age determination at this stage.

Although Chapter 5 showed that inshore-offshore migration of *M. capensis* coincided with translucent zone formation on their otoliths (Fig. 5.9a), there was not enough variation in the GLM explained by the position of the shelf (depth category) on which fish were captured. However, depth category usually ranked second or high in the model selection table (Appendix 6.2, Table A6.2a). Influences of the depth category are probably contained within the area influences of predicting presence of translucent zones (per cm fish length) in the GLM. The double shelf-break is more pronounced in northern and central Namibia, while the continental shelf is much narrower in southern Namibia (Fig. 2.1; Monteiro *et al.*, 2005; van der Plas *et al.*, 2008); and *M. capensis* are usually found closer inshore in the south. Morales-Nin *et al.* (1998) ascribe some of the variability in zone formation of *M. merluccius* to differences in mobility between males and females and individuals migrating in and out of different areas causing additional translucent zones to be formed. This could be the case for *M. capensis* found in northern Namibia; forming

additional translucent zones due to an increased mobility as a result of a wider continental shelf in the north. To decouple the influences of area and depth, following from Chapter 5 and this chapter, a more detailed sampling approach is needed with a larger sample of otoliths from all areas and all depths. It would also be a great advantage to follow specific depths and temperatures *M. capensis* are exposed to by using data storage tags, similar to those used for a study on Atlantic *G. morhua* (Hüssy *et al.*, 2010). In addition, it is recommended that diet and nutritional condition of *M. capensis* be linked with areas and depth (for example by looking at depth- and area-specific condition factor) and ultimately with translucent zone formation.

There was a 6-week lag from daylight duration (peak on 21 December) to SST (peak on 8 February) (Fig. 6.7). This indicates that SST is forced (directly) by solar heating and (indirectly) by season. The wind-driven upwelling cycle in the northern Benguela diminishes to reach a minimum in autumn (February). The maximum SST is therefore reached as upwelling diminishes. Maximum bottom temperatures are reached by 25 March. The upwelling cycle starts again in winter and reaches a peak with minimum temperatures in spring (SST minimum 10 August, Fig. 6.6). When upwelling conditions are at their peak in August–September, the maximum area (up to 400 km along the Namibian coast) is influenced by upwelled water (Campillo-Campbell and Gordoa, 2004). The minimum bottom temperatures reached by 24 September (Fig. 6.6) are then probably also caused by the upwelling peak in spring, upwelling also affecting the water up to a depth of 250 m (Stander, 1967). Temperature anomalies are then forced by wind-driven upwelling and differences between years driven by the differences in onset and intensity of upwelling (Bartholomae and van der Plas, 2007).

The errors / smoothing out of variability introduced with back-calculation of translucent zone formation dates are (1) smoothing out the TL-OD variability between fish (2) assuming constant growth rates for all fish in all areas in all years and seasons and (3) assuming constant growth rates between translucent and opaque zones. The back-calculated dates would therefore be more variable between individuals and possibly extend in both directions (Szedlmayer and Beyer, 2011),

but the general comparisons between cohorts could still be made as the same simplifying assumptions were made for all.

The 23°S latitude shows a difference of less than three hours between maximum and minimum daylight duration (Fig. 6.6). This is a small difference compared to higher latitudes, where the effects of daylight duration on translucent zone formation may be more applicable (e.g. Szedlmayer and Beyer, 2011). So it is no surprise that translucent zone formation was not temporally correlated with daylight duration (Fig. 6.8A). There was no temporal correlation between translucent zone formation events and oxygen conditions (Fig. 6.8C) or SST, or SST anomalies or SST change (Fig. 6.8C) marking the "onset" of events.

It is not clear whether growth rates of young fish are slower in months in which translucent zones are formed as the length-frequency distribution data (Figs 4.1 and 4.2) and growth curve comparison data (Fig. 2.7) were too coarse and did not span a long enough continuous time period for one cohort to calculate season-specific growth rates. The optimum growth temperature of *M. capensis* is also not known. However, their preferred temperature range is 4–12°C (Inada, 1981). The preferred temperature has been shown to be a good predictor of the optimum temperature for growth (Jobling, 1981; McCauley and Casselman, 1981). This means that not only cold temperatures, but also temperatures warmer than 12°C could result in reduced growth rates (due to reduced feeding and possibly reduced activity) of *M. capensis*. Metabolic stress, for example as resulting from reduced feeding, may be more pronounced at warm temperatures (Hüssy and Mosegaard, 2004; Hüssy *et al.*, 2004). This may be a reason for translucent zones being formed at extremely warm as well as extremely cold temperatures (Fig. 6.9), but showing a significant temporal correlation with warm temperatures (Fig. 6.8E). Generally two translucent zones tend to be formed in summer/autumn and one in winter/spring (Fig. 6.3; Chapter 4), and so generally more events occur during the warmer periods (February to June).

Given that translucent zones form more frequently during periods of warm temperatures, and the northern latitudes of Namibia generally showing SSTs of at least four degrees higher than at 23°S (Fig. 6.4), it is possible that warmer

temperatures in the north cause more translucent zone formation "events", hence more translucent zones per fish length (Figs 6.1 and 6.2a). Since translucent zone formation events were also linked with the lowest and highest temperatures, extreme and variable conditions would result in more translucent zones being formed. Northern Namibia is generally exposed to more variable conditions. Fig. 6.4 shows that there is a 12°C difference between minimum and maximum SSTs at 17°S, and only an 8°C difference between minimum and maximum SSTs from 23°S and southwards. The reason for this is that northern Namibia is affected first and more often by the intrusion of the Angola-Benguela Front (ABF), the zone where the nutrient-poor water from the Angola-current meets the nutrient-rich northward-flowing Benguela current (Shannon, 1985). Autumn is often marked with intrusion of highly saline and warm water mixed with the cold, less saline upwelled South Atlantic Central Water (Stander, 1976; Shannon, 1986). The ABF can move northwards and further southwards in certain years, often affecting northern Namibia, sometimes central Namibia, but very seldom southern Namibia, where consistent upwelling usually prevails (Batholomae and van der Plas, 2007). Warm SSTs (> 16°C) usually show a higher variability of bottom temperatures (Fig. 6.5), meaning that a higher variability of bottom temperatures is expected in northern Namibia. The temperature variability increasing from the south to the north of Namibia could be another reason for translucent zone formation events increasing from south to north of Namibia. Pilling *et al.* (2007) showed that a narrower translucent zone was formed in warmer years in North Sea *G. morhua*, and growth started up to a month earlier. It is possible that the *M. capensis* in northern Namibia have narrower translucent zones but formed more frequently than on fish in southern Namibia. No difference in appearance (width or clarity) between winter/spring and summer/autumn translucent zones or those from fish from northern or southern Namibia were visible under the light microscope. However, chemical differences or physical differences that are not visible under the light microscope may exist between different zones and this warrants further study.

The area-specific timing of translucent zone formation may explain the continuous and overlapping "events" in Fig. 6.3. Apparent "secondary" events may be those of fish from the south, while the early events may generally pertain to fish from the north. However, the 2002 cohort generally showed formation of T3 and T4 zones on

the smallest fish (L_{50} of 15–25 cm) for the northern, central and southern areas (Fig. 6.1), while for fish larger than 45 cm, fish from the 2002 cohort had the fewest translucent zones (Fig. 6.2b). Even within each area, the cohorts showed differences in timing. The periods of "events" of T3 and T4 formation of the 2002 cohort were November–December of 2003, February–March of 2004 and May–June of 2004 (Fig. 6.3). This spanned an anomalously warm spring, an anomalously cool summer, and again an anomalously warm to variable period of SSTs with cool bottom temperatures, respectively (Figs 6.6 and 6.7). If translucent zones are formed at extreme temperatures, this could be the reason for the early / additional translucent zones being deposited on fish of the 2002 cohort over that period. However, the differences between maximum and minimum bottom temperatures were smaller than in other years over that period (Fig. 6.6). It is difficult to unravel temperature signals on such a large scale as reasons for (early) translucent zone formation additional to the regular biannual translucent zones in certain cohorts (Chapter 4). However, overall it seems there are no specific temperature cues to translucent zone formation.

In line with expectation from theory, Baumann *et al.* (2006) showed that Baltic sprat *Sprattus sprattus* young-of-the-year could reach their maximum growth rates earlier (at younger ages) at higher temperatures. The opposite could be expected for translucent zone formation, i.e. that minimum growth rate or "translucent zone formation" would occur earlier at lower temperatures with *M. capensis*. However, no consistent link between the cohorts' individual timing and anomalous conditions in the particular years could be detected. This could be due to random variation, even within cohorts and within areas, following more specific localised conditions. Wilson *et al.* (2011) stated it was more difficult to explain within-sample variation of growth and first translucent zone formation of walleye pollock *Theragra chalcogramma* suggesting that even individuals could differ in their responses to the annual cycle. Another explanation could be that translucent zone formation of *M. capensis* is more closely linked to age and the individual cohorts' hatchdates, masked by differences in growth rates. Fish sampled of the same length could be older in some cohorts, and therefore having lived through more seasons, formed more translucent zones per cm fish length. These differences can only be decoupled with monthly area-specific length-frequency distributions, which would make it

possible to independently calculate somatic growth rates, and link these to translucent zone formation and other various events in the life history of the fish. In a recent paper investigating macrostructure of *M. polli* and *M. senegalensis* otoliths, Rey *et al.* (2012) concluded that translucent zone formation was related to a specific endogenous event (such as spawning), rather than a precise environmental event, partially concurring with results in this chapter. However, not enough variation of translucent zone formation per fish length was explained by fish maturity stage (Appendix 6.2, Table A6.2a). In Chapter 5, confirming earlier results by Assorov and Berenbeim (1983) and Kainge *et al.* (2007), hake exhibited two spawning periods, showing strong evidence for biannuality. It is possible that these periods are indirectly associated with their translucent zone formation. Admassu and Casselman (2000) showed that adult tilapia *Oreochromis niloticus* from Lake Awassa formed biannuli and also showed biannual recruitment. It is possible that there is an indirect link between periods of spawning and translucent zone formation. The link is not direct as sexually immature fish also form translucent zones and no significant link between mature fish and maturity stage was shown here. In fact, if the results of Singh *et al.* (2011) also pertain to northern Benguela *M. capensis*, none or very few of the fish investigated here should be sexually mature.

An indirect link with biannuality may be predominant in tropical (23°N–23°S) and south latitude temperate (23°–45°S) regions, as shown in a summary of 23 studies by Beckman and Wilson (1995) showing a peak in translucent zones in (December), April, and June–August (tropical regions) and February–March (temperate regions). The northern Benguela spans both of these regions, by the definition of Beckman and Wilson (1995), the warm tropical northern part of Namibia and the cold temperate southern part, with the added effect of seasonality and variability of a wind-driven upwelling system. The conditions specific to the northern Benguela may also cause the biannuality linked with minimum and maximum temperatures (February–March and August–September).

There are a few examples for which differences in seasonality between the northern and southern Benguela have been documented. For example, continuous breeding activity throughout the year has been observed in African penguins in Namibia

(Kemper, 2006a), but with distinct biannual moult peaks in summer (December–January, secondary peak) and autumn (April–May, primary peak). This is much in contrast with monomodal moult peaks of penguins from other regions, including the southern Benguela (Kemper, 2006b). The cues for this could be first endogenous, when adapted to the Namibian specific temperate environment, while the individual variation and responses could be different and could be a response to localised environmental variability.

The absence of a link between translucent zone formation and a temperature change, or other environmental signals was recently confirmed by Hüssy (2010), who used daily increments to test patterns in opacity and translucency on Baltic *G. morhua* otoliths, and showed that there was no link between translucency and cold water temperatures in a system with far more pronounced seasonality than the northern Benguela. Other authors have also shown that there is no relationship between temperature and zone formation (e.g. Nelson and Manooch, 1982; Natanson, 1993; Brouwer and Griffiths, 2004; Szedlmayer and Beyer, 2011). This, and the fact that translucent zones were most significantly predicted by fish length (see Appendix 6.2, Table A6.2b) may mean that, in line with thinking of Chapter 5, ICSEAF (1983), Campana (1984) and Geffen and Nash (1995) that translucent zone formation on *M. capensis* otoliths is possibly driven by internal rhythms that may be linked to biannuality. Variability within these rhythms is caused by environmental variability, such as increased temperature variability in northern Namibia, which can cause formation of additional translucent zones on *M. capensis* otoliths. However, further research on nutritional condition and the fish' response to specific temperature conditions is needed. Rearing experiments to test specific responses to specific conditions are not possible at this stage for hake. However, it is possible to study the environmental conditions they are exposed to with data storage tags similar to those used for a study on Atlantic *G. morhua* (Hüssy *et al.*, 2010), and this is recommended for *M. capensis*.

6.6. Conclusions and recommendations

This chapter is a first attempt to link translucent zone formation on *M. capensis* otoliths with other important events in their life history using statistical models. It illustrates the need for more detailed specific data collection (especially seasonal conditional status, otolith zonation and data storage tags) for further linking of these events. Fish caught in the north of Namibia (< 20.5°S) consistently showed earlier formation of translucent zones and therefore more translucent zones at the same fish lengths as fish from the central and southern areas. Differences between timing of translucent zone formation and cohorts were detected for the T1, T3 and T4 zones.

Events of translucent zone formation were significantly correlated with periods of warm bottom temperatures, but took place at times of minimum and maximum temperatures. The differences between areas could be linked to warmer water or higher variability in temperature or a wider shelf in northern Namibia compared to southern Namibia. While it is very difficult to tease apart the exact influences of environmental or any other variables on translucent zone formation, it is clear that the primary association is the length of the fish.

The variability of number of translucent zones at fish length between northern and southern Namibia should not influence the methods for routine age determination described in Chapter 4.

Appendix 6.1

Namibian *M. capensis* back-calculated fish total length (cm) (Equation 6.3) for each translucent zone one to six (T1–T6) compared between female (F) and male (M) fish. The plots show means with 95 % confidence intervals and sample sizes of each (n). The plot was generated in R version 2.9.1 (R Development Core Team, 2009) using the library 'gplots' (Warnes *et al.*, 2009).

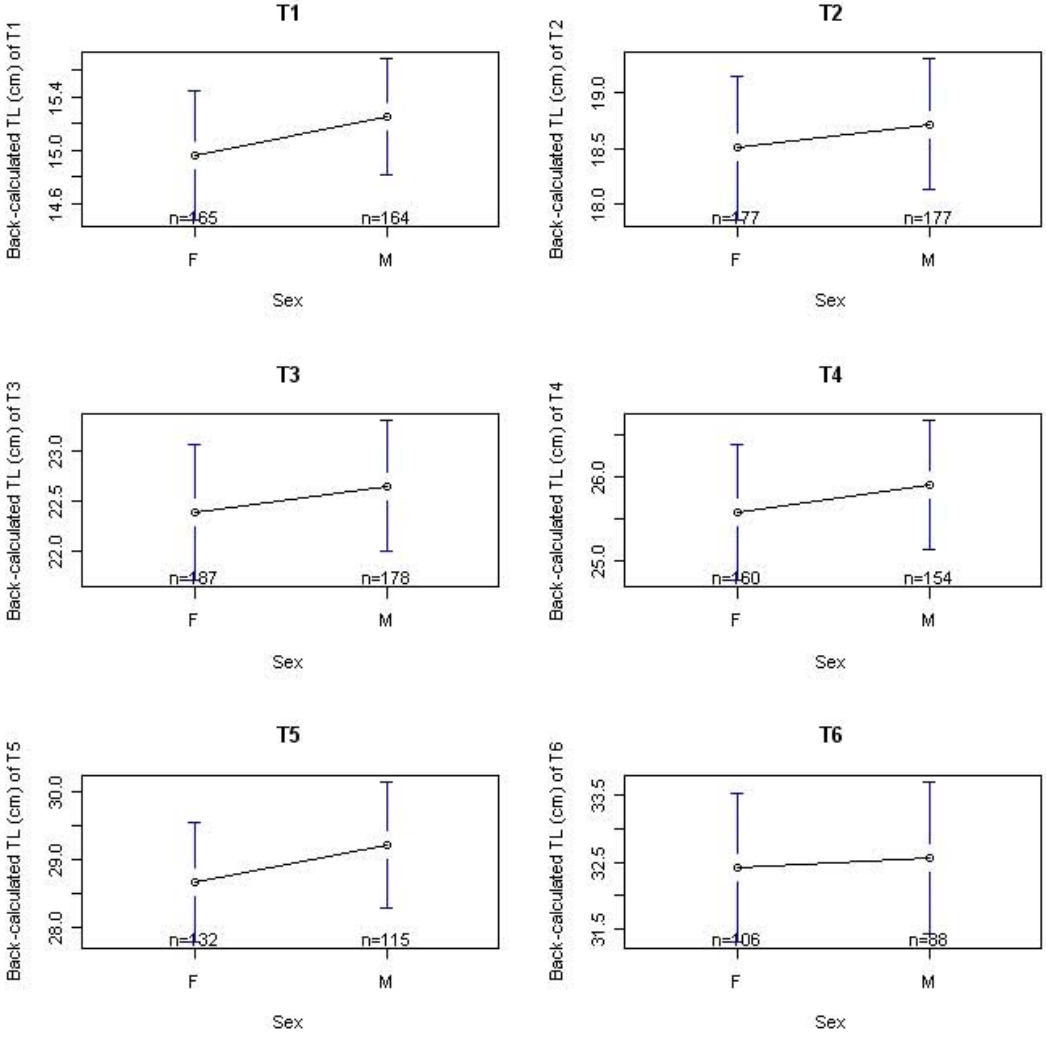

Appendix 6.2

Table A6.2a Comparisons of Binomial Generalised Linear Models (GLM) to predict the presence of each translucent zone **i.** T1, **ii.** T2, **iii.** T3, **iv.** T4, **v.** T5 and **vi.** T6 on *M. capensis* otoliths based on fish length in cm (TL), cohort (three levels), area (three levels), depth category (DepthCat, three levels) and maturity stage (Stage, three levels), n = 451. Candidate models include the global model (Equation 6.1) with five factors and 12 (of the best by the step function) reduced models. Models are ranked by Akaike's information criterion (AIC). K is the number of parameters, including the intercept. Support for each model is expressed relative to the best model (ΔAIC= difference between model AIC and best model AIC). "No conv" means the global model did not converge.

i. T1

Number of effects	Candidate models (model structure)	K	AIC	ΔAIC
3	**TL+Cohort+Area**	**6**	**80.2**	
4	TL+Cohort+Area+DepthCat	8	82.7	2.5
4	TL+Cohort+Area+Stage	8	84.2	4.0
5	TL+Cohort+Area+DepthCat+Stage	10	86.7	6.5
2	TL+Cohort	4	93.7	13.5
3	TL+Cohort+DepthCat	6	97.3	17.1
2	TL+Area	4	100.3	20.0
4	TL+Cohort+DepthCat+Stage	8	101.3	21.1
3	TL+Area+DepthCat	6	102.0	21.8
4	TL+Area+DepthCat+Stage	8	106.0	25.7
1	TL	2	106.5	26.3
2	TL+DepthCat	4	109.3	29.0
2	TL+Stage	4	110.4	30.2

ii. T2

Number of effects	Candidate models (model structure)	K	AIC	ΔAIC
2	**TL+Area**	**4**	**19.9**	
3	TL+Cohort+Area+DepthCat	8	20.6	0.8
4	TL+Cohort+Area+Stage	8	24.2	4.4
1	TL	2	26.0	6.1
2	TL+Cohort	4	27.5	7.6
3	TL+Cohort+Area+DepthCat	6	29.5	9.7
2	TL+Stage	4	29.8	9.9
4	TL+Cohort+DepthCat+Stage	8	32.9	13.0
2	TL+DepthCat	4	255.9	236.0
5	TL+Cohort+Area+DepthCat+Stage	10	No conv	
3	TL+Area+DepthCat	6	No conv	
4	TL+Cohort+Area+DepthCat	8	No conv	
4	TL+Area+DepthCat+Stage	8	No conv	

Table A6.2a (continued)

iii. T3

Number of effects	Candidate models (model structure)	K	AIC	ΔAIC
3	**TL+Cohort+Area**	**6**	**97.4**	
4	TL+Cohort+Area+Stage	8	100.8	3.5
2	TL+Cohort	4	100.9	3.6
4	TL+Cohort+Area+DepthCat	8	101.1	3.7
4	TL+Cohort+DepthCat+Stage	8	104.5	7.1
5	TL+Cohort+Area+DepthCat+Stage	10	104.5	7.1
3	TL+Cohort+Stage	6	104.5	7.1
3	TL+Area+Stage	6	107.8	10.4
2	TL+Area	4	108.4	11.0
4	TL+Area+DepthCat+Stage	8	108.9	11.6
2	TL+Stage	4	109.5	12.1
1	TL	2	111.4	14.0
2	TL+DepthCat	4	114.8	17.5

iv. T4

Number of effects	Candidate models (model structure)	K	AIC	ΔAIC
3	**TL+Cohort+Area**	**6**	**290.4**	
4	TL+Cohort+Area+Stage	8	293.4	3.0
4	TL+Cohort+Area+DepthCat	8	294.0	3.5
2	TL+Area	4	296.4	5.9
5	TL+Cohort+Area+DepthCat+Stage	10	296.9	6.5
3	TL+Area+Stage	6	297.7	7.2
2	TL+Cohort	4	298.3	7.8
3	TL+Cohort+Stage	6	300.2	9.8
4	TL+Area+DepthCat+Stage	8	300.7	10.3
1	TL	2	301.7	11.3
4	TL+Cohort+DepthCat+Stage	8	302.2	11.8
2	TL+Stage	4	303.3	12.8
2	TL+DepthCat	4	304.6	14.1

v. T5

Number of effects	Candidate models (model structure)	K	AIC	ΔAIC
2	**TL+Area**	**4**	**318.4**	
3	TL+Cohort+Area	6	320.1	1.8
3	TL+Area+DepthCat	6	320.6	2.3
4	TL+Cohort+Area+DepthCat	8	322.5	4.1
4	TL+Area+DepthCat+Stage	8	322.7	4.4
4	TL+Cohort+Area+Stage	8	322.8	4.4
5	TL+Cohort+Area+DepthCat+Stage	10	325.3	7.0
2	TL+DepthCat	4	327.2	8.8
1	TL	2	330.4	12.0
3	TL+Cohort+DepthCat	6	330.5	12.2
2	TL+Stage	4	332.8	14.5
4	TL+Cohort+DepthCat+Stage	8	333.5	15.1
2	TL+Cohort	4	333.6	15.2

Table A6.2a (continued)

vi. T6

Number of effects	Candidate models (model structure)	K	AIC	ΔAIC
2	**TL+Area**	**4**	**325.0**	
3	TL+Area+DepthCat	6	328.2	3.2
3	TL+Cohort+Area	6	328.5	3.5
4	TL+Cohort+Area+DepthCat	8	331.3	6.3
4	TL+Area+DepthCat+Stage	8	331.5	6.5
4	TL+Cohort+Area+Stage	8	331.6	6.6
5	TL+Cohort+Area+DepthCat+Stage	10	334.3	9.3
1	TL	2	339.0	14.0
2	TL+DepthCat	4	339.6	14.6
2	TL+DepthCat	4	339.6	14.6
3	TL+Cohort+DepthCat	6	340.5	15.5
2	TL+Cohort	4	340.6	15.6
4	TL+Cohort+DepthCat+Stage	8	343.2	18.2

Table A6.2b Parameter estimates with standard error (SE) and p-values (Pr(>|z|)) of models with lowest AIC (Table A6.2a) for a binomial GLMs predicting the presence of translucent zone **i.** T1, **ii.** T2, **iii.** T3, **iv.** T4, **v.** T5 and **vi.** T6 on *M. capensis* otoliths based on fish length in cm (*TL*), Cohort (1996 base level) and Area (Central area base level, North = N, South = S). Parameter coefficients with p-values < 0.05 are highlighted (bold).

i. T1

Term	Estimate	SE	Pr(>|z|)
Intercept	-0.430	3130.1	1.00
TL	**0.997**	**0.286**	**0.000484**
Cohort 1998	-11.7	3130	0.997
Cohort 2002	-8.51	3130	0.998
Area N	19.1	3120.8	0.995
Area S	**-2.27**	**0.838**	**0.00688**

ii. T2

Term	Estimate	SE	Pr(>|z|)
Intercept	**-17.4**	**4.99**	**0.000496**
TL	**1.07**	**0.292**	**0.000248**
Area N	**5.35**	**2.47**	**0.0299**
Area S	-0.216	3.37	0.949

iii. T3

Coefficients	Estimate	SE	Pr(>|z|)
Intercept	**-11.5**	**2.30**	**0.000001**
TL	**0.607**	**0.0962**	**<0.000001**
Cohort 1998	-1.30	0.788	0.0994
Cohort 2002	1.89	1.07	0.0760
Area N	1.37	0.920	0.138
Area S	-1.15	0.738	0.118

iv. T4

Coefficients	Estimate	SE	Pr(>|z|)
Intercept	**-5.82**	**0.727**	**<0.000001**
TL	**0.224**	**0.0223**	**<0.000001**
Cohort 1998	-0.269	0.411	0.513
Cohort 2002	**0.861**	**0.408**	**0.0350**
Area N	**1.13**	**0.424**	**0.00790**
Area S	-0.329	0.354	0.351

v. T5

Coefficients	Estimate	SE	Pr(>|z|)
Intercept	**-6.21**	**0.611**	**<0.000001**
TL	**0.206**	**0.0186**	**<0.000001**
Area N	**0.848**	**0.357**	**0.0176**
Area S	**-0.720**	**0.347**	**0.0377**

vi. T6

Coefficients	Estimate	SE	Pr(>|z|)
Intercept	**-7.39**	**0.726**	**<0.000001**
TL	**0.204**	**0.0192**	**<0.000001**
Area N	**1.24**	**0.352**	**0.000432**
Area S	-0.265	0.354	0.453

Appendix 6.3

Regression of 6-week-lagged bottom temperature at station 2340 (23°S line, 40 nautical miles offshore, 144 m average bottom depth) against average sea surface temperature in the 23° block in the period 1996 to 2006.

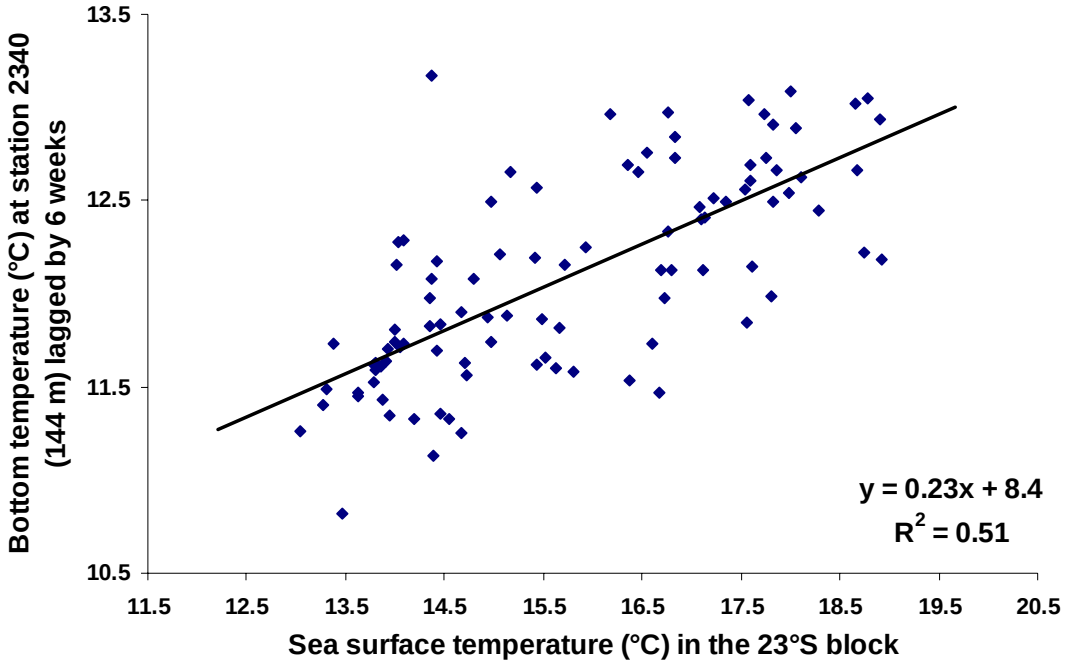

CHAPTER 7
Synthesis and conclusions

In this thesis it was shown that growth rates, hatchdates, year-class strength and age validation of juvenile *M. capensis* can be studied using otoliths recovered from Namibian fur seal scats (Chapters 2–4). This can be done because the diet of fur seals in Namibia mainly consists of *M. capensis* (Mecenero *et al.*, 2006a). This is unique to Namibia because of the low abundance of sardine and other small pelagic fish species, which are usually preferred by fur seals as a food source, in the northern Benguela (Heymans *et al.*, 2004; van der Lingen *et al.*, 2006).

Advances were made towards growth rate estimation and age validation of *M. capensis* in Namibia. The synthesis and recommendations for the Namibian routine age determination programme as well as possible consequences of the fast growth rates to the stock assessment are discussed in Section 7.1. In addition, progress was made with respect to understanding the timing of spawning, distribution, spawning locations, alongshore migration and inshore-offshore migration of *M. capensis*. Together with environmental variables, these were related to translucent zone formation on *M. capensis* otoliths and are synthesized in Section 7.2.

7.1 Age and growth of Namibian *M. capensis* and the possible consequences for fisheries research and stock assessment

The first overall objective of this thesis was to calculate growth rates of *M. capensis* using available data other than that obtained from age information on otoliths. It was shown that *M. capensis* juveniles grow faster than previously thought (Chapter 2). This was supported by survey and commercial length-frequency data of adult *M. capensis* (Chapter 4). Juveniles (Chapter 2) as well as adults (Chapter 4) showed growth rates twice as fast as most recently described for this species (Wilhelm *et al.*, 2007), but comparable to those recently described for *M. merluccius* (de Pontual *et al.*, 2006; Piñeiro *et al.*, 2007) and *M. gayi* (Goicochea *et al.*, 2010). The number of translucent zones per cm fish length was similar to that described recently for *M. senegalensis* (Rey *et al.*, 2012).

This identifies hakes in general and *M. capensis* in particular, as more r-selected life history strategists compared with other gadoids.

The second objective was to validate translucent zone formation on otoliths and to describe a new routine age determination method for *M. capensis*. The underlying hypothesis that *M. capensis* translucent zones would be formed once per annum after the first annulus was shown not to hold. Translucent zones were formed in the first summer and subsequent winter/spring and summer/autumn of the first 1.5 years of life of *M. capensis* (Chapter 3). After that, translucent zone formation occurred at least twice per year in winter/spring, autumn and summer (Chapter 4). Ages had thus been previously overestimated by using the method of counting one translucent zone per year. A new method of annual age determination was described and recommendations made for conversion of old to new age data (Chapter 4). The recommendations for otolith sampling and methods for Namibian hake routine age determination following from Chapters 2–5 are summarised in Table 7.1, adding an overall recommendation for *M. paradoxus* research and monitoring work to be done.

Table 7.1 Summary of recommendations for age validation method, age determination methods, age sampling for management purposes of Namibian *M. capensis*. See Chapters 2 to 5 for details.

1. Edge analysis should not be used as an age validation method, even for young fast-growing fish.
2. The simplest age determination method should be used for routine annual age determination of *M. capensis*. Three steps should be followed for this:
   a. Under the assumption of the present growth rates continuing, the first visible translucent zone at ≥ 7.5 mm diameter should be assigned as the first annulus (age group 1), regardless of the presence or number of translucent zones present before the annulus.
   b. The number of translucent zones after the assigned age group 1 should be counted. This count should be divided by two.
   c. Age group = Integer of [1 + (count after assigned age group 1 / 2)].
   d. Growth rates, measurements and age determination methods should be re-evaluated once the stock recovers to sustainable levels in the future.
3. For the purpose of stock assessment, new input age data should be obtained using the conversion presented in Table 4.7.
4. The current method of otolith sampling should be sufficient to cover the entire *M. capensis* stock. Sampling currently takes 10 fish per cm-length-class in each of the northern and southern legs of each survey. Even if northern and southern aggregations show differences in biannual ages, this sampling method covers each area sufficiently to be separated after age determination. No area-specific age determination adjustments should be made at this stage.
5. *M. paradoxus* age validation and age determination research and monitoring should be conducted.

The consequences of fast growth rates and biannual translucent zone formation of *M. capensis* in Namibia for the recovery and productivity of the stock are investigated in the final objective of this thesis. A simple age-structured production model (ASPM) was used for that purpose. It is expected that a fast-growing *M. capensis* stock would be able to withstand higher fishing mortality because of the implied higher natural mortality or stock productivity. More K-selected species such as slow-growing *M. capensis* would take longer to recover once fished down (Adams, 1980).

Input parameters to the ASPM that would be affected by fast growth rates, and therefore smaller lengths-at-age, were calculated: proportions mature, weight-at-age and selectivity-at-age as outlined in Table 7.2. The slow growth rate data (Table 7.2, column A) were taken from Wilhelm *et al.* (2007) and are used in the current Namibian hake assessment (Kirchner, 2010; Kirchner *et al.*, 2011). The expected length (L_a) at age group a was calculated using the von Bertalanffy growth function (VBGF), from Wilhelm *et al.* (2007) for slow growth, and from Chapters 2 and 4 for fast growth:

$$L_a = L_\infty \left[1 - e^{-K(a - t_0)}\right] \qquad (7.1),$$

where a is age group a (years), L_∞ is the asymptotic length (cm), K is the growth coefficient (years^{-1}) and t_0 is the theoretical age (years) at length zero (Table 7.2). Weight (W) (g) at age a was calculated from the length-at-age using the weight-length equation:

$$W = a' (L_a)^{b'} \qquad (7.2),$$

where a' and b' are constants calculated for Namibian *M. capensis* from research survey data (Wilhelm *et al.*, 2007). Mid-year lengths were calculated by adding 0.5 years to age group a, and mid-year weights calculated from mid-year-lengths using Equation 7.2 (Table 7.2). Proportion mature at age-group a (P_a) was calculated for slow growth data using the logistic function (ogive):

$$P_a = \frac{1}{1 + e^{\frac{-(a - a_{50})}{\delta}}} \qquad (7.3),$$

where a_{50} (years) is the age at which 50 % of the fish are sexually mature and δ is the width of the maturity ogive (years). The maturity-at-age parameters a_{50} (1.67 years) and δ (0.728 years) (Wilhelm *et al.*, 2007) were converted to maturity-at-length parameters L_{50} (cm) and δ (cm) (Table 7.2), and these were used to convert the

proportions mature from length-at-age data.

The commercial selectivity-at-age (proportion of fish selected by the fishery in age group a (S_a)), was estimated by fitting a two-stage selectivity curve (Equations 7.4a and b) to the model-estimated commercial selectivity (1990–2000, Kirchner, 2010). This is (a) a logistic function, modified to include (b) a decrease in selectivity at older ages:

$$S_a = \frac{1}{1 + e^{\frac{-(a - S_{50})}{\Delta}}} \quad (7.4a),$$

where S_{50} is the age at 50 % selectivity (years) and Δ is the width of the ascending part of the logistic ogive (years). S_a was modified to include a decrease in selectivity from age group a_{decr} onwards:

$$S_a = S_a e^{-v(a - a_{decr})} \quad (7.4b),$$

where v is the rate of decrease in selectivity with age for fish older than a_{decr} (Rademeyer, 2003; Kirchner, 2010), with a_{decr} set at 4 years (Kirchner, 2010). S_{50}, Δ and v were estimated at 2.5 years, 0.44 years and 0.10 year^{-1} respectively. These were converted to selectivity-at-length parameters, using the length at mid-year age because commercial catches were removed in the model in the middle of the year (see Table 7.5). Selectivity-at-length parameters (Table 7.2, column A) were used to convert the proportions mature from length-at-age for the fast growth data (Table 7.2, column B).

Table 7.2 shows that because of the differences in length-at-age between the slow growth (A) and the fast growth (B) populations, weight-at-age (g) almost doubles for slow compared with fast growth data, from age group 3 years onwards. Maturity increases by about 10 % in age groups 2 and 3, but decreases by 5–7 % in age groups 0 and 1, and the age at full selectivity ($S_a \sim 1$) changes from age group 4 to 3 years from slow to fast growth inputs.

The maximum age (that fish survive to) was changed from 7 to 5 years from the slow growth (A) to the fast growth model (B).

All of these parameters would affect the stock dynamics, sometimes in a trade-off. The potential effects of these on a stock assessment model were tested.

Table 7.2 Differences in input parameters used for age-structured population models of Namibian *M. capensis* assuming **A.** slow growth rates (Wilhelm *et al.*, 2007) and **B.** fast growth rates (Chapter 4).

	A. *M. capensis* - slow growth					**B. *M. capensis* - fast growth**				
Parameters	**Length (cm)**	**Begin-year weight (g)**	**Mid-year weight (g)**	**Proportion mature**	**Selectivity (proportion)**	**Length (cm)**	**Begin-year weight (g)**	**Mid-year weight (g)**	**Proportion mature**	**Selectivity (proportion)**
L_∞ **(cm)**	149					134				
K **(years^{-1})**	0.0609					0.127				
t_0 **(years)**	-1.28					-0.049				
a'		0.0051	0.0051				0.0051	0.0051		
b'		3.08	3.08				3.08	3.08		
$L_{50\,(cm)}$				24.8					24.8	
δ **(cm)**				5.21					5.21	
S_{50} *(cm)*					30.7					30.7
δ **(cm)**					3.19					3.19
v					45.9					45.9
L_{decr}					0.0192					0.0192
Age (years)										
0	11.2	8.8		0.07		0.8	0.0		0.01	
0.5	15.4		23.1		0.0080	9.0		4.5		0.0011
1.0	19.4	47.2		0.26		16.7	29.8		0.17	
1.5	23.3		83.0		0.088	23.9		90.1		0.11
2.0	27.1	131.9		0.61		30.7	194.1		0.76	
2.5	30.8		195.0		0.50	37.1		346.5		0.88
3.0	34.3	273.3		0.86		43.0	548.7		0.97	
3.5	37.8		367.1		0.90	48.6		799.7		0.94
4.0	41.1	476.8		0.96		53.9	1096.9		1.00	
4.5	44.4		602.6		0.99	58.8		1436.5		0.78
5.0	47.5	744.4		0.99		63.4	1813.9		1.00	
5.5	50.6		902.0		0.91	67.8		2224.3		0.66
6.0	53.5	1074.9		1.00						
6.5	56.4		1262.8		0.82					
7.0	59.2	1465.2		1.00						
7.5	61.9		1681.3		0.73					

A slow-growing *M. capensis* stock (Case A) was compared with a fast-growing *M. capensis* stock (Case B) using the different growth rates, maximum age groups, proportions mature, weight-at-age and selectivity-at-age parameters as outlined in Table 7.2. Natural mortality (*M*) values were fixed for both cases at the age-dependent natural mortality values used in the current base case assessment in Namibia (Table 7.3; Kirchner, 2010).

Table 7.3 Natural mortality (*M*) at age fixed for both cases A and B (Kirchner, 2010).

Age group	*M*
0	1.424
1	0.712
2	0.570
3	0.500
4	0.456
5	0.424
6	0.400

A simple ASPM (Hilborn, 1990) was applied using data and equations outlined in Tables 7.4 and 7.5, respectively. In order to get the models to fit, no plus-groups were used (Table 7.5). This means it was assumed that after the maximum age group *m*, all fish would die, which is different to previous stock assessment models on Namibian hake (Rademeyer, 2003; Kirchner, 2010). The maximum age group *m* was changed from 7 to 5 years from Case A to Case B.

The catchability coefficient *q*, steepness parameter *h* and pristine spawning stock biomass K^{Sp} were estimated for both cases. The current estimated spawning stock biomass B^{Sp}_{2011}, depletion level in 1990 B^{Sp}_{1990}/K^{Sp}, current depletion level B^{Sp}_{2011}/K^{Sp} and the rate of recovery by 2016 (short-term) assuming no catch for the next five years, $B^{sp}_{2016}/B^{sp}_{2011}$, were compared between both cases.

Table 7.4 Input data used for the simple ASPM of Namibian *M. capensis*. Catch is from the Namibian total landings of hake (MFMR, Namibia) and the observed catch-per-unit effort (CPUE) series is based on estimates of Kirchner (2010).

	Catch ('000 tonnes)	**Observed CPUE (tonnes h^{-1})**
1964	47.9	4500
1965	193.2	4327
1966	334.6	4036
1967	394.4	3743
1968	630.4	3315
1969	526.7	3018
1970	627.2	2856
1971	595.2	2681
1972	820.1	2266
1973	668.0	1816
1974	514.6	1501
1975	488.2	1488
1976	601.0	1495
1977	431.5	1455
1978	379.4	1429
1979	310.2	1404
1980	171.8	1396
1981	211.5	1333
1982	307.1	1210
1983	339.6	1288
1984	365.0	1622
1985	386.2	1736
1986	381.2	1656
1987	300.2	1584
1988	336.0	1416
1989	309.3	1146
1990	132.4	726
1991	56.1	795
1992	87.5	889
1993	108.0	883
1994	112.2	877
1995	130.4	771
1996	129.1	674
1997	116.6	676
1998	106.8	710
1999	157.9	662
2000	171.5	565
2001	174.1	478
2002	156.5	430
2003	189.3	376
2004	173.9	383
2005	158.1	455
2006	136.8	562
2007	125.5	601
2008	126.3	612
2009	130.0	634
2010	135.0	693

Table 7.5 Equations for the simple age-structured production model of *M. capensis* (Hilborn, 1990).

1. $N_{0,0} = R_0$

2. $R_0 = \dfrac{K^{Sp}}{\left(\sum_{a=0}^{m-1} p_a \cdot w_a \cdot e^{-M \cdot a}\right)}$

3. $N_{0,a} = R_0 \cdot e^{-M \cdot a} \qquad (a > 0)$

4. $N_{y+1,0} = R_{y+1}$

5. $N_{y+1,a+1} = \left(N_{y,a} e^{-M/2} - \sum C_{y,a}\right) e^{-M/2} \quad (a > 0)$

6. $C_{y,a} = N_{y,a} \cdot e^{-M/2} \cdot S_a \cdot F_y$

7. $F_y = \dfrac{Y_y}{\sum_{a=0}^{m} N_{y,a} \cdot e^{-M/2} \cdot S_a \cdot w_{a+1/2}}$

8. $EB_y = \sum_{a=0}^{m} w_{a+1/2} S_a N_{y,a} e^{-M/2}$

9. $R_y = \dfrac{B_y^{sp}}{\alpha + \beta(B_y^{sp})}$

10. $B_y^{sp} = \sum_{a=0}^{m} p_a w_a N_{y,a}$

11. $\varepsilon_y = \lambda n I_y - \lambda n (qEB_y)$

12. $\hat{\sigma}^2 = \sum_{n} \frac{1}{n} \left(\varepsilon_y\right)^2$

13. $-\lambda n L = \frac{n}{2}\left(\lambda n \sigma^2\right) + \frac{n}{2}$

Equations 1–3 denote initial conditions given initial equilibrium age structure (pristine levels, in 1963). Equations 4–5 reflect Pope's approximation to the more customary Baranov catch equations.

$N_{0,a}$ is the number of fish of age *a* at the start of year *0* (1963).

$N_{y,a}$ is the number of fish of age *a* at the start of year *y*.

R_y is the number of recruits at the start of year *y*, related deterministically to the spawning stock biomass (B_y^{sp}) by the Beverton-Holt stock-recruitment relationship (Equation 9).

B_y^{sp} is the spawning biomass at the start of year *y* (Equation 10).

M denotes the constant natural mortality rate of fish of all ages (input, Table 7.3).

$C_{y,a}$ is the number of fish of age *a* caught in year *y* (Equation 6).

m is the maximum age group considered

S_a is the age-specific commercial selectivity (for all fleets and gear combined, assumed to be constant over the years, input, Table 7.4).

F_y is the fully selected fishing mortality in year *y* (Equation 7).

Y_y is the total observed yield by weight in year *y* (input, Table 7.4).

$w_{a+1/2}$ is the mid-year weight of a fish of age *a* + ½ (input, Table 7.2).

EB_y is the model estimate of the mid-year exploitable ("available") biomass, calculated by converting the numbers-at-age into mid-year weights at each age and applying natural mortality for half the year (Equation 8).

α and β are spawning stock biomass-recruitment relationship parameters, with 0 recruitment variability assumed.

The stock-recruitment relationship (Equation 9) is re-parameterised in terms of the pristine (unexploited) equilibrium spawning stock biomass K^{sp} and the steepness parameter h of the stock-recruitment relationship, where
h is the fraction of pristine recruitment that results when spawning stock biomass drops to 20 % of its pristine level, with re-estimated stock-recruitment parameters

$\alpha = \frac{K^{sp}(1-h)}{4hR_0}$ and $\beta = \frac{5h-1}{4hR_0}$ (Francis, 1992; Haddon, 2001).

w_a is the begin-year weight of fish of age a (input, Table 7.2),

p_a is the proportion of fish of age a that are mature (input, Table 7.2),

h and K^{Sp} were estimated for both models (Table 7.5).

The model was fitted to the "Observed CPUE" abundance index (Table 7.4) data to estimate model parameters assuming that the observed abundance index is log-normally distributed about its expected value. Contributions of this series to the negative log-likelihood ($-\lambda nL$, Equation 13) are given by Equations 11 and 12, where

ε_y from $N\left(0,\left(\sigma_y\right)^2\right)$,

I_y is the abundance index for year y,

$\hat{q}E\hat{B}_y$ is the corresponding model estimate with EB_y being the model estimate of biomass (Equation 8) and $\hat{q}$ the catchability coefficient for the abundance index (estimated as a parameter).

n is the number of data points for the observed abundance index.

After substituting estimates of σ^2 (Equation 12) into Equation 13, the negative log-likelihood ($-lnL$) is minimised to find the estimates of q, h and K^{Sp}.

The results showed that with a faster growth rate (Case B), a smaller K^{Sp} and higher h are estimated than with a slow growth rate (Case A, Table 7.6). These parameter estimates result in a 50 % smaller estimated current spawning stock biomass (B_{2011}) for the fast-growth model, but a similar depletion level (B_{2011}/Ksp). The results also show that the initial response to exploitation of a fast-growth *M. capensis* was severe, being reduced to 5 % of pristine levels in 1990 (Table 7.6; Fig. 7.1). However, with a higher h value, the population has a greater productivity, and the recovery rate of a fast-growing resource is much faster than for a slow-growing resource. After 1990, the fast-growing resource (Case B) recovered from 5 to 9 % depletion level, while the slow-growing resource (Case A) further declined from 22 % to 12 %. Assuming no catches are taken in the next five years, the recovery of the fast-growing resource (Case B) would be double the rate of a slow-growing resource (Case A) (Table 7.6; Fig. 7.1). The fast-growing resource showed a better fit to the data than the slow-growing resource (Table 7.6; Fig. 7.1).

Table 7.6 Results of the three estimated parameters and the indicators using **A.** the slow growth rate data (Table 7.4, A) and **B.** the fast growth rate data (Table 7.4, B) for Namibian *M. capensis*.

	A. *M. capensis* – slow growth	**B. *M. capensis* - fast growth**
K^{sp} ('000 tonnes)	5604	3153
h	0.232	0.384
q	0.711	1.82
B_{2011} ('000 tonnes)	651	284
B_{1990}/K^{sp}	0.22	0.051
Depletion B_{2011}/K^{sp}	0.12	0.090
Recovery B_{2016}/B_{2011}	1.304	2.634
- lnL	-9.26	-10.62

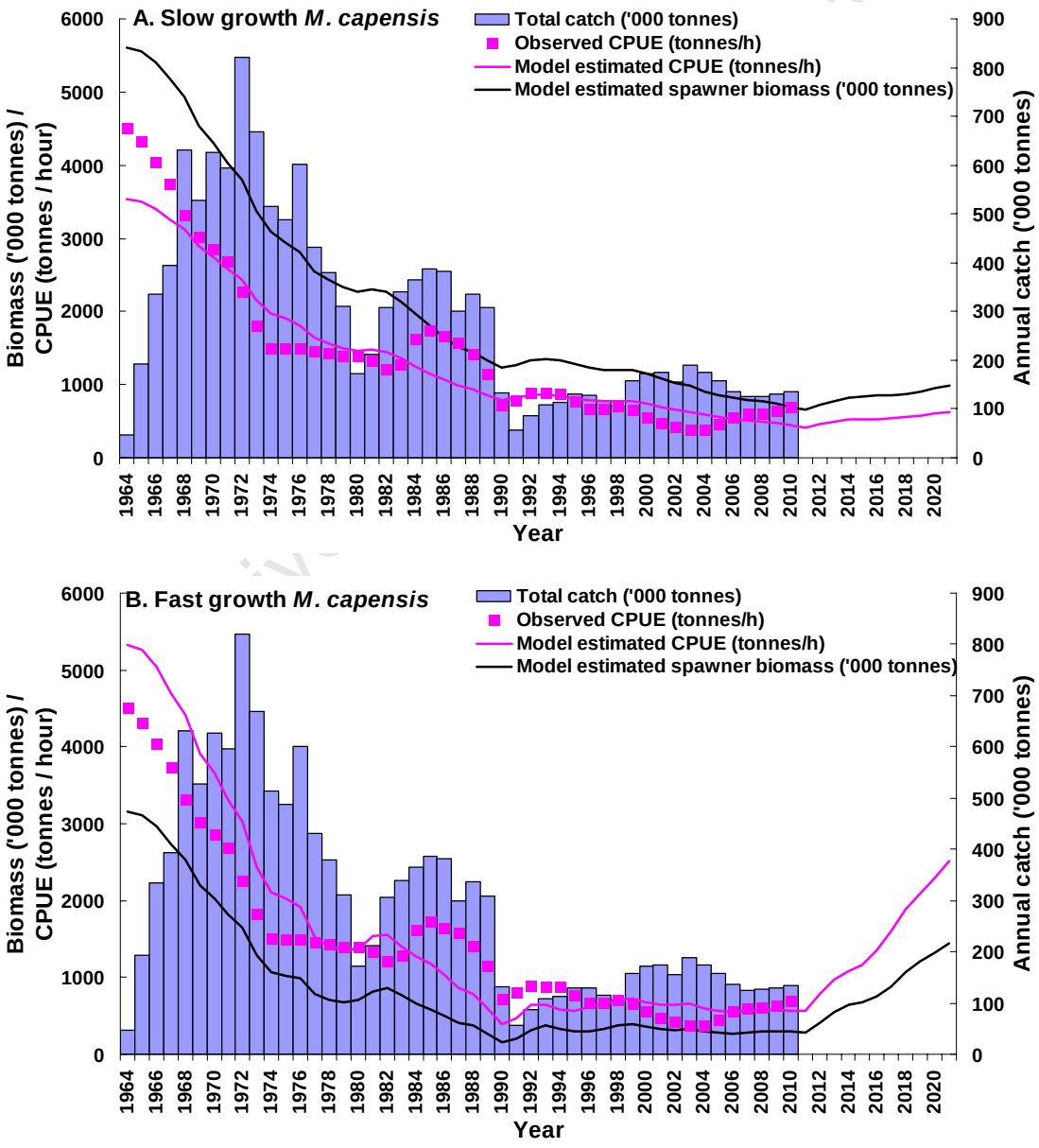

Figure 7.1 Results of the simple age-structured production model using **A.** slow growth rate data (Table 7.2, A) and **B.** fast growth rate data (Table 7.2, B) for Namibian *M. capensis*.

A smaller current biomass is expected for a fast-growing stock than for a slow-growing stock, which in turn could mean the stock is sensitive to variability in catches or large catches. The stock also might be more reactive to environmental fluctuations as there are fewer age groups, which would be regarded as a buffer for large natural mortality due to environmental fluctuations. The fishing selectivity of younger age-groups increases because of the larger lengths-at age of the fast-growth resource (Table 7.2, B). However, the age-at-maturity also decreases which compensates for this change in population age structure.

Alternatively, it is possible that the fast-growing *M. capensis* stock could have a higher natural mortality rate than previously thought, which could also mean higher resilience to fishing but also higher variability and thus greater risk involved with its current fishing strategy. This needs further investigation.

An increased length (and age) at 50 % maturity (54 cm) has been recently observed for *M. capensis* (Singh *et al.*, 2011). The high length-at-maturity could have happened as a tactic to compensate for fishing pressures (Rochet, 2000; Table 1.1), or could be an effect of previous erroneous calculations. More detailed studies should be carried out testing the consequences of (1) higher maturity- and selectivity-at-age as shown in Table 7.2, (2) a higher expected length at maturity as shown by Singh *et al.* (2011) and (3) fitting the model to detailed "new" catch-at-age data for all fleets and surveys using the conversion method outlined in Table 7.1, points 2 and 3.

It is likely that *M. paradoxus* is a more K-selected species than *M. capensis*, with slow growth rates (Botha, 1971; 1980; Wilhelm *et al.*, 2007). Translucent zones on *M. paradoxus* otoliths have a regular and clear appearance, and fewer "double rings" are apparent than for *M. capensis*. They are therefore easier to interpret (ICSEAF, 1983; BENEFIT, 2004b; 2005). Translucent zones on *M. paradoxus* otoliths are thus likely to be formed once per year and growth rates are probably similar to those previously estimated (Wilhelm *et al.*, 2007). More specifically, because *M. capensis* live at shallower bottom depths than *M. paradoxus*, they are exposed to more variable environmental fluctuations, as coastal upwelling affects water on the mid-shelf. Their distribution spans slightly further north than that of *M. paradoxus* (Table 1.2). They undergo vertical migration to a meso-pelagic environment, on a daily basis as well as

during spawning, all of these factors exposing them to variable environmental conditions. Because growth rate and natural mortality are often positively correlated (Pauly, 1980) and high natural mortality is often linked with highly variable and unpredictable environments (Adams, 1980), *M. capensis* should show a much higher natural mortality than *M. paradoxus*. This means *M. paradoxus* would be expected to be a more K-selected strategist with much slower growth rates and lower natural mortality and productivity than *M. capensis* (Adams, 1980). In terms of management recommendations for both hake species in Namibia, *M. paradoxus* should therefore be fished according to more conservative fishing strategies applied to less productive species. At present in Namibia, management does not reflect this, as *M. paradoxus* is fished at higher catch rates than *M. capensis*, and *M. capensis* juveniles are protected by the 200/300 m depth restriction. Adjustments to the management strategies that will follow a split-species management approach should take these results and hypotheses into consideration. In order to achieve more specific recommendations, age validation and age determination research on *M. paradoxus* needs to be carried out (Table 7.1, 5).

7.2 Spawning, recruitment and migration of Namibian *M. capensis* – in relation to translucent zone formation in their otoliths

It was shown that *M. capensis* from fur seal scats hatched mainly in winter (23 June), ranging from 20 May to 20 July among cohorts (Chapter 2). Spawning and nursery areas of *M. capensis* consisted of a central (20.5–25.5°S) and a southern (25.5–29°S) aggregation, indicating that the *M. capensis* aggregations have shifted southward in recent years (Chapter 5). The timing of hatchdates between the two areas usually differs by 3–4 months. Most hatchdates calculated of the young-of-the year from the central nursery aggregations ranged between April and July and September–October in a secondary mode. Those from the southern aggregations mainly ranged between September and October (Fig. 7.2). The hypothesis that hatchdates consisted of one peak, first supported in Chapter 2, was thus not supported by data in Chapter 5. Rather, hatchdates were consistently separated by a few months (between areas) concurring with previous studies on Namibian *M. capensis* (Assorov and Berenbeim, 1983; Olivar *et al.*, 1988), as well as studies on South African *M. capensis* (Botha, 1986), European hake (Arneri and Morales-Nin, 2000) and Chilean hake (Landaeta and Castro, 2006).

The calculated June–July hatchdate from fur seal scat samples in Chapter 2, as opposed to a double peak shown in Chapter 5, could be caused by the over-riding presence of small hake from central Namibia available to fur seals in most years, and samples from that area mostly stemming from a winter hatchdate period (Fig. 5.3). Off northern and southern Namibia, fur seals forage up to 500 m bottom depth and off central Namibia up to 200 m bottom depth (Skern-Mauritzen *et al.*, 2009). This means they would feed on 18 to 25 cm hake most often off southern Namibia, and on < 18 cm hake off central Namibia. As can be seen in Fig. 2.7, small hake samples in the fur seal diet often stem from the Cape Cross colony, which is at ~ 21°S. These small fish often seem to be from two different periods (e.g. Figs 2.7f and 2.7k), while this cannot always be seen for larger fish due to their higher variation of lengths-at-age, and their disappearance out of the feeding range of fur seals in central Namibia. In addition, and supported by this argument, it is possible that the early growth rates and variation of hatchdates of young *M. capensis* calculated in Chapter 2 were under-estimated (Fig. 2.8 should have a wider range, and possibly a forward shift). As indicated in Figs 2.7l and m, it is possible to calculate a much faster rate for young *M. capensis* from the 2004 and 2005 cohorts, placing their hatchdates generally in August–September. However, even with spring-spawned cohorts, this would not change the conclusions of age validation, with the annuli still falling in the winter–spring range (Fig. 3.5).

The hypothesis that recruitment strength was dependent on timing of hatchdates was also not supported by these data (Chapters 2 and 5). Rather, it seems that recruitment strength is dependent on a long spawning season from the northern as well as the southern spawning aggregations. Strong recruitment followed when bimodal peaks could be seen in young-of-the-year *M. capensis* in the fur seal scat samples (Chapters 2 and 5), or in the middle of the hatchdate range (Fig. 2.8). For example, the strong year-classes of 1996 and 2004 (Fig. 2.8) were from multiple spawning peaks (March, May, July and November of 1996; May, July, September, October of 2004; Table 5.2). This recruitment hypothesis should be further investigated by more regular sampling of juvenile fish, focussing on the small juvenile fish (< 6 cm) that are not fully sampled by fur seals, and not at all sampled by research surveys.

At present, within the ASPM, recruitment "happens" at the beginning of the calendar year (1 January) and catches are taken in the middle of the year (1 July) (Tables 7.2

and 7.5). However, hatchdates are calculated for mid-winter from the fur seal scat index (Chapter 2). Growth rates calculated in Chapters 2 and 3, which are used here (Table 7.2, B), and should be used for future assessments, assume a 1 July hatchdate. The theoretical spawning stock biomass calculated for the beginning of the calendar year should actually be calculated from "mid-year weights" (Tables 7.2 and 7.5). This is not a problem when stocks are considered individually, as the biomass calculations are just moved half a year forward. However, for future stock assessments this should be noted and it is recommended that the catches be adjusted to be "taken" at 1 January and the spawning stock biomass calculated for 1 July within the ASPM.

In the current stock assessment model the recruitment index calculated from fur seal scat samples is used as a time series for fitting (Kirchner, 2010). The results of the stock assessment model show that the variability in recruitment observed in the seal scat data is not observed in the catch-at-age data. When the seal scat data are given most weight, the model-expected catch-at-age data fit the observed catch-at-age data the worst (Kirchner, 2010). This is because the recruitment index from seal scat data is calculated for a hatchdate of 1 July and named after the hatching year, but the recruitment in the model is taken at a hatchdate of 1 January and the survey catch-at-age data is calculated for February. Since ages are only taken as integers, the recruitment index is therefore mismatched by one year. For example, the 1996 cohort would be 0 years old on 1 January 1997 and for the 1997 February survey, but is now taken as 1-year-olds assuming that recruitment happens in January. Secondly, the slow-growth data are used in the current ASPM for stock assessment. Summarising results on cohorts presented from Chapters 2 and 4 shows that the cohorts identified from the seal scat recruitment index (Fig. 2.8) can be followed very well in the survey and commercial length-frequency distributions (Figs 4.1 and 4.2). The 2002, 1996 and 2007 cohorts are three of the four strongest cohorts identified from fur seal scat data (Fig. 2.8). Assuming the cohorts mainly stem from the mid-winter period, the 2002 cohort should thus be 2.5 years old in the "Feb 2005" survey, the 1996 cohort should be 2.5 years old in "Feb 1999" and the 2007 cohort should be 0.5 years old in "Feb 2008" (Fig. 4.1). All of these can be seen as strong year-classes in Fig. 4.1. In addition, the strong 2007 cohort (Fig. 2.8) can be followed from 0+-year-olds from "2008 Jun" to "2009 Nov" as 2-year-olds (Fig. 4.2). Fish of those sizes (< 30 cm) are not normally selected in the commercial fishery. This cohort presented as particularly strong

throughout that year (Fig. 4.2). Thus, using the fast growth rate catch-at-age data (converted using Table 4.6) as well as shifting the assessment and catches back by half a year (or else moving the seal scat index forward by half a year into the next calendar year), would improve the results in the ASPM, and cohorts would be followed better through the fishery.

Given the results of biannual translucent zone formation presented in Chapters 2–4, additional hypotheses on causes of translucent zone formation were developed and tested in Chapters 5 and 6. The previously defined "demersal ring" was invalidated (Chapters 3 and 5), supporting the hypothesis that the pre-annual translucent zones on *M. capensis* are not caused by "demersal settlement". The second part of the hypothesis was also supported as translucent zone formation frequently coincided with inshore-offshore and alongshore migration of *M. capensis* (Chapter 5). The same proportion of fish that had migrated, for example, from the inner-shelf to the mid-shelf, tended to have a certain translucent zone present on their otoliths, showing that the causes of movement and zone formation could be related to the same endogenous cues at certain fish lengths. It was hypothesized that translucent zone formation happens first in response to an endogenous cue, and second in response to an environmental change. The life history of hake up to four years of age and their movement and how this related to translucent zone formation is illustrated in Figure 7.2.

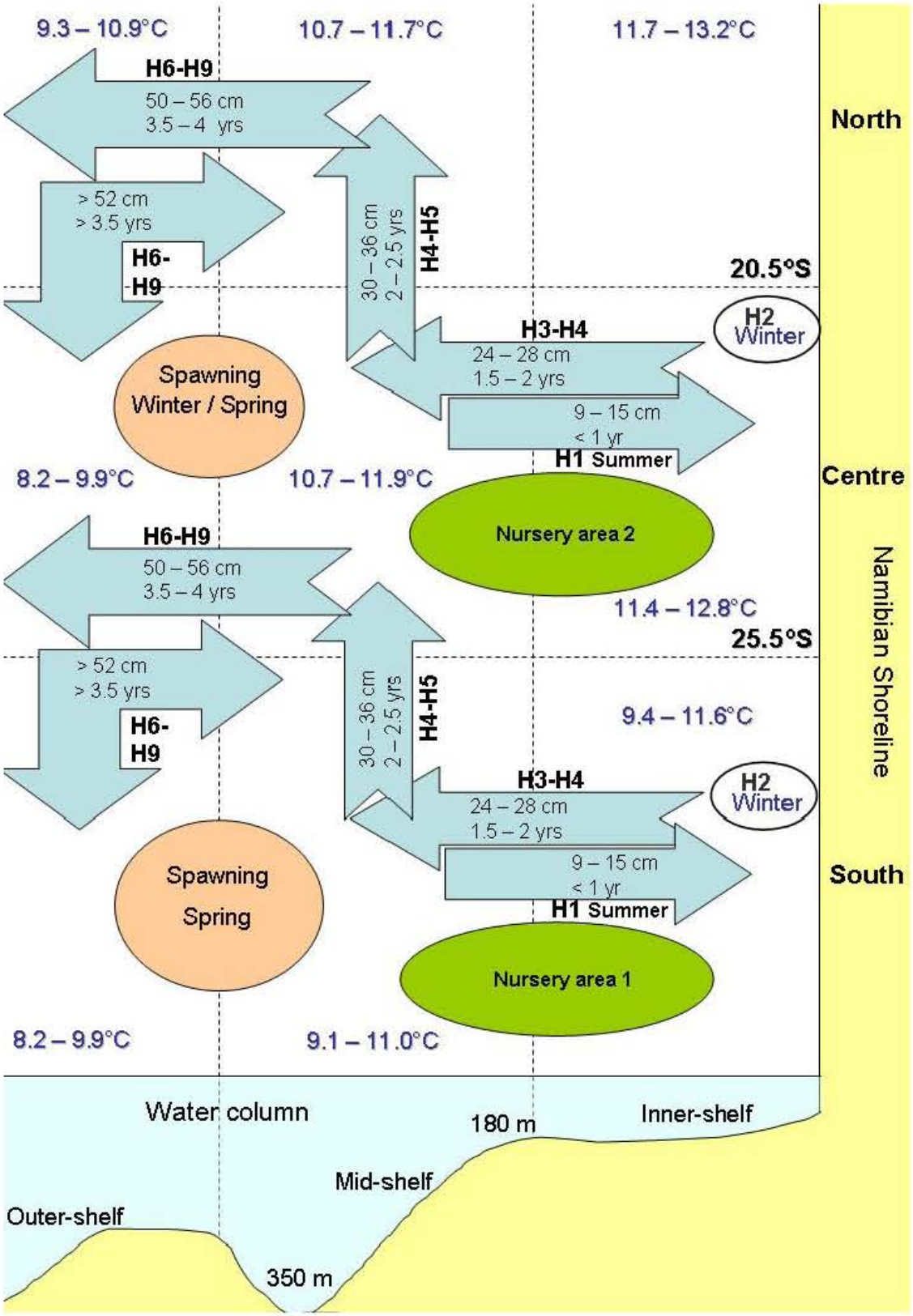

Figure 7.2 Summary of life history of Namibian *M. capensis* (nursery areas, migration, spawning) related to translucent zone formation as presented in Chapters 2 to 5 and including mean temperatures (°C) in blue text (ranges refer to summer and winter mean monthly temperatures).

The presence of translucent zones on *M. capensis* otoliths was most strongly associated with fish length. Presence of zones T1–T6 per cm fish length was most strongly associated with area (north, centre or south) in which the fish were captured, or cohort (1996, 1998 or 2002) to which the fish belonged. Fish caught in the northern area consistently showed earliest formation of translucent zones T1–T6, and therefore most number of translucent zones per cm fish length. Translucent zone formation in general fell more often into summer–autumn , being temporally correlated with warm bottom temperatures (Chapter 6), invalidating the "winter translucent zone" hypothesis from earlier literature (ICSEAF, 1983). Early and increased formation of translucent zones in fish in northern Namibia could be caused by warm temperatures and more variable environment of the north caused by the north-south movement of the Angola-Benguela front.

Translucent zone formation did not significantly coincide with low oxygen water or a preceding drop in temperature (Chapter 6). This did not support the hypothesis that translucent zones are formed in response to a temperature drop, or increase, or any other environmental change (Schramm, 1989). Presence of translucent zones at a certain fish length was not associated with depth category, although the width and steepness of the continental shelf and position of the shelf break in northern and central Namibia may have a different effect on fish behaviour and migration, and thus also cause additional translucent zones to be formed. The presence of translucent zones at a certain fish length was not dependent on the fish's maturity stage. However, a biannual trigger of spawning may be indirectly linked to biannual translucent zone formation.

It is recommended that area-specific monthly length-frequency distributions are analysed for growth rate differences (between areas and seasons). This could be done, for example, using monthly commercial samples collected (for both *M. capensis* and *M. paradoxus*) in Namibia. Also, coupled with this, environmental measurements should be matched with otoliths collected on a monthly basis. The sampling design should allow matching translucent and opaque edges (of the same cohort) with recent environmental conditions, previous translucent zones, fish condition factor (indicating nutritional status), and gonadosomatic index of individual fish. Coupled with this, it would be an advantage if diet studies could be added to the sampling programme.

Hake are opportunistic feeders (Roel and Macpherson, 1988) so their diet will change seasonally, but during their life history the diet of South African *M. capensis* (on the west coast) gradually changes from a crustacean-dominated diet to a fish-dominated diet (80 % crustaceans by wet mass at < 20 cm to 20 % at > 50 cm) (Punt and Leslie, 1992). A more detailed diet by length analysis showed that Argentine hake *M. hubbsi* changed from a small lightfish and pelagic crustacean dominated diet (90 % by wet mass) at 7–16 cm to a diet dominated by anchovy (19–52 cm), to a cannibalistic diet (Ocampo Reinaldo *et al.*, 2011). The onset of piscivory can result in a dramatic increase in growth rates (Buijse and Houthuijzen, 1992; Juanes and Conover, 1994; Sogard, 1997). Translucent zone formation could follow a change in somatic growth rate. Diet coupled with changes in nutritional level (condition factor) of *M. capensis*, especially for juvenile fish, should be studied, separated for different size classes, to investigate the change to piscivory or any other seasonal nutritional level change and whether this is related to zone formation. Again, fish at sizes that are sampled by fur seals, and smaller fish should be included in this research sampling programme.

While the temporal and spatial frequency and accuracy of otolith sampling made it difficult to decouple the exact influences of depth, maturity stage or environmental variables on translucent zone formation, it seems that the number of translucent zones was always most strongly associated with fish length. This means again that as long as their growth rates remain constant, the methods of age determination described here (Table 7.1) can be applied to *M. capensis*.

In summary, this thesis has confirmed the importance of otoliths in studies of the life history of fish. Studies on otoliths in this thesis have provided new and valuable insights. It is shown that *M. capensis* in the northern Benguela consist of one single stock with two centres of gravity of spawning and nursery areas. A plausible migration pattern of Namibian *M. capensis* for the past 20 years is presented. *M. capensis* have faster growth rates and are more pronounced r-strategists than previously observed. As a result, they could be more sensitive to short-term fishing pressures but also faster to recover when fishing is reduced. Translucent zones are formed at least twice per year in their otoliths. Implications for the routine age determination methods are described, and age conversion recommendations are made. The findings of this research have direct value for stock assessments, and also towards greater understanding of the ecology of a dominant species of the northern Benguela offshore ecosystem.

REFERENCES

Adams, P. B. 1980. Life history patterns in marine fishes and their consequences for fisheries management. Fishery Bulletin, 78 (1): 1–12.

Admassu, D., and Casselman, J. M. 2000. Otolith age determination for adult tilapia, *Oreochromis niloticus* L. from Lake Awassa (Ethiopian Rift Valley) by interpreting biannuli and differentiating biannual recruitment. Hydrobiologia, 418: 15–28.

Akaike, H. 1973. Information theory as an extension of the maximum likelihood principle. *In* Second international symposium on information theory, pp. 267–281. Ed. by B. N. Petrov, and F. Csaki. Akademiai Kiado.

Anon. 1986. Report of the standing committee on stock assessment (STOCK). *In* Proceedings and reports of meetings 1985, Part II, pp. 51–95. The International Commission for Southeast Atlantic Fisheries, Madrid, Spain.

Anon. 2004. Hake quota goes up. The Namibian, 20. 4. 2004. http://www.namibian.com.na/

Anon. 2006. Report of the BCLME Joint hake research planning workshop (Namibia and South Africa), 9–12 May 2006, Cape Town, South Africa: 6 pp.

Arneri, E., and Morales-Nin, B. Y. O. 2000. Aspects of the early life history of European hake from the central Adriatic. Journal of Fish Biology, 56 (6): 1368–1380.

Assorov, V. V., and Berenbeim, D. Y. 1983. Spawning grounds and cycles of Cape hakes in the southeast Atlantic. Collection of Scientific Papers of the International Commission for Southeast Atlantic Fisheries, 10 (i): 27–30.

Bailey, K. M., Francis, R. C., and Stevens, P. R. 1982. The life history and fishery of pacific whiting, *Merlucclus productus*. CalCOFI Report, 23: 81–98.

Bal, G., Rovot, E., Prévost, E., Piou, C., and Baglinière, J. L. 2011. Effect of water temperature and density of juvenile salmonids on growth of young-of-the-year Atlantic salmon *Salmo salar*. Journal of Fish Biology, 78: 1002–1022.

Bartholomae, C. H., and van der Plas, A. K. 2007. Towards the development of environmental indices for the Namibian shelf, with particular reference to fisheries management. African Journal of Marine Science, 29 (1): 25–35.

Bartolino, V., Ottavi, A., Colloca, F., Ardizzone, G. D., and Stefánsson, G. 2008. Bathymetric preferences of juvenile European hake (*Merluccius merluccius*). ICES Journal of Marine Science, 65 (6): 963–969.

Baumann, H., Gröhsler, T., Kornilovs, G., Makarchouk, A., Feldmann, V., and Temming, A. 2006. Temperature-induced regional and temporal growth differences in Baltic young-of-the-year sprat *Sprattus sprattus*. Marine Ecology Progress Series, 317: 225–236.

Beamish, C. A., Booth, A. J., and Deacon, N. 2005. Age, growth and reproduction of largemouth bass, *Micropterus salmoides,* in Lake Manyame, Zimbabwe. African Zoology, 40 (1): 63–69.

Beamish, R. J. 1979. Differences in the age of Pacific hake (*Merluccius productus*) using whole otoliths and sectioned otoliths. Journal of the Fisheries Research Board Canada, 36: 141–151.

Beamish, R. J., and McFarlane, G. A. 1983. The forgotten requirement for age validation in fisheries biology. Transactions of the American Fisheries Society, 112 (6): 735–743.

Beckman, D. W., Stanley, A. L., Render, J. H., and Wilson, C. A. 1990. Age and growth of black drum in Louisiana waters in the Gulf of Mexico. Transactions of the American Fisheries Society, 119: 537–544.

Beckman, D. W., and Wilson, C. A. 1995. Seasonal timing of opaque zone formation in fish otoliths. *In* Recent developments in fish otolith research, pp. 27–43. Ed. by D. H. Secor, J. M. Dean, and S. E. Campana. University of South Carolina Press, Columbia, USA.

Begg, G. A., Campana, S. E., Fowler, A. J., and Suthers, I. M. 2005. Otolith research and application: current directions in innovation and implementation. Marine and Freshwater Research, 56 (5): 477–483.

Belcari, P., Ligas, A., and Viva, C. 2006. Age determination and growth of juveniles of the European hake, *Merluccius merluccius* (L., 1758), in the northern Tyrrhenian Sea (NW Mediterranean). Fisheries Research, 78: 211–217.

BENEFIT. 2004a. Formal Report: BENEFIT / NRF Stock Assessment Workshop 2004 (12 – 17 January 2004, University of Cape Town), BENEFIT/NRF Stock assessment workshop, January 2004, Cape Town, South Africa: 18 pp.

BENEFIT. 2004b. Report of the 2004 BENEFIT hake and *Dentex* otolith reading workshop, Zoology department, University of Cape Town, South Africa, 22 June – 2 July 2004: 26 pp.

BENEFIT. 2005. Report of the 2005 BENEFIT hake otolith reading workshop. National Marine Information and Research Centre, Swakopmund, Namibia, 19–30 September 2005: 20 pp.

Bentz, K. L. M. 1976. Gill arch morphology of the Cape hakes *Merluccius capensis* Cast. and *M. paradoxus* Franca. Fisheries Bulletin of South Africa, 8: 17–22.

Bernardes, R. A. 2002. Age, growth and longevity of the gray triggerfish, *Balistes capriscus* (Tetraodontiformes: Balistidae), from the Southeastern Brazilian Coast. Scientia Marina, 66 (2): 167–173.

Bertignac, M., and de Pontual, H. 2007. Consequences of bias in age estimation on assessment of the northern stock of European hake (*Merluccius merluccius*) and on management advice. ICES Journal of Marine Science, 64: 981–988.

Beverton, R. J. H., and Holt, S. J. 1957a. Growth and feeding. Section 9. *In* On the dynamics of exploited fish populations. Fishery Investigations, Series II, Volume XIX: 96–135. Blackburn Press, London.

Beverton, R. J. H., and Holt, S. J. 1957b. Estimation of the total mortality coefficients ($F + M$), and the maximum age, t. Section13. *In* On the dynamics of exploited fish populations. Fishery Investigations, Series II, Volume XIX: 178–189. Blackburn Press, London.

Beverton, R. J. H., and Holt, S. J. 1959. A review of the life spans and mortality rates in nature, and their relation to growth and other physiological characteristics. Ciba Foundation of Colloquial Ageing, 5: 142–177.

Bliss, C. I. 1958. Periodic regression in biology and climatology. Bulletin of the Conneticut Agricultural Experimental Station New Haven, 615: 1–55.

Botha, L. 1970. The growth of Cape hake *Merluccius capensis*. Investigational Report of the Division of Sea Fisheries Research of South Africa, 82: 1–9.

Botha, L. 1971. Growth and otolith morphology of the Cape hakes *Merluccius capensis* Cast. and *M. paradoxus* Franca. Investigational Report of the Division of Sea Fisheries Research of South Africa, 97: 1–32.

Botha, L. 1973. Migrations and spawning behaviour of the Cape hakes. South African Shipping News and Fishing Industry Review, 28 (4): 62–67.

Botha, L. 1980. The biology of the Cape hake *Merluccius capensis* Cast. and *M. paradoxus* Franca. PhD thesis, Stellenbosch University, South Africa: 182 pp.

Botha, L. 1985. Occurrence and distribution of Cape hakes *Merluccius capensis* Cast. and *M. paradoxus* Franca in the Cape of Good hope area. South African Journal of Marine Science, 3: 179–190.

Botha, L. 1986. Reproduction, sex ratio and rate of natural mortality of Cape hakes *Merluccius capensis* Cast. and *M. paradoxus* Franca in the Cape of Good Hope area. South African Journal of Marine Science, 4: 23–35.

Boyer, D. C., Cole, J., and Bartholomae, C. H. 2000. Southwestern Africa: Northern Benguela Current Region. Marine Pollution Bulletin, 41: 123–140.

Bremner, J. M. 1983. Biogenic sediments on the South West African (Namibian) continental margin. *In* Coastal Upwelling: Its Sedimentary Record Part B: Sedimentary Records of Ancient Coastal Upwelling, pp. 73–103. Ed. by J. Thiede, and E. Suess. Plenum Press, New York.

Brinkman, F. V. 2007. Analysis of annuli in otoliths, age distribution and growth rates of the Namibian hake (*Merluccius capensis*). MSc dissertation, University of Algrave, Lisboa, Portugal: 79 pp.

Brothers, E. B. 1979. Age and growth studies on tropical fishes. *In* Stock assessment for tropical small-scale fisheries, pp. 119–136. Ed. by S. B. Saila, and P. M. Roedel. University of Rhode Island International Center for Marine Research Development, Kingston, RI, USA.

Brouwer, S. L., and Griffiths, M. H. 2004. Age and growth of *Argyrozona argyrozona* (Pisces: Sparidae) in a marine protected area: an evaluation of methods based on whole otoliths, sectioned otoliths and mark-recapture. Fisheries Research, 67: 1–12.

Buckland, S. T. 1984. Monte-Carlo confidence intervals. Biometrics, 40: 811–817.

Buckland, S. T., Burnham, K. P., and Augustin, N. H. 1997. Model selection: An integral part of inference. Biometrics, 53: 603–618.

Buijse, A. D., and Houthuijzen, R. P. 1992. Piscivory, growth, and size-selective mortality of age 0 pikeperch (*Sfizosfedion lucioperca*). Canadian Journal of Fisheries and Aquatic Sciences, 49: 894–902.

Burmeister, L.-M. 2001. Depth-stratified density estimates and distribution of the Cape hake *Merluccius capensis* and *M. paradoxus* off Namibia, deduced from survey data, 1990–1999. South African Journal of Marine Science, 23: 347–356.

Burmeister, L.-M. 2005. Is there a single stock of *Merluccius paradoxus* in the Benguela ecosystem? African Journal of Marine Science, 27: 23–32.

Butterworth, D. S., and Geromont, H. F. 2001. Evaluation of a range of possible simple interim management procedures for the Namibian hake fishery. South African Journal of Marine Science, 23: 357–374.

Butterworth, D. S., and Rademeyer, R. A. 2005. Sustainable management initiatives for the southern African hake fisheries over recent years. Bulletin of Marine Science, 76 (2): 287–319.

Buratti, C. C., and Santos, B. A. 2010. Otolith microstructure and pelagic larval duration in two stocks of the Argentine hake, *Merluccius hubbsi*. Fisheries Research, 106: 2–7.

Cabo, F. L. 1965. Las merluzas atlanticas. Publicaciones Técnicas de la Junta de Estudios de Pesca Maritima, Madrid, 4: 2–8.

Campana, S. E. 1984. Interactive effects of age and environmental modifiers on the production of daily growth increments in otoliths of plainfin midshipman (*Porichthys notatus*). Fishery Bulletin, 82 (1): 165–177.

Campana, S. E. 2001. Review paper: Accuracy, precision and quality control in age determination, including a review of the use and abuse of age validation methods. Journal of Fish Biology, 59: 197–242.

Campana, S. E. 2005. Otolith science entering the 21st century. Marine and Freshwater Research, 56 (5): 485–495.

Campillo-Campbell, C., and Gordoa, A. 2004. Physical and biological variability in the Namibian upwelling system: October 1997–October 2001. Deep-Sea Research II, 51: 147–158.

Cappo, M., Eden, P., Newman, S. J., and Robertson, S. G. 2000. A new approach to validation of periodicity and timing of opaque zone formation in the otoliths of eleven species of *Lutjanus* from the central Great Barrier Reef. Fishery Bulletin, 98: 474–488.

Casselman, J. M. 1983. Age and growth assessment of fish from their calcified structures – techniques and tools. US Department of Commerce, NOAA Technical Report NMFS, 8: 1–17.

Casselman, J. M. 1987. Determination of age and growth. *In* The biology of fish growth, pp. 209–242. Ed. by A. H. Weatherley and H. S. Gill. Academic Press, London.

Casselman, J. M. 1990. Growth and relative size of calcified structures of fish. Transactions of the American Fisheries Society, 119: 673–688.

Chidlow, J. A., Simpfendorfer, C. A., and Russ, G. R. 2007. Variable growth band deposition leads to age and growth uncertainty in the western wobbegong shark, *Orectolobus hutchinsi*. Marine and Freshwater Research, 58: 856–865.

Chlapowski, K. 1974. Length composition and maturity of hakes *Merluccius capensis* and *M. paradoxus* caught in the ICSEAF area during the period from November 1972 to January 1973. Collection of Scientific Papers of the International Commission for Southeast Atlantic Fisheries, 1: 182–192.

Chlapowski, K. 1977. Food and feeding of hake in South West African seas. Collection of Scientific Papers of the International Commission for Southeast Atlantic Fisheries, 4: 115–120.

Christiansen, H. E., Glorioso, P. D., Olivieri, C. E., 1986. Aplicación de la histología en la determinación de los efectivos de merluza (*Merluccius hubbsi*). Tipificación de tejidos, cálculos de fecundidad y vinculación con las condiciones ambientales. Publicaciones Comisión Técnica Mixta Frente Marítimo, 1 (2): 567–574.

Clayden, A. D. 1972. Simulation of the changes in abundance of the cod (*Gadus morhua* L.) and the distribution of fishing in the north Atlantic. Fishery Investigations, 27 (1): 1–58.

Cochrane, K. L., Augustyn, C. J., Bianchi, G., de Barros, P., Fairweather, T. P., Iitembu, J., Japp, D. W., Kanandjembo, A., Kilongo, K., Moroff, N., Nel, D. C., Roux, J.-P., Shannon, L. J., van Zyl, B. J., and Vaz-Velho, F. 2007. Results and conclusions of the project "Ecosystem approaches for fisheries management in the Benguela Current Large Marine Ecosystem". FAO Fisheries Circular, 1026: 167 pp.

Colloca, F., Gentiloni, P., Belluscio, A., Carpentieri, P., and Ardizzone, G. D. 2003. Analysis and validation of annual increments in otoliths of European hake (*Merluccius merluccius*) in the central Mediterranean Sea. Archive of Fishery and Marine Research, 50 (2): 175–192.

Courbin, N., Fablet, R., Mellon, C., and de Pontual, H. 2007. Are hake otolith macrostructures randomly deposited? Insights from an unsupervised statistical and quantitative approach applied to Mediterranean hake otoliths. ICES Journal of Marine Science, 64 (6): 1191–1201.

Crawford, R. J. M., Shannon, L. V., and Pollock, D. E. 1987. The Benguela ecosystem. Part IV. The major fish and invertebrate resources. Oceanography and Marine Biology: An Annual Review, 25: 353–505.

Cushing, D. H. 1975. Marine ecology and fisheries. Cambridge University Press, Cambridge: 278 pp.

de Bruyn, A. M. H., and Meeuwig, J. J. 2001. Detecting lunar cycles in marine ecology: periodic regression versus categorical ANOVA. Marine Ecology Progress Series, 214: 307–310.

de Bruyn, P. J. N., Bester, M. N., Kirkman, S. P., Mecenero, S., Roux, J.-P., and Klages, N. T. W. 2005. Cephalopod diet of the Cape fur seal, *Arctocephalus pusillus pusillus*, along the Namibian coast: variation due to location. African Zoology, 40 (2): 261–270.

de Bruyn, P. J. N., Bester, M. N., Mecenero, S., Kirkman, S. P., Roux, J.-P., and Klages, N. T. W. 2003. Temporal variation of cephalopods in the diet of Cape fur seals in Namibia. South African Journal of Wildlife Research, 33 (2): 85–96.

de Decker, A. H. B. 1970. Notes on an oxygen-depleted sub-surface current off the west coast of South Africa. Investigational Report of the Division of Sea Fisheries Research of South Africa, 84: 24 pp.

de Pontual, H., Groison, A.-L., Piñeiro, C., and Bertignac, M. 2006. Evidence of underestimation of European hake growth in the Bay of Biscay, and its relationship with bias in the agreed method of age estimation. ICES Journal of Marine Science, 63: 1674–1681.

Dellinger, T., and Trillmich, F. 1988. Estimating diet composition from scat analysis in otariid seals (*Otariidae*): is it reliable? Canadian Journal of Zoology, 66: 1865–1870.

Dorn, M. W. 1995. The effects of age composition and oceanographic conditions on the annual migration of Pacific whiting, *Merluccius productus*. CalCOFI Report, 36: 97–105.

Duncombe Rae, C. M. 2005. A demonstration of the hydrographic partition of the Benguela upwelling ecosystem at 26º40′S. African Journal of Marine Science, 27 (3): 617–628.

Efron, B., and Tibshirani, R. 1986. Bootstrap methods for standard errors, confidence intervals, and other measures of statistical accuracy. Statistical Science, 1 (1): 54–77.

Elago, P. N. 2002. Trawling and longlining in the Namibian hake industry. MSc dissertation, University of Tromsø, Norway: 53 pp.

Fabens, A. J. 1965. Properties and fitting of the von Bertalanffy growth curve. Growth, 29 (3): 265–289.

FAO. 2007. http://www.fao.org/fi/oldsite/FCP/en/NAM/profile.htm

Fletcher, W. J., and Blight, S. J. 1996. Validity of using translucent zones of otoliths to age pilchard *Sardinops sagax neopilchardus* from Albany, Western Australia. Marine and Freshwater Research, 47: 617–624.

Flury, B. D., and Levri, E. P. 1999. Periodic logistic regression. Ecology, 80 (7): 2254–2260.

Fournier, D. A., Hampton, J., and Sibert, J. R. 1998. MULTIFAN-CL: a length-based, age-structured model for fisheries stock assessment, with application to South Pacific albacore, *Thunnus alalunga*. Canadian Journal of Fisheries and Aquatic Sciences, 55: 2105–2116.

Franca, P. 1960. Nova contribuição para o conhecimento do género Merluccius no Atlântico oriental ao sul do Equador. Memoria Junta Investigaciones Ultramarina Seriés, 2 (18): 57–101.

Francis, R. I. C. C. 1992. Use of risk analysis to assess fishery management strategies: A case study using orange roughy (*Hoplostethus atlanticus*) on the Chatham Rise, New Zealand. Canadian Journal of Fisheries and Aquatic Sciences, 49 (5): 922–930.

Gammelsrød, T., Bartholomae, C. H., Boyer, D. C., Filipe, V. L. L., and O'Toole, M. J. 1998. Intrusion of warm surface water along the Angolan-Namibian coast in February–March 1995: the 1995 Benguela Niño. South African Journal of Marine Science, 19: 41–56.

Garcia Rey, M., and Grobler, J. 2011. Spain's hake appetite threatens Namibia's most valuable fish. The Namibian, 07. 10. 2011. http://www.namibian.com.na/news/full-story/archive/2011/october/article/spains-hake-appetite-threatens-namibias-most-valuable-fish-1/

Gayanilo, F. C., Sparre, P., and Pauly, D. 2005. The FAO-ICLARM stock assessment tools II (FISAT II). Revised version. User's guide. FAO Computerized Information Series (Fisheries), 8: 168 pp.

Geffen, A. J., and Nash, R. D. M. 1995. Periodicity of otolith check formation in the juvenile plaice *Pleuronectes platessa* L. *In* Recent developments in fish otolith research, pp. 65–73. Ed. by D. H. Secor, J. M. Dean, and S. E. Campana. University of South Carolina Press, Columbia, USA.

GFCM. 1982. Report of the technical consultation on methodologies used for fish age-reading, Montpellier, 5–9 October 1981. FAO Fisheries Report, 257: 109 pp.

Godinho, M. L., Afonso, M. H., and Morgado, C. 2001. Age and growth of hake *Merluccius merluccius* Linnaeus, 1758 from the Northeast Atlantic (ICES division IXa). Boletín del Instituto Español de Oceanografía, 17 (3–4): 255–262.

Goicochea, C., Wosnitza-Mendo, C., Mostacero, J., and Moquillaza, P. 2010. Periodicidad de formación de anillos de crecimiento en otolitos de la merluza peruana *Merluccius gayi peruanus* Ginsburg [Periodicity of growth ring formation in otoliths of Peruvian hake *Merluccius gayi peruanus* Ginsburg]. Informes del Instituto del Mar del Perú, 37 (3–4): 79–83.

Gordoa, A., and Duarte, C. M. 1991. Size-dependent spatial distribution of hake (*Merluccius capensis* and *Merluccius paradoxus)* in Namibian waters. Canadian Journal of Fisheries and Aquatic Sciences, 48: 2095–2099.

Gordoa, A., and Duarte, C. M. 1992. Size-dependent density of the demersal fish off Namibia: Patterns within and among species. Canadian Journal of Fisheries and Aquatic Sciences, 49 (10): 1990–1993.

Gordoa, A., and Hightower, J. E. 1991. Changes in catchability in a bottom trawl fishery for Cape hake (*Merluccius capensis*). Canadian Journal of Fisheries and Aquatic Sciences, 48: 1887–1895.

Gordoa, A., Lesch, H., and Rodergas, S. 2006. Bycatch: complementary information for understanding fish behaviour. Namibian Cape hake (*M. capensis* and *M. paradoxus*) as a case study. ICES Journal of Marine Science, 63 (8): 1513–1519.

Gordoa, A., and Macpherson, E. 1989. Biomass indices and recruitment levels for hake and other commercial species in ICSEAF divisions 1.4 and 1.5 from 1988 surveys. Collection of Scientific Papers of the International Commission for Southeast Atlantic Fisheries, 16 (i): 103–118.

Gordoa, A., and Macpherson, E. 1990. Food selection by a sit-and-wait predator, the monkfish, *Lophius upsicephalus*, off Namibia (South West Africa). Environmental Biology of Fishes, 27 (1): 71–76.

Gordoa, A., and MacPherson, E. 1991. Diurnal variation in the feeding activity and catch rate of Cape hake (*Merluccius capensis* and *M. paradoxus*) off Namibia. Fisheries Research, 12 (4): 299–305.

Gordoa, A., Macpherson, E., and Olivar, M. P. 1995. Biology and fisheries of Namibian hakes (*M. capensis* and *M. paradoxus*). Chapter 3. *In* Hake fisheries ecology and markets, pp. 49–79. Ed. by J. Alheit, and T. J. Pitcher. Chapman & Hall, London.

Gordoa, A., Masó, M., and Voges, E. 2000. Monthly variability in the catchability of Nambian hake and its relationship with environmental seasonality. Fisheries Research, 48: 185–195.

Gordoa, A., Raventós, N., and Dealie, F. F. 2001. Comparison between micro- and macro-structure readings in the age estimations of Cape hake. Journal of Fish Biology, 59: 1153–1163.

Gordon, J. D. M, and Duncan, J. A. R. 1987. Deep-sea bottom-living fishes at two repeat stations at 2200 and 2900 m in the Rockall Trough, northeastern Atlantic Ocean. Marine Biology, 96: 309–325.

Grant, W. S., Becker, I. I., and Leslie, R. W. 1988. Evolutionary divergence between sympatric species of southern African hakes *Merluccius capensis* and *M. paradoxus*. I. Electrophoretic analysis of proteins. Heredity, 61: 13–20.

Grant, W. S., Leslie, R. W., and Becker, I. I. 1987. Genetic stock structure of the southern African hakes *Merluccius capensis* and *M. paradoxus*. Marine Ecology Progress Series, 41: 9–20.

Grote, B. 2010. The early life strategy of Cape hakes in the Benguela upwelling system off South Africa. PhD thesis, Universität Bremen, Germany: 153 pp.

Guevara-Carrasco, R., and Lleonart, J. 2008. Dynamics and fishery of the Peruvian hake: Between nature and man. Journal of Marine Systems, 71: 249–259.

Haddon, M. 2001. Modelling and quantitative methods in fisheries. Chapman & Hall/CRC, London: 406 pp.

Hamukuaya, H., O'Toole, M. J., and Woodhead, P. M. J. 1998. Observations of severe hypoxia and offshore displacement of Cape hake over the Namibian shelf. South African Journal of Marine Science, 19: 57–59.

Helser, T. E., and Brodziak, J. K. T. 1998. Impacts of density-dependent growth and maturation on assessment advice to rebuild depleted U.S. silver hake (*Merluccius bilinearis*) stocks. Canadian Journal of Fisheries and Aquatic Sciences, 55 (4): 882–892.

Hecht, T. 1980. A comparison of the otolith and scale methods of ageing, and the growth of *Sarotherodon mossambicus* (Pisces: Cichlidae) in a Venda impoundment (southern Africa). South African Journal of Zoology, 15 (4): 222–228.

Heymans, J. J., Shannon, L. J., and Jarre, A. 2004. Changes in the northern Benguela ecosystem over three decades: 1970s, 1980s, and 1990s. Ecological Modelling, 172 (2–4): 175–195.

Hickling, C. F. 1933. The natural history of the hake. Part IV Age determination and the growth rate. Fishery Investigations, Series II, Volume 13 (ii): 20–83.

Hilborn, R. 1990. Estimating the parameters of full age-structured models from catch and abundance data. International North Pacific Fisheries Commission Bulletin, 50: 207–213.

Hjort, J. 1914. Fluctuations in the great fisheries of northern Europe viewed in the light of biological research. Rapports Et Procès-Verbaux Des Rèunions, Conseil International Pour L'exploration De La Mer, 20: 228 pp.

Horn, P. L. 1997. An ageing methodology, growth parameters and estimates of mortality for hake (*Merluccius australis*) from around the South Island, New Zealand. Marine and Freshwater Research, 27: 145–155.

Horne, J. K., and Smith, P. E. 1997. Space and time scales in Pacific hake recruitment processes: Latitudinal variation over annual cycles. CalCOFI Report, 38: 90–102.

Hunt, J. J. 1980. Guidelines for age determination of silver hake, *Merluccius bilinearis*, using otoliths. Journal of Northwest Atlantic Fishery Science, 1: 65–80.

Hutchings, L., Barange, M., Bloomer, S. F., Boyd, A. J., Crawford, R. J. M., Huggett, J. A., Kerstan, M., Korrûbel, J. L., De Oliveira, J. A. A., Painting, S. J., Richardson, A. J., Shannon, L. J., Schülein, F. H., van der Lingen, C. D., and Verheye, H. M. 1998. Multiple factors affecting South African anchovy recruitment in the spawning, transport and nursery areas. South African Journal of Marine Science, 19: 211–225.

Hutchings, L., Beckley, L. E., Griffiths, M. H., Roberts, M. J., Sundby, S., and van der Lingen, C. D. 2002. Spawning on the edge: spawning grounds and nursery areas around the southern African coastline. Marine and Freshwater Research, 53: 307–318.

Hüssy, K. 2010. Why is age determination of Baltic cod (*Gadus morhua*) so difficult? ICES Journal of Marine Science, 67: 1198–1205.

Hüssy, K., Hinrichsen, H.-H., Fey, D. P., Walther, Y., and Velasco, A. 2010. The use of otolith microstructure to estimate age in adult Atlantic cod *Gadus morhua*. Journal of Fish Biology, 76: 1640–1654.

Hüssy, K., and Mosegaard, H. 2004. Atlantic cod (*Gadus morhua*) growth and otolith accretion characteristics modelled in a bioenergetics context. Canadian Journal of Fisheries and Aquatic Sciences, 61: 1021–1031.

Hüssy, K., Mosegaard, H., and Jessen, F. 2004. Effect of age and temperature on amino acid composition and the content of different protein types of juvenile Atlantic cod (*Gadus morhua*) otoliths. Canadian Journal of Fisheries and Aquatic Sciences, 61: 1012–1020.

Hyams, D. G. 2010. CurveExpert software. http://www.curveexpert.net/.

ICSEAF. 1983. Otolith interpretation guide, Hake. International Commission for Southeast Atlantic Fisheries, 1: 70 pp.

Iilende, T., Strømme, T., and Johnsen, E. 2001. Dynamics of the pelagic component of the Namibian hake stocks. South African Journal of Marine Science, 23: 337–346.

Inada, T. 1981. Studies on the merluccid fishes. Bulletin of Far Seas Fisheries Research Laboratory (Shimizu), 18: 172 pp.

Investment House Namibia. 2011. Namibia macro-economic outlook 2011–2012. Namibian Economic Research, 2 March 2011: 54 pp. http://www.investmenthousenamibia.com/IHN_Economic_outlook_2011.pdf

Jarre[-Teichmann], A., Shannon, L. J., Moloney, C. L., and Wickens, P. A. 1998. Comparing trophic flows in the southern Benguela to those in other upwelling ecosystems. South African Journal of Marine Science, 19: 391–414.

Jobling, M. 1981. Temperature tolerance and the final preferendum rapid methods for the assessment of optimum growth temperatures. Journal of Fish Biology, 19: 439–455.

Johnsen, E., and Iilende, T. 2007. Factors affecting the diel variation in commercial CPUE of Namibian hake – Can new information improve standard survey estimates? Fisheries Research, 88: 70–79.

Johnsen, E., and Kathena, J. N. 2011. A robust method to separate Namibian commercial hake catches by species – a necessary step towards a biologically realistic hake stock assessment. Submitted to African Journal of Marine Science: 27 pp.

Johnson, J. B., and Omland, K. S. 2004. Model selection in ecology and evolution. TRENDS in Ecology and Evolution, 19 (2): 101–108.

Juanes, F., and Conover, D. O. 1994. Rapid growth, high feeding rates, and early piscivory in young-of-the year bluefish (*Pomatomus saltatrix*). Canadian Journal of Fisheries and Aquatic Sciences, 51: 1752–1761.

Kacher, M., and Amara, R. 2005. Distribution and growth of 0-group European hake in the Bay of Biscay and Celtic Sea: a spatial and inter-annual analyses. Fisheries Research, 71 (3): 373–378.

Kainge, P., Kathena, J. N., Iitembu, J., and Wedeinge, J. 2006. Surveys of the hake Stocks 10 January – 19 February 2006. National Marine Information and Research Centre (NatMIRC), Swakopmund, Namibia: 75 pp.

Kainge, P., Kjesbu, O. S., Thorsen, A., and Salvanes, A. G. 2007. *Merluccius capensis* spawn in Namibian waters, but do *M. paradoxus*? African Journal of Marine Science, 29 (3): 379–392.

Kalish, J. M., Beamish, R. J., Brothers, E. B., Casselman, J. M., Francis, R. I. C. C., Mosegaard, H., Panfili, J., Prince, E. R., Thresher, R. E., Wilson, C. A., and Wright, P. J. 1995. Glossary for otolith studies. *In* Recent developments in fish otolith research, pp. 723–729. Ed. by D. H. Secor, J. M. Dean, and S. E. Campana. University of South Carolina Press, Columbia, USA.

Kashava, S. 2009. Age and growth of Namibian Cape hake (*Merluccius capensis*). Open Section Project for Experiential Learning for the Diploma in Fisheries Resource Management, Cape Peninsula University of Technology, Cape Town, South Africa: 21 pp.

Kathena, J. N. 2004. A species separated study of catch per unit of effort in the Namibian hake fishery. MPhil dissertation, University of Bergen, Norway: 57 pp.

Kawahara, S., and Nagai, T. 1980. Mixing of three species of *Merluccius* in the ICSEAF area. Collection of Scientific Papers of the International Commission for Southeast Atlantic Fisheries, 7 (ii): 169–174.

Kemper, J. 2006a. Breeding seasonality patterns and factors influencing breeding success of African Penguins *Spheniscus demersus* in Namibia. Chapter Three. *In* Heading towards extinction? Demography of the African penguin in Namibia, pp. 39–64. PhD thesis, University of Cape Town, South Africa.

Kemper, J. 2006b. Effect of age and breeding status on moult phenology of adult African Penguins *Spheniscus demersus* in Namibia. Chapter Seven. *In* Heading towards extinction? Demography of the African penguin in Namibia, pp. 113–137. PhD thesis, University of Cape Town, South Africa.

Kimura, D. K., Kastelle, C. R., Goetz, B. J., Gburski, C. M., and Buslov, A. V. 2006. Corroborating the ages of walleye pollock (*Theragra chalcogramma*). Marine and Freshwater Research, 57: 323–332.

Kimura, D. K., Mandapat, R. R., and Oxford, S. L. 1979. Method, validity, and variability in the age determination of yellowtail rockfish (*Sebastes flavidus*) using otoliths. Journal of the Fisheries Research Board of Canada, 36: 377–383.

Kirchner, C. H. 2010. Determinants of resource rents in the Namibian hake industry. MBA research report, University of Cape Town, South Africa: 95 pp.

Kirchner, C. H., Kainge, P., and Kathena, J. N. 2011. Evaluation of the status of the Namibian hake resource (*Merluccius* spp.) using statistical catch-at-age analysis. MARAM International Fisheries Stock Assessment Review Workshop, November 2011, Cape Town, South Africa, MARAM IWS/DEC11/H/MODEL/BG2: 39 pp.

Kirkman, S. P., Mecenero, S., Roux, J.-P., Meÿer, M. A., and Kotze, P. G. H. 2007. Monitoring the diet of Cape fur seals. Chapter 1. *In* Annex 2: Manual of methods for monitoring Cape fur seals. Final report of the BCLME (Benguela Current Large Marine Ecosystem) project on top predators as biological indicators of ecosystem

change in the BCLME. LMR/EAF/03/02: pp. 5–16. Ed. by S. P. Kirkman. Cape Town, South Africa. http://web.uct.ac.za/depts/stats/adu/bclme_report.htm

Ladah, L. B., Tapia, F. J., Pineda, J., and López, M. 2005. Spatially heterogeneous, synchronous settlement of *Chthamalus* spp. larvae in northern Baja California. Marine Ecology Progress Series, 302: 177–185.

Landaeta, M. F., and Castro, L. R. 2006. Spawning and larval survival of the Chilean hake *Merluccius gayi* under later summer conditions in the Gulf of Arauco, central Chile. Fisheries Research, 77: 115–121.

Laslett, G. M., Eveson, J. P., and Polacheck, T. 2004. Fitting growth models to length frequency data. ICES Journal of Marine Science, 61: 218–230.

Lehodey, P., and Grandperrin, R. 1996. Age and growth of the alfonsino *Beryx splendens* over the seamounts off New Caledonia. Marine Biology, 125: 249–258.

Lloris, D., Matallanas, J., and Oliver, P. 2005. Hakes of the world (Family Merlucciidae). An annotated and illustrated catalogue of hake species known to date. FAO Species Catalogue for Fishery Purposes, 2: 57 pp.

Ludynia, K., Roux J.-P., Jones, R., Kemper, J., and Underhill, L. G. 2010. Surviving off junk: Low-energy prey dominates the diet of African penguins *Spheniscus demersus* at Mercury Island, Namibia, between 1996 and 2009. African Journal of Marince Science, 32: 562–572.

Lutjeharms, J. R. E., and Valentine, H. R. 1987. Water types and volumetric considerations of the South-East Atlantic upwelling regime. South African Journal of Marine Science, 5: 63–71.

Macchi, G. J., Pájaro, M., and Ehrlich, M. 2004. Seasonal egg production pattern of the Patagonian stock of Argentine hake (*Merluccius hubbsi*). Fisheries Research, 67 (1): 25–38.

Macchi, G. J., Pájaro, M., and Madirolas, A. 2005. Can a change in the spawning pattern of Argentine hake (*Merluccius hubbsi*) affect its recruitment? Fishery Bulletin, 103 (2): 445–452.

MacDonald, P. D. M., and Pitcher, T. J. 1979. Age-groups from size-frequency data: A versatile and efficient method of analyzing distribution mixtures. Journal of the Fisheries Research Board Canada, 36: 987–1001.

Mackas, D. L., Kieser, R., Saunders, M., Yelland, D. R., Brown, R. M., and Moore, D. F. 1997. Aggregation of euphausiids and Pacific hake (*Merluccius productus*) along the outer continental shelf off Vancouver Island. Canadian Journal of Fisheries and Aquatic Sciences, 54: 2080–2097.

MacLean, J. A., and Evans, D. O. 1981. The stock concept, discreteness of fish stocks and fisheries management. Canadian Journal of Fisheries and Aquatic Sciences, 38 (12): 1889–1898.

Macpherson, E. 1976. Relative growth of *Merluccius capensis*. Collection of Scientific Papers of the International Commission for Southeast Atlantic Fisheries, 3: 115–118.

Macpherson, E., and Duarte, C. M. 1991. Bathymetric trends in demersal fish size: is there a general relationship? Marine Ecology Progress Series, 71: 103–112.

Macpherson, E., and Gordoa, A. 1994. Effect of prey densities on cannibalism in Cape hake (*Merluccius capensis*) off Namibia. Marine Biology, 119 (1): 145–149.

Macpherson, E., Masó, M., Barange, M., and Gordoa, A. 1991. Relationship between measurements of hake biomass and sea surface temperature off southern Namibia. South African Journal of Marine Science, 10: 213–217.

Macpherson, E., and Roel, B. A. 1987. Trophic relationships in the demersal fish community off Namibia. South African Journal of Marine Science, 5: 585–596.

Macpherson, E., Roel, B. A., and Morales, B. Y. O. 1985. Reclutamiento de la merluza y abundancía y distribución de differentes especies comerciales en las divisiones 1.4 y 1.5 durante 1983–1984. Collection of Scientific Papers of the International Commission for Southeast Atlantic Fisheries, 12 (ii): 1–61.

Maree, R. 1999. Environmental influences on the daytime vertical distribution of Cape hakes and implications for demersal trawl estimates of hake abundance off the west coast of South Africa. Rhodes University, Grahamstown, South Africa: 97 pp.

Mas-Riera, J. 1991. Changes during growth in the retinal structure of three hake species, *Merluccius* spp. (Teleostei: Gadiformes), in relation to their depth distribution and feeding. Journal of Experimental Marine Biology and Ecology, 152 (1): 91–104.

Mas-Riera, J., Lombarte, A., Gordoa, A., and Macpherson, E. 1990. Influence of Benguela upwelling on the structure of demersal fish populations off Namibia. Marine Biology, 104 (2): 175–182.

Maynou, F., Lleonart, J., and Cartes, J. E. 2003. Seasonal and spatial variability of hake (*Merluccius merluccius* L.) recruitment in the NW Mediterranean. Fisheries Research, 60: 65–78.

McCauley, R. W., and Casselman, J. M. 1981. The final preferendum as an index of the temperature for optimum growth in fish. *In* Aquaculture in heated effluents and recirculation systems, Volume II, Proceedings of the World Symposium, Stavanger, Norway, May 28–30, 1980, pp. 81–93. Ed. by K. Tiews. Heenemann Verlagsgesellschaft, Berlin.

McQueen, N., and Griffiths, M. H. 2004. Influence of sample size and sampling frequency on the quantitative dietary description of a predatory fish in the Benguela ecosystem. African Journal of Marine Science, 26 (1): 205–217.

Mecenero, S. 2005. Investigating fur seal diet using scats: recommendations for sampling and analysis. Chapter 8. *In* The diet of the Cape fur seal *Arctocephalus pusillus pusillus* in Namibia: variability and fishery interactions, pp. 135–181. PhD thesis, University of Cape Town, South Africa.

Mecenero, S., Roux, J.-P., Underhill, L. G., and Bester, M. N. 2006a. Diet of Cape fur seals *Arctocephalus pusillus pusillus* at three mainland breeding colonies in Namibia. 1. Spatial variation. African Journal of Marine Science, 28 (1): 57–71.

Mecenero, S., Roux, J.-P., Underhill, L. G., and Kirkman, S. P. 2006b. Diet of Cape fur seals *Arctocephalus pusillus pusillus* at three mainland breeding colonies in Namibia. 2. Temporal variation. African Journal of Marine Science, 28 (1): 73–88.

MFMR. 1991. Towards responsible development of the Fisheries Sector. White paper of the Ministry of Fisheries and Marine Resources, Republic of Namibia: 65 pp.

MFMR. 1992. Sea Fisheries Act (Act no. 29 of 1992). Government Gazette, Republic of Namibia, 493: 57 pp.

MFMR. 2000. Marine Resources Act 2000 (Act no. 27 of 2000). Government Gazette, Republic of Namibia, 2458: 4 pp.

MFMR. 2003. Statistics. www.mfmr.gov.na http://209.88.21.36/opencms/opencms/grnnet/MFMR/Fishing_Industry/statistics.html

MFMR. 2004. Namibia's Marine Resources Policy. Towards responsible development and management of the Marine Resources Sector. Ministry of Fisheries and Marine Resources, Republic of Namibia: 23 pp. http://209.88.21.36/opencms/export/sites/default/grnnet/MFMR/Laws_and_Policies/docs/whitepaper.pdf

Millar, D. 1996. Diet composition estimates for *Arctocephalus pusillus pusillus* from prey remains in the faeces. An experimental evaluation. BSc (Honours) dissertation, University of Cape Town, South Africa: 25 pp.

Millar, D. L. 2000. Distribution and abundance of Cape hakes (*Merluccius capensis* and *Merluccius paradoxus*) in relation to environmental variation in the southern Benguela system. MSc dissertation, University of Cape Town, South Africa: 126 pp.

Miller, J. A., Wells, B. K., Sogard, S. M., Grimes, C. B., and Cailliet, G. M. 2010. Introduction to proceedings of the 4th International Otolith Symposium. Environmental Biology of Fishes, 89 (3–4): 203–207.

Mohrholz, V., Bartholomae, C. H., van der Plas, A. K., and Lass, H. U. 2008. The seasonal variability of the northern Benguela undercurrent and its relation to the oxygen budget on the shelf. Continental Shelf Research, 28: 424–441.

Mombeck, F. 1969. Vorläufiger Bericht über Seehecht-Untersuchungen im SO Atlantik Institut für Seefischerei der Bundesforschungsanstalt für Fischerei, Aussenstelle, Bremerhaven. Archiv für Fischereiwissenschaft, 21: 45–61.

Mombeck, F. 1971. 3. Mitteilung über Seehecht im SO Atlantik: Alter und Wachstum. Archiv für Fischereiwissenschaft, 22: H–I.

Monteiro, P. M. S., Nelson, G., van der Plas, A. K., Mabille, E., Bailey, G. W., and Klingelhoeffer, E. 2005. Internal tide-shelf topography interactions as a forcing factor governing the large-scale distribution and burial fluxes of particulate organic matter (POM) in the Benguela upwelling system. Continental Shelf Research, 25: 1864–1876.

Morales, B. Y. O., and Payne, A. I. L. 1985. A note on the interpretation of hake otoliths. Collection of Scientific Papers of the International Commission for Southeast Atlantic Fisheries, 12 (ii): 69–79.

Morales-Nin, B. Y. O. 1987. The influence of environmental factors on microstructure of otoliths of three demersal fish species caught off Namibia. South African Journal of Marine Science, 5: 255–262.

Morales-Nin, B. Y. O. 1991. Growth of Cape hake *Merluccius capensis* off Namibia determined by means of length frequency analysis and age/length data. South African Journal of Marine Science, 10: 53–60.

Morales-Nin, B. Y. O. 2000. Review of the growth regulation processes of otolith daily increment formation. Fisheries Research, 46: 53–67.

Morales-Nin, B. Y. O. 2001. Mediterranean deep-water fish age determination and age validation: the state of the art. Fisheries Research, 51: 377–383.

Morales-Nin, B. Y. O. and Aldebert, Y. 1997. Growth of juvenile *Merluccius merluccius* in the Gulf of Lions (NW Mediterranean) based on otolith microstructure and length-frequency analysis. Fisheries Research, 30: 77–85.

Morales-Nin, B. Y. O., Bjelland, R. M., and Moksness, E., 2005. Otolith microstructure of a hatchery reared European hake (*Merluccius merluccius*). Fisheries Research, 74: 300–305.

Morales-Nin, B. Y. O., and Panfili, J. 2005. Seasonality in the deep sea and tropics revisited: what can otoliths tell us? Marine and Freshwater Research, 56 (5): 585–598.

Morales-Nin, B. Y. O., and Ralston, S. 1990. Age and growth of *Lutjanus kasmira* in Hawaiian waters. Journal of Fish Biology, 36: 191–203.

Morales-Nin, B. Y. O., Torres, G. J., Lombarte, A., and Recasens, L. 1998. Otolith growth and age estimation in the European hake. Journal of Fish Biology, 53: 1155–1168.

Morales-Nin, B. Y. O. and Moranta, J. 2004. Recruitment and post-settlement growth of juvenile *Merluccius merluccius* on the western Mediterranean shelf. Scientia Marina, 68: 399–409.

Moranta, J., Palmer, M., Massutí, E., Stefanescu, C., and Morales-Nin, B. Y. O. 2004. Body fish size tendencies within and among species in the deep-sea of the western Mediterranean. Scientia Marina, 68 (S3): 141–152.

MRAG. 2005. Review of impacts of Illegal, Unreported and Unregulated fishing on developing countries. Final Report, July 2005: 176 pp. http://webarchive.nationalarchives.gov.uk/+/http:/www.dfid.gov.uk/pubs/files/illegal-fishing-mrag-report.pdf

Natanson, L. J. 1993. Effect of temperature on band deposition in the little skate, *Raja erinacea*. Copeia, 1993 (1): 199–206.

Natanson, L. J., and Cailliet, G. M. 1990. Vertebral growth zone deposition in Pacific angel sharks. Copeia, 1990: 1133–1145.

Natanson, L. J., Wintner, S. P., Johansson, F., Piercy, A., Campbell, P., De Maddalena, A., Gulak, S. J. B., Human, B., Fulgosi, F. C., Ebert, D. A., Hemida, F., Mollen, F. H., Vanni, S., Burgess, G. H., Compagno, L. J. V., and Wedderburn-Maxwell, A. 2008. Ontogenetic vertebral growth patterns in the basking shark *Cetorhinus maximus*. Marine Ecology Progress Series, 361: 267–278.

Nelson, G., and Hutchings, L. 1983. The Benguela upwelling area. Progress in Oceanography, 12: 333–356.

Nelson, R. S., and Manooch, C. S. III. 1982. Growth and mortality of red snapper in the West-Central Atlantic Ocean and Northern Gulf of Mexico. Transactions of the American Fisheries Society, 111: 465–475.

Nichy, F. E. 1969. Growth patterns on otoliths from young silver hake, *Merluccius bilinearis* (Mitch.). International Commission for Northeast Atlantic Fisheries Selected Papers, 6: 107–117.

Norbis, W., Lorenzo, M. I., and Torres, G. J. 1999. Intra-annual growth variations of young-of-the-year hake (*Merluccius hubbsi*) of the Uruguayan continental shelf based on otolith analysis. Fisheries Research, 44 (2): 129–137.

O'Toole, M. J. 1976. Distribution and abundance of the hake *Merluccius* spp. off South West Africa 1972–1974. Collection of Scientific Papers of the International Commission for Southeast Atlantic Fisheries, 2: 151–158.

O'Toole, M. J. 1978. Aspects of the early life history of the hake, *Merluccius capensis* Castelnau, off South West Africa. Fisheries Bulletin of South Africa, 10: 20–36.

Ocampo Reinaldo, M., González, R., and Romero, M. A. 2011. Feeding strategy and cannibalism of the Argentine hake *Merluccius hubbsi*. Journal of Fish Biology, 79: 1795–1814.

Oelofsen, B. W. 1999. Fisheries management: the Namibian approach. ICES Journal of Marine Science, 56 (6): 999–1004.

Olivar, M.-P. 1990. Spatial patterns of ichthyoplankton distribution in relation to hydrographic features in the northern Benguela region. Marine Biology, 106: 39–48.

Olivar, M.-P., Rubiés, P., and Salat, J. 1988. Early life history and spawning of *Merluccius capensis* Castelnau in the northern Benguela current. South African Journal of Marine Science, 6: 245–254.

Olivar, M.-P., and Shelton, P. A. 1993. Larval fish assemblages of the Benguela current. Chapter 2. *In* Advances in the early life history of fishes, pp. 450–474. Ed. by H. G. Moser, P. E. Smith, and L. A. Fuiman.

Otxotorena, U., Díez, G., López de Abechuco, E., Santurtún, M., and Lucio, P. 2010. Estimation of age and growth of juvenile hakes (*Merluccius merluccius* Linneaus,

1758) of the Bay of Biscay and Great Sole by means of the analysis of macro and microstructure of the otoliths. Fisheries Research, 106: 337–343.
Panfili, J., de Pontual, H., Troadec, H., and Wright, P. J. 2002. Manual of Fish Sclerochronology. Ifremer-IRD coedition. http://archimer.ifremer.fr/doc/00017/12801/, Brest, France. 464 pp.
Pannella, G. 1971. Fish otoliths: Daily growth layers and periodical patterns. Science, 173: 1124–1127.
Pannella, G. 1974. Otolith growth patterns: an aid in age determination in temperate and tropical fishes. *In* Aging of fish, pp. 28–39. Ed. by T. B. Bagenal. Unwin Brothers Limited, Old Woking, Surrey, UK.
Pannella, G. 1980. Growth patterns in fish sagittae. *In* Sceletal growth of aquatic organisma: Biological records of environmental change, pp. 519–560. Ed. by D. C. Rhoads, and R. A. Lutz. Plenum Press, New York.
Parker, H. W., and Stott, F. C. 1965. Age, size and vertebral calcification in the basking shark, *Cetorhinus maximus* (Gunnerus). Zoologische Mededelingen, 40: 305–319.
Pauly, D. 1980. On the interrelationship between natural mortality, growth parameters, and mean environmental temperature in 175 fish stocks. Journal du Conseil International pour l'Exploration de la Mer, 39 (2): 175–192.
Pawson, M. G., and Jennings, S. 1996. A critique of methods for stock identification in marine capture fisheries. ICES Journal of Marine Science, 25: 203–217.
Payá Contreras, I. 2002. An overview of the Chilean hake (*Merluccius gayi gayi*) fishery. BENEFIT/NRF Stock assessment workshop, January 2004, Cape Town, South Africa. Unpublished report: 28 pp.
Payne, A. I. L. 1989. Cape hakes. *In* Oceans of life off southern Africa, pp. 136–147. Ed. by A. I. L. Payne, and R. J. M. Crawford. Vlaeberg Publishers, Cape Town, South Africa.
Payne, A. I. L., and Punt, A. E. 1995. Biology and fisheries of South African hakes (*M. capensis* and *M. paradoxus*). Chapter 2. *In* Hake fisheries ecology and markets, pp. 15–47. Ed. by J. Alheit, and T. J. Pitcher. Chapman & Hall, London.
Payne, A. I. L., Rose, B., and Leslie, R. W. 1987. Feeding of hake and a first attempt at determining their trophic role in the South African west coast marine environment. African Journal of Marine Science, 5: 471–501.
Pearson, D. E. 1996. Timing of hyaline-zone formation as related to sex, location, and year of capture in otoliths of the widow rockfish, *Sebastes entomelas*. Fishery Bulletin, 94: 190–197.
Pepin, P. and Myers, R. A. 1991. Significance of egg and larval size to recruitment variability of temperate marine fish. Canadian Journal of Fisheries and Aquatic Sciences, 48: 1820–1828.
Petersen, C. G. J. 1891. Eine Methode zur Bestimmung des Alters und des Wuchses des Fisches. Mitteilungen des Deutschen Seefischerei-Vereins, 11: 226–235.
Pillar, S. C., and Barange, M. 1995. Diel feeding periodicity, daily ration and vertical migration of juvenile Cape hake off the west coast of South Africa. Journal of Fish Biology, 47: 753–768.
Pillar, S. C., and Barange, M. 1997. Diel variability in bottom trawl catches and feeding activity of the Cape hakes off the west coast of South Africa. ICES Journal of Marine Science, 54: 485–499.
Pilling, G. M., Millner, R. S., Easy, M. W., Maxwell, D. L., and Tidd, A. N. 2007. Phenology and North Sea cod *Gadus morhua* L.: has climate change affected otolith annulus formation and growth? Journal of Fish Biology, 70: 584–599.

Pinheiro, J., Bates, D., DebRoy, S., Sarkar, D., and the R Core team. 2009. nlme: Linear and Nonlinear Mixed Effects Models. R package version 3: 92 pp.

Piñeiro, C., and Hunt, J. J. 1989. Comparative study on growth of European hake (*Merluccius merluccius* L.) from southern stock using whole and sectioned otoliths, and length frequency distributions. ICES CM, 1989/G 37: 16 pp.

Piñeiro, C., Rey, J., de Pontual, H., and García, A. 2008. Growth of Northwest Iberian juvenile hake estimated by combining sagittal and transversal otolith microstructure analyses. Fisheries Research, 93: 173–178.

Piñeiro, C., Rey, J., de Pontual, H., and Goñi, R. 2007. Tag and recapture of European hake (*Merluccius merluccius* L.) off the Northwest Iberian Peninsula: First results support fast growth hypothesis. Fisheries Research, 88: 150–154.

Piñeiro, C., and Saínza, M. 2003. Age estimation, growth and maturity of the European hake (*Merluccius merluccius* (Linnaeus, 1758)) from Iberian Atlantic waters. ICES Journal of Marine Science, 60 (5): 1086–1102.

Polloni, P. T., Haedrich, R. L., Rowe, G. T., and Clifford, C. H. 1979. The size-depth relationship in deep ocean animals. Internationale Revue der gesamten Hydrobiologie und Hydrographie, 64: 39–46.

Porebski, J. 1976. The morphology and distribution of hake *Merluccius* spp. in early stages of development, as a basis for determination of regions and periods of concentration of the species. Collection of Scientific Papers of the International Commission for Southeast Atlantic Fisheries, 3: 165–173.

Pozo Arteaga, E. 1976. Some data on the biology of the Cape hake (*Merluccius capensis*) inhabiting the Cunene and Cape Cross divisions of the ICSEAF area. Collection of Scientific Papers of the International Commission for Southeast Atlantic Fisheries, 3: 179–185.

Pratt, H. L., and Casey, J. G. 1983. Age and growth of the shortfin mako *Isurus oxyringhus*, using four methods. Canadian Journal of Fisheries and Aquatic Sciences, 40: 1944–1957.

Preñski, L. 1978. Studies on hake, *Merluccius capensis*, in ICSEAF Divisions 1.4 and 1.5 in 1977. Collection of Scientific Papers of the International Commission for Southeast Atlantic Fisheries, 5: 89–94.

Pschenichnii, B. P. 1976. On some changes in linear length of South African hake *Merluccius merluccius capensis*. Collection of Scientific Papers of the International Commission for Southeast Atlantic Fisheries, 3: 175–178.

Punt, A. E., and Leslie, R. W. 1991. Estimates of some biological parameters for the Cape hakes off the South African west coast. South African Journal of Marine Science, 10: 271–284.

Punt, A. E., and Leslie, R. W. 1992. Estimation of the annual consumption of food by Cape hake *Merluccius capensis* and *M. paradoxus* off the South African west coast. South African Journal of Marine Science, 12: 611–634.

Punt, A. E., and Leslie, R. W. 1995. The effects of future consumption by the Cape fur seal on catches and catch rates of the Cape hakes. 1. Feeding and diet of the Cape hakes *Merluccius capensis* and *M. paradoxus*. South African Journal of Marine Science, 16: 37–55.

R Development Core Team. 2009. R: A language and environment for statistical computing. R Foundation for Statistical Computing, Vienna, Austria. ISBN 3-900051-07-0, URL http://www.R-project.org

Rademeyer, R. A. 2003. Assessment of and management procedures for the hake stocks off southern Africa. MSc dissertation, University of Cape Town, South Africa: 214 pp.

Recasens, L., Chiericoni, V., and Belcari, P. 2008. Spawning pattern and batch fecundity of the European hake (*Merluccius merluccius* (Linnaeus, 1758)) in the western Mediterranean. Scientia Marina, 72(4): 721-732.

Relini, L. O., Papaconstantinou, C., Jukic-Peladic, S., de Sola, L. G., Piccinetti, C., Kavadas, S., and Rossi, M. 2002. Distribution of the Mediterranean hake populations (*Merluccius merluccius smiridus* Rafinesque, 1810) (Ostheichthyes: Gadiformes) based on six years monitoring by trawl-surveys: some implications for management. Scientia Marina, 66 (S2): 21–38.

Renzi, M. A., and Pérez, M. A. 1992. Un criterio pra la determinacion de la edad en juveniles de merluza (*Merluccius hubbsi*) mediante la lectura de otolitos. Frente Maritimo, 11 (A): 15–31.

Rey, J., Fernández-Peralta, L., Esteban, A., García-Cancela, R., Salmerón, F., Ángel Puerto, M., and Piñeiro, C. 2012. Does otolith macrostructure record environmental or biological events? The case of black hake (*Merluccius polli* and *Merluccius senegalensis*). Fisheries Research, 113: 159–172.

Ricker, W. E. 1975. Computation and interpretation of biological statistics of fish populations. Bulletin of the Fisheries Research Board of Canada, 191: xviii + 382 pp.

Rochet, M. 2000. A comparative approach to life-history strategies and tactics among four orders of teleost fish. ICES Journal of Marine Science, 57 (2): 228–239.

Roel, B. A., and Bailey, G. W. 1987. Preliminary investigations of the relationship between hake abundance and hydrological parameters in the Benguela system. Collection of Scientific Papers of the International Commission for Southeast Atlantic Fisheries, 14 (ii): 193–201.

Roel, B. A., and Macpherson, E. 1988. Feeding of *Merluccius capensis* and *M. paradoxus* off Namibia. South African Journal of Marine Science, 6: 227–243.

Roux, E. R. 1947. Growth rates of the South African hake or stockfish. South African Journal of Science, 1 (2): 46–48.

Roux, J.-P. 2004. Cape hakes (*Merluccius capensis*) as prey of Cape fur seals in Namibia: prey size, juvenile hake growth rates and hake cohort strength estimations from scats analysis (1994–2003). BENEFIT / NRF Stock assessment workshop, January 2004, Cape Town, South Africa, BEN/JAN04/NH/3c: 14 pp.

Roux, J.-P. 2006. Juvenile Cape hake (*Merluccius capensis*) and early growth parameters, birth date estimates and recruitment index: the 2005 cohort. Hake working group document, Ministry of Fisheries and Marine Resources, Namibia, 24 November 2006: 3 pp.

Roux, J.-P., and Shannon, L. J. 2004. Ecosystem approach to fisheries management in the northern Benguela: the Namibian experience. African Journal of Marine Science, 26: 79–93.

Saetersdal, G., and Villegas, L. 1968. Estudio del tamaño, crecimiento y madurez de la merluza (*Merluccius gayi*) en aguas chilenas. Publicasiones del Instituto de Fomento Pesquero, Santiago, Chile, 34: 52 pp. (In Spanish, with English abstract)

Salat, J., Masó, M., and Boyd, A. 1992. Water mass distribution and geostrophic circulation off Namibia during April 1986. Continent Shelf Research, 12: 355–366.

Saunders, M. W., and McFarlane, G. A. 1997. Observations on the spawning distribution and biology of offshore Pacific hake (*Merluccius productus*). CalCOFI Report, 38: 147–157.

Schill, D. J. 2009. Population studies of desert redband trout. PhD thesis, University of Idaho, USA: 186 pp.

Schill, D. J., Mamer, E. R. J. M., and LaBar, G. W. 2010. Validation of scales and otoliths for estimating age of redband trout in high desert streams of Idaho. Environmental Biology of Fishes, 89: 319–332.

Schramm, H. L. 1989. Formulation of annuli in otoliths of bluegills. Transactions of the American Fisheries Society, 118: 546–555.

Shannon, L. J., and Jarre[-Teichmann], A. 1999. A model of trophic flows in the northern Benguela upwelling system during the 1980s. South African Journal of Marine Science, 21: 349–366.

Shannon, L. J., and Roux, J.-P. 2000. Trophic interactions in the Benguela ecosystem and their implications for multispecies management of fisheries. Report for the period December 1998 – December 1999. Implementation of the Kyoto conference plans of action. Component 2: Multispecies management, GCP/INT/643/JPN 2.3: 6 pp.

Shannon, L. J., Roux, J.-P., and Jarre, A. 2001. Trophic interactions in the Benguela ecosystem and their implications for multispecies management of fisheries. Report on progress to January 2001: Exploring multispecies management options using the completed Northern Benguela Ecosystem Model, GCP/INT/643/JPN 2.4: 56 pp.

Shannon, L. V. 1985. The Benguela ecosystem. Part I. Evolution of the Benguela, physical features and processes. Oceanography and Marine Biology Annual Review, 23: 105–182.

Shannon, L. V. 1986. Some distinguishing features of the Benguela system. Collection of Scientific Papers of the International Commission for Southeast Atlantic Fisheries, 13 (ii): 225–228.

Shannon, L. V., Boyd, A. J., Brundrit, G. B., and Tauton-Clark, J. 1986. On the existence of an EI Niño-type phenomenon in the Benguela System. Journal of Marine Research, 44 (3): 495–520.

Shannon, L. V., Crawford, R. J. M., Brundrit, G. B., and Underhill, L. G. 1988. Responses of fish populations in the Benguela ecosystem to environmental change. Journal du Conseil International pour l'Exploration de la Mer, 45: 5–12.

Singh, S., Melo, Y. C., and Glazer, J. P. 2011. Merluccius *capensis* and *M. paradoxus* length at 50% maturity based on histological analyses of gonads from surveys. Demersal working group document, Department of Agriculture, Forestry and Fisheries, Cape Town, South Africa, FISHERIES/2011/JUL/SWG-DEM/33: 6 pp.

Skern-Mauritzen, M., Kirkman, S. P., Olsen, E., Bjørge, A., Drapeau, L., Meÿer, M. A., Roux, J.-P., Swanson, S., and Oosthuizen, W. H. 2009. Do inter-colony differences in Cape fur seal foraging behaviour reflect large-scale changes in the northern Benguela ecosystem? African Journal of Marine Science, 31 (3): 399–408.

Smale, M. J., Watson, G., and Hecht, T. 1995. Otolith atlas of southern African marine fishes, 1. JLB Smith Institute of Ichthyology, Grahamstown, South Africa: 149 plates + xiv + 253 pp.

Smith, A. D. M. (Chair), Fernandez, C., Parma, A., and Punt, A. E. 2011. International review panel report for the 2011 International Fisheries Stock Assessment Workshop 28 November – 2 December 2011, UCT. MARAM International Fisheries Stock Assessment Review Workshop, November 2011, Cape Town, South Africa: 20 pp.

Snelgrove, P. V. R., and Haedrich, R. L. 1985. Structure of the deep demersal fish fauna off Newfoundland. Marine Ecology Progress Series, 27: 99–107.

Sogard, S. M. 1997. Size-selective mortality in the juvenile stage of teleost fishes: a review. Bulletin of Marine Science, 63 (3): 1129–1157.

Sparre, P., and Venema, S. C. 1998. Introduction to tropical fish stock assessment. Part 1. Manual. FAO Fisheries Technical Paper, 306 (1): 407 pp.

Stearns, S. C. 1976. Life history tactics: a review of the ideas. The Quarterly Review of Biology, 51: 3–47.

Stander, G. H. 1967. The Benguela current off South West Africa. Fisheries Bulletin of South Africa, 4: 1–7.

Stearns, S. C. 1989. Trade-offs in life-history evolution. Functional Ecology, 3 (3): 259–268.

Stearns, S. C. 2000. Life history evolution: successes, limitations, and prospects. Naturwissenschaften, 87: 476–486.

Stefanescu, C., Rucabado, J., and Lloris, D. 1992. Depth-size trends in western Mediterranean demersal deep-sea fishes. Marine Ecology Progress Series, 81: 205–213.

Stenevik, E. K., Lipinski, M. R., and Zaera, D. 2009. 2009 BCC survey No. 2. Transboundary survey between Namibia and South Africa with focus on the juvenile stage of deep water hake, 21 February – 5 March 2009. Cruise report No 2/2009. FAO PROJECT: CCP/INT/003/NOR. Cruise reports *Dr. Fridtjof Nansen* EAF-N2009/2, Bergen, Norway: 62 pp.

Steves, B. P., and Cowen, R. K. 2000. Settlement, growth, and movement of silver hake *Merluccius bilinearis* in nursery habitat on the New York Night continental shelf. Marine Ecology Progress Series, 196: 279–290.

Sundby, S., Boyd, A. J., Hutchings, L., O'Toole, M. J., Thorisson, K., and Thorsen, A. 2001. Interaction between Cape hake spawning and the circulation in the northern Benguela upwelling ecosystem. South African Journal of Marine Science, 23: 317–336.

Svedäng, H., Righton, D., and Jonsson, P. 2007. Migratory behaviour of Atlantic cod *Gadus morhua:* natal homing is the prime stock-separating mechanism. Marine Ecology Progress Series, 345: 1–12.

Szedlmayer, S. T., and Beyer, S. G. 2011. Validation of annual periodicity in otoliths of red snapper, *Lutjanus campechanus*. Environmental Biology of Fishes, 91: 219–230.

Tolimieri, N., and Levin, P. S. 2006. Assemblage structure of eastern Pacific groundfishes on the U.S. continental slope in relation to physical and environmental variables. Transactions of the American Fisheries Society, 135 (2): 317–332.

Traut, P. J. 1996. Diet and annual consumption for the Cape hakes on the Namibian shelf, with special reference to cannibalism. MPhil dissertation, University of Bergen, Norway: 66 pp.

Tserpes, G., Politou, C.-Y., Peristeraki, P., Kallianiotis, A., and Papaconstantinou, C. 2008. Identification of hake distribution pattern and nursery grounds in the Hellenic seas by means of generalized additive models. Hydrobiologia, 612: 125–133.

van der Lingen, C. D., Hutchings, L., Merkle, D., van der Westhuizen, J. J., and Nelson, G. 2001. Comparative spawning habitats of anchovy (*Engraulis capensis*) and sardine (*Sardinops sagax*) in the southern Benguela upwelling ecosystem. *In* Spatial processes and management of marine populations, pp. 185–209. Ed. by G. H. Kruse, N. Bez, A. J. Booth, M. Dorn, S. Hills, R. Lipcius, D. Pelletier, C. Roy, S. J. Smith, and D. Witherell. Alaska Sea Grant College Program, AK-SG-01-02, Fairbanks, USA.

van der Lingen, C. D., Shannon, L. J., Cury, P. M., Kreiner, A., Moloney, C. L., Roux, J.-P., and Vaz-Velho, F. 2006. Resource and ecosystem variability, including regime shifts, in the Benguela current system. Chapter 8. *In* The Benguela: Predicting a large marine environment, Large Marine Ecosystems, 14: 147–185. Ed. by L. V.

Shannon, G. Hempel, P. Malanotte-Rizzli, C. L. Moloney, and J. Woods. Elsevier, Amsterdam.

van der Plas, A., Titus, J., Louw, D., and Kreiner, A. 2008. Oceanographic survey of transect 23°S as well as 20°, 18°, and 16°S off the coast of Namibia. 27 February to 23 March 2008. Ministry of Fisheries and Marine Resources, Swakopmund, Namibia. Cruise Report no. MOM 0308-01 R.V. Welwitschia: 15 pp.

van der Westhuizen, A. 2001. A decade of exploitation and management of the Namibian hake stocks. South African Journal of Marine Science, 23: 307–315.

van Eck, T. H. 1969. The South African hake, *Merluccius capensis* or *Merluccius paradoxus*? South African Shipping News and Fishing Industry Review, 24: 95–97.

Vilizzi, L., and Walker, K. F. 1999. Age and growth of the common carp, *Cyprinius carpio*, in the River Murray, Australia: validation, consistency of age interpretation, and growth models. Environmental Biology of Fishes, 54: 77–106.

Voges, E. 1995. Attempts to validate the age readings of Cape hake, *Merluccius capensis*, off Namibia. *In* Proceedings of the 6th annual research meeting of the Ministry of Fisheries and Marine Resources held at Swakopmund on 21–22 February 1995, pp. 80–89. Ministry of Fisheries and Marine Resources, Swakopmund, Namibia.

Voges, E., Gordoa, A., Bartholomae, C. H., and Field, J. G. 2002. Estimating the probability of different levels of recruitment for Cape hakes *Merluccius capensis* off Namibia using environmental indices. Fisheries Research, 58: 333–340.

von Bertalanffy, L. 1960. Principles and theory of growth. *In* Functional Aspects of Normal and Malignant Growth, pp. 137–259. Ed. by W. W. Nowinsky. Elsevier, Amsterdam.

von der Heyden, S., Lipinski, M. R., and Matthee, C. A. 2007a. Mitochondrial DNA analyses of the Cape hakes reveal an expanding, panmictic population for *Merluccius capensis* and population structuring for mature fish in *Merluccius paradoxus*. Molecular Phylogenetics and Evolution, 42: 517–527.

von der Heyden, S., Lipinski, M. R., and Matthee, C. A. 2007b. Species-specific genetic markers for identification of early life-history stages of Cape hakes, *Merluccius capensis* and *Merluccius paradoxus* in the southern Benguela Current. Journal of Fish Biology, 70 (Suppl. B): 262–268.

Warnes, G. R. Includes R source code and/or documentation contributed by (in alphabetical order): Bolker, B., Bonebakker, L., Gentleman, R., Huber, W., Liaw, A., Lumley, T., Maechler, M., Magnusson, A., Moeller, S., Schwartz, M., and Venables, B. 2009. gplots: Various R programming tools for plotting data. R package version 2.7.4. http://CRAN.R-project.org/package=gplots

Watermeyer, K. E., Shannon, L. J., Roux, J.-P., and Griffiths, C. L. 2008. Changes in the trophic structure of the northern Benguela before and after the onset of industrial fishing. African Journal of Marine Science, 30 (2): 383–403.

Weidlich, B. 2006. Hake needs protection: Minister. The Namibian, 3. 11. 2006. http://www.namibian.com.na/

West, W. M. 2009. Age determination, back-calculation of ring formation date and growth of Namibian shallow-water hake (*Merluccius capensis*). BSc (Honours) dissertation, University of Cape Town, South Africa: 43 pp.

Weyl, O. L. F., and Booth, A. J. 1999. On the life history of a cyprinid fish, *Labeo cylindricus*. Environmental Biology of Fishes, 55: 215–225.

Wilhelm, M. R. 2005. Indirect age validation, growth and age at sexual maturity of the hakes, *Merluccius capensis* and *M. paradoxus*, off Namibia. *In* Southern African Marine Science Symposium (SAMSS), ORI: Durban, South Africa.2005 (12): 84.

Wilhelm, M. R., Brinkman, F. V., Mweenda, T., and Kashava, S. 2007. Age distributions, length- weight- and maturity-at-age data of the Namibian hakes, *Merluccius capensis* and *M. paradoxus*, updated for the 2007 assessment. Hake demersal working group report, February 2007, Ministry of Fisheries and Marine Resources, Swakopmund, Namibia, DWG/HK/07/04: 15 pp.

Wilhelm, M. R., Durholtz, M. D., and Kirchner, C. H. 2008. The effects of ageing biases on stock assessment and management advice: A case study on Namibian horse mackerel. African Journal of Marine Science, 30 (2): 255–261.

Williams, E. H., and Ralston, S. 2002. Distribution and co-occurrence of rockfishes (Family: Sebastidae) over trawlable shelf and slope habitats of California and southern Oregon. Fishery Bulletin, 100 (4): 836–855.

Wilson, M. T., Mier, K. L., and Dougherty, A. 2011. The first annulus of otoliths: a tool for studying intra-annual growth of walleye pollock (*Theragra chalcogramma*). Environmental Biology of Fishes, 92: 53–63.

Winker, H., Weyl, O. L. F., Booth, A. J., and Ellender, B. R. 2010. Validating and corroborating the deposition of two annual growth zones in astericus otoliths of common carp *Cyprinus carpio* from South Africa's largest impoundment. Journal of Fish Biology, 77 (10): 2210–2228.

Woodhead, P. M., Hamukuaya, H., O'Toole, M. J., and McEnroe, M. 1998. Effects of oxygen depletion in shelf waters on hake populations off central and northern Namibia. *In* International Symposium, Environmental Variability in the South East Atlantic. Ed. by V. Shannon, and M. J. O'Toole. National Marine Information and Research Centre, Swakopmund, Namibia: 10 pp.

Woodhead, P. M., Hamukuaya, H., O'Toole, M. J., Strømme, T., Saetersdal, G., and Reiss, M., 1997. Catastrophic loss of two billion Cape hake recruits during widespread anoxia in the Benguela Current off Namibia. ICES International Symposium on Recruitment Dynamics of Exploited Marine Populations, Physical-Biological Interactions, September 22–24 1997: 105–106.

Wright, P. J., Talbot, C., and Thorpe, J. E. 1992. Otolith calcification in Atlantic salmon parr, *Salmo salar* L., and its relation to photoperiod and calcium metabolism. Journal of Fish Biology, 40: 779–790.

Wysokiñski, A. 1982. An attempt to apply analysis of modal lengths to the determination of growth of young hake (*Merluccius capensis*) / Essai d'application de l'analyse des longueurs modales pour la determination de la croissance du jeune merlu (*Merluccius capensis*). Collection of Scientific Papers of the International Commission for Southeast Atlantic Fisheries, 9 (ii): 343–352.

Wysokiñski, A. 1983. Photographic guide for determination from otoliths of the age of young hake *Merluccius capensis* from South West Africa (Namibia). South African Journal of Marine Science, 1: 19–55.

Yosef, T.-G., and Casselman, J. M. 1995. A procedure for increasing the precision of otolith age determination of tropical fish by differentiating biannual recruitment. *In* Recent developments in fish otolith research, pp. 247–269. Ed. by D. H. Secor, J. M. Dean, and S. E. Campana. University of South Carolina Press, Columbia, USA.

Zuur, A. F. 2010. AED: Data files used in mixed effects models and extensions in ecology with R. (2009). Zuur *et al.* (2009). R package version 1.0.

Zuur, A. F., Ieno, E. N., Walker, N. J., Saveliev, A. A., and Smith, G. M. 2009. Mixed effects models and extensions in ecology with R. Springer, New York: 574 pp.